# IMPACT OF NUCLEAR THERMAL PROPULSION ON THE NASA 90-DAY STUDY'S BASELINE MISSIONS FOR THE SPACE EXPLORATION INITIATIVE

by

FRED GEORGE WILLIAM KENNEDY, III

S.B., Aeronautics and Astronautics, Massachusetts Institute of Technology

(1990)

SUBMITTED TO THE DEPARTMENT OF
AERONAUTICS AND ASTRONAUTICS
IN PARTIAL FULFILLMENT OF THE REQUIREMENTS
FOR THE DEGREE OF

MASTER OF SCIENCE

at the

MASSACHUSETTS INSTITUTE OF TECHNOLOGY
February, 1992



Signature of Author_____
Department of Aeronautics and Astronautics
23 October 1991

Certified by_____
Joseph F. Shea
Adjunct Professor, Aeronautics and Astronautics
Thesis Supervisor

Accepted by_____
Professor Harold Y. Wachman
Chairman, Department Graduate Committee
Department of Aeronautics and Astronautics

# IMPACT OF NUCLEAR THERMAL PROPULSION ON THE NASA 90-DAY STUDY'S BASELINE MISSIONS FOR THE SPACE EXPLORATION INITIATIVE

by

FRED GEORGE WILLIAM KENNEDY, III

Submitted to the Department of Aeronautics and Astronautics
on October 23, 1991, in partial fulfillment of the
requirements for the Degree of Master of Science in
Aeronautics and Astronautics

## ABSTRACT

NASA's 90-Day Study on the implementation of the Space Exploration Initiative concluded that chemical propulsion assisted by aerobraking at Mars and Earth would provide the safest, lowest-cost architecture available to mission planners; such a choice dictates long-duration flights to minimize total transfer delta-V and sets very restrictive ceilings on entry speeds at both planets to allow aerobraking. The Study has come under fire for essentially disregarding problems associated with long-duration spaceflight, namely zero-g deterioration of human bone and musculature, as well as crew radiation exposure due to galactic background radiation and occasional solar particle events. Advanced forms of propulsion were not effectively explored and yet represent important alternative means for reaching the moon and Mars; some, such as nuclear thermal systems like NERVA and its descendants, could reduce travel time and/or mission mass in low Earth orbit.

This report investigated the use of nuclear thermal propulsion (NTP) for orbital transfer, ascent/descent from the moon and Mars, and as propulsion for a launch vehicle's upper stages. The 90-Day Study was examined in depth and parametric studies involving thrust, thrust-to-weight, and specific impulse were performed to determine if initial mission masses could be reduced or payload delivery to the moon or Mars increased by replacing the chemical/aerobrake scheme with higher-specific impulse nuclear thermal propulsion systems.

Gas-core reactors and NERVA were found to be too large for the missions under consideration; newer concepts such as the high thrust-to-weight particle bed reactor could decrease initial mass for a given payload and trajectory by almost a factor of two under the chemical/aerobrake baseline. Specifications for the particle bed reactor were an $I_{sp}$ of 1000 s., a total thrust in the 300 kN range, and an engine thrust-to-weight of 30; such a design was seen to be technologically feasible while offering the best performance of any of the engines studied. Variable duration missions were also examined; it was seen that the use of nuclear thermal propulsion could in some instances reduce total trip time to Mars from 565 to 300 days. The use of NTP for launch vehicle upper stages was found to allow a doubling of payload; however, upper stages will require strict engine-out requirements and very high reliability to

ensure that that the nuclear stage reaches orbit. Lunar and Martian ascent/descent missions did not profit from the use of nuclear propulsion primarily because of the operational complexity entailed, especially in the areas of crew egress and cargo offloading following touchdown on the lunar or Martian surface.

Following the mission analysis, the impact of replacing the chemical/aerobraking scheme with NTP on the design and operations of the various missions--orbital transfer, ascent/descent, and upper stage use--was investigated. It was seen that, while nuclear thermal systems could provide substantial benefits for orbital transfer, their use for launch vehicles and ascent/descent vehicles entailed significant operational problems that might preclude their use in these missions entirely. These problems included crew egress and cargo offloading problems mentioned previously, docking and rendezvous errors, reentry of active reactors into the Earth's atmosphere, and disposal of reactors at end-of-life.

Thesis Supervisor: Dr. Joseph F. Shea
Title: Adjunct Professor of Aeronautics and Astronautics

**ACKNOWLEDGEMENTS**

I am indebted to a number of people without whom this effort would not have been possible: Prof. Joseph Shea, a fantastic mentor and teacher, who provided the impetus for my work, critiqued it tirelessly and encouraged me to examine all aspects of a problem; Prof. Edward Greitzer and Dr. Choon Tan, whose support during my first term of graduate school allowed me to be able to pick and choose the work of my choice; Alissa Fitzgerald, friend and 'sanity check,' whose advice frequently provided useful insights; Vickie Garbarino, who has put up with me during the entire process of producing this thesis and somehow still seems to enjoy my company; and, of course, my parents Col. Fred and Claudette Kennedy, as well as my brother James, for their continued love and support.

## TABLE OF CONTENTS

ABSTRACT....1
ACKNOWLEDGEMENTS....3
TABLE OF CONTENTS....4
LIST OF FIGURES....6
LIST OF TABLES....8
1.0 INTRODUCTION....9
1.1 NASA Scheduling and Baseline Designs....10
1.1.1 Option I....11
1.1.2 Option V....14
1.1.3 Mission Scenarios....17
1.1.3.1 Lunar Reference Missions....17
1.1.3.2 Mars Reference Missions....20
1.1.4 Transfer and Excursion Vehicle design....23
1.1.5 Earth-To-Orbit (ETO) Vehicle design....29
1.2 Propulsion and Astrodynamics....31
1.2.1 Lunar Trajectories....34
1.2.2 Mars Trajectories....34
1.2.3. Evaluation of the 90-Day Study Architecture....39
1.2.3.1 Aerobraking....39
1.2.3.2 Earth-To-Orbit Delivery and On-Orbit Assembly....40
1.2.3.3 Effect of Lengthy Missions....41
2.0 NTP ENGINE DESIGN....46
2.1 Design Approach....46
2.2 NTP Engine Options....51
2.2.1 Solid-Core Reactors (SCR)....51
2.2.1.1 ROVER/NERVA/Cermet....53
2.2.1.2 Particle-Bed Reactors....56
2.2.2 Gas-Core Reactors (GCR)....58
2.2.2.1 Open-Cycle....59
2.2.2.2 Closed-Cycle....61
3.0 NUCLEAR PROPULSION AND THE NASA BASELINE MISSIONS....65
3.1 Effect of Specific Impulse (Isp), Thrust (T), and Thrust-to-Weight (T/W)....65
3.1.1 Fixed Mission Duration (NASA Baseline Missions)....69
3.1.1.1 Orbital Transfer NTP....69
3.1.1.1.1 All-Propulsive Missions....71
3.1.1.1.2 Aerobraked Missions....78
3.1.1.2 LV Upper Stage NTP....83
3.1.1.3 Ascent/Descent NTP....86
3.1.2 Variable Duration Missions....88
3.1.2.1 Short Stay Missions....91
3.1.2.2 Medium Stay Missions....93
3.1.2.3 Long Stay Missions....95
3.1.2.4 Protracted Stay Missions....98
3.1.2.5 All-Up Alternatives to the Baseline....101
3.1.2.6 Split Mission Alternatives to the Baseline....105
3.1.2.7 Results of Mission Analysis....110
3.2 Impact on OTV, ADV, and LV Design....115
3.2.1 Orbital Transfer Vehicle Design....115
3.2.1.1 Engine Cluster Sizing....115

3.2.1.2 Engine Cycle and Pressurization Schemes....116
3.2.1.3 Radiation Enviroment and Shielding Requirements....120
3.2.1.4 Tank Construction....140
3.2.2 Ascent/Descent Vehicle Design....142
3.2.3 Launch Vehicle Design....143
3.3 Impact on orbital operations....145
3.3.1 Cooldown, Serviceability, and EVA....145
3.3.2 Docking and Maneuvering Near Manned Stations....148
3.3.3 Flyover....152
3.3.4 Disposal methods....154
3.4 Impact on Surface Facilities and Surface Operations....158
3.4.1 Earthbound Facilities....158
3.4.2 Extraterrestrial Facilities....160
4.0 SUMMARY AND CONCLUSIONS....161
4.1 Conclusions....161
4.1.1 Issues of Performance....161
4.1.2 Issues of Construction, Operation, and Testing....163
BIBLIOGRAPHY....168
APPENDIX A....171

## LIST OF FIGURES

Figure 1 Key Characteristics of Reference Approaches,....10
Figure 2 Cumulative Launches to LEO (Option I vs. Option V)....11
Figure 3 Option I Operations Schedule....12
Figure 4 Option V Operations Schedule....13
Figure 5 Total mass delivered to LEO....14
Figure 6 Total mass delivered to lunar surface....15
Figure 7 Total mass delivered to LEO....15
Figure 8 Total mass delivered to Mars....16
Figure 9 Total Payload to LEO (supporting both Mars and Lunar operations)....16
Figure 10 Option I Lunar Flight 0....18
Figure 11 Option I Mars Flight 6....22
Figure 12 Paired Lunar Transfer Vehicle (LTV) and Lunar Excursion Vehicle (LEV)....24
Figure 13 Paired Mars Transfer Vehicle (MTV) and Mars Excursion Vehicle (MEV)....25
Figure 14 STS-Derived Launch Vehicles....30
Figure 15 NTS-Derived Launch Vehicles....31
Figure 16 Aspects of the generic lunar transfer....34
Figure 17 2007 960-Day Conjunction-Class Mission....35
Figure 18 2007 560-Day Opposition-Class Mission....36
Figure 19 Hohmann Transfer....37
Figure 20 NERVA engine (hot bleed cycle)....54
Figure 21 Possible engine scheme for the Fixed Particle Bed Reactor....57
Figure 22 Open Cycle Gas Core Reactor engine concept....60
Figure 23 Closed Cycle Gas Core Reactor engine concept....63
Figure 24 Option I Mars Flight 1....67
Figure 25 Option I Mars Flight 1....68
Figure 26 Performance of NTP versus NASA's Mars Option I....72
Figure 27 NTP versus Option I....73
Figure 28 Performance of nuclear thermal options against NASA's baseline Option I....77
Figure 29 Performance of nuclear options versus the NASA baseline....77
Figure 30 Total payload in LEO required to support....79
Figure 31 Total payload delivery to LEO required to support....80
Figure 32 NTP with Aerobraking versus Option I....81
Figure 33 NTP with Aerobraking versus Option I....82
Figure 34 Hypothetical next-generation launch vehicle....84
Figure 35 Payload delivered to LEO by a nuclear second stage....85
Figure 36 Payload delivered to LEO by a nuclear second stage....86
Figure 37 Lunar excursion vehicle mass allowance....87
Figure 38 Mars excursion vehicle mass allowance....88
Figure 39 200-day trip time with 30-day stay, for the period 2000-2016....90
Figure 40 Envelope of 30-day stay missions for variable trip time....90
Figure 41 Envelope for 60-Day stay times....92
Figure 42 Envelope for 90-Day stay times....92
Figure 43 500/240 mission opportunities....93
Figure 44 Envelope for 240-Day stay times....94
Figure 45 Envelope for 180-Day stay times....94
Figure 46 Envelope for 300-Day stay times....95
Figure 47 850/500 mission opportunties....96

Figure 48 850/550 mission opportunities ..... 96
Figure 49 Envelope of 500-Day stay times ..... 97
Figure 50 Envelope of 550-Day stay times ..... 97
Figure 51 1000/750 mission opportunities ..... 98
Figure 52 Envelope of 700-Day stay times ..... 99
Figure 53 Envelope of 750-Day stay times ..... 99
Figure 54 1000/850 mission opportunities ..... 100
Figure 55 Envelope of 850-Day stay times ..... 100
Figure 56 Δv mission requirements for 350/30 and 450/30, 2000-2006 ..... 102
Figure 57 Option I Flight 1 (565/30) ..... 103
Figure 58 Alternate 350/30 ..... 103
Figure 59 Opportunities for the 850/500 and 900/500 ..... 104
Figure 60 Option I Flight 6 ..... 105
Figure 61 Alternate 850/500 ..... 105
Figure 62 Option I Mars Flight 1 Split Mission (cargo flight) ..... 106
Figure 63 Option I Mars Flight 1 Split Mission (crew flight) ..... 107
Figure 64 Flowchart of mission analysis perfomed ..... 113
Figure 65 Fixed payload, variable IMLEO results for Option I ..... 114
Figure 66 Performance of NTP options versus the NASA baseline ..... 114
Figure 67 Hypothetical Mars Transfer Vehicle incorporating ..... 116
Figure 68 Engine cycle options ..... 119
Figure 69 Separation distances required to achieve given dose rates ..... 123
Figure 70 Shielding depth necessary to hold absorbed gamma ..... 128
Figure 71 Shielding depth for gamma dose of 2.5 rem (60 m. separation) ..... 129
Figure 72 Shielding depth for gamma dose of 2.5 rem (120 m. separation) ..... 129
Figure 73 Tungsten shield depth necessary to hold absorbed gamma ..... 130
Figure 74 LiH neutron shield thickness required to hold absorbed dose to 2.5 rem, for 30, 60, and 120 m. separation distances ..... 131
Figure 75 LH2 neutron shield depth (total dose = 2.5 rem) ..... 131
Figure 76 Gamma shielding depth required for reactor power levels of ..... 135
Figure 77 LiH neutron shield depth (given a lead or tungsten ..... 136
Figure 78 Structural and shielding mass for various ..... 137
Figure 79 Total structural and shielding mass ..... 138
Figure 80 Hypothetical MTV with conical propellant tanks ..... 141
Figure 81 Dose rate/unit power (rem/s./MW) ..... 147
Figure 82 Accumulated gamma radiation dose (rem/MW) at separation distances of 200 m, 2 km, and 20 km, assuming exposure begins ..... 148
Figure 83 Departure of transfer vehicle from Freedom or ..... 150
Figure 84 Overflight Model ..... 152
Figure 85 Total absorbed dose received at a lunar base due ..... 154

## LIST OF TABLES

Table 1 Option I Lunar Flight 0 Manifest ..... 17
Table 2 Option I Lunar Flight 0 Mission Event List ..... 19
Table 3 Option I Lunar Flight 5 Manifest ..... 20
Table 4 Option I Mars Flight 3 Manifest ..... 20
Table 5 Option I Mars Flight 5 Manifest ..... 21
Table 6 Option I Flight 6 Mission Event List ..... 23
Table 7 Lunar Transfer Vehicle (LTV) ..... 26
Table 8 Lunar Excursion Vehicle (LEV) ..... 27
Table 9 Mars Transfer Vehicle (MTV) ..... 28
Table 10 Mars Excursion Vehicle (MEV) ..... 29
Table 11 Key Characteristics of Conjunction- and Opposition-Class Missions ..... 37
Table 12 Mars Missions, Options I and V ..... 38
Table 13 NCRP Career Limit Radiation Exposure in Rem ..... 43
Table 14 $I_{sp}$ Variation among Propellant ..... 50
Table 15 Engine Designs Considered in Analysis ..... 51
Table 16 Mars Mission Δv requirements ..... 70
Table 17 NTP Engine Staging for Fixed IMLEO ..... 75
Table 18 Option I Mars Flight 6 Mission Event List ..... 76
Table 19 Option I Lunar Flight 0 Mission Event List ..... 78
Table 20 Encounter Mass in Low Mars Orbit ..... 81
Table 21 Mars Mission Δv requirements ..... 87
Table 22 Option I Mars Flight 1 and Alternatives ..... 102
Table 23 Option I Mars Flight 6 and Alternatives ..... 104
Table 24 Option I Mars Flight I Payload ..... 107
Table 25 Option I Mars Flight 1 and Alternatives ..... 108
Table 26 Option I Mars Flight 1 Mission Event List ..... 109
Table 27 Option I Mars Flight 1 Mission Event List ..... 110
Table 28 Removal Cross-Sections for Fast Neutrons ..... 124
Table 29 Linear Attenuation Coefficients for Gamma Radiation ..... 127
Table 30 Inverse Mass Absorption Coefficients for Gamma Radiation ..... 134
Table 31 Inverse Mass Absorption Coefficients for Neutron Radiation ..... 134
Table 32 Properties of Structural Materials ..... 139
Table 33 Mass and Dimension Requirements for ..... 140
Table 34 Disposal of reactors in LEO ..... 157

## 1.0 INTRODUCTION

President Bush's speech of July 20, 1989 spelled out the administration's support for a return to manned exploration of the solar system, comprised of the establishment of a permanent human presence on the moon early in the 21st century and, at a later time, the emplacement of manned settlements on Mars. The National Space Council was directed to uncover mission architectures that would allow this plan to proceed. From the preface of NASA's 90-day study:

> "To support this endeavor, NASA administrator Richard H. Truly created a task force to conduct a 90-day study of the main elements of a Human Exploration Initiative. The Initiative described in this report encompasses robotic as well as human missions. It is, nonetheless, a distinctly human adventure in the broadest sense, involving not only human space travelers, but also extending into the solar system the skills, imagination, and support of people who will never leave the Earth."[1]

The 90-day study team developed five 'reference approaches,' offered principally as alternatives in scheduling. The emphasis of each is explained in the report as follows: balance and speed (Option I); the earliest possible landing on Mars (II); reduced logistics from Earth (III); schedule adapted to Space Station Freedom (IV); and reduced scale (V).[2] It is interesting to note that there are no differences in technology between the reference approaches--the differences lie mainly in the startup times for certain key assets--such as the lunar oxygen plant or the emplacement of materials on Mars. Figure 1 shows the characteristics of each of NASA's five approaches.

The purpose of this study is to consider options I and V in detail (II, III, and IV are simple variants of I and were not analyzed in depth by NASA) and to present the impact of a different technology--in this case, nuclear thermal or 'direct-heating' propulsion (NTP), as an alternative to the baseline (cryogenic LOX-$LH_2$) currently being viewed for use. NTP's capabilities, specifically high specific impulse (800+ s.) and thrust levels of up to 2000 kN, offer the possibility of mitigating long-term crew exposure to hazards such as zero-gravity and galactic cosmic radiation (by lowering trip times) or cutting the overall mass launched to LEO. The 90-Day Study considered the impact of NTP on a single Mars mission, but did not examine plans that integrated this technology into an architecture--this is the gap that this paper will attempt to fill. This paper will attempt to show that great propellant mass savings (and/or substantial

---

[1] Report of the 90-Day Study on Human Exploration of the Moon and Mars, p. i, Aaron Cohen, et. al., November 1989

[2] ibid., pp. 1-3

decreases in transit times) are possible as specific impulse approaches 1000 s. and fuel needs decline, but this advantage may be offset by the significant radioactivity in the vicinity of these engines both during operation and following shutdown. Proper shielding of the engines should result in minimal risk to humans (and sensitive instrumentation), allowing such hazards to become less potentially lethal. However, in our society, there are important questions regarding public opinion and the use of nuclear power under any conditions, no matter how infinitesimal the probability of failure. These and other considerations will be addressed within this report.

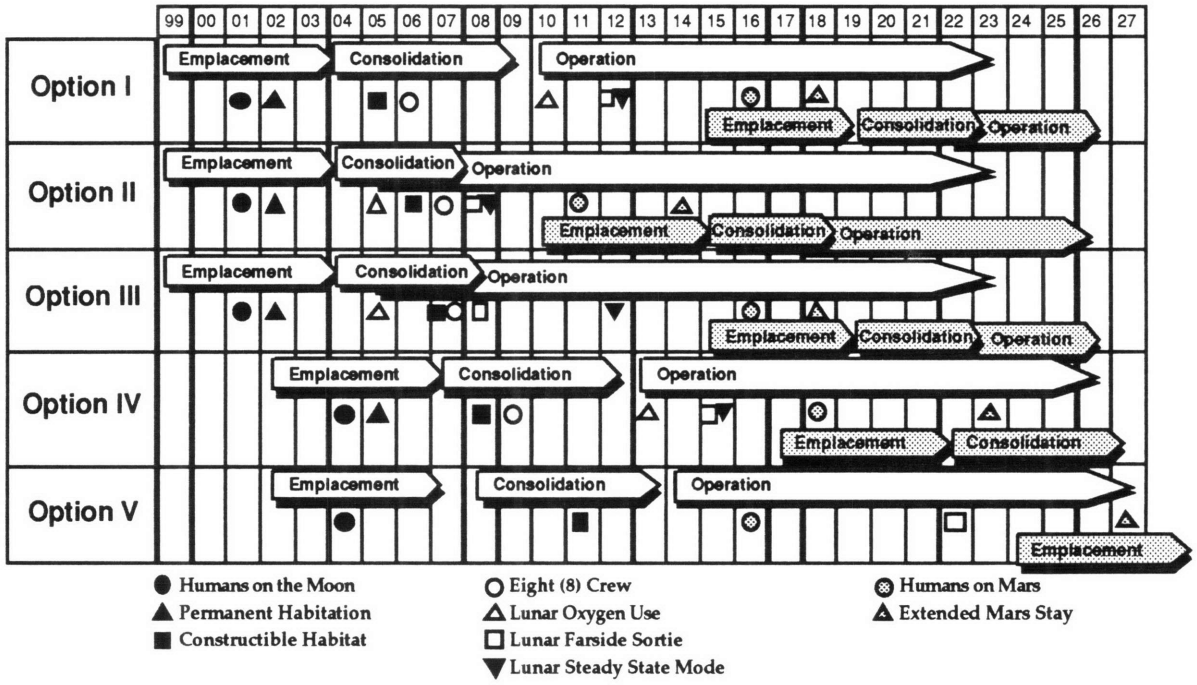


**Figure 1 Key Characteristics of Reference Approaches, Options I-V [NASA, 1989]**

## 1.1 NASA Scheduling and Baseline Designs

The NASA 90-day study's options I and V both use the baseline technologies to settle the moon and advance to Mars; however, Option I presents a "serial" approach, in which the lunar settlement is fully developed (circa 2012) before the Mars missions are begun. Option V, which reflects the strategy of 'reduced scale,' allows parallel development of the moon and Mars. However, Option V never achieves several significant milestones, among them (1) permanent habitation of the lunar surface; (2) exploitation of lunar resources, such as oxygen, and (3) consolidation of a Mars outpost. Extended Martian stays (600 days) in the Option V timeline begin nine years after the Option I date.

### 1.1.1 Option I[3]

The lunar colonization portion of Option I is characterized by 43 flights to the lunar surface between 1999 and 2026; 112 heavy-lift launch vehicle (HLLV's) flights and 34 shuttle flights are required to loft the required payload into low earth orbit (Fig.'s 2, 3).[4] The lunar transfer vehicle (LTV) and excursion vehicle (LEV) are sent, unmanned, to the moon in July 1999, delivering a rover and materials necessary to ready the area for human habitation. The 150 mT lunar transfer vehicle will provide a habitat for the crew on its 3 1/2-day transit to and from the moon. The lunar excursion vehicle, approximately 50 mT when fully loaded with propellant, would separate from the LTV upon insertion into lunar orbit and would carry crew and cargo to

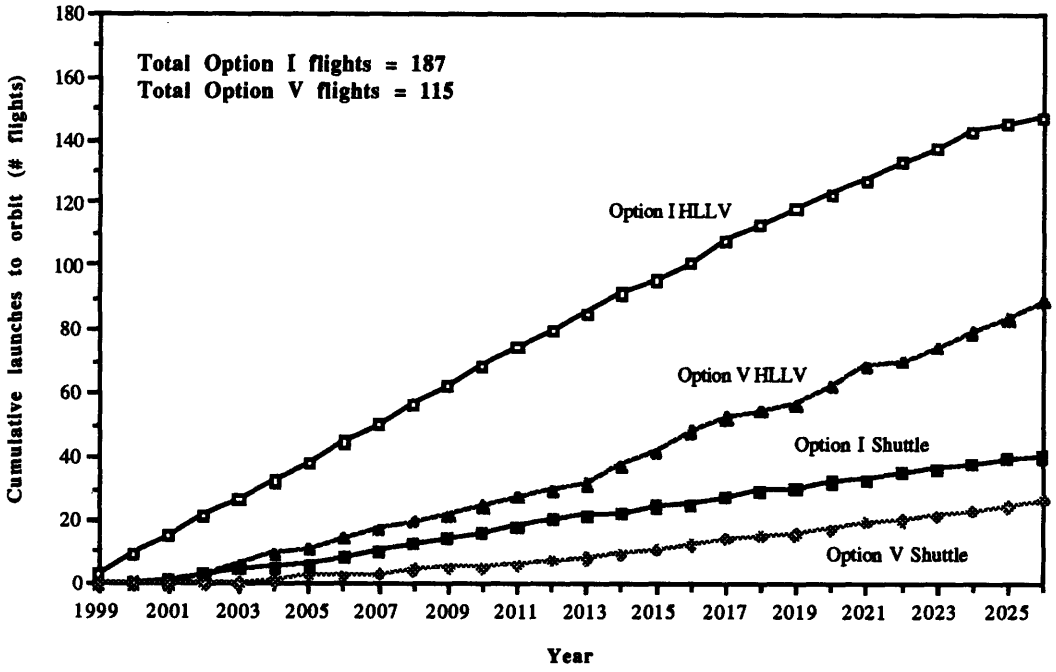


**Figure 2 Cumulative Launches to LEO (Option I vs. Option V)**

and from the lunar surface. The LEV would have a cargo capacity of 15 mT (unmanned version) or 33 mT (manned). A year later, the power system, habitation module, and airlock

---

[3] ibid., pp. 4-1 - 4-5

[4] Databook for the 90-Day Study on Human Exploration of the Moon and Mars, Doug Cooke, et. al., December 1989 -- The lunar heavy-lift launch vehicle was postulated to be able to deliver anywhere from 61 to 98 mT of payload to a 407-km. circular orbit, allowing a single lunar mission to be delivered in two or three launches; the Mars HLLV would place 140 mT in LEO, requiring five to seven launches.

are left on the lunar surface in anticipation of the arrival of the first four crew members. These astronauts will land in 2001. Permanent occupancy of the moon begins in 2002, and with the third crew later that same year, twelve-month duty cycles begin. Clearly, these dates cannot be any longer be considered credible, due to current budgetary constraints and the uncertainty as to what form, if any, a Space Exploration Initiative might take.

By 2006, the crew is expanded to eight; two years later, the original nuclear power plant is increased in size to deliver 550 KW. At this point, the lunar outpost is capable of conducting research into all aspects of the Martian mission, including simulation of a 1000-day Mars expedition for the purpose of developing technologies to prevent zero-gravity debilitation of humans.

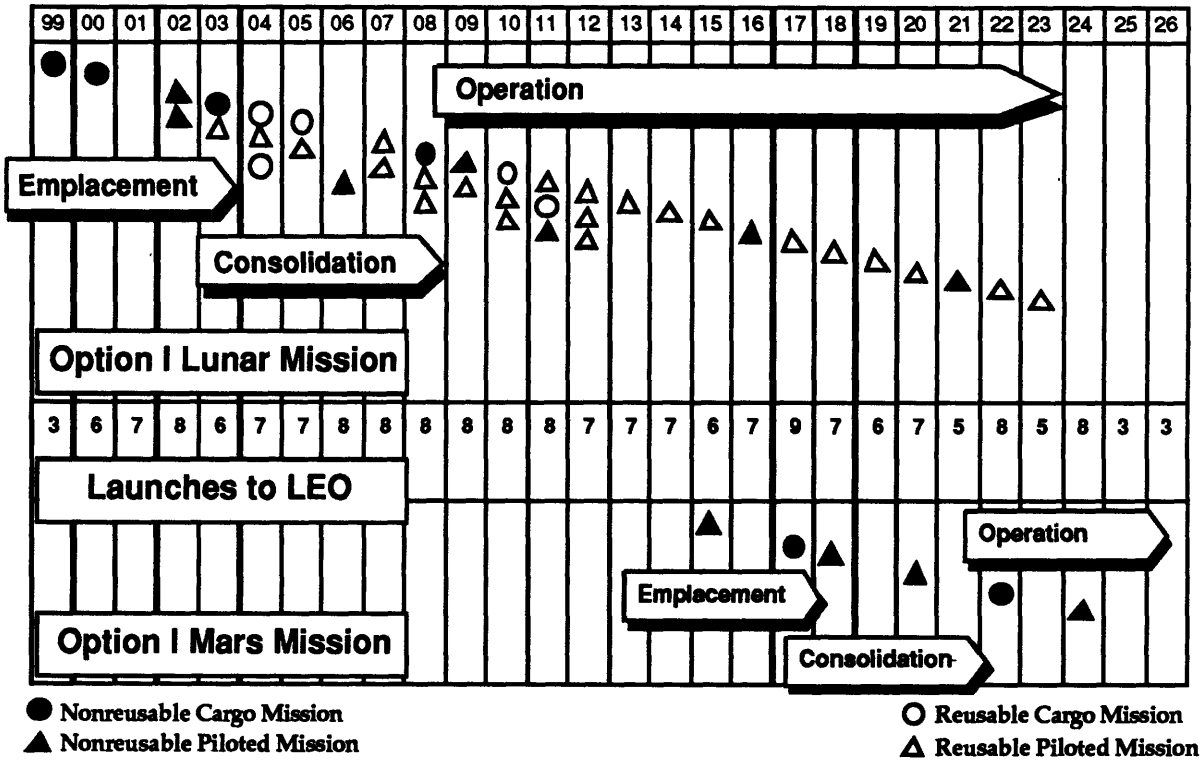


**Figure 3 Option I Operations Schedule (derived from the Databook for the 90-Day Study on Human Exploration of the moon and Mars)**

Option I assumes lunar oxygen production after 2010 and steady-state operation after 2012, which is defined as one flight per year to the moon with four crew members on station for twelve months.

Mars expeditions begin in 2015, following precursor missions and construction of the Mars Transfer and Excursion Vehicles (MTV and MEV) at Space Station Freedom. The Mars transfer vehicle, which would provide living quarters for the lengthy transit from Earth to Mars

and return, would mass between 600 and 850 mT and would be mated to an excursion vehicle which would separate on insertion into Mars orbit. The piloted Mars excursion vehicle, which would transfer crew and cargo from low orbit to the surface and back, would mass approximately 80 mT when loaded with cargo and propellant, of which no more than 25 mT would be payload. The cargo version of the MEV would be capable of carrying as much as 80 mT of payload from orbit to the surface. 35 HLLV and 6 shuttle flights fulfill the Earth-LEO payload requirement. Seven missions, of which five are piloted, are planned between 2015 and 2024, after which steady-state operations commence. Habitat and power systems leave with the first flight, in conjunction with scientific instrumentation and teleoperated rovers. Permanent habitats and emplacement materials leave with the second flight, a cargo run, in order to prepare for the arrival of four crew members (intended to remain on the Martian surface for an extended stay of 600 days) in 2018. By 2025, additional flights would leave Earth as needed only to resupply the Mars outpost.

It is important to note that, in both Options, precursor missions to the moon and Mars are launched by expendable vehicles, such as those currently in the national inventory (e.g. Titan IV or Delta II). This study will not examine these precursor missions.

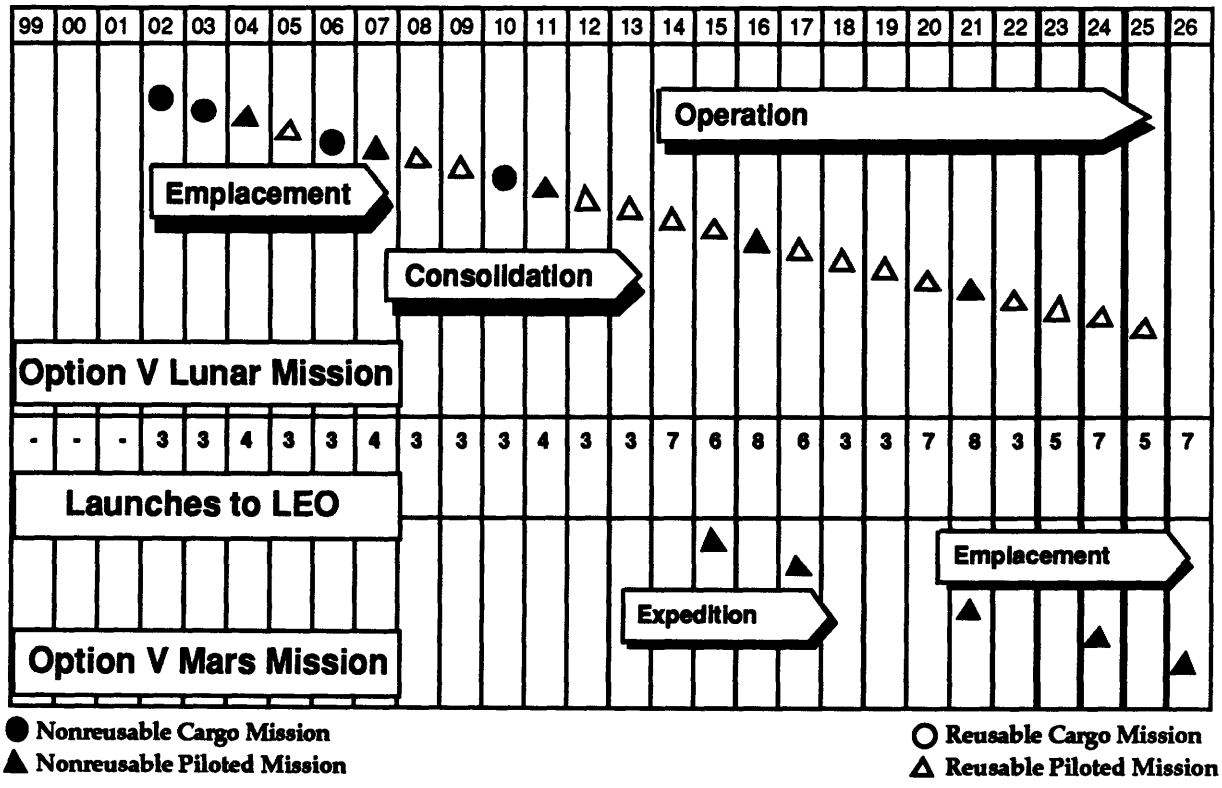


**Figure 4 Option V Operations Schedule (derived from the Databook for the 90-Day Study on Human Exploration of the moon and Mars)**

### 1.1.2 Option V[5]

The 'reduced-scale' of this option is seen in the payload deposited in LEO--60 HLLV and 21 shuttle launches send the necessary materials to set up lunar housekeeping (Fig.'s 4, 5, 6). Unlike Option I, Option V never reaches steady-state operations; humans reach the moon only in 2004 and are not intended to take part in a duty cycle that would afford permanent occupation. Science tends to be conducted through greater use of teleoperation.

The unmanned LTV/LEV test occurs in 2002, followed by emplacement of habitation and power facilities in the next year. By 2011, astronauts experiment with lunar oxygen production and remain for 180 days. Two years later, a piloted flight arrives to occupy the facility for 600 days (in order to gather data pertaining to the 2015 Mars expedition).

The focus of the Mars phase is on exploration. The initial piloted flights (three of the four planned) concern themselves principally with locating the optimum site for human habitation.

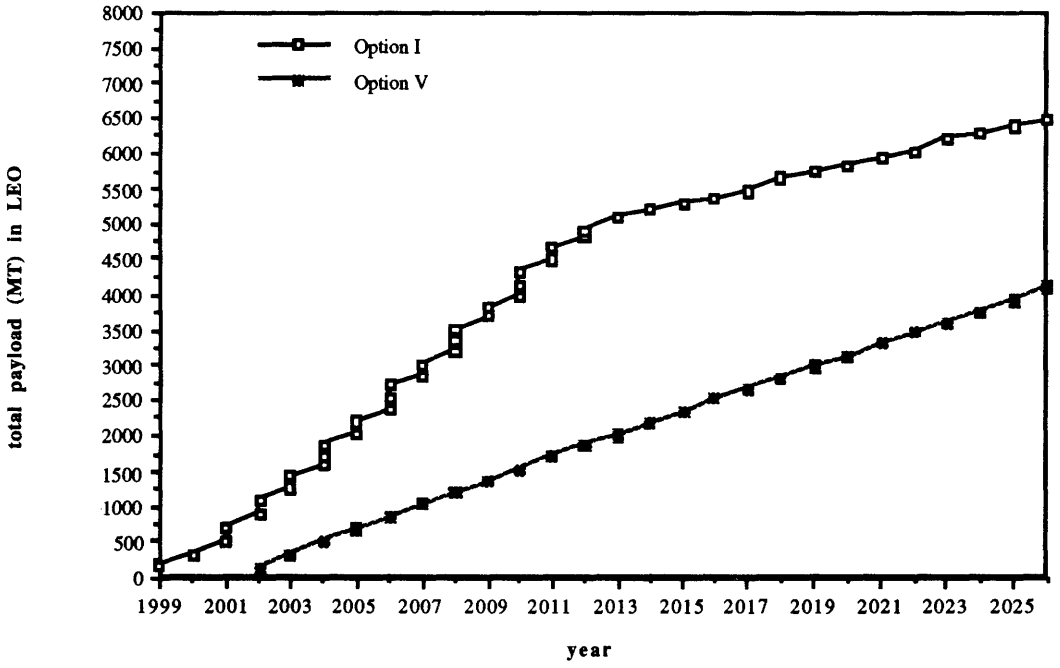


**Figure 5 Total mass delivered to LEO (Supporting lunar operations, Option I vs. Option V)**

[5] 90-Day Study, pp. 4-7 - 4-10

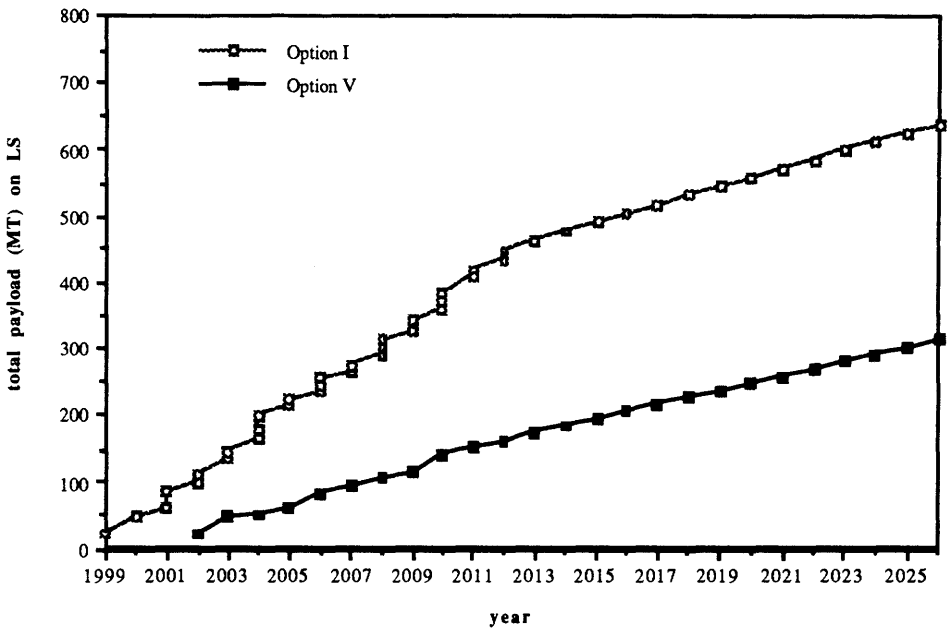


**Figure 6 Total mass delivered to lunar surface (Option I vs. Option V)**

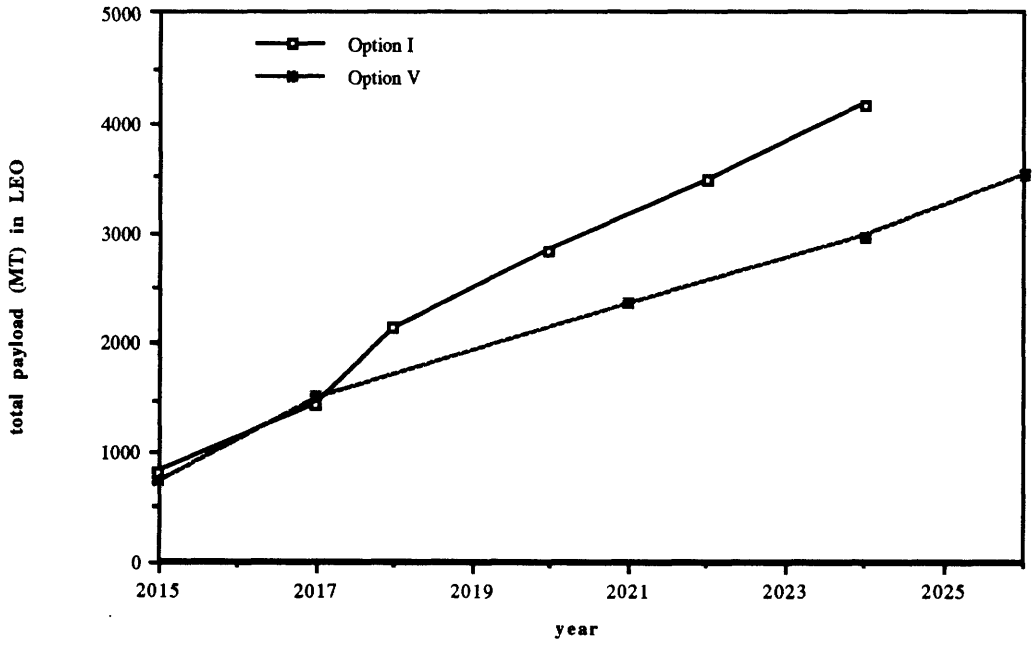


**Figure 7 Total mass delivered to LEO (Supporting Mars operations, Option I vs. Option V)**

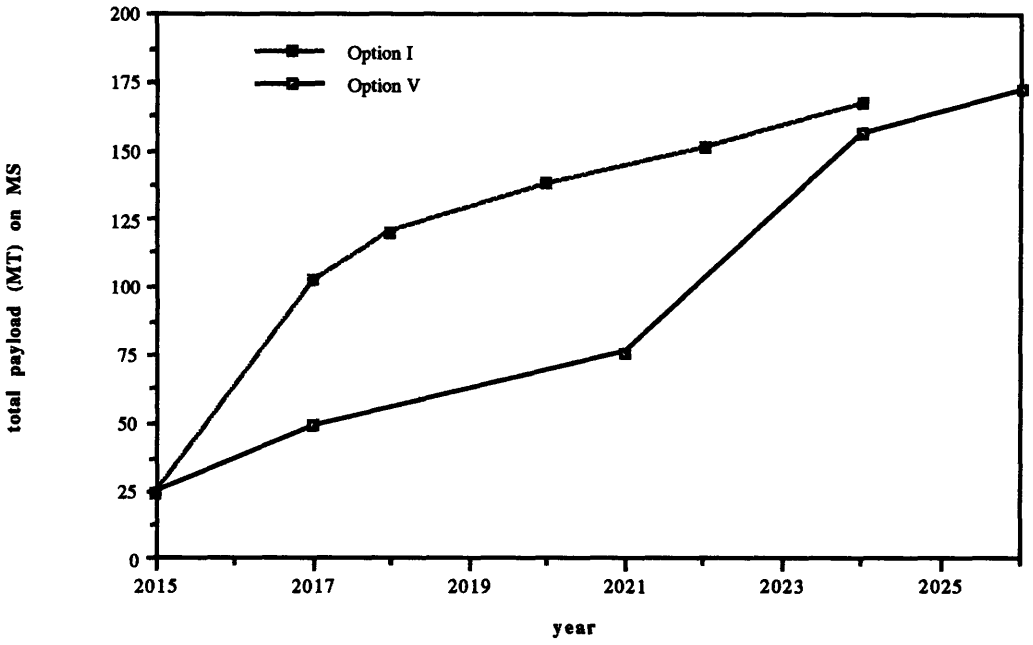


**Figure 8 Total mass delivered to Mars (Option I vs. Option V)**

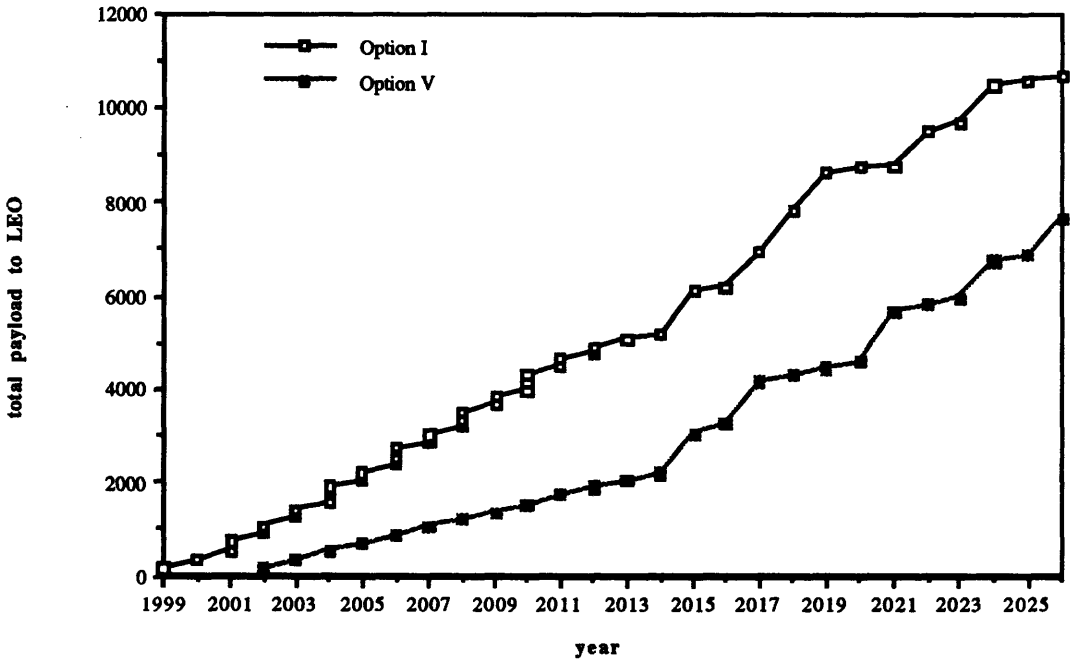


**Figure 9 Total Payload to LEO (supporting both Mars and Lunar operations, Option I vs. Option V)**

The fourth manned mission, which would not get underway until November 2026, occupies the selected outpost--placed there in 2025 by a cargo mission--for 600 days. Option V assumes additional flights beyond the fourth piloted mission but does not elaborate except to say that, "consolidation and occupation of the Mars outpost will follow." The Mars expedition and emplacement requires a total of 29 HLLV and 5 shuttle flights (Fig.'s 7, 8). The total number of Earth-LEO flights for Option V (115) is substantially smaller than that for Option I (187) (Fig. 9). It is necessary to point out, however, that Option I, which attempts a quick settlement of both Mars and Earth, clearly achieves a greater level of extraterrestrial human presence and a lesser reliance on telerobotic exploration.

### 1.1.3 Mission scenarios[6]

It is important to reemphasize that, while Options I and V have quite disparate schedules, as a result of their differing scope, the separate flights (lunar or Martian) performed are accomplished with the same technology and in essentially the same manner.

#### 1.1.3.1 Lunar reference missions

Generic lunar flights begin at Space Station Freedom; they tend to have similar $\Delta V$ figures--to within a few hundred meters per second--for various required maneuvers and are therefore not as difficult to plan as Martian flights. Those flights that return to LEO are distinguished by the

**Table 1 Option I Lunar Flight 0 Manifest [NASA, 1989]**

| | |
|---|---|
| Cargo Lunar Excursion Vehicle (LEV-C) | 5.10 MT |
| LEV-C Propellant | 16.80 |
| Cargo Lunar Transfer Vehicle (LTV-C) | 7.60 |
| LTV-C Propellant | 102.20 |
| LTV-C Tanks | 5.70 |
| | |
| Payload Unloader | 10.00 |
| Attachments for Payload Unloader | 6.33 |
| Excavation Pyrotechnics | 3.68 |
| Communication Equipment | 0.94 |
| Unpressurized Manned Rover (with telerobotic adapter kit) | 1.47 |
| Margin | 0.00 |
| **IMLEO** | **159.80 MT** |

[6] Databook for the 90-day Study, Sections 5.1.1, 5.1.2

use of an aerobrake to slow the vehicle into orbit. As a reference, Option I's first cargo flight ('flight 0'), with a launch date of July 1999, is described in detail. Flight 0's initial mass in low earth orbit (IMLEO) is 159.80 MT. This mass is divided among components of the missions as shown in Table 1.

The flight leaves Freedom and performs a translunar injection (TLI) burn of 3300 m/s, using 80.45 MT of propellant (see Table 1). The TLI propellant tanks are jettisoned after the burn's completion. After three days in transit and midcourse corrections totalling a $\Delta V$ of 10 m/s, the LTV-C performs a lunar orbit insertion (LOI) burn of 1100 m/s. Fine-tuning of the lunar orbit is made and the LEV-C decouples from the LTV; it then retrofires and lands on the lunar surface ($\Delta V$ = 2000 m/s). The excursion vehicle unloads its payload unloader and various other materials. It remains on the lunar surface and is not reused. The LTV-C drops its LOI tanks, uses 2.85 MT of its propellant for its trans-Earth injection (TEI) of 1100 m/s, and aerobrakes on return to Earth. The LTV uses its remaining fuel to circularize its orbit into that of Freedom's (310 m/s) (Fig. 10).

Some events listed (e.g. LEV-C ascent propellant use) are, of course, necessary to some missions and not to others. All possible planned events are shown to illustrate what might

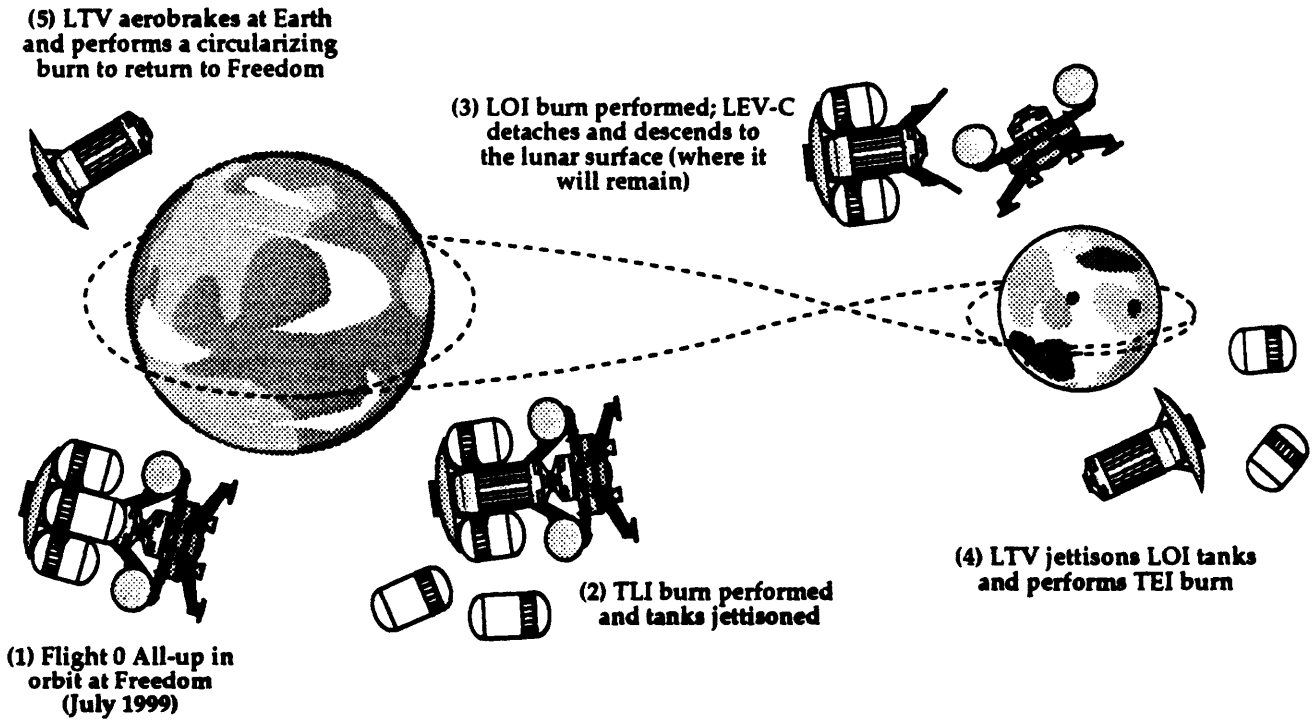


**Figure 10 Option I Lunar Flight 0 [NASA, 1989]**

happen on any given mission.

The second mission is Option I's Flight 5, a piloted mission scheduled for July 2002. IMLEO is 189.0 MT; the manifest is detailed in Table 3. The flight here is quite similar to the cargo flight of Table 1. The LTV/LEV pair leave Freedom and perform the TLI and LOI burns (total propellant burned = 113.94 MT), releasing empty tanks along the way. The crew transfers to the LEV, which then descends from lunar orbit; supplies and materials are unloaded and the habitat prepared for a full year's residence. The LTV-P in lunar orbit returns to Freedom in order to be reused for a cargo mission in January 2003 (propellant used = 5.76 MT). The lunar outpost crew returns to Earth in July 2003. Note: (1) The lack of a lunar transfer vehicle in orbit overhead prevents a return by astronauts in case of an emergency, requiring the crew to wait at least 3 1/2 days before a vehicle could arrive, assuming it could be fueled for the transfer in that time, and (2) during the year-long duty cycle, the lunar excursion vehicle will be sitting on the lunar surface, presumably with a full load of ascent fuel. The issue of how one might prevent cryogenic fluid boiloff in the severe lunar thermal environment over such an extended period is not addressed by the 90-Day Study.

**Table 2 Option I Lunar Flight 0 Mission Event List (derived from the Databook for the 90-Day Study on Human Exploration of the Moon and Mars)**

| *Mission Event* | *Total Vehicle Mass* (MT) | *Change in Mass* (MT) | *Delta-V* (m/s) |
|---|---|---|---|
| IMLEO | **159.80** | | |
| Pre-injection preparation propellant | 159.80 | 0.00 | |
| Translunar injection propellant | 79.35 | 80.45 | 3300 |
| Jettison TLI tanks | 75.05 | 4.30 | |
| TLI coast propellant | 74.89 | 0.16 | 10 |
| Lunar orbit insertion propellant | 59.30 | 15.59 | 1100 |
| Lunar orbit operations propellant | 59.30 | 0.00 | |
| Deploy additional payloads | 59.30 | 0.00 | |
| Lunar payload to lunar surface | 15.00 | 44.30 | |
| Jettison LOI tanks | 13.70 | 1.30 | |
| Trans-Earth injection propellant | 10.85 | 2.85 | 1100 |
| Trans-Earth coast propellant | 10.83 | 0.02 | 10 |
| Earth orbit operations propellant | 10.81 | 0.01 | 6 |
| Post-aerobrake circularize | 10.13 | 0.69 | 310 |
| Final LTV-C mass in LEO | **10.13** | | |
| | | | |
| Lunar payload total mass | **44.30** | | |
| Pre-deorbit preparation propellant | 43.82 | 0.48 | 50 |
| Lunar descent propellant | 28.25 | 15.57 | 2000 |
| Lunar payload (dry) | 5.85 | 22.40 | |
| Moon surface science | 5.85 | 0.00 | |
| Moon surface consumables | 5.85 | 0.00 | |
| LEV-C total mass prior to ascent | **5.85** | | |
| LEV-C ascent propellant | 5.85 | 0.00 | |
| Crew | 5.85 | 0.00 | |
| LEV-C final mass | **5.85** | | |

**Table 3 Option I Lunar Flight 5 Manifest (from the Databook for the 90-Day Study on Human Exploration of the Moon and Mars)**

| | |
|---|---|
| LEV-P (Personnel) | 8.70 MT |
| LEV-P Propellant | 22.80 |
| LTV-P | 14.20 |
| LTV-P Tanks | 5.70 |
| LTV-P Propellant | 121.70 |
| **4 crew for 12 months** | |
| 4 EMU's | 0.71 |
| Crew Supplies | 6.24 |
| Optical Telescope | 0.50 |
| Particles and Fields Instruments | 1.00 |
| Biostack, Aseptic Samplers | 0.05 |
| 2 UV-Visible Interferometer Elements | 2.00 |
| Spares (unspecified) | 2.25 |
| Margin | 3.10 |
| **IMLEO** | **189.00 MT** |

## 1.1.3.2 Mars Reference Missions

90-day study Mars flights typically last 500 days or longer and are *far more restricted in terms of launch and arrival dates than their lunar counterparts*, since the amount of velocity change needed to place payloads on the surface of Mars can be extremely sensitive to variations

**Table 4 Option I Mars Flight 3 Manifest (from the Databook for the 90-Day Study on Human Exploration of the Moon and Mars)**

| | |
|---|---|
| Personnel Mars Excursion Vehicle (MEV-P) | 23.00 MT |
| MEV-P Propellant | 32.50 |
| Personnel Mars Transfer Vehicle (MTV-P) | 122.90 |
| MTV-P Propellant | 495.30 |
| | |
| **4 crew for 600 days** | |
| 6 EMU's | 1.06 |
| Crew Supplies | 9.33 |
| Mars ISRU Water Demonstration | 0.23 |
| Unpressurized Manned Rover (with telerobotic adapter kit) | 1.47 |
| Geologic Equipment w/drill | 1.00 |
| Portable Geophysical Traverse Package | 0.10 |
| Particles and Fields Instruments | 2.25 |
| Teleoperated Rover | 0.60 |
| Plant/Animal/Microbe Instruments | 2.30 |
| Spares (unspecified) | 1.25 |
| Margin | 6.70 |
| **IMLEO** | **698.70 MT** |

in time of launch and mission duration and can vary by tens of thousands of meters per second. The intricacies of trajectory analysis with respect to interplanetary travel are reasonably complex and will be addressed further in Section 1.2.

Option I's Flight 3 to Mars, a piloted flight intended to be launched from Freedom on or around 5 June 2018, fires its trans-Mars injection (TMI) stage for a $\Delta V$ of 4500 m/s and then separates from the main MTV/MEV pair. The mission encounters Mars after 100 days of travel, at which point the MEV detaches from the MTV. Both spacecraft shed their excess velocity by aerobraking and decelerate into an eccentric elliptical orbit about the planet. Following these maneuvers, the MEV and MTV dock in orbit and the crew transfers to the excursion vehicle and descend to the Martian surface.

After unloading, the four personnel settle down for a stay of over 600 days. The MEV ascent stage and crew return to Mars orbit and transfer to the MTV, which fires its TEI stage ($\Delta V$ = 2000 m/s) and jettisons it shortly thereafter. On 14 November 2020, 135 days after leaving Mars, the MTV deploys its aerobrake and decelerates into LEO. The transfer times for this mission are quite short, and occur only for long-duration stay missions, when the stay time is on the order of 500-700 days. Short-duration stay missions used by the 90-Day Study tend to very long transfer times--on the order of a year in some cases--due to the use of Venus gravity-assist maneuvers to lower overall delta-V.

The second reference Mars mission is Option I's Flight 5, a cargo flight intended to leave Freedom on 11 September 2022 and arrive in low Mars orbit (LMO) on 12 March 2023. Its manifest is as follows:

**Table 5 Option I Mars Flight 5 Manifest (from the Databook for the 90-Day Study on Human Exploration of the Moon and Mars)**

| | |
|---|---|
| Cargo Mars Excursion Vehicle (MEV-P) | 32.30 MT |
| MEV-C Propellant | 45.70 |
| Cargo Mars Transfer Vehicle (MTV-P) | 48.50 |
| MTV-C Propellant | 393.60 |
| | |
| Mars Surface Water Pilot Plant | 8.05 |
| Spares (unspecified) | 5.00 |
| Margin | 86.90 |
| **IMLEO** | **620.10 MT** |

The MTV-C fires and releases its spent TMI stage ($\Delta V$ = 4250 m/s), placing it on a 182-day transfer trajectory. Just prior to the Mars encounter, the MTV and MEV separate and aerobrake in the manner described in Flight 3. In the case of cargo flights, the MTV and MEV are both excursion vehicles; the two descend and unload a water production facility and spare materials, remaining on the Martian surface.

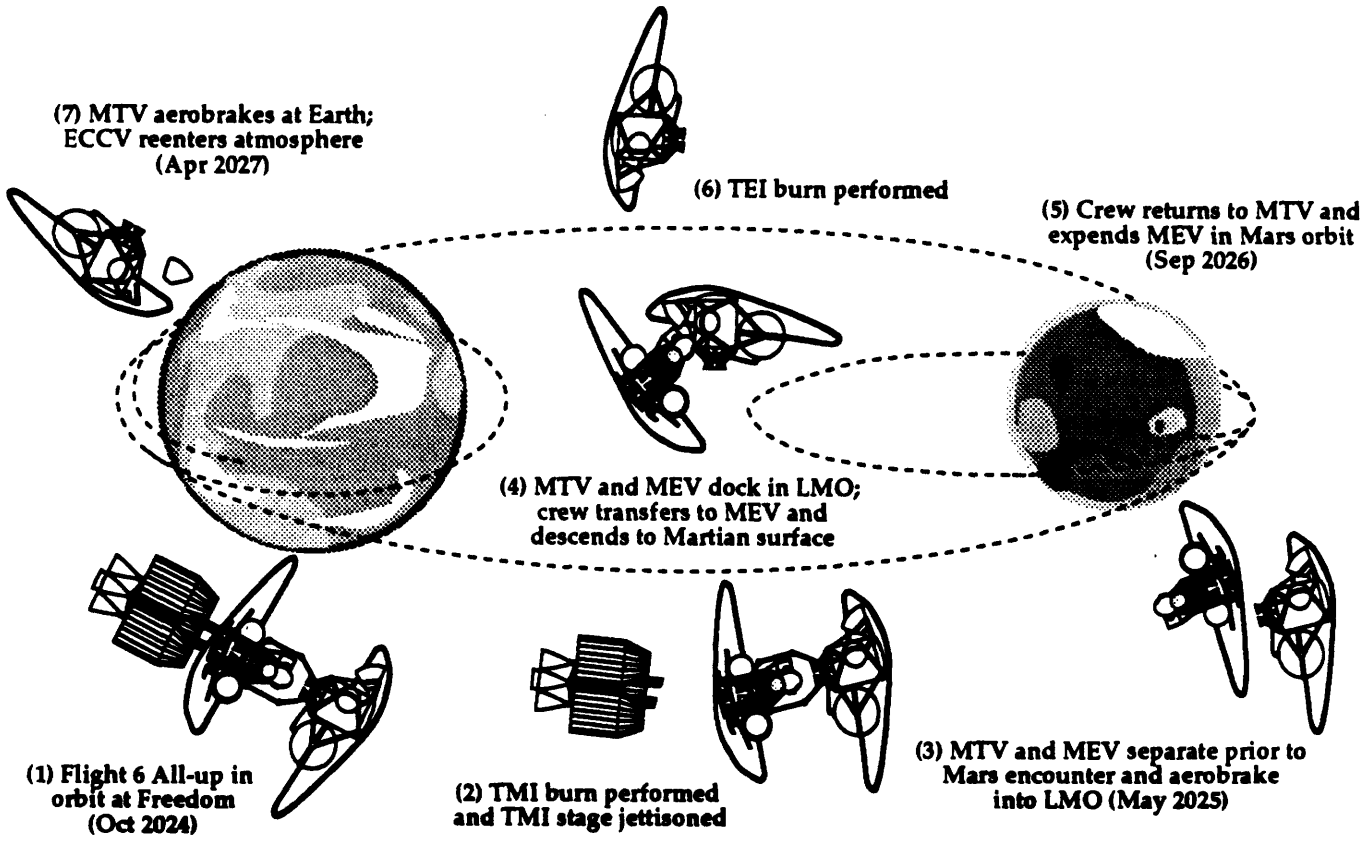


**Figure 11 Option I Mars Flight 6 [NASA, 1989]**

The table below (Table 6) illustrates the mission events of Option I's Flight 6, the final piloted mission explicitly described in the 90-Day Study (Fig. 11).[7]

**Table 6 Option I Flight 6 Mission Event List (derived from the Databook for the 90-Day Study)**

| *Mission Event* | *Total Vehicle Mass* (MT) | *Change in Mass* (MT) | *Delta-V* (m/s) |
|---|---|---|---|
| IMLEO | **678.70** | | |
| Pre-injection preparation propellant | 649.41 | 29.29 | 0 |
| Trans-Mars injection propellant | 260.62 | 388.79 | 4250 |
| Jettison TMI stage | 205.62 | 55.00 | |
| Jettison Earth-Mars consumables | 201.82 | 3.80 | |
| Trans-Mars coast propellant | 198.00 | 3.82 | 90 |
| Mars orbit insertion propellant | 197.29 | 0.71 | 17 |
| Mars orbit operations propellant | 193.56 | 3.73 | 90 |
| Deploy payloads/jettison aerobrake | 186.96 | 6.60 | |
| Mars payload to Mars surface | 116.06 | 70.90 | |
| Mars orbit consumables | 116.06 | 0.00 | |
| Trans-Earth injection propellant | 82.22 | 33.84 | 1625 |
| Jettison TEI stage | 71.82 | 10.40 | |
| Mars-Earth consumables | 68.02 | 3.80 | |
| Trans-Earth coast propellant | 66.58 | 1.44 | 101 |
| Earth orbit operations propellant | 64.68 | 1.89 | 136 |
| Mars-Earth aerobrake | 43.98 | 20.70 | |
| Final LTV-C mass in LEO | 43.98 | | |
| | | | |
| Mars payload total mass | **70.90** | | |
| Pre-deorbit preparation propellant | 70.90 | 0.00 | |
| Mars descent propellant | 52.61 | 18.29 | 1360 |
| Mars payload (dry) | 46.54 | 6.07 | |
| Mars surface science | 46.54 | 0.00 | |
| Mars surface consumables | 37.21 | 9.33 | |
| MEV-P ascent stage prior to ascent | **37.21** | | |
| MEV-P ascent propellant | 10.50 | 26.70 | 5763 |
| Crew | 10.50 | 0.00 | |
| MEV-P final mass | **10.50** | | |

### 1.1.4 Transfer and Excursion Vehicle design

To achieve the aims of Options I and V, the 90-day study team sketched out designs for four spacecraft that would be the focus of all transport, manned or unmanned, to the moon and Mars (Fig.'s 12, 13). These vehicles are the orbital transfer and excursion vehicles mentioned in a.iii; they are constructed on-orbit--at Freedom--and their key characteristics are described in the tables below.

---

[7] There is in fact a Flight 7 obliquely mentioned in the Databook, to be launched in 2026, but it is neither given a manifest nor is it referred to in the 90-Day Study itself.

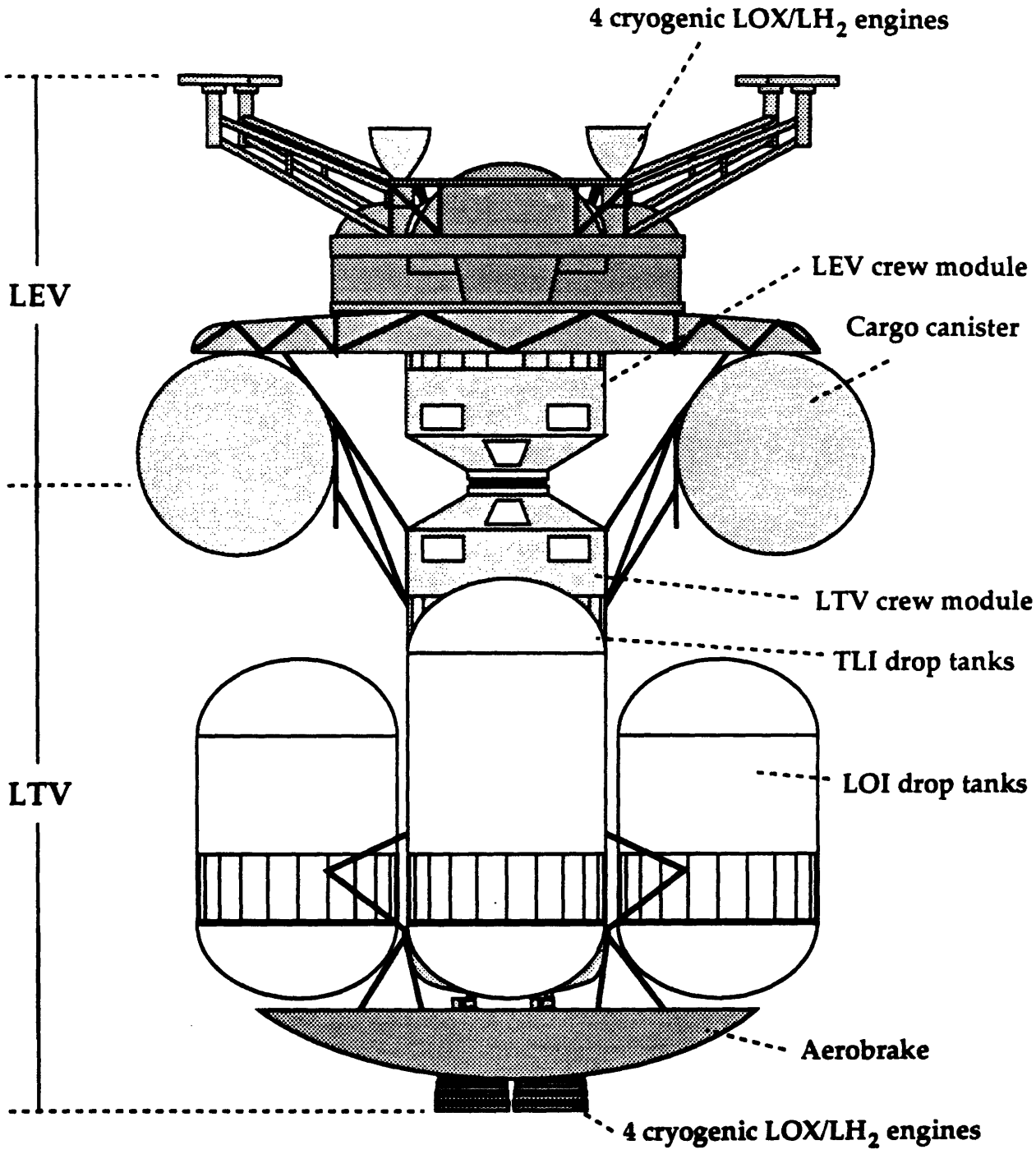


**Figure 12 Paired Lunar Transfer Vehicle (LTV) and Lunar Excursion Vehicle (LEV) [NASA, 1989]**

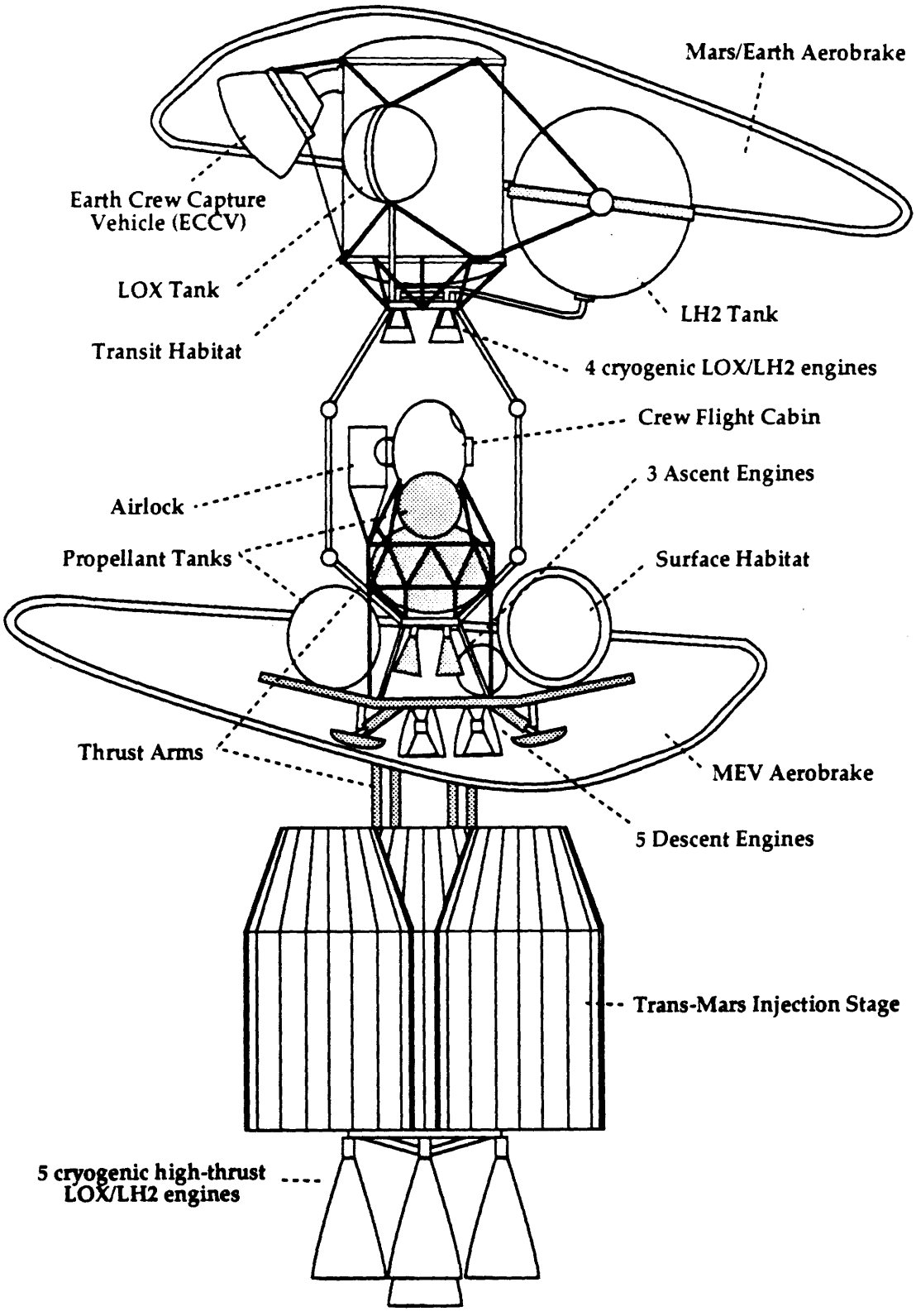


**Figure 13 Paired Mars Transfer Vehicle (MTV) and Mars Excursion Vehicle (MEV) [NASA, 1989]**

The first LTV-C's (cargo vehicles) would be expendable, with the first returning to Freedom for inspection. Later LTV's would return to LEO and be based there for reuse. The personnel

**Table 7 Lunar Transfer Vehicle (LTV)**

| | |
|---|---|
| Dimensions | 15.2 m x 14.4 m (aerobrake diameter = 13.7 m) |
| Mass | LTV core (8.1 MT)<br>core module propellant load (6.4 MT)<br>LTV tanks (5.8 MT)<br>LTV tank propellant load (129.8 MT)<br>crew module (7.6 MT) |
| Power | solar arrays; batteries or fuel cells |
| Propulsion | 4 cryogenic LOX-$LH_2$ engines ($I_{sp}$ = 481 s, thrust = 89 kN, total thrust = 356 kN) |
| Aerobrake | reusable for 5 missions; composite structure |
| Crew module | supports four crew for 4 days on translunar segment; 7 days for return to Freedom |
| Artificial gravity | none |
| Radiation protection | water-filled shielding |

vehicles are essentially the same as the the cargo carriers, outside of the addition of a crew module. The crew would work in a zero-gravity environment during their transfer from LEO to the lunar surface and would be protected against possible solar flares by water-filled radiation shielding. All versions are 1-1/2 stage vehicles which rely on both their cryogenic engines and an aerobrake for maneuvering between the Earth and moon. The LOX-$LH_2$ engines provide slightly higher specific impulse than that currently found in the Space Shuttle Main Engine (SSME). From the 90-day study:

> "Lunar transfer vehicle engines were selected on the basis of vehicle thrust-to-weight, number of engines, throttle range, and man-rating. The need for man-rating with multiple engines for engine-out capability, the desire for a common engine, and the excursion vehicle touchdown 'g' limit with a throttling requirement of less than 20:1 resulted in the selection of four engines at 89 kilonewtons."[8]

The lunar excursion vehicle's two variants, the LEV-C and LEV-P, are designed to transport four personnel and/or various cargo from LLO to the lunar surface and return. Like their transfer vehicle counterparts, later models would be based on the lunar surface for reuse, while the earliest craft would be expended on the moon. The total payload delivered to the lunar surface by a single excursion vehicle would be 15 MT (LEV-P) or 33 MT (LEV-C). The excursion vehicle's propulsion system is identical in design to that of the transfer vehicle--the

---

[8] 90-Day Study, p. 3-18

**Table 8 Lunar Excursion Vehicle (LEV)**

| | |
|---|---|
| Dimensions | 11.3 m x 8.5 m |
| Mass | LTV core (5.6 MT)<br>propellant load (23 MT)<br>crew module (3.6 MT) |
| Power | 4 O-$H_2$ fuel cells |
| Propulsion | 4 cryogenic LOX-$LH_2$ engines ($I_{sp}$ = 465 s,thrust = 89 kN, total thrust = 356 kN) |
| Aerobrake | none |
| Crew module | supports four crew for 4 days on translunar segment (2 days on descent, 2 days on ascent) |
| Artificial gravity | none |
| Radiation protection | none |
| Guidance and navigation | astronauts involved in docking of LEV/LTV; separate radar systems for docking and landing |

difference in specific impulse between the two systems is due to the greater expansion ratio achieved by the transfer vehicle's nozzles. Other common systems (LEV/LTV) include the reaction control system, avionics and software, and communications.[9]

The reusable LEV's will be based on the lunar surface, necessitating propellant storage for relatively long periods of time (up to 30 days) before use. For longer stays, "it will require surface support..."[10] The vehicle's crew module will allow up to four days of habitation, for use principally in 'initial surface operations' and preparation for return to Earth. There is no protection provided against solar radiation.

Propellant reserves for both the LEV and LTV were computed assuming a 2% overall reserve and allowing for the following variations in $\Delta V$: (1) 200 m/s during TLI; (2) 100 m/s during LOI; and (3) 100 m/s during TEI. Hardware weight design margins were determined based on the technological level of the subsystem--a figure of 5% was used for 'existing or slightly modified hardware,' 10-15% for new designs based on current technology, and 15-25% on 'new designs using advanced technologies.'[11]

The Mars vehicle, again of two forms, MTV-C and MTV-P, is expendable after use and is intended to move cargo and crew from LEO to Mars and back. Like the other vehicles, it is

---

[9] ibid., p. 3-20

[10] ibid., p. 3-21

[11] Databook, Section 5.2.1.1

constructed on-orbit. The TMI stage, which is composed of five high-thrust engines and up to three additional propellant tanks, is jettisoned after use; the remaining core module continues on to Mars.

**Table 9 Mars Transfer Vehicle (MTV)**

| | |
|---|---|
| Dimensions | 58 m x 21.1 m (aerobrake diameter = 30 m) |
| Mass | TMI stage (539 MT)<br>aerobrake (20.7 MT)<br>crew module (41 MT)<br>crew capture vehicle (7.5 MT)<br>TEI stage (84.5 MT) |
| Power | solar arrays and battery storage |
| Propulsion | TMI stage: 5 cryogenic LOX-$LH_2$ engines ($I_{sp}$ = 475 s, thrust = 890 kN, total thrust = 4450 kN)<br>TEI stage: 4 cryogenic LOX-LH2 engines (Isp = 481 s, thrust = 89 kN, total thrust = 356 kN) |
| Aerobrake | composite structure; used at both Mars and Earth |
| Crew module | supports four crew for 500+ days |
| Artificial gravity | none |
| Radiation protection | storm shelter |

The MTV separates from its companion MEV at Mars encounter, upon which both aerobrake through the atmosphere and dock in orbit above the planet. The aerobrakes used are the same; the MTV aerobrake would be used again after TEI and encounter at Earth. The TEI engines are those designed for the LTV and preserve commonality among propulsion systems; they deliver one-tenth the thrust of the TMI engines. For long missions such as those analyzed in the 90-Day Study, power can be generated only by solar or nuclear systems--in this case, solar arrays are used to provide electrical power to the transfer crew module. Life support is designed to recycle water and oxygen.[12]

The MEV-C and MEV-P transfer materials and personnel from Mars orbit to the planetary surface, and return the personnel and any outgoing cargo to the MTV after the end of a Martian expedition. The MEV can transport 25 MT of payload to the surface of Mars. The MEV crew module is similar to that designed for the LEV, although it is capable of supporting the four crew members aboard for thirty days, in case of difficulties in starting up the Martian habitat.

---

[12] ibid., Section 5.2.2

**Table 10 Mars Excursion Vehicle (MEV)**

| | |
|---|---|
| Dimensions | 22.5 m x 14.3 m (aerobrake diameter = 30 m) |
| Mass | ascent vehicle (28.4 MT)<br>aerobrake (9.3 MT)<br>descent stage (17.8 MT)<br>surface payload (25 MT) |
| Power | solar arrays for surface deployment, fuel cells |
| Propulsion | descent stage: 5 cryogenic LOX-$LH_2$ engines ($I_{sp}$ = 465 s, thrust = 89 kN, total thrust = 445 kN)<br>ascent stage: 3 cryogenic LOX-$LH_2$ engines (Isp = 465 s, thrust = 89 kN, total thrust = 267 kN) |
| Aerobrake | design identical to MTV aerobrake; provides aeromaneuver capability |
| Crew module | supports four crew for 30 days |
| Artificial gravity | none |
| Radiation protection | none |

On departure, the ascent stage separates from the main MEV, using three cryogenic engines (again, based on the LEV design).[13]

### 1.1.5 Earth-To-Orbit (ETO) Vehicle design

Options I and V use existing expendable launch vehicles for their precursor missions to both the moon and Mars. For the large amounts of payload that will be lofted into orbit to support the outposts on the moon and Mars, the 90-Day Study proposed several alternatives. The first of these is Shuttle-C, an unmanned version of the STS; a much larger STS-derived vehicle would be used for Mars missions. Several National Transportation System (NTS) vehicles, the product of a joint NASA-DoD venture formerly titled ALS (Advanced Launch System), are offered as an option (after 1999) to continuing use of the STS systems. The Shuttle itself would also be used, although in a greatly reduced role.

Shuttle-C, and a derivative design that incorporates a slightly larger payload shroud to accommodate outsize payloads (e.g. aerobrake sections), would be used for Earth-to-orbit in support of lunar missions (Fig. 14). Shuttle-C's capacity is 71 MT, with an envelope of 4.6 m diameter x 25m length. The outsize design would allow only 61 MT, but an envelope of 7.6 m x 27.4 m. Shuttle-C's propulsion is similar that of the current Shuttle: core propulsion is composed of three Space Shuttle Main Engines (SSME's; $I_{sp}$ = 455 s, total sea-level thrust = 4950 kN, LOX-$LH_2$) firing concurrently with two solid rocket boosters (SRB's; $I_{sp}$ = 250 s.,

---

[13] ibid.

total thrust = 23760 kN, ammonium perchlorate/aluminum). As with the the original STS, Shuttle-C is a 1-1/2 stage vehicle.

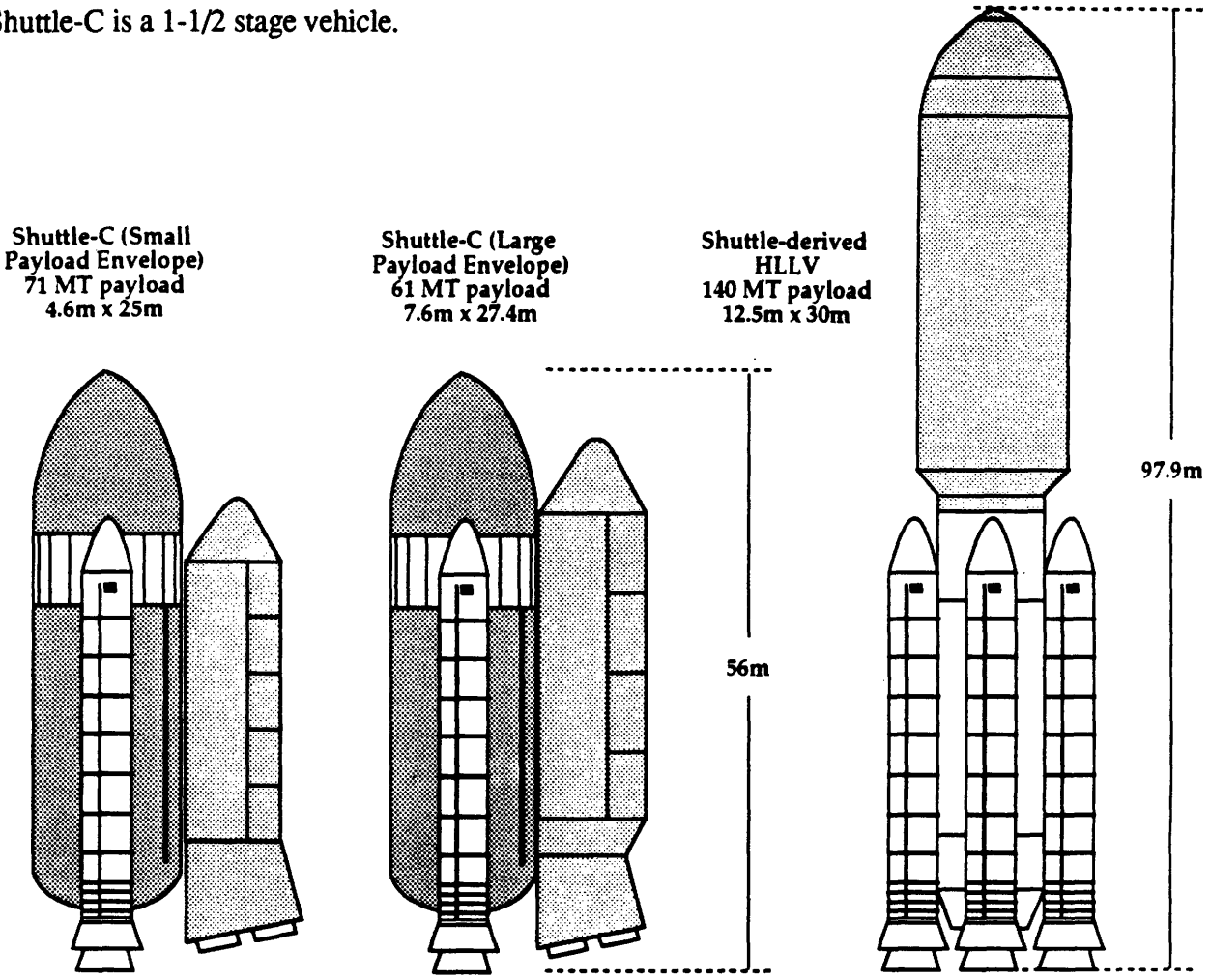


**Figure 14 STS-Derived Launch Vehicles [NASA, 1989]**

For Mars support, an STS-derived heavy-lift launch vehicle would allow ETO transport of a 140 MT payload to Freedom's orbit (407 km, 28.5° inclination). The payload shroud would be 12.5 m x 30 m. This HLLV would use four SRB's and a core system of four or five SSME's; the core propulsion and avionics would be reusable.

NTS options (Fig. 15) allow fewer ETO flights; the stated objective of NTS is to provide "low cost per flight, high reliability, and high operability."[14] The reference design consists of a booster vehicle and core stage, both powered by LOX-$LH_2$ engines (six in the booster and three in the core vehicle), with a payload capacity of 52.3 MT. The designs considered for the 90-

[14] 90-Day Study, p. 5-6

Day Study would involve the addition of a second booster for the lunar program (allowing a net payload of 98.2 MT and a payload envelope of 10 m diameter x 30 m length) and a third booster for the Mars portion of the mission (net payload = 140 MT, envelope of 12.5 m x 30 m). A transfer stage would be required to circularize the payload at Freedom's altitude.

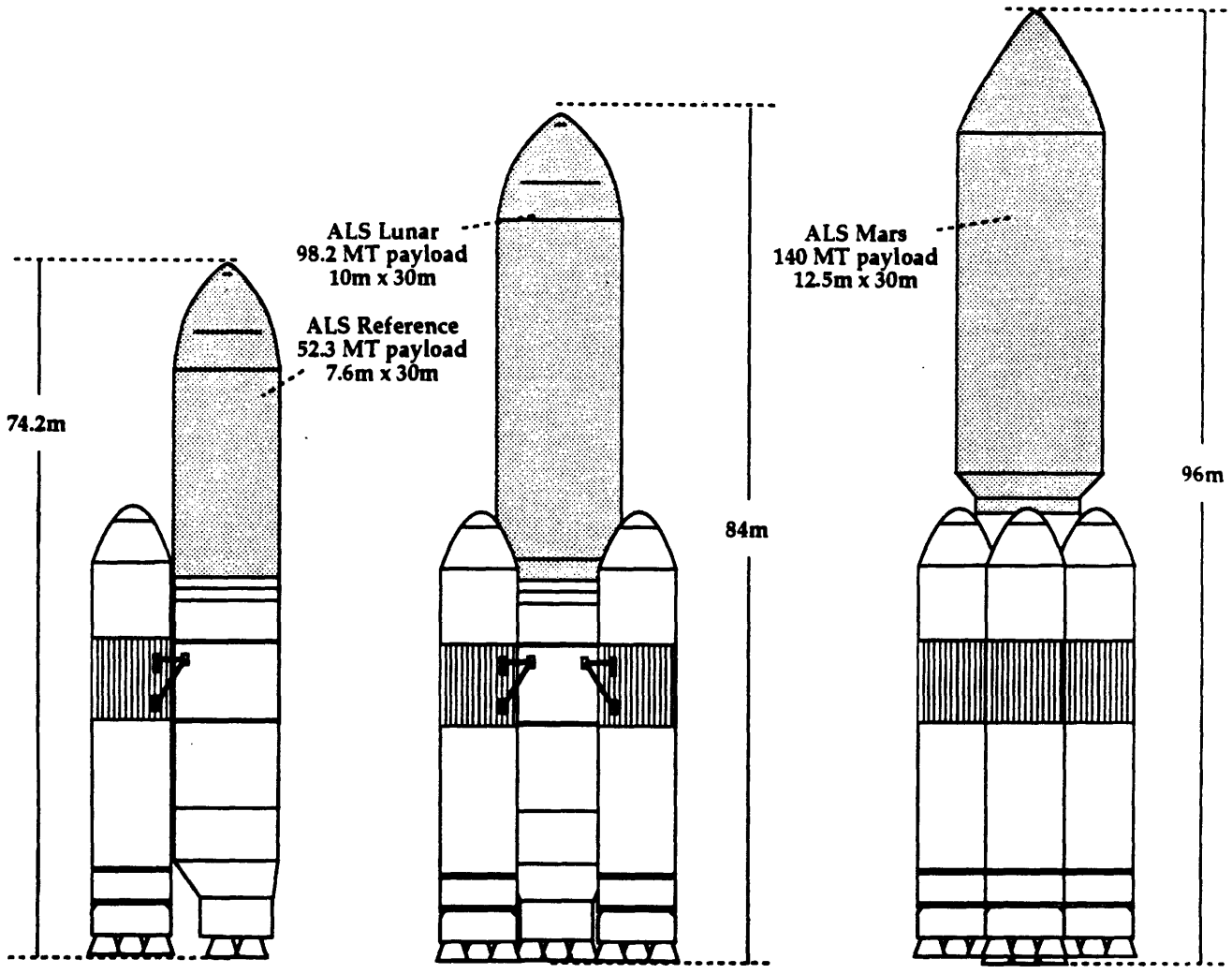


**Figure 15 NTS-Derived Launch Vehicles [NASA, 1989]**

## 1.2 Propulsion and Astrodynamics

Orbital transfer between the Earth and the moon or Mars require significant expenditures of energy to accomplish changes in velocity on the order of 1000 -10000 m/s. Launching payloads into LEO typically requires upwards of 7700 m/s (this value can be derived directly from the equation for circular orbit velocity at Freedom's altitude); accounting for gravity and drag losses could bring this figure as high as 9200 m/s. Faster transfers to the moon and Mars.

which will be discussed later in this study, may result in $\Delta V$ figures in the tens of thousands of meters per second. These high velocity changes result in the burning of large quantities of propellant, as illustrated by the rocket equation:

$$\frac{m_f}{m_o} = e^{\left[\frac{\Delta v}{g I_{sp}}\right]} \tag{1}$$

Here, $m_f/m_o$ is the amount of spacecraft mass at burnout ($m_f$) relative to the initial mass $m_o$. This is the reciprocal of what is usually defined as the 'mass ratio,'.

Specific impulse ($I_{sp}$) itself is a function primarily of the square root of the expelled propellant's temperature (a function of $T_o$) divided by its molecular weight (M). The governing equation (in vacuum) is:

$$I_{sp} = \sqrt{\left(\frac{2\gamma}{\gamma - 1}\right)\left(\frac{RT_o}{g^2 M}\right)} \tag{2}$$

R here is the universal gas constant (8.314 J/mol°K), $\gamma$ is the ratio of specific heats, and g is the gravitational acceleration at the Earth's surface. g is added to the definition of specific impulse to give it a value in seconds, allowing it to be a figure of merit in both the English and SI systems of measurement. Specific impulse can be thought of as the amount of impulse delivered per unit mass of propellant, or 'kick' per kilogram. The benefits derived from an increased $I_{sp}$, then, drive the designer to higher temperatures and lower molecular weights. Tested nuclear thermal designs, such as the pioneering NERVA reactors of the 1960's and early 70's, used diatomic hydrogen ($H_2$) as the working fluid, achieving exhaust temperatures as high as 2500 K and specific impulses above 800 s. Obviously, $H_2$ (with only the exception of dissociated H) provides the smallest molecular weight of any possible propellant. The challenge is to develop a propulsion method that heats it to the high temperatures necessary to achieve large values of $I_{sp}$.

Thrust and thrust-to-weight ratio (T/W) are also prominent figures of merit in the analysis of lunar and Mars missions. Since thrust and T/W dictate vehicle acceleration, they will have a direct impact on the impulsive nature of the boost phases (TMI, TEI, TLI burns). Vehicle maneuvers of the type found in the 90-Day Study are generally treated as if they were instantaneous--for high thrust-to-weight this usually results in a high degree of agreement between the actual $\Delta V$ figures and the predicted values for impulsive burns. However, for lower-thrust vehicles (NTP to some extent, and electric propulsion methods in particular), the gravity losses incurred could require a substantial amount of extra propellant, growing larger as the mission's impulsive $\Delta V$ increases. (For example, the Mars transfer analysis in Chapter 3.0 is based on algorithms that assume a direct escape from Space Station Freedom's orbit at 407 km x 407 km; in fact, a three-impulse escape would be performed in order to minimize

gravitational losses and prevent additional propellant consumption; this is explained further in Section 1.2.2)

## 1.2.1 Lunar Trajectories

Lunar transits (Fig. 16) are detailed in Section 1.1.3.1. Some of the difficulties associated with long-term travel to the Mars will obviously not present difficulties on translunar flights. Permanent deterioration of human bone in zero-g will not take on the degree of significance that it has achieved in discussions of the Mars mission, due to the relatively short transfer time; likewise, cosmic radiation will also not be a factor during the transfer (although it will during lengthy stays on the lunar surface). The trip time is already reasonably short, especially by comparison to the much longer and more costly Mars flights, and there is little present advantage to decreasing it. More important is increasing the ratio of lunar payload mass to total mass delivered to LEO--this will be the focus of lunar studies in Chapter 3.0 of this paper.

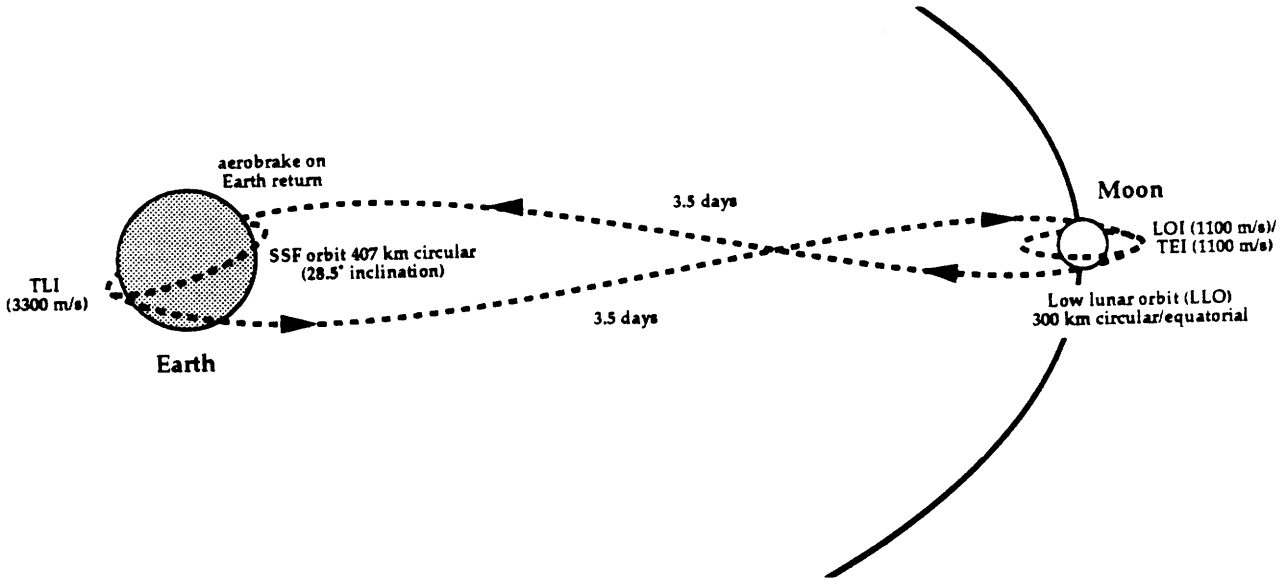


**Figure 16 Aspects of the generic lunar transfer**

## 1.2.2 Mars Trajectories[16]

90-Day Study Mars round-trips typically last 500-1000 days. They will begin, as did lunar missions, at Space Station Freedom's 407 km x 407 km circular parking orbit. A three-impulse sequence is used to achieve trans-Mars injection: (1) the orbital apogee is raised from 407 km to 142500 km; (2) the perigee is lowered from 407 to 185 km; and (3) the injection impulse is

---

[16] Fast Round-Trip Mars Trajectories, Sam Wilson, NASA LBJ Space Flight Center, 1990

applied at perigee to place the spacecraft on its way to encounter at Mars. This approach is used to minimize penalty ΔV's for non-impulsive burns within the gravitational influence of a major body (e.g. Earth, Mars). For near-minimum-energy transfers, the apogee-raising burn is the largest impulse of the three, at 2937 m/s. The second (apogee) burn is extremely small (~7 m/s), while the third burn's value can be calculated from:

$$\Delta v = \sqrt{\frac{2\mu}{r} + v_\infty^2} - \sqrt{\mu\left(\frac{2}{r} - \frac{1}{a}\right)} \qquad (3)$$

Here, ΔV is the difference between the injection velocity, represented by the first radical, and the perigee velocity at the 185 x 142500 km orbit. Physically, the quantity $2\mu/r$ represents the energy of an escape orbit for a given r, while the v-infinity term represents energy over escape; v-infinity is the velocity of the vehicle at infinite separation from the center of mass. The second radical is a variation of the simple vis-viva equation and gives the velocity of the transfer vehicle prior to the impulsive burn at perigee. A 5000 m/s impulsive burn (implying a v-infinity of 6500 m/s) performed in one step is thus almost exactly equal to the three-impulse burn (2937 m/s, 7 m/s, 2033 m/s). Thus, there is no "ΔV" savings; however, *each burn is smaller and limits the gravity losses associated with finite burn times.*

At Mars, the spacecraft is captured into a 250 km x 34000 km elliptical parking orbit. Planetary operations commence, and following the return of crew and/or cargo to the transfer vehicle, the vessel circularizes its orbit at 34000 km to allow optimal insertion into a trans-Earth

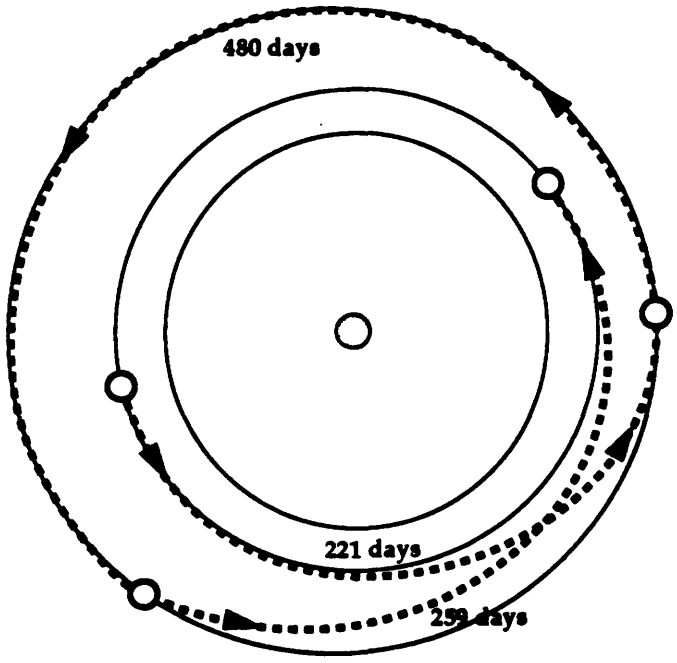


**Figure 17 2007 960-Day Conjunction-Class Mission [Wilson, 1990]**

trajectory. The periapse altitude is dropped once again to 250 km, and the TEI burn performed. On encounter at Earth, the vehicle aerocaptures into a 185 km x 142500 km orbit, whereupon (in the case of a piloted MTV) the crew can return immediately to the surface in the ECCV.

The two classes of trajectories considered in the 90-Day Study were the conjunction-class and opposition-class missions. A conjunction-class mission (sometimes referred to as a double-Hohmann, Fig. 17) are distinguished by the fact that a conjunction of the Earth and Mars occurs near the midpoint of the round-trip; those of the opposition-class (Fig. 18) are similarly distinguished by the single opposition (Earth and Mars) that occurs at some point during the mission.

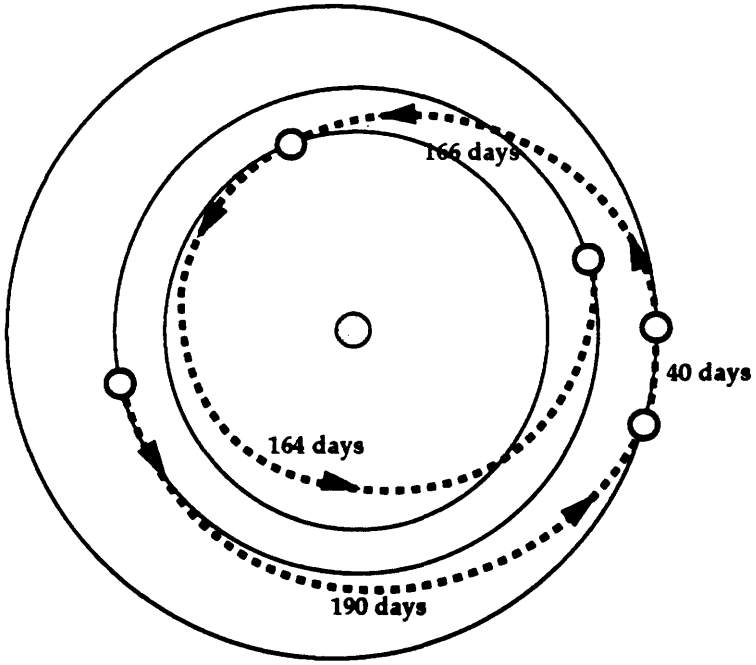


**Figure 18 2007 560-Day Opposition-Class Mission [Wilson, 1990]**

These orbits can be further classified as Type I or II, depending upon whether the transfer angle traversed by the vehicle is less or greater than 180° (the transfer angle is simply the angle between the departure planet at time of departure and the encounter planet at the time of arrival, with the sun at vertex). Assuming circular, coplanar orbits for the Earth and Mars, the minimum $\Delta V$ would be achieved by cotangential impulsive firings, once for TMI, the second for Mars orbit insertion. These firings would take place 258 days and 180° apart, and would incur the lowest propulsive mass penalty of any powered maneuver. However, Mars' orbit is not circular but is reasonably eccentric (e=.093), allowing Mars to range between 1.395 and 1.665 AU (132 to 173 million km) in its distance from the Sun. In addition, a true Hohmann transfer of the type just described is made impossible by virtue of the fact that Mars is inclined 1.85° to the ecliptic (Fig. 19). Since these orbits are calculated using a two-body model

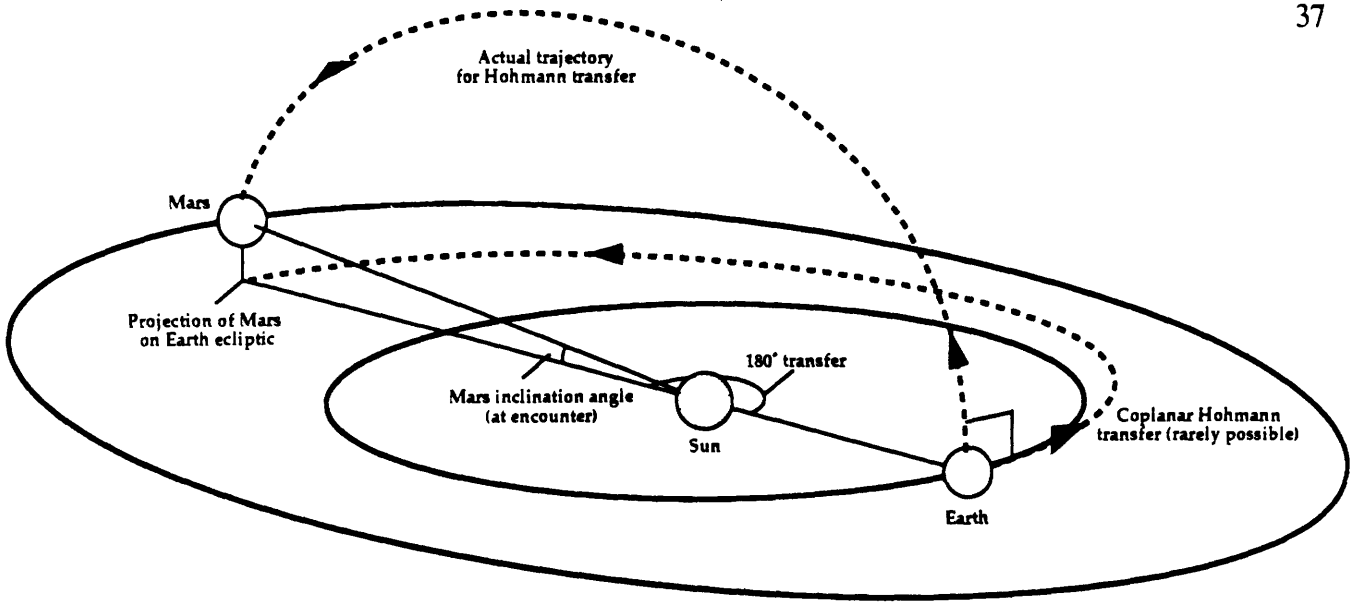


**Figure 19 Hohmann Transfer**

**Table 11 Key Characteristics of Conjunction- and Opposition-Class Missions (from Fast Round-Trip Mars Trajectories)**

| Characteristic | Conjunction Missions | Opposition Missions |
|---|---|---|
| Geometry | (1) intersection of outgoing and incoming transfer orbits; (2) the near-symmetry about a line drawn through the sun and that intersection; and (3) bounding of both trajectories by the orbits of Earth and Mars | (1) Short Mars stop; (2) asymmetry of transfer arcs; and (3) passage inside the orbit of Venus |
| Transfer Time | near-Hohmann transfer (~258 d.) used for both legs minimizes total $\Delta V$; total mission time of ~1000 d. | 450-600 days (in 90-Day Study); can be much shorter |
| Venus Swingby | not possible | reduces total $\Delta V$ but is difficult to coordinate synodic periods of Venus and Mars |
| Variations | relatively small from year to year | wide variations with a cyclic period of 16 years |

(spacecraft and sun), neglecting the masses of planets, any trajectory within the system will be sun-centered--which will require that the transfer orbit be inclined at a large angle to the ecliptic in order to intercept Mars at the trajectory's apohelion.[17] For a Hohmann transfer, this

[17] Of course, it is possible to achieve a 'perfect' Hohmann transfer twice every Martian year (687 d.), when Mars crosses the plane of the ecliptic. This would clearly curtail launch opportunities, however, since there is little likelihood that the Earth would oblige us by being in position during the exceedingly short windows available.

inclination must be 90°, demanding an immense ΔV (~40 km/sec) and consequent expenditure of fuel. The large inclination change ΔV requirement drops off drastically as the transfer angle moves away from 180°. For this reason, near-Hohmann transfers and not pure Hohmann transfers are used--moving the planetary encounter by only a few degrees reduces the firing angle and thus the plane change Δv.

The eccentricity of Mars also affects what would otherwise be regular opportunities to journey to Mars. The synodic period of Mars, defined as the time between successive oppositions or conjunctions of Mars, is 780 days; this would seem to suggest that launch windows would reoccur on the order of every two years. However, Mars' eccentricity causes a 16-year cycle of variation in launch windows. S. Wilson notes in Fast Round-Trip Mars Trajectories, "the requirement for short missions is near the 16-year minimum in 2003, and near the maximum in 2009."[18]

Option I Flights 1 and 2 are both opposition-class missions with total trip times of 565 and 490 days, respectively. They require Venus swingbys (VSB) early in the trans-Mars segment (150-170 days) to reduce the total ΔV but do so at the expense of increasing transit time. Option V Flights 1-3 are also opposition class with trip times comparable to those of Option I.

**Table 12 Mars Missions, Options I and V (derived from the Databook for the 90-Day Study)***

| Mission | Type | Mission dates | Stay Time | Trip Time | delta-V (m/s) |
|---|---|---|---|---|---|
| Option I -1 | Opposition (VSB) | May 2015-Dec 2016 | 30 d | 565 d | 6617 |
| -2 | Opposition (VSB) | Mar 2017-Jul 2018 | 30 d | 490 d | 6419 |
| -3 | Conjunction | Jun 2018-Nov 2020 | 659 d | 894 d | 6103 |
| -4 | Conjunction | Aug 2020-Jan 2023 | 621 d | 903 d | 6159 |
| -5 | Conjunction | Sep 2022-Mar 2025 | 526 d | 917 d | 5513 |
| -6 | Conjunction | Oct 2024-Apr 2027 | 484 d | 927 d | 5091 |
| Option V -1 | Opposition (VSB) | May 2015-Dec 2016 | 30 d | 564 d | 6616 |
| -2 | Opposition (VSB) | Mar 2017-Aug 2018 | 60 d | 520 d | 7022 |
| -3 | Opposition (VSB) | Aug 2021-Aug 2023 | 90 d | 723 d | 8441 |
| -4 | Conjunction | Oct 2024-Apr 2027 | 484 d | 927 d | 5091 |
| -5 | Conjunction | Nov 2026-Jun 2029 | 474 d | 932 d | 4689 |

*piloted missions in boldface

Option I's Flights 3-6 and Option V's Flights 4 and 5 are all conjunction-class with trip times in excess of 890 days. They allow long stay times on the Martian surface and typically have small ΔV requirements. Option I's Flights 2 and 5 (also, Option V's Flight 4) are cargo missions and

[18] Mars Trajectories, p. 511

do not return to Earth; however, they were analyzed assuming a return flight and could be used in such a manner if necessary (for instance, if a piloted flight were to be postponed). Table 12 Δv data is based on the computed impulsive burn with no margin included.

While the missions proposed by the 90-Day Study minimize total propulsive ΔV through the use of conjunction-class near-Hohmann transfers and aerobraking at Mars and Earth, at the expense of very long trip times, shorter missions with higher ΔV totals are plausible and within the range of current technology (both NTP and otherwise). They may, in fact, prove to be necessary if other methods of preventing long-duration mission difficulties cannot be found. The effect of these shorter missions on the NASA baseline will be addressed in Section 3.0.

### 1.2.3. Evaluation of the 90-Day Study Architecture

This evaluation will only consider the impact of the Architecture's propulsion decisions--it will not address issues that fall outside the scope of the study. The 90-Day Study relies on a cryogenic LOX-$LH_2$ system to perform all major propulsive burns--the specific impulse of these engines will fall in the 465-481 s. range and will require large propellant expenditures in order to achieve mass requirements in Mars orbit. The comparatively low technical risk of developing such an engine is at least partially offset by the difficulty of storing cryogenic propellants for a year or more before use. The architecture, in an attempt to achieve the lowest possible Δv figures, requires the development of aerobrake technology to take the place of propulsive capture at Mars and Earth, and at Earth on the return journey from the moon. These aerobrakes tend to have mass fractions approaching .10. Aerobraking places firm restrictions on EOI and MOI Δv (with entry velocity ceilings of 12.5 km/s. and 9.5 km/s., respectively) due to material limitations imposed by atmospheric heating of the brake. In addition, the use of cryogenic propulsion drove the 90-Day designers to consider minimum-energy trajectories entailing generally long total mission times. When possible, Venus swingbys (VSB) were utilized, saving Δv but raising transfer times. All opposition-class missions (30-90 day stay times) examined by Options I and V used either an inbound- or outbound-VSB. The conjunction-class missions (stays in excess of 450 days) incurred lower Δv at the expense of extremely long total trips. The shortest transfers of the 90-Day Study were found in Option I's Flight 3, with a 100-day outbound and a 135-day inbound transit. However, this was by far the most optimistic mission: No opposition mission required less than 460 days en route, while Option V's Flight 3 requires 633 days of travel.

**1.2.3.1 Aerobraking:** The largest prospective benefit of a low-$I_{sp}$ cryogenic engine, namely its low technical risk, is compromised by the difficulties associated with the proposed aerobrake, technology which has not yet been tested (although the Aeroassist Flight

Experiment, AFE, is still scheduled to be launched in May 1994). The lack of a comprehensive database on Mars' atmospheric composition introduces serious uncertainties into what form atmospheric variations may take during aerocapture. This will require extensive control capability of the brake itself--and since the ability to control the brake is heavily dependent on the vehicle's center-of-mass, careful placement of various subsystems as well as a pre-capture inventory will be required to assure that all items are properly stowed. The prospect of dust storms on the planet at a mission's arrival, where particulate matter can be lofted far higher than in Earth's atmosphere (above 50 km) raises the possibility of dangerous erosion of the brake and an increase in brake mass to forestall this contingency. While initial studies[19] seem to indicate that the increase is 'modest,' perhaps 8.7% of the total brake mass (given an aerobraked vehicle mass of 6 mT, much lower than could be expected in a manned Mars mission), estimation of the critical parameters, such as dust particle size and required braking altitude, can still only be considered preliminary without further investigation of the Martian atmosphere. Global dust storms are believed to occur over approximately 10% of every Martian year, while local atmospheric disturbances raise the probability of encounter with a dust storm to 50%[20]. Finally, there is a question as to what form aerocapture loads will take and what effect they may have on the MTV and/or MEV structure. Mission failure due to aerocapture may not be catastrophic (in the form of burnup on entry) but may force an abort due to insufficient braking force applied to slow the vehicle into an elliptical capture orbit. Any backup to the aerobrake would necessarily be in the form of a propulsive system--which begs the question, in a mission where success relies so heavily on the performance of a single component, as to why a brake should be baselined. An all-propulsive system would be composed of an engine cluster, of which only a fraction of the engines would be required to fire upon orbital insertion.

**1.2.3.2 Earth-To-Orbit Delivery and On-Orbit Assembly:** The 90-Day Study Options require 187 launches (I) and 115 launches (V), respectively. The NASA 90-Day Study mentions, "Approximately 75% of the mass delivered to LEO is lunar transfer vehicle propellant."[21] Higher-$I_{sp}$ alternatives might reduce this mass. Likewise, much of the MTV mass is propellant for the TMI burn.

---

[19] Aerobraking in a Dusty Martian Atmosphere, p.1, P. Papadopolous, AIAA 90-1700, 1990

[20] ibid.

[21] 90-Day Study, p. 5-3

No existing launch system (or, for that matter, any of the proposed systems in the 90-Day Study) are capable of launching all-up missions that could depart for Mars or the moon immediately upon insertion into LEO. The mass and dimensional requirements for the lunar mission, never lower than 92 mT (Option I) and generally much higher (as high as 197 mT), are usually above even the Mars HLLV's payload delivery of 140 mT. Even when the mass requirements for a mission are under HLLV ceilings, the assembled payloads are outsize and would not fit within the payload shroud. The Mars vehicles are far too large to be transferred to LEO in anything but constructible sections. Nuclear thermal propulsion offers the possibility of reducing the propellant necessary to propel the vehicle to Mars and thus the number of launch vehicles required to assemble a vehicle in LEO. This reduction in total launch-to-orbit missions would increase reliability--needing a smaller number of successful launches in sequence to construct the MTV/MEV system--and ease construction difficulties. If two ETO missions could put the necessary Mars mission equipment in LEO (as opposed to the five to seven launches planned in the 90-Day Study), the amount of human EVA and/or teleoperation would be reduced significantly, with a corresponding decrease in risk to the astronauts.

Since lengthy on-orbit construction implies the need for a 'transportation node,' such as the converted Space Station Freedom in the 90-Day Study, a decline in the number of assemblies might allow the architecture to discard Freedom as a necessary stop on the way to Mars. In turn, this would simplify the modifications made to Freedom's design in the Study in order to prepare it for SEI missions. Lunar missions might still require an LEO staging base, as the LEV was designed to be reusable and based in LEO. Direct reentry of the crew via an ECCV-style capsule would necessitate delivery of separate capsules on every subsequent manned mission.

**1.2.3.3 Effect of Lengthy Missions:** The effect of long missions on crew members is a second and more important issue. The biomedical problems of extended travel in interplanetary space fall into:

(1) Microgravity exposure and its effects on various parts of the body,

(2) Increased cancer risk, as well as increased risk of death from solar particle events,

(3) Increased probability of medical emergencies and crew behavior problems,

(4) The necessity for closed-cycle life support to minimize mass requirements.

Clearly, onboard hardware, as well as sensitive Mars payloads, would not be immune from failure over long periods of use (or disuse).

Microgravity results in changes to the human cardiovascular system, neurovestibular effects, and (perhaps most alarmingly) the breakdown of bone and muscle tissue, some of which may not be reversible. The heart muscle has a tendency to shrink, while it has been

mentioned[22] that blood pressure regulation in the human body may be damaged after long exposure to zero-g--damage that is only partially reversible. Neurovestibular effects include sensory perception conflicts between visual, tactile, and inner-ear signals. (This results in the common short-term 'space-sickness' problems.) Whether the human body eventually adapts to such conflicts is still an open question, and bears directly on the crew's ability to perform under such adverse conditions. Finally, bone and muscle deconditioning poses what may be the most serious difficulty. Skylab results[23] indicate that 160 to 170 mg of calcium was lost in crew members' urine per day throughout the course of their missions (the longest of which lasted 84 days). There does not seem to be any grounds to believe that such calcium loss will decrease as mission time extends--as evidenced by Soviet missions. This calcium loss is important not only because it results in a greater probability of bone fracture but also because (1) increased urinary calcium could lead to renal stone formation, and (2) bone fractures tend to heal improperly when the bone involved is not loaded. W. DeCampli notes: "It is well-known that, if you unload a lower extremity bone after tibial/fibular fracture, it will not heal. In fact, it can reach a point where it becomes what we call a 'non-union' fracture. And that requires an operation before an astronaut can walk."[24] Artificial gravity, achievable by spinning the transfer vehicle or crew area, may be a possible countermeasure. Another suggestion is the prescription of drugs to mitigate these effects. Muscle deconditioning, less serious than bone demineralization, could be slowed by exercise, as was done aboard Skylab and the Soviet space stations. Neuromuscular stimulation and the donning of special pressurized suits has been offered as a possible alternative to long periods of intense exercise.

Radiation in the form of galactic cosmic rays (GCR), normally shielded by the Earth's atmosphere, will shower a Mars transfer vehicle for the entire duration of the mission. GCR will be accompanied by even more dangerous solar flare and solar particle events (SPEs). These events are rare and short-lived (on the order of 30-100 minutes)[25] , yet they can result in large radiation dosages delivered to the MTV crew. The National Council on Radiation

---

[22] Medical Problems Associated with Long-Duration Space Flights, pp. 202-203, W. DeCampli, in The Human Quest in Space (24th Goddard Memorial Symposium), AAS Science and Technology Series, Vol. 65, 1987

[23] ibid., p. 206

[24] ibid., p. 210

[25] Radiation Hazards in Low Earth Orbit, Polar Orbit, Geosynchronous Orbit, and Deep Space, p. 74, P. McCormack, in Working in Orbit and Beyond: The Challenges of Space Medicine, AAS Science and Technology Series, Vol. 72, 1989

Protection (NCRP) provides a career limit for absorbed radiation (Table 13). The dose equivalent, measured in REM (Radiation Equivalent Man) is the product of the actual radiation dose, measured in rads, and the Radiation Biological Effectiveness (RBE, which is dependent upon the amount of energy deposited in living matter by a given form of radiation).

**Table 13 NCRP Career Limit Radiation Exposure in rem (from Radiation Hazards)**

| Lifetime Excess Risk of Fatal Cancer | Age at First Exposure (yrs.) | 25 | 35 | 45 | 55 |
|---|---|---|---|---|---|
| | Men | 150 | 250 | 325 | 400 |
| 3% | Women | 100 | 175 | 250 | 300 |

The NCRP limit is based on a 3% excess risk of fatal cancer incurred by the dose received for a specific age group and gender. P. McCormack notes:

> "Such a lifetime risk is comparable to the risks in occupations such as construction and agriculture, but is greater than for terrestrial radiation-exposed workers. A 3% lifetime excess risk of death from cancer seems reasonable."[26]

For a given shielding depth of 2.5 g/cm$^2$ of aluminum, the yearly dose in interplanetary space form GCR would be approximately 47 rem. For 633 days in transit, the crew would suffer an absorbed dose of 82 rem. The yearly dose limit set by NCRP is 50 rem/year--so that the 90-Day Study comes very close to exceeding the recommended safety standards even with 'storm shelters' aboard its transfer vehicles. SPEs and solar flares could add significantly to the accumulated dose, even with thick shielding (on the order of 70 g/cm$^2$), since secondary radiation during the particle event would be far and away the greatest contributor to total dose. McCormack notes that, with shielding as stated, a worst-case particle event (based on a 1972 flare) would produce an accumulated dose of 2.2 rem--but that the buildup of secondary particles would inflict an additional 236 rem on the astronauts, far above the safe limit.[27] On long missions, especially during the active phase of the solar cycle, there is great incentive to reduce the mission duration (or at least the transfer duration) and prevent this clear threat to astronaut health.

---

[26] ibid., p. 61

[27] ibid., p. 74

SPEs (and GCR to a much lesser extent) could deliver significant doses to sensitive instrumentation such as integrated circuits, which may require radiation hardening or be susceptible to failure. Shorter missions would reduce the likelihood of an SPE and the subsequent failures in electronic systems associated with operation in an high radiation environment.

The NASA study intends to use closed-cycle (regenerative) life support for lunar and Mars habitats, as well as the Mars Transfer Vehicles. To date, only open-loop systems have been used--A Mars mission with an open-loop system would require large quantities of breathable air, food, and water. One estimate from Smylie and Reumont's "Life-Support Systems" in Manned Spacecraft Systems has a mass requirement of 23.3 lbm (10.6 kg) of $O_2$, water for drinking and washing, and food. If the system could be closed and food produced on board, the total weight of the vehicle could be reduced. The 90-Day Study assumes the possibility of developing such systems, yet they entail substantial problems--nutrient requirements in space are not yet well understood, while complete closure could result in a toxic environment. Bioregenerative cycles are currently being researched, but there is little hard data available on the realizability of such systems.

Other long-term issues involve the probability of medical emergencies occurring during the mission. Surgery aboard ship would be difficult and dangerous, with little in the way of surplus medical supplies and a high chance of infection (with contaminants such as urine, fecal matter, and hair permeating the cabin). Crew behavioral problems could arise during lengthy trips due to the lack of privacy, social and physical isolation, and perhaps simple disagreements among members.[28]

The hazards associated with the 90-Day Study's lengthy missions, combined with the use of such a questionably effective technology as aerobraking, argue for a careful consideration of alternatives to the cryo/aerobrake baseline before eliminating them--The 90-Day Study's cursory inspection of these other propulsion methods was not sufficient to draw the conclusions necessary to do so. Two of the more realizable techniques include nuclear thermal and nuclear electric propulsion--nuclear electric systems will not be examined here because they are low-thrust devices incapable of shortening transfer times between Mars and Earth (although they are certainly capable of reducing the IMLEO of cargo missions, especially for nonperishable

---

[28] Consideration for Solar System Exploration: A System to Mars, pp. 107-108, A. Nicogossian and V. Garshnek, in Working in Orbit and Beyond: The Challenges for Space Medicine

supplies, such as habitat structures or power plants). Nuclear thermal systems, such as those discussed in the next section, have been researched for decades.

## 2.0 NTP ENGINE DESIGN

Nuclear thermal propulsion is not a new idea; it has been in existence since the concept of nuclear fission was first put into practice. 1955 saw the inception of Project Rover, an effort to develop a solid-core nuclear rocket with diatomic hydrogen as the working fluid. With the possibility of specific impulses near 1000 s. and moderate thrust-to-weight (T/W ~ 5), the nuclear rocket was seen as a serious alternative for upper-stage Earth-to-orbit use, and later as a concept for both Mars missions and (in the 1980's) LEO-GEO transfers. NERVA (Nuclear Engine for Rocket Vehicle Application) designs were constructed and tested until the program's termination in 1973 due to budgetary considerations; NASA concentrated on the development of a Space Transportation System (STS), which culminated in the present Space Shuttle. Nevertheless, The Rover-NERVA project was a success--the NERVA small engine, which could have fit within the cargo bay of the shuttle, produced a thrust of 72 kN (T/W = 2.88) at an $I_{sp}$ of 875 s. No actual flight test had been performed by the time NERVA was canceled.

Other fission-based concepts would keep the solid core (PBR, NERVA and NERVA derivatives) or allow it to melt (gas-core rockets); hydrogen would still be the primary propellant. The PBR (particle-bed reactor) has not been tested as a unit, but would theoretically provide higher T/W and $I_{sp}$ than their NERVA counterparts. Advanced designs, such as the open- and closed-cycle gas-core engines, have not been given serious consideration but deserve further study since their benefits (specific impulses in the thousands of seconds, thrust values on the par of NERVA) could allow greatly reduced trip times or greatly increased payload ratios for interplanetary travel. All fission-based concepts suffer from high neutron and gamma-ray fluxes, potentially deadly to crew and destructive to sensitive cargo; shielding is thus a primary requirement for all NTP methods and may well constitute a significant fraction of the total propulsive system mass. This study will not consider any form of fusion-based reactor, primarily due to the fact that these engines are unlikely to be ready by the 2000-2015 time frame (not to mention their predicted mass, on the order of a thousand mT).

### 2.1 Design Approach

The two main drivers behind designing a nuclear thermal rocket are (1) significantly higher $I_{sp}$ at (2) thrust levels high enough to keep gravity losses relatively low. Current high-$I_{sp}$ chemical propulsion relies on a chemical reaction between liquid oxygen and liquid hydrogen to heat the resulting propellant mixture to high temperatures (typically above 3000°K). This effluent is expanded through a nozzle and provides specific impulses at the 460 s. level. Engine thrust-to-weight levels are generally very high, in the range of 50. The NASA 90-Day Study presumes the development of excursion vehicle engines with an $I_{sp}$ of 481 s.; 500 s. is

frequently taken to be the limit for improvement of cryogenic chemical engines.[29] Yet, since the specific impulse directly affects the amount of payload that can be placed on Mars or the moon for a given $\Delta V$ (Eq. 1), there is great incentive to increase $I_{sp}$ and thus payload (or, for a given payload deposited at Mars or moon, decrease total trip time). Some proven technologies, such as electrothermal engines (arcjets, resistojets), could give specific impulses as high as 2000 s., while electrostatic ion engines promise perhaps 25000 s. This large increase in $I_{sp}$ is almost completely negated by such engines' exceedingly low thrust-to-weight, ranging between $10^{-5}$ to $10^{-2}$.[30] Such low thrust levels will require very long burn times--on the order of the total transfer time, with interplanetary trajectories tending to consist of ever-widening spirals out of one gravitational well, a heliocentric transfer (similar to that found for high-thrust trajectories), and a tightening spiral into the encounter planet's gravitational well. The non-impulsive nature of low-thrust burns is such that, while total $\Delta v$ is increased, propellant consumption is low enough (due to the engine's high $I_{sp}$) to offset it.

The nuclear thermal rocket can be thought of as a compromise between these very high-$I_{sp}$/very low thrust alternatives and the common chemical rocket engine, although it certainly shares more in common with the chemical engine than the electric vehicles. The parameters of the nuclear thermal engine can be analyzed in a manner similar to that used to examine the performance of a chemical system; the model to be used assumes (1) the working fluid to be a perfect gas of constant composition, (2) the heating of the propellant be approximated by a isobaric model, and (3) the expansion to be steady, one-dimensional, and isentropic.[31] The nuclear thermal rocket's $I_{sp}$, given the conditions of this model, can be determined from the previously stated Eq. 2:

$$I_{sp} = \sqrt{\left(\frac{2\gamma}{\gamma - 1}\right)\left(\frac{RT_o}{g^2 M}\right)} \qquad (4)$$

This ideal specific impulse is usually not determined directly from thrust chamber conditions but from the quotient of the effective exhaust velocity $u_e$, and g, the gravitational acceleration at Earth's surface:

---

[29] Exotic chemical options, such as the use of metastable (H as opposed to $H_2$) or tripropellants, may extend this range somewhat, but do not hold out any hope for $I_{sp}$ figures in the range promised by solid-core NTP.

[30] Rocket Propulsion Elements: An Introduction to the Engineering of Rockets, p. 31, G. Sutton, Wiley-Interscience, 1986

[31] Mechanics and Thermodynamics of Propulsion, pp. 356-7, Hill & Peterson, Addison-Wesley, 1970

$$u_e = \sqrt{\left(\frac{2\gamma}{\gamma - 1}\right)\left(\frac{RT_o}{M}\right)} \tag{5}$$

This exhaust velocity is the velocity of the propellant upon exit from the nozzle of the propulsion system; it is dependent not only on the properties of the thrust chamber itself (propellant $\gamma$, M, $T_O$), but also on the construction of the nozzle and ambient conditions outside the vehicle. The equations above assume perfect expansion to vacuum (i.e. ambient pressure = 0). The exhaust velocity $u_e$ can be defined as the product of two terms, c* and $c^T$ ($u_e = c^* c^T$).

$$c^* = \sqrt{\frac{\left(\frac{\gamma + 1}{2}\right)^{\left(\frac{\gamma+1}{\gamma-1}\right)}}{\gamma}\left(\frac{RT_o}{M}\right)} \tag{6}$$

This quantity, the characteristic velocity, is a function of only the chamber conditions, dependent as it is on the ratio of specific heats $\gamma$, the universal gas constant R, chamber temperature $T_O$, and the molecular weight of the propellant species M. The characteristic velocity c* of the engine can also be described by:

$$c^* = \frac{P_o A^*}{\dot{m}} \tag{7}$$

Here, $P_O$ is the engine's chamber pressure, A* is the nozzle throat area, and $\dot{m}$ is the mass flow rate of the propellant.

The coefficient of thrust, $c^T$, is dependent somewhat on chamber conditions but mostly upon ambient conditions and nozzle properties. The thrust coefficient is defined as:

$$c^T = \sqrt{\frac{2\gamma^2\left(\frac{\gamma + 1}{2}\right)^{\left(\frac{\gamma+1}{\gamma-1}\right)}}{\gamma - 1}\left(1 - \left(\frac{P_e}{P_o}\right)^{\left(\frac{\gamma-1}{\gamma}\right)}\right)} + \left(\frac{P_e - P_a}{P_o}\right)\left(\frac{A_e}{A^*}\right) \tag{8}$$

The variables not previously defined in prior equations are: $P_e$, the nozzle exit pressure; $P_a$, the ambient (outside) pressure; and $A_e$, the exit area of the nozzle. For the purposes of calculating $I_{sp}$ and exhaust velocity based on an engine's operating conditions, perfect expansion to vacuum was assumed--this sends both the ratio of exit pressure to chamber pressure and the ratio of (exit pressure - ambient pressure) to chamber pressure to zero, simplifying the basic equation for $c^T$:

$$c^{T}_{ideal} = \sqrt{\frac{2\gamma^2\left(\frac{\gamma+1}{2}\right)^{\left(\frac{\gamma+1}{\gamma-1}\right)}}{\gamma-1}} \tag{9}$$

This approximation seems quite reasonable in light of the fact that these engines will be used primarily for orbit transfer (and thus in vacuum) and will be designed to have large expansion ratios and thus large nozzle area ratios. Finally, the assumption of constant g holds true for many cases, since for solid-core rockets, the chamber is not sufficiently hot (although it is almost hot enough) to dissociate diatomic hydrogen, while for gas-core rockets (where such dissociation is a goal, since the decrease in molecular weight by half is a substantial benefit) the design imperative would be to prevent recombination of H into $H_2$ inside the rocket nozzle and prevent the accompanying drop in $I_{sp}$.

The other important parameter is thrust (T), measured in newtons (N) or kilonewtons (kN). As mentioned previously, the chemical engine may develop very high thrust, in the range of thousands of kN and with an effective T/W ratio of 50. Thrust is defined as:

$$T = \dot{m}u_e \tag{10}$$

Combined with the definition of c*, specific impulse and thrust can be related through the equation

$$I_{sp} = \frac{c^* c^T}{g} = \frac{T}{\dot{m}g,} \tag{11}$$

and the engine's 'jet power', **P**, measured in watts (W) or in this report primarily as megawatts (MW), can then be defined as:

$$P = \frac{1}{2}\dot{m}u_e^2 = \frac{1}{2}Tu_e \tag{12}$$

One optimistic estimate for the upper bound on solid-core NTP chamber temperature is given by the designers of the particle-bed reactor concept.[32] They suggest that 3500 K is achievable with a particular PBR design; since this engine would use hydrogen as the propellant, it is simple to calculate the engine's ideal specific impulse. Hydrogen has an exceedingly high constant-pressure specific heat (14209 J/kg °K) and (obviously) the lowest molecular weight of

---

[32] Particle-Bed Reactor Propulsion Vehicle Performance and Characteristics as an Orbital Transfer Rocket, p. 375, from Space Nuclear Power Systems, Powell et. al, Brookhaven National Laboratory, 1986

any element (.002 kg/mol).[33] The value for specific impulse is calculated to be 1018 s., and constitutes a plausible upper limit on solid-core nuclear rockets, given reasonable advances in materials technology.

With the 3500 K temperature above, and *assuming no dissociation of the fluid*, it can be seen how various other propellants provide significantly degraded performance in comparison to hydrogen:

**Table 14 $I_{sp}$ Variation among Propellant Types (no dissociation; $T_0$ = 3500 K)**

| Propellant Type | Molecular Weight (kg/mol) | $C_p$ (J/kg K) | Ideal $I_{sp}$ (s.) |
|---|---|---|---|
| $H_2$ | .002 | 14209 | **1018** |
| He | .004 | 5193 | **615** |
| $CH_4$ | .016 | 2254 | **405** |
| $CO_2$ | .044 | 842 | **248** |

Methane ($CH_4$) has a molecular weight only eight times greater than hydrogen but a specific heat nearly seven times less. Its $I_{sp}$ is lower than what could be achieved by contemporary chemical engines--even if it dissociates, the achievable $I_{sp}$ is only raised to around 671 s.,[34] a definite improvement over cryogenic chemical rockets but not substantially greater than what could be accomplished by exotic tripropellant combinations, were it determined that they were achievable. Similarly, carbon dioxide has been suggested as an indigenous propellant extractable from the Martian atmosphere for use in a NERVA-derivative engine. With total dissociation at 3500 K, the maximum attainable specific impulse would only be 381 s.[35] This appears to argue against the use of $CO_2$ on the grounds that the propellant mass saved by consuming materials produced in situ might not make up for the initial investment in engine research and development necessary to produce a working solid-core propulsion system, especially when combined with the mass of the indigenous propellant extraction system. Another question that arises in the use of indigenous Martian $CO_2$ is that of vastly increased engine corrosion in the presence of dissociated oxygen at high temperature. Therefore, most

---

[33] Dissociated hydrogen offers the advantage of higher Cp (20910 J/kg °K) and lower molecular weight (.001 kg/mol).

[34] Nuclear Thermal Rockets Using Indigenous Martian Propellants, R. Zubrin, Martin Marietta Astronautics, 1989

[35] ibid.

work in the field has been concentrated on producing a nuclear thermal rocket that would use hydrogen as its primary propellant. Nevertheless, this issue will be readdressed in Chapter 3.0.

## 2.2 NTP Engine Options

Fission-based NTP engines are divided neatly into two camps: solid-core reactors (SCR), which would have operating temperatures in the 3000 K range and specific impulses ≤1000 s., and gas-core reactors (GCR), with operating temperatures as high as $10^5$ K and $I_{sp}$ values ranging up to perhaps 7000 s. (These last are almost entirely theoretical designs) Liquid-core or 'colloidal' reactors, the obvious intermediate design, are generally lumped in with the rotating particle bed reactor, which will be described in Section 2.2.1.2. Table 14 illustrates three SCR and three GCR engine types that will be analyzed in Section 3.0. The Cermet NERVA derivative is based on the NERVA design and is discussed in 2.2.1.1. The Open-Cycle and Light-Bulb reactors are detailed in 2.2.2.

**Table 15 Engine Designs Considered in Analysis**

| Engine | Thrust (kN) | Isp (s.) | Power (MW) | T/W | type |
|---|---|---|---|---|---|
| NERVA | 330 | 825 | 1575 | 3.1 | SCR |
| Cermet NDR | 132 | 927 | 600 | 5.7 | SCR |
| FPBR | 68 | 900 | 300 | 7.7 - 45 | SCR |
| Open Cycle (1) | 220 | 5000 | 7500 | 0.18 | GCR |
| Open Cycle (2) | 1760 | 1800 | 22000 | 1.4 | GCR |
| Light Bulb | 405 | 1870 | 4600 | 1.3 | GCR |

### 2.2.1 Solid-Core Reactors (SCR)

The solid-core reactor relies on the fission of uranium ($U^{233}$ or $U^{235}$) and the 200 MeV (200 x $10^6$ electron volts) of energy released per fission event to heat a gaseous propellant stream to high temperatures in much the same way that Earth-based nuclear reactors heat a fluid (e.g. light water, liquid metals) to generate electricity. Whereas the Earth-based reactors run fluids through a closed-cycle pumping system, a space-based propulsion reactor is of necessity an open-cycle, releasing the hot propellant to provide thrust. Solid-core reactors have intrinsic design limits based on high-temperature material strength; much of the work in these engines has gone into increasing the amount of thermal energy transferred to the propellant without overstressing the structure of the system.

In the reactors discussed, fission is accomplished by 'thermalized' neutrons, particles having energies in the .025 eV range (rather, those neutrons that have interacted with the surrounding medium enough to slow them to 'thermal' speeds). Faster neutrons, with energies as high as

15 MeV, will usually not interact with materials within the reactor and are therefore counted as 'leakage'. When the thermal neutrons are captured by a large fuel nucleus such as $U^{233}$, the nucleus generally fissions into two roughly equal fragments and several neutrons, in addition to prompt $\gamma$-rays. Secondary neutrinos, electrons ($\beta$-rays) and $\gamma$-rays are released as the fission fragments decay into simpler elements. The bulk of the heat generated is left with the fission fragments (168 MeV out of the 200 MeV available), which transfer their thermal energy to the surrounding fuel; fragments tend not to travel far after a fission incident. Of the neutrons produced, enough are captured by nearby nuclei to continue the fission chain reaction; the rest are lost to capture or leakage outside the fuel elements.

The main components of a fission reactor for any application are the (1) fuel, (2) cladding, (3) moderator, (4) reflector, (5) coolant, and (6) shielding. The fuel is $U^{233}$ or $U^{235}$: Provided there is a critical mass of the fuel in the reactor, an ongoing chain reaction may be maintained. This critical mass will vary from isotope to isotope and from reactor design to design. The cladding, which is the structural support, fission fragment containment, and corrosion preventive for the fuel loading, is quite unlike that found in ground-based power reactors. In fact, there is no true 'clad,' for the fuel material in some space reactors (e.g. NERVA) is distributed throughout the moderating graphite.

The moderator is generally a block of material surrounding the fuel elements. Its purpose is simply to slow fast neutrons produced by fission (since they may have energies in the MeV range). Preferred moderating material is dense and of low molecular weight, since neutrons are capable of transferring a sizeable portion of their energy to these molecules,[36] essentially stopping them in their tracks so that they remain in the vicinity of the fuel and contribute to the fission process. Ground-based reactors tend to the use of heavy water ($D_2O$), water, and, more recently, graphite (in high-temperature gas-cooled reactor prototypes, similar in design to space-based reactors).

The reflector's purpose is to 'reflect' neutrons not thermalized by the moderator back into the core, where they may interact with the fuel there. In the vicinity of the reflector are generally found the control drums, which rotate to control the reactivity of the core, and may also be used to 'scram,' or quickly shut down, the engine. Constructed from both neutron-reflecting material (BeO, or possibly graphite--the material is also a capable moderator) and an effective neutron absorber (boron carbide, $B_4C$, is one), the drums can dampen reactivity by exposing

---

[36] Nuclear Reactor Analysis, pp. 28-29, A.F. Henry, MIT Press, 1986

the $B_4C$ sections of the drums to the core and increase the reactor's fission rate by exposing the BeO.

In a space-based propulsion reactor, the coolant performs double duty as propellant. A coolant should ideally have a high heat capacity so as to engender a high amount of thermal energy transfer to the fluid. Hydrogen possesses far and away the highest heat capacity and, as previously mentioned, is also clearly superior as a propellant. However, hydrogen is difficult to work with at high temperatures due to its propensity for chemical reaction with many materials, making such non-reactive gases as helium more attractive. In addition, liquid hydrogen is very light (~70 $kg/m^3$), necessitating more structure for tankage than, say, the equivalent mass of liquid oxygen. Investigations by the National Aerospace Plane (NASP) program into slush hydrogen may reveal methods for reducing this structure.

Shielding, an issue dealt with in ground reactors by adding meters of steel-reinforced concrete, is far more difficult in space, where mass is at a premium. $\alpha$- and $\beta$-rays are easily stopped by thin shields, and are not determining factors in shield type; the main problems are high-energy neutrons and $\gamma$-rays, which can traverse several centimeters of tungsten or lead virtually undiminished in intensity. This leads, given the possibility of nuclear-propelled manned missions, to very thick shields (and/or large separation distances between sensitive portions of the cargo/crew area and the engine cluster) and constraints on extravehicular activity outside a definite 'safety cone' while the reactor is in operation. $\gamma$-rays are attenuated only through the use of high-density, high-atomic weight materials (lead, uranium, and tungsten being possible candidates). Neutron attenuation is provided by low-molecular weight, low-density materials such as lithium hydride. The hydrogen nuclei act as effective moderators, slowing down the neutrons so that they may be absorbed by $Li^6$. It is also possible to use the hydrogen stored in propellant tanks as a further means of reducing neutron fluence.

#### 2.2.1.1 ROVER/NERVA/Cermet

As mentioned in the beginning of this section, Project ROVER was begun during the 1950's to develop a high-specific impulse, moderate thrust-to-weight nuclear thermal engine. In the NERVA program, the core was comprised of 1100 fuel elements. These elements were constructed from "coated uranium carbide particles dispersed in a graphite matrix....Each element contained 19 coated coolant channels."[37] $LH_2$ flowed from the propellant tank through the turbopump and into a nozzle cooling jacket. The hydrogen was heated in the jacket and

---

[37] Nuclear Propulsion--A Vital Technology for the Exploration of Mars and the Planets Beyond, NASA Technical Memorandum, S. Borowski, 1987

continues through (1) the beryllium reflector , (2) the radiation shield, and (3) into the core itself. After being heated to nearly 2500 K at a pressure of 30 atm, the propellant entered the nozzle and was blasted out of the rear of the engine. There was tendency in earlier NERVA designs for the hydrogen to combine with the graphite and erode the channel walls; designers partially succeeded in fixing this problem by coating the channels with tantalum, niobium, and zirconium carbides. 3% of the hydrogen was diverted from the main flow and mixed with cold hydrogen to provide fluid for the turbine inlet necessary to turn the pump. The turbine exhaust was released at lower temperature, driving down the engine's overall $I_{sp}$ by a small percentage. Assuming that the turbine exhaust to be released at 0 $I_{sp}$ would drive the engine's specific impulse down by only 3%, or about 25 s. This cycle was dubbed 'hot-bleed' (Fig. 20), and has since been reexamined in the design of NERVA derivatives (NDRs)--with the turbine exhaust reentering the core and exiting with the main propellant flow (this variant is known as the 'full flow-topping cycle').

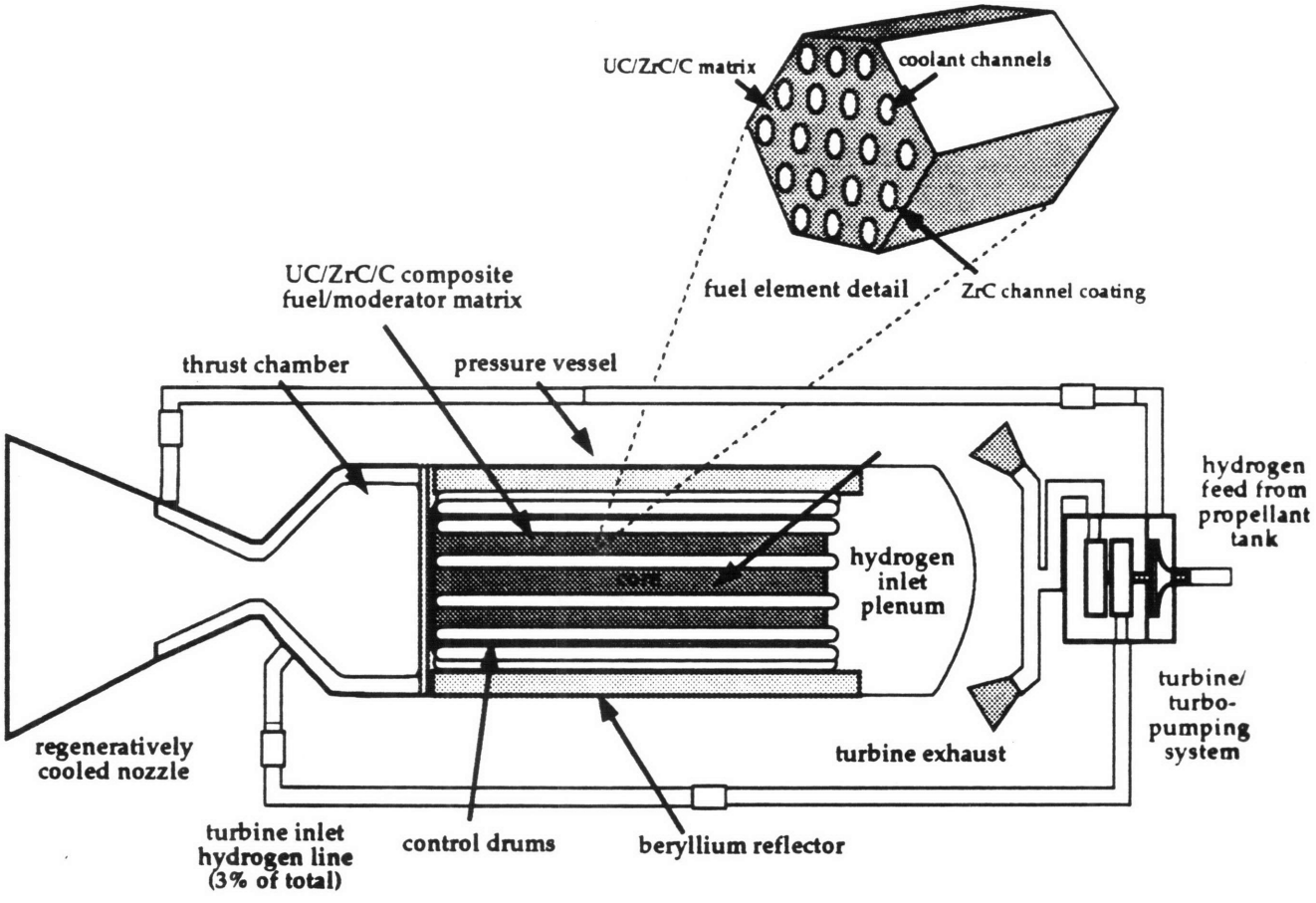


**Figure 20 NERVA engine (hot bleed cycle)**

NERVA requirements allowed for a ramp-up to full-power in approximately 30 s., with a cooldown period after shutdown to allow reactor decay heat to escape. Early mission plans to use NERVA engines for a lunar shuttle vehicle, described by J. Altseimer in his "Operating Characteristics and Requirements for the NERVA Flight Engine," would require 6% of the total propellant mass to be used during the cooldown phase. The level of decay power necessitated that hydrogen continue to flow through the core even after shutdown, lowering NERVA's effective specific impulse (since the flow would occur at lower than nominal chamber temperature) to the 400-500 s. range. This problem was circumvented to some degree by using the cooldown propellant to provide a portion of the maneuvering $\Delta V$. These cooldown periods, in the specific example of the nuclear lunar shuttle, might last on the order of ten hours or more

The NERVA flight engine was expected to provide 330 kN of thrust at an $I_{sp}$ of 825 s and a power level of 1575 MW. The engine mass was expected to be ~11000 kg without the addition of an external shield necessary to man-rate the vehicle (The shield would have raised the engine mass to 15000 kg). Without a shield, the NERVA design could have a thrust-to-weight ratio of ~3.1.[38]

Cermet reactors, which use a fuel design different from that in NERVA, have also been given recent consideration for use in thermal propulsion. These engines have been advocated by Argonne National Laboratory and General Electric as a candidate for nuclear propulsion missions. The fissile material is uranium dioxide ($UO_2$) embedded in a tungsten-rhenium matrix. The coolant channels are likewise coated with tungsten. This allowed the cermet designers to circumvent NERVA's greatest problem, the erosion of the graphite blocks by hydrogen propellant. The cermet reactor was projected to weigh 1880 kg with a thermal power of 600 MW, thrust of 132 kN and, from:

$$P = \frac{1}{2}\dot{m}u_e^2 = \frac{1}{2}Tu_e \tag{13}$$

an exhaust velocity of 9000 m/s ($I_{sp}$ ~ 927 s.). Assuming 500 kg of pumping system raises the total non-shielded mass to 2380 kg and gives a T/W of 5.66. The cermet reactor would suffer from the same problems as NERVA (slow transient response at startup and shutdown) and would have pumping systems and a nozzle with requirements 'very similar' to that of

---

[38] Operating Characteristics and Requirements for the NERVA Flight Stage, AIAA 70-676, J. Altseimer et. al., 1970

NERVA.[39] However, since tungsten is an excellent shielding material and a major component of the cermet reactor, it is likely that it would have a significantly smaller dedicated gamma radiation shield.

#### 2.2.1.2 Particle-Bed Reactors

There are two basic forms of the particle-bed reactor (PBR), the fixed-bed reactor (FPBR) and the rotating-bed reactor (RPBR). Most interest to date has concentrated on the FPBR, but the RPBR will also be examined, because it allows for the possibility of liquefaction of a portion of the core itself--providing higher specific impulse than could be gained from a solid-core reactor.

A representative FPBR point design[40] is composed of nineteen fuel elements, twelve control rods, moderator, and reflector. The fuel elements are annular packed beds of coated particulate fuel (particle diameter ~ 500-700 mm), kept in place by two cylindrical porous shells, or 'frits.' The fuel particles are composed of $UC_2$ coated with zirconium carbide and pyrolitic carbon; in this way, the fissile uranium is encased in high-temperature resistant material to resist fission fragment release. The frits themselves have a pore size of 40 mm and will pass gaseous hydrogen propellant while containing the particle bed. This hydrogen passes from the outer frit at 300 K, through the particle bed, and emerges at 3000 K into a central channel. The severe thermal gradient--and thus, thermal stress--encountered in the bed is nullified by the particulate nature of the fuel itself. This was not possible in the design of NERVA (where the fuel and moderator was an integrated block of material susceptible to cracking under the thermal loads), but allows a much faster ramp-up to full power in the FPBR, on the order of several seconds. In addition, very high power densities--perhaps up to 50000 $MW/m^3$ of bed--are possible, with the increased surface area available for heating. NERVA engines were constrained by the geometry of their cores--heat transfer was directly proportional to the coolant channel area per engine volume. Since the FPBR does not rely on coolant channels but on hydrogen flow into a packed bed of hot particles, the bed area/reactor volume ratio is much larger. The FPBR's performance could outstrip NERVA designs by a factor of ten and consequently allow much

---

[39] Use of Cermet-Fueled Nuclear Reactors for Direct Nuclear Propulsion, S. Bhattacharyya, 1988

[40] Particle Bed Reactor Propulsion Vehicle, pp. 375-377

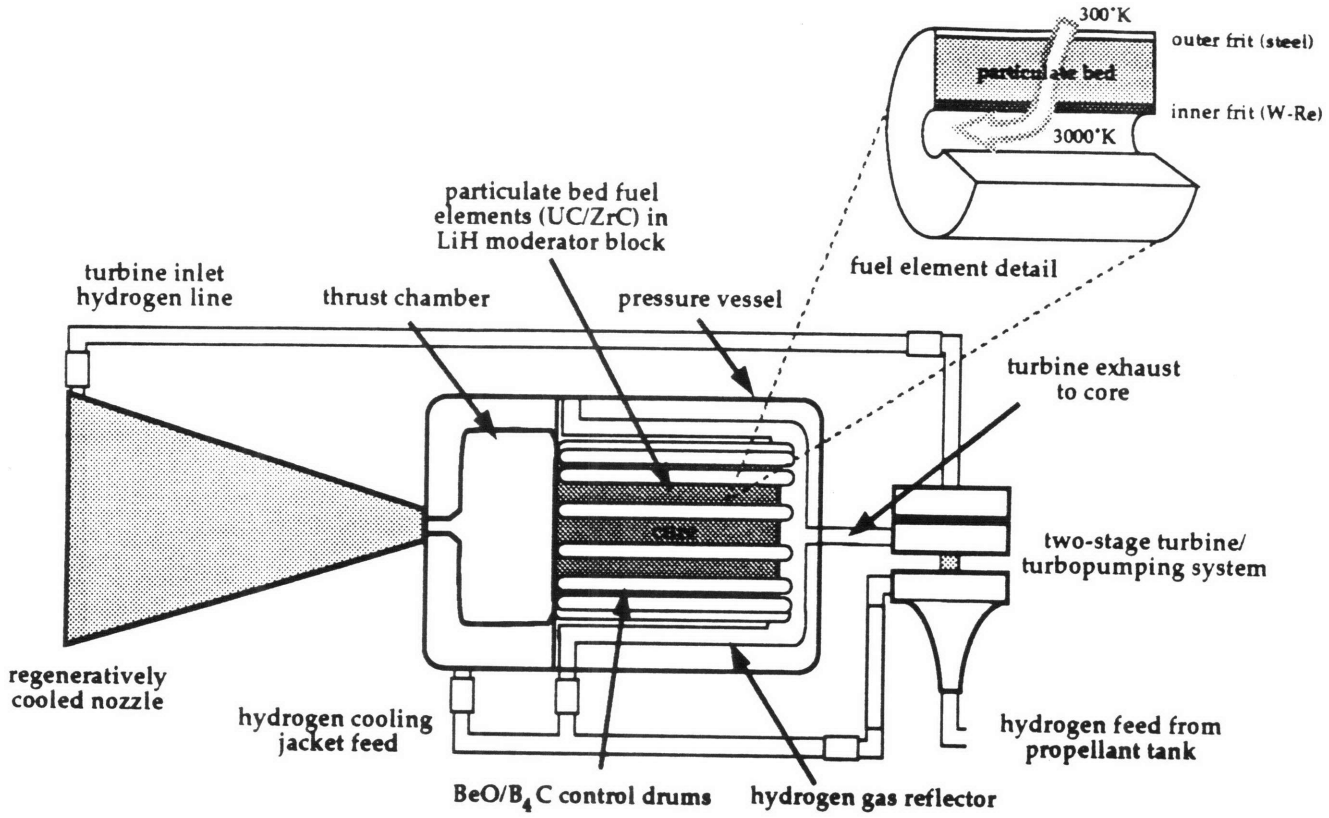


**Figure 21 Possible engine scheme for the Fixed Particle Bed Reactor (FPBR)**

lower reactor mass and thus a higher engine thrust-to-weight ratio. Regenerative cooling of the thrust chamber and nozzle was not explicitly planned, but is certainly possible by routing a fraction of the total propellant through a cooling jacket and running the turbopump system off of this flow (Fig. 21).

The fuel elements are embedded in a block of moderating material, possibly LiH or $ZrH_{1.7}$, and surrounded by a stainless steel pressure vessel. The hydrogen passing through the outside of the core acts as the reflector and can affect the neutron fluence, thus allowing a measure of independent control (outside of the control drums) of core reactivity. The nineteen fuel elements empty their coolant into a thrust chamber and vent the propellant through a high-temperature (carbon-carbon composite) nozzle.

The major constraint on PBR design is the 'hot frit' temperature, which serves as a limit on the temperature of the exhaust gas and, thus, the specific impulse achievable by the FPBR. The cold frit (at 300 K) is not as much of a design issue, obviously, so long as it can withstand the 60 atm pressure in the core. Nevertheless, the cold frit must be resistant to 'clogging' of its pores, and must properly spread the hydrogen propellant throughout the bed to prevent 'hot spots' from developing. At ten times this temperature, however, the hot frit must be made of very heat-resistant materials; in the case of the PBR design at issue, the frit is composed of a tungsten-rhenium alloy. Carbon composites and metal carbides have also been proposed as

substitutes for W-Re--C-C is lighter and is not as susceptible to activation by the radiation environment in the engine. Given an Isp of 900 s. and a power level of 300 MW, the engine's thrust can be determined via equation (12): Powell's FPBR is capable of thrust levels approaching 68 kN with a mass (core only) of as little as 300 kg. If no shield mass is included, and 500 kg of pumping system and structure is added, a T/W of ~7 is possible. While a pressurized gas feed system is plausible, it is more effective in conjunction with engines that produce low thrust or operate for very short burn times. Since these engines can be expected to operate for 14 minutes or longer (given the assumptions in Section 3.0), a pumping system was presumed to be used. Recent work by the NASA Synthesis Group indicates a requirement for T/W values in the range of 30-40 and a thrust of 300-400 kN--the FPBR represents the only engine design that might permit such performance.

The rotating particle-bed reactor attempts to solve the hot-frit problem by eliminating the need for an inner frit entirely. The RPBR core is spun by a drive motor to provide enough centripetal force on the bed to hold it against the outer (cold) frit. With no thermal constraint on the hot side of the bed besides the melting point of the fuel particles themselves, the temperature of the chamber could rise to 3500 K (the melting point of ZrC is ~3800 K; that of $UC_2$, 2600 K).[41] With the higher temperature, a specific impulse of nearly 1000 s. is achievable. Unfortunately, a failure of the drive motor would probably allow the release of highly radioactive fuel and fission products, while the motor itself and the need for redundancy in the drive system would entail additional structural mass and design complexity. Nevertheless, an increase of 100 s. of $I_{sp}$ is significant, allowing for decreased initial mass requirements.

In the case of the liquid annular or colloidal rotating bed reactor, a portion of the fuel liquefies and allows hydrogen exit temperatures near 5500 K. Hydrogen will dissociate at this level, and the specific impulse could theoretically be increased to 1550 s.

### 2.2.2 Gas-Core Reactors (GCR)

The fundamental difference between the solid-core and gas-core reactors is based on their operating temperatures; this affects all facets of the gas-core design. Whereas 1000 s. represents an upper limit to the performance of SCR, GCR rockets could well have specific impulses in excess of 5000 s., were they found to be possible--the question is in much doubt. The mass and complexity of the GCR have precluded any from being built--tests to determine if the basic modelling assumptions are correct were performed in the 1960's and early 70's, and

---

[41] Evaluation of Advanced Nuclear Reactor Concepts for Space Applications, S. Harms, NRRT-N-89-023, 1987

set aside after the cancellation of NERVA. Now that the SEI has made manned Mars missions a possibility, and such difficult problems as zero-g debilitation have arisen, there has been a resurgence of interest in the design of these very-high $I_{sp}$, moderate thrust designs.

#### 2.2.2.1 Open-Cycle

The Open-Cycle Gas-Core Reactor (OCGCR), sometimes referred to as the coaxial flow gas-core, is an attempt to reach beyond the material limitations imposed by SCR. Fissioning uranium is heated to exceedingly high temperatures ($10^5$ K) and pressures of perhaps 2000 atm. Under these conditions, the uranium fuel will exist only as a gas or plasma--it may not touch the walls of its chamber and introduces serious confinement problems. The fuel is surrounded by an envelope of tungsten-seeded hydrogen gas, which is heated upon contact with the fissioning uranium and is released through a nozzle. The OCGCR design also allows a certain amount of uranium and fission products to escape, which therefore requires a substantial inventory of fuel to replace that lost in the exhaust. The amount lost to space is projected to be not more than 1% of the hydrogen mass flow rate.[42] This 'small' amount will certainly be a point of contention, however, with a public sensitized to the dangers of nuclear devices. The comparative difficulty of testing this design will tax the ingenuity of gas-core engine designers.

The hydrogen is injected through the porous walls of the confinement chamber and is seeded with tungsten or carbon particles to prevent the walls from absorbing the majority of the incident radiation--hydrogen is essentially transparent at temperatures below $10^4$ K.[43] The moderating material in this GCR concept is BeO, which was selected primarily because of its ability to operate at gas-core temperatures in the presence of hydrogen. The moderator itself is regeneratively cooled by the hydrogen propellant prior to the stream entering the core (Fig. 22). The reference design from R.G. Ragsdale via Borowski's article "Nuclear Propulsion--A Vital Technology" assumes a specific impulse of 5000 s., a thrust of 220 kN, a thermal power level of 7500 MW, and a total mass of 123 mT. This leads to a thrust-to-weight of .1825, much lower than the solid-core reactors examined above, but still far higher than electric propulsion concepts. It will be seen, however, that the requirements for a near-impulsive burn will disqualify this engine from further consideration based on this low T/W figure. A second point

---

[42] Nuclear Propulsion--A Vital Technology, p. 18

[43] Review of Fission Engine Concepts, Journal of Spacecraft, Vol. 9, No. 9, K. Thom ,1972

design, with an Isp of 1800 s. and a thrust of 1760 kN, would have a system mass of 126 mT, a power level of 22000 MW, and a higher thrust-to-weight (1.42).[44]

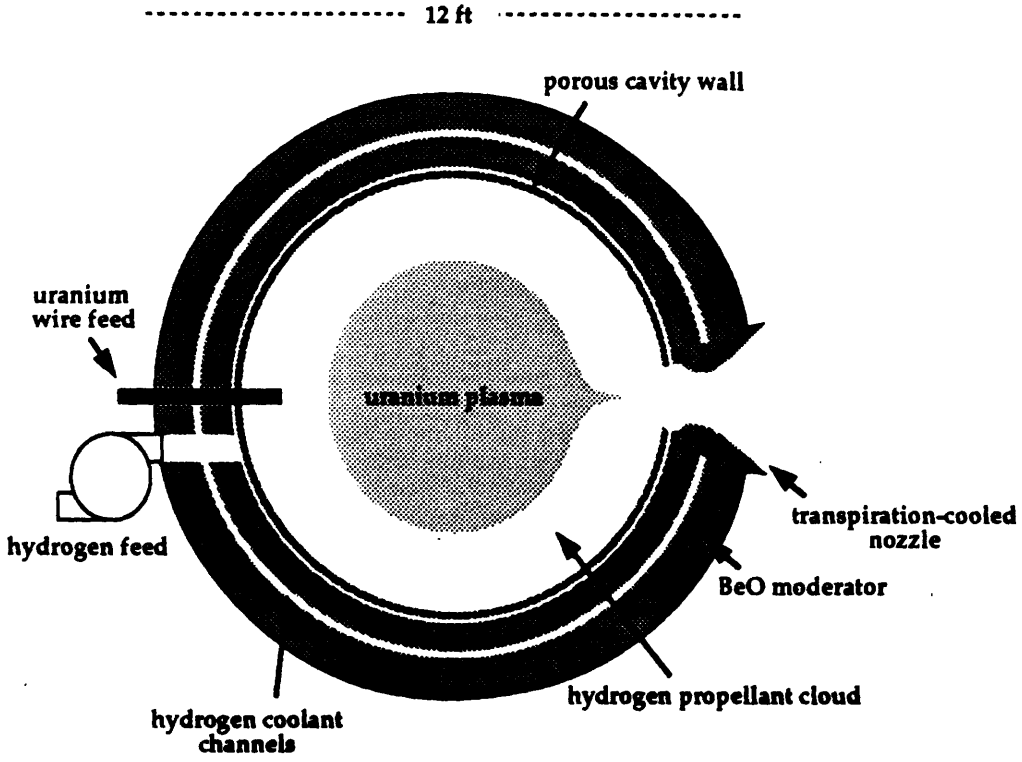


**Figure 22 Open Cycle Gas Core Reactor engine concept**

The major issues involved with the OCGCR are (1) containment of the uranium fuel, (2) construction of a reactor pressure vessel and nozzle capable of withstanding the high pressures and temperatures it will encounter, (3) thermal energy transfer to the hydrogen propellant, and (4) criticality of the uranium fuel. The containment problem could pose problems unlikely to be solved--even at 1% of the propellant flow rate, fuel and fission product loss could total 20 kg or more after a 500 s. burn involving the reference design above. This could well prove unacceptable to a populace sensitized to the hazards of nuclear waste material, even if the waste were released far from Earth. The precise methodology for shutting the engine down following a burn must also be addressed.

Fuel criticality of the fissioning plasma was the subject of much scrutiny during the 1960's and 70's. Gaseous $UF_6$ was rf- or inductively heated to temperatures comparable to that

---

[44] Gas-Core Nuclear Rocket Engine Technology Status, Journal of Spacecraft, Vol. 7, No. 12, p. 1391, G. McLafferty, 1970

expected to exist in GCR engines, and while plasma fission had not yet been performed, such experiments were in the planning stage:

> "Plans are to employ a ballistic piston to compress $U^{235}F_6$, for a short time, to a density greater than $10^{19}$ particles/$cm^3$, and to expose the compressed plasma to the neutron flux of a research reactor....One can envision a gradual expansion of this technique to eventually incorporate short-time flow confinement and flow-heating experiments."[45]

Furthermore, recent work indicates that critical fuel loading--the amount of uranium in the fissioning plasma necessary to continue the chain reaction--is extremely dependent on the geometry of the containment cavity. If the uranium cloud can be restricted to a small portion of the chamber, fuel and fission product loss can be minimized. B. Schnitzler, in his "Gas Core Reactors for Direct Nuclear Propulsion," notes that decreasing the volume fraction (the ratio of fuel cloud volume to chamber volume) of the fuel cloud from ~1 to approximately 30% requires a ten to fifteenfold increase in the critical fuel loading. This is a direct result of neutron upscatter and capture by a larger and larger quantity of hydrogen propellant, and also requires higher operating pressures (to confine the fuel cloud in a smaller volume). This drives the designer to higher containment structure mass and argues for a trade study to determine the optimum critical loading of fuel, given an 'acceptable' fuel loss rate.

It is important to note that, while gas-core proponents were enthusiastic about the eventual success of the coaxial engine, there is as yet no proof-of-concept and certainly no working model of an open-cycle engine.

#### 2.2.2.2 Closed-Cycle

The closed-cycle gas-core reactor (CCGCR or 'light-bulb' reactor) is a design that attempts to solve the problem of fuel and fission product loss by encasing the fissioning plasma inside a high-temperature transparent casing--affectionately referred to as the 'light-bulb.' The reference design (Fig. 23) is composed of seven reactors, each containing a uranium plasma separated from the hydrogen propellant it heats. A neon buffer gas injected radially into the chamber creates a vortex which prevents the hot plasma from contacting the 'light-bulb's' walls. It is removed from the chamber and scrubbed for fission products and fuel--the fuel being reintroduced into the fuel region. The design suffers from material limits unlike that found in the open-cycle engine; the thin containment vessels must be able to withstand the enormous flux of radiant energy emitted from the fissioning plasma without melting or fracturing; this lowers

---

[45] Review of Fission Engine Concepts, p. 635

the effective "chamber temperature" achievable by the light-bulb design and thus specific impulse. The containment vessel walls have been assumed to be constructed from either fused silica or single-crystal BeO. McLafferty comments, "...because of the finite absorption of fused silica in the ultraviolet and its low thermal conductivity, the transparent walls must be thin, on the order of .005 in. in the representative engine..."[46] Such light walls will pose serious--if not insurmountable--structural problems in an engine with a fuel cavity pressure of 500 atm and a hydrogen pressure of 250 atm; the stress seen at the wall, related to the ratio of cavity radius (1.15 ft) to wall thickness, would be on the order of 70000 $MN/m^2$ (1 x $10^7$ psi). Another issue arises:

> "The transparent wall material dividing the propellant and fuel regions of a nuclear light bulb engine must be transparent to the wavelengths of the radiant energy emitted from the fuel region. This energy is contained mostly in the wavelength region between 0.1 and 4.0 m. Results...of measurements of the transmission characteristics of fused silica indicate that exposure of the specimen to neutron and gamma irradiation resulted in an increase in the absorption coefficient in the ultraviolet...."[47]

This phenomenon is called nuclear-induced coloration; McLafferty mentions that such coloration can be reversed by heating the silica to approximately 1100 K--which sets a constraint on the silica wall operating temperature--but the issue had not been resolved at the time of his writing and there was some question as to whether the amount of ultraviolet absorption might be even higher than originally anticipated. It was later determined that the actual wall width could be increased to between .01 and .015 in., due to 'radiation annealing,' a process of coloration reversal.[48] At the high dose rates (> $10^6$ rad/s.) likely to be found in the light bulb engine, it was experimentally determined that the absorption coefficient in the UV decreased dramatically. The question of wall fabrication and fragility, even at widths of .01 in., is nevertheless a design issue of major importance.

The hydrogen propellant is not in contact with the plasma as in the coaxial flow design but is injected into the engine around the plasma containment vessel. The reference design uses seeded tungsten particles (4% by mass) in the propellant to prevent too large a deposition of heat in the engine's structure. For the design in question, the heat deposition was given as 2% of the total generated. Hydrogen is regeneratively circulated throughout the engine to cool the

---

[46] Gas-Core Nuclear Rocket Engine Technology Status, p. 1395

[47] ibid., p. 1395

[48] Summary of the Performance Characteristics of the Nuclear Light-Bulb Engine, AIAA 71-642, T. Latham, 1971

BeO/graphite moderator and is transpired through the skin of the nozzle to similarly limit its temperature.

The reference design for the CCGCR predicts a propellant exit temperature of 12000°R (~6700 K), a specific impulse of 1870 s., 4600 MW of power, a thrust of 405 kN, and a T/W of 1.27.[49] Latham comments that the nuclear light bulb could be expected to perform at an $I_{sp}$ of as high as 3200 s. with some modifications to the reference design (including the addition of a radiator to reject heat from the moderator material), and with engine T/W ratios perhaps as high as 6.9.

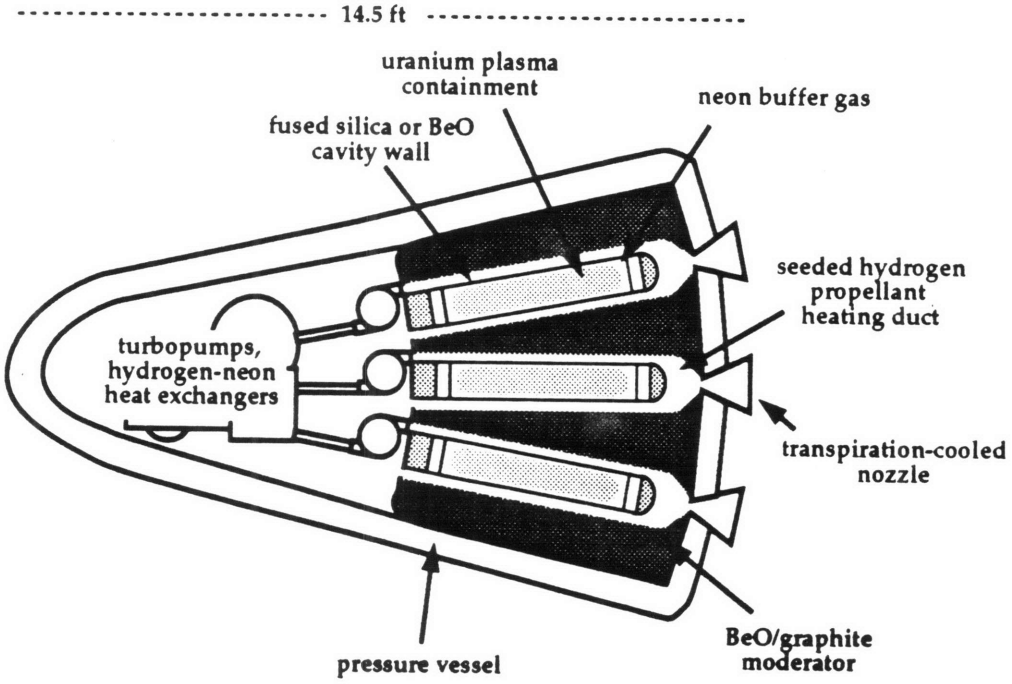


**Figure 23 Closed Cycle Gas Core Reactor engine concept**

Major advances in structures will clearly have to be made before a closed-cycle gas-core engine can be developed. In the open-cycle gas-core, the main issue was one of fluid dynamics and containment. Here, the basic questions are: (1) whether or not the fissioning plasma can be contained by any known material, given the stresses that will be seen in the transparent wall, (2) how gamma and neutron radiation will change the properties of the transparent wall over time--especially its resistance to heat transfer, and (3) uranium plasma criticality. Both gas-core

---

[49] Criticality Studies of a Nuclear Light Bulb Engine, Journal of Spacecraft, Vol. 6, No. 19, p. 1148, T. Latham, 1969

engines have major design issues yet to be resolved before testing can begin. This clearly distinguishes them from their solid-core counterparts, of which one (NERVA) has already been constructed and tested.

## 3.0 NUCLEAR PROPULSION AND THE NASA BASELINE MISSIONS

This chapter will discuss the results of several studies which were performed to determine (1) how specific impulse, thrust, and thrust/weight affect the range of NTP engine options available to the SEI mission designer; (2) what modifications or additions these nuclear thermal engines will require in the design of transfer vehicles, ascent/descent vehicles, and launch vehicles; (3) what effect the use of the engines will have on orbital operations; and (4) how the use of NTP will affect the design of planetary surface systems and habitats, including ground support and Earth-based infrastructure. For part (1) , the six engines discussed in the previous section will be analyzed in detail--and a baseline engine selected on the basis of its performance. This engine will then be examined more fully in the context of a Mars architecture in parts (2), (3), and (4).

### 3.1 Effect of Specific Impulse ($I_{sp}$), Thrust (T), and Thrust-to-Weight (T/W)

These three parameters, Isp, thrust, and thrust-to-weight, are natural measures to determine optimal engine classes for a given mission. Specific impulse (for a given $\Delta V$) is related directly to propellant mass through the rocket equation. For low values of $\Delta V$, such as those of the NASA baseline missions (where the advantage of short trip time is essentially sacrificed to reduce the total mission $\Delta V$), high-$I_{sp}$ engines are not as clearly superior to cryogenic chemical engines as they are for sprint missions; this is due entirely to the nature of the exponential curve of the rocket equation. Modest propellant mass savings can still be exploited, however, except in the case of the most massive engines (open-cycle gas cores, and the closed-cycle light bulb engines to a lesser extent).

This study is intended to focus primarily on high- or moderate-thrust alternatives to the cryogenic baseline of the 90-day study. As such, one of the requirements placed on the NTP engines is that they must be capable of what is defined as a 'near-impulsive' burn. An impulsive burn occurs over essentially zero time--this is a good approximation for high thrust-to-weight cryogenic engines but tends to break down for NTP options. The near-impulsive burn is one in which an additional $\Delta V$ (the 'performance penalty') can be approximated by the equation[50] :

$$\Delta v_p = \frac{gI_{sp}}{4}(\omega_s T)^2\left[\frac{-2gI_{sp}}{\Delta v_I} + \coth\left(\frac{\Delta v_I}{2gI_{sp}}\right)\right] \qquad (14)$$

---

[50] An Analytic Study of the Impulsive Approximation, H. Robbins, AIAA Journal, August 1966

This equation was derived from Robbins' work in his 1966 analysis of the impulsive approximation. $\Delta v_p$ is the performance penalty associated with a specific burn, while $\Delta v_I$ represents the impulsive $\Delta V$. T is the burn time, and $\omega_s$ is the Schuler frequency, defined by:

$$\omega_s = \sqrt{\frac{GM_p}{r^3}} \tag{15}$$

G is the gravitational constant, r represents the radius of the circular orbit, and $M_p$ is the planetary mass about which the maneuver is being done. Robbins notes that this approximation breaks down rapidly when the product ($\omega_s T$) exceeds 1, although it is quite accurate up to 1. Beyond this limit, it is necessary to numerically integrate the equations of motion, as there is no closed-form solution to the problem. Since the Schuler frequency can be calculated for a specific orbit, a threshold T can be found beyond which the approximation (14) will not hold beyond it. For the 407 km circular orbit at Freedom, the maximum burn time was found to be 885 s. The Mars capture orbit (250 km x 34000 km) was conservatively approximated by a 250 km circular orbit; this gave a critical burn time at Mars of 1064 s. The true value will obviously be higher, but the 1064-s. limit was used for subsequent calculations.

Now that the maximum allowable burn times are known, it is possible to determine the average thrust required to perform at least a near-impulsive burn for the given mission IMLEO/IMLMO and engine type. With F defined as the engine thrust, $m_p$ defined as the consumed propellant mass, and $m_o$ as the initial mass in Mars or Earth orbit, the total impulse I is:

$$I = \int_0^T F\,dt = m_p u_e = m_o\left(1 - e^{\frac{\Delta v}{g I_{sp}}}\right) g I_{sp} \tag{16}$$

Then the average thrust required to boost a given initial mass near-impulsively is given by:

$$\bar{F} = \frac{I}{T} \tag{17}$$

Finally, given the specific engine design, it is possible to determine the number of engines required to achieve that level of thrust. For instance, the FPBR design (68 kN/engine, $I_{sp}$ = 900 s.) could be used to boost Option I's Mars Flight I on its first, or apogee-raising, impulse (IMLEO = 832.2 mT, $\Delta v$ = 2937 m/s). The average thrust required is 2350 kN, which necessitates 2350 kN/68 kN/engine, or 35 engines. In contrast, NERVA engines (330

kN/engine, $I_{sp}$ = 825 s.) allow for an average thrust of 2316 kN, thus 2316 kN/330 kN/engine, or 7 engines. The total mass of a 7-engine NERVA cluster is 77 mT--while the 35-engine FPBR cluster is only 28 mT, a significant mass savings over NERVA.[51] It is important to note that the issue of engine sizing and redundancy is addressed further in 3.2.1.1; the large numbers of FPBR and Cermet engines reflect the lack of consideration here for such sizing. Clearly, an engine such as the FPBR could be made larger to preclude structural mass penalties associated with the use of many engines in tandem. The performance penalty associated with this near-impulsive burn is quite small--about 4% of the total burn. Any study-generated Δv value will have a 15% margin to cover launch windows and finite-burn losses: Therefore, it will not be necessary to add the performance penalty to the impulsive Δv but will be assumed to be small under the stringent conditions applied (namely, that the burn must be 'near-impulsive'). Launch windows generated for NTP vehicles typically last two months.

The large mass gap between the NERVA and FPBR designs for Option I's Flight 1

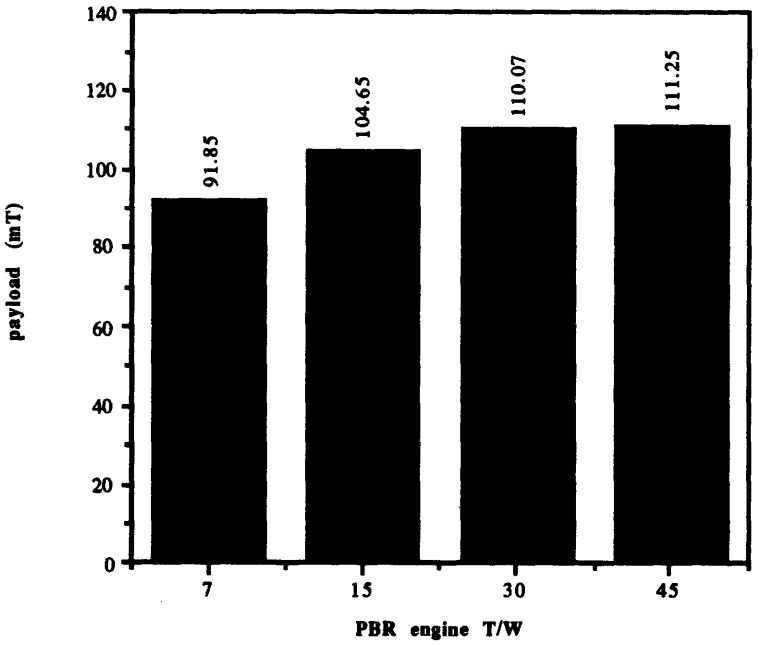


**Figure 24 Option I Mars Flight 1**
**Fixed IMLEO and variable payload delivery with**
**FPBR thrust-to-weight varying from 7 to 45**

---

[51] Note that this does not address the question of extra mass in terms of shielding and supporting structure. This will be included in the 25% margin discussed in Section 3.1.1.

illuminates the importance of engine thrust-to-weight (T/W). The difference between the two engines' performance in terms of Δv is fairly small (75 s.) but the amount of mass required to produce such performance in a NERVA-based system is significantly larger--by 50 mT--than that required of a PBR system. An FPBR-propelled Option I Flight 1 was examined more fully to determine its sensitivity to engine thrust-to-weight. For fixed IMLEO, the deliverable payload to Mars increases as T/W increases from 7 to 45; however, the payload bonus received for

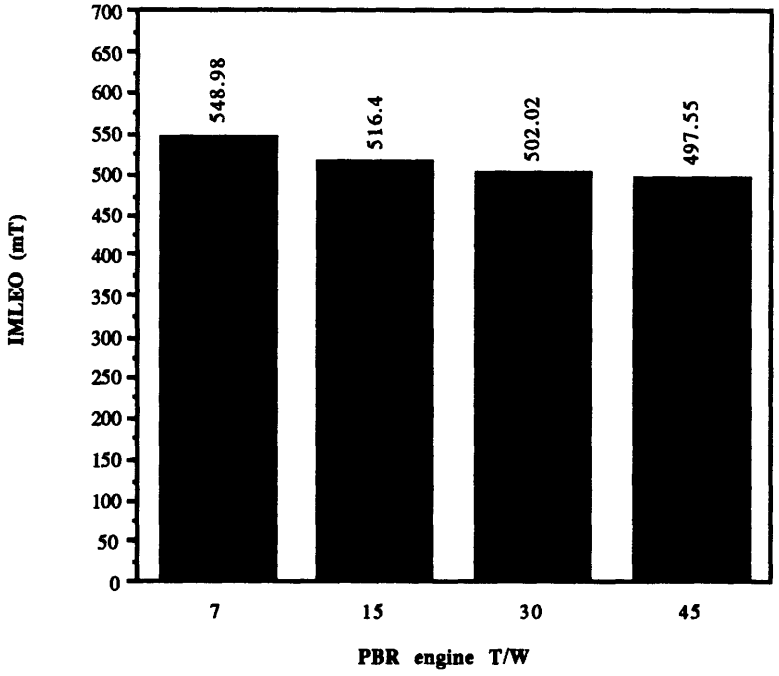


**Figure 25 Option I Mars Flight 1**
**Fixed payload delivery and variable IMLEO with**
**FPBR thrust-to-weight varying from 7 to 45**

doubling T/W from 7 to 15 (14 mT) is over twice that received for doubling from 15 to 30. The 1 mT difference between T/W=30 and 45 clearly show that there is little incentive to continue reaching for higher thrust-to-weight than ~30 (Fig. 24). Similarly, figure 25 indicates that higher thrust-to-weight can lower IMLEO for fixed Mars payload. These smaller increases result from the fact that the FPBR engine mass is fixed at 1 mT; since at least one engine is necessary to initiate a maneuver, and since at higher T/W only a very few engines are needed, the total mass savings gained by decreasing the number of necessary engines grows smaller

with increasing T/W. The limit on such mass savings is reached when one engine is capable of performing the TMI burn.

The lunar transfers most clearly demonstrate the need for light systems. Here, overall mass savings in the 90-Day Study and in this paper are achieved by reusing the LTV and LEV for five missions. In the next section, it will be seen that the lunar missions require two NERVA engines (27.5 mT, with a 25% margin) or nine FPBR engines (9 mT). The difference between the two--18.5 mT--is structure that will be paid for five times over in propellant mass. This mass problem is even more marked in the gas-core engines, making them completely unable to compete with chemical or FPBR engines for lunar missions: An engine cluster composed of one Open-Cycle #2 engine (157.5 mT, $I_{sp}$ = 1800 s., F = 1760 kN) would be easily sufficient to propel the lunar mission, but its mass is higher than some of the later mission IMLEO figures. While it could be argued that this engine would be reusable and would pay for itself in the long term, this is not where the high-$I_{sp}$ engines could be utilized most effectively. Their particular importance lies in their ability to achieve vastly shortened trip times at reasonable propellant cost. Such variable duration mission alternatives will be examined in detail in Section 3.1.2.

### 3.1.1 Fixed Mission Duration (NASA Baseline Missions)

This section examines the performance of nuclear thermal systems against the NASA baseline lunar and Mars missions, fixing the mission profile and duration. The NTP systems outlined in Chapter 2.0 were rated against the NASA baseline on the basis of (1) fixed IMLEO and FMLEO (Final Mass in Low Earth Orbit), with variable payload delivered to the moon or Mars, and (2) variable IMLEO, with a fixed (baseline delivery) payload delivered to the moon or Mars. In the first part of this study, the NTP systems were used only for orbital transfer--their prospective abilities for use aboard a launch vehicle upper stage and ascent/descent vehicles will be addressed later. The use and consequences of a Mars/Earth or Earth-only (lunar missions) aerobrake is addressed.

The second half of this section will examine how the NTP options provide SEI missions with the capability to perform faster transfers to Mars, assuming once again (1) fixed IMLEO/FMLEO, (2) fixed payload delivered to the lunar or Martian surface, and (3) baseline stay time. Aerobraking, upper stage use, and planetary ascent/descent use of NTP engines is also addressed.

**3.1.1.1 Orbital Transfer NTP:** The NASA 90-Day Study Mars missions are near-minimum energy trips that require from 565 to almost 1000 days to complete. Stay times typically run from 30 days to as many as 600 days. The 90-Day Study Databook provided

trajectory data for Option I and Option V missions but did not give MOI or EOI Δv figures--since an aerobrake was used to produce the velocity changes on encounter at Mars and return to Earth. MULIMP ("Multiple Impulse")[52], software developed by the Illinois Institute of Technology and continued by SAIC for use on personal computers, was used to determine the MOI and EOI impulsive burns necessary for a non-aerobraking NTP-propelled mission (Table 15). The 90-Day Study used MULIMP extensively. The SAIC program uses a Lambert algorithm to find an orbit connecting two specified points. Detailed information on the solution to the Lambert problem is available[53], but the pertinent astrodynamics will not be further discussed here.

These values were supplemented by a 15% margin in order to account for finite-burn losses detailed in Section 3.1, as well as to cover "reasonable" launch windows. The 90-Day Study contingency provides for "2% Δv reserves, 2% for performance uncertainties, finite burn losses

**Table 16 Mars Mission Δv requirements (EOI Δv of 0 m/s represents a direct entry upon return to Earth)**

| Mission | | TMI delta-V (m/s) | MOI delta-V (m/s) | TEI delta-V (m/s) | EOI delta-V (m/s) |
|---|---|---|---|---|---|
| Option I -1 | Opposition (VSB) | 4500 | 4447 | 3400 | 0 |
| -2 | Opposition (VSB) | 4225 | 4421 | | |
| -3 | Conjunction | 4500 | 4479 | 2000 | 5311 |
| -4 | Conjunction | 4600 | 4418 | 1975 | 5314 |
| -5 | Conjunction | 4250 | 2254 | | |
| -6 | Conjunction | 4250 | 2454 | 1625 | 5284 |
| Option V -1 | Opposition (VSB) | 4500 | 4440 | **3130** | 0 |
| -2 | Opposition (VSB) | 4275 | 3003 | **3399** | 0 |
| -3 | Opposition (VSB) | 4630 | 2947 | **4635** | 0 |
| -4 | Conjunction | 4225 | 2454 | | |
| -5 | Conjunction | 4025 | 3255 | 1000 | 5295 |

calculated and added to the impulsive Δv, and Δv reserve requirements for launch windows from LEO."[54] These launch windows were not explicitly spelled out in the 90-Day Study but

---

[52] MULIMP, Macintosh II software, SAIC, 1991

[53] An Introduction to the Mathematics and Methods of Astrodynamics,pp. 295-342, R. Battin, AIAA Education Series, 1987

[54] Databook, Section 5.2.2

were implicitly mentioned in the transfer vehicle requirements. Maximum Δv figures were specified, as opposed to launch window durations. This resulted in Δv reserves ranging from 5% in the case of most unmanned vehicles' burns to as high as 25% in the case of Option I's Flight 1 (TEI). Most margins fell in the 15% range and this value was therefore used as a representative margin for all MULIMP-calculated Δv figures. It is interesting to note that several Option V's Mars missions were designed assuming impulsive TEI Δv values several hundred m/s *lower* than the figures provided by MULIMP. This discrepancy is not explained in the 90-Day Study, although it might be due to a difference in departure orbits used in the 90-Day Study and that specified for this study. The numbers used by the 90-Day Study missions were used for evaluation of NTP options when they were greater than their MULIMP-generated counterparts but were otherwise discarded in favor of the MULIMP + 15% figures.
The boldfaced values in Option V represent disagreement between MULIMP and the 90-Day Study figures for the TEI burn. In addition, it is important to note that those missions (Option V's Flights 1-3, as well as Option I Flight 1) are direct-entry; they do not attempt to rendezvous with Space Station Freedom on return to Earth.

**3.1.1.1.1 All-Propulsive Missions:** The first study of NTP options using the baseline duration specifications assumed:

(1) Baseline payload delivery to be constant for the study,

(2) the initial mass in low Earth orbit, and thus the total LEO payload necessary to support lunar and Martian missions, would be the figure of merit,

(3) a mass margin of 25% would be added to NTP engine estimates to cover shielding requirements, extra support structure and tankage requirements,

(4) reusability would not be considered an important factor in Mars missions; i.e. engines would be staged and discarded at various points along the mission timeline to improve fuel consumption,

(5) Ascent/descent would be performed by the baseline MEV and LEV,

(6) Aerobraking would not be considered. In the case of lunar missions, the aerobrake mass (~3 mT) was kept in the manifest as additional margin (in the NTP/aerobrake portion of this study, this mass is then actively used to brake the LTV).

Both Options I and V were considered for this study, although results are presented only for Option I. Only half of the Option I lunar flights were examined, but the trend is clear even for the first few flights.

Since mission IMLEO was variable for this portion of the study, the number of engines required to perform various impulsive burns was determined through iteration; an estimate of the number of engines necessary was used and the new IMLEO calculated. In turn, this IMLEO

value allowed resizing of the engine cluster until the number of engines was capable of providing sufficient thrust for the burn in question. Thrust requirements are further discussed in the second part of this section, where mission IMLEO is held fixed and the total delivered payload allowed to vary.

Figure 26 shows the results of this study--FPBR and the Light Bulb can both cut substantially into the LEO support payload necessary for the Mars missions. Both the Cermet NDR (not shown) and FPBR reduced total LEO support by over 700 mT (the equivalent of six 90-Day Study Mars HLLV's). NERVA's design was incapable of matching the baseline IMLEO; likewise, neither open-cycle gas-core design was able to approach the cryo/aerobrake performance.

The following table illustrates engine performance for a specific piloted Mars mission, Option I Flight 1:

| Engine type | IMLEO | Savings over baseline |
|---|---|---|
| Baseline cryo/aerobrake | 832.20 mT | |
| NERVA | 826.35 | 5.85 mT |
| FPBR (T/W = 7) | 578.42 | 253.78 |
| FPBR (T/W = 30) | 502.02 | 330.18 |
| Cermet NDR | 619.95 | 212.25 |
| Light Bulb | 688.45 | 143.75 |

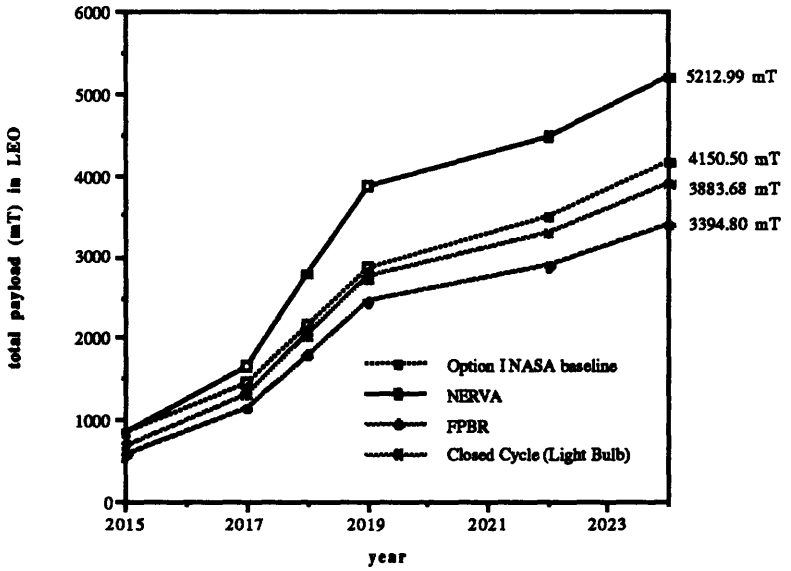


**Figure 26 Performance of NTP versus NASA's Mars Option I (variable IMLEO, fixed payload); total payload delivered to LEO to support Mars missions**

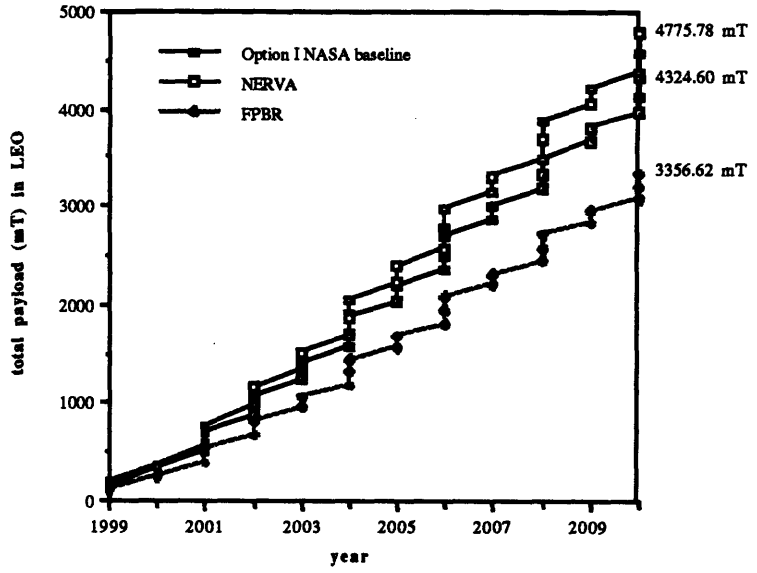


**Figure 27 NTP versus Option I; total payload delivery to LEO supporting lunar missions**

The lunar missions (Fig. 27) showed similar results: NERVA and the open-cycle engines could not achieve the baseline, while (in this case) the relatively large mass of the Light Bulb and the requirement for reusability prevented it from taking full advantage of its high $I_{sp}$. Nevertheless, the Light Bulb LTV was shown to be capable of emplacing the baseline payload for a total shipment to LEO of 4168.53 mT, 150 mT lower than the cryo/aerobrake missions. FPBR and Cermet both produced the lowest figures, in the range of 3400 mT.

The second half of this study will consider payload increases possible for a fixed IMLEO, but it is important to note that it is far more likely that payload requirements will be specified in advance. Thus, it is reasonable to assume that any savings in IMLEO as a result of improved engine performance will be of more importance to the SEI mission designer than possible payload increases for a given IMLEO. Nevertheless, such payload increases will be detailed below.

Assumptions for the second half of this study include:

(1) Baseline IMLEO and FMLEO to be constant for the study,

(2) the *delivered payload to the Martian surface* would be the figure of merit,

(3) a mass margin of 25% would be added to NTP engine estimates,

(4) reusability would not be considered,

(5) Ascent/descent would be performed by the baseline design MEV's. Since many of the alternatives produced substantially higher payloads, this is not completely accurate, since an MEV intended to handle payloads in the tens of metric tons could clearly not handle hundreds of metric tons and not face a redesign. Finally,

(6) Aerobraking would not be considered.

To achieve the stringent conditions imposed on overall vehicle thrust-to-weight required the NERVA MTV-P to have 7 engines for TMI. This value was determined assuming $\Delta v_{TMI,\,1}$ = 2937 m/s, the first and largest $\Delta v$ of the three-impulse burn. Using the limiting burn time and the IMLEO (832.2 mT) required 2350 kN as previously stated, or 7 engines at TMI. The burn time threshold similarly set limits on the number of engines needed to provide a near-impulsive burn at MOI, TEI, and EOI. The NERVA-propelled MTV-P was determined to use the following staging plan:

(1) TMI: Three impulse burn is followed by jettison of two engines,

(2) MOI: Perigee capture is followed by the release of four engines, and

(3) TEI/EOI: Both trans-Earth injection and Earth-orbit insertion are accomplished by the remaining NERVA engine, which is released before crew return vehicle reentry.

The cluster and staging requirements were determined in similar fashion for the other nuclear thermal engines, and summarized in Table 17. These numbers were modified slightly in the case of the Light Bulb engine, where it was possible to perform two missions with less engines (Opt I-3, Opt V-5, specifically).

The Open Cycle 1 Engine was incapable of performing any of the Mars missions--its thrust-to-weight of 0.18 disqualified it from consideration as a true 'near-impulsive' engine. At the Open Cycle 1's thrust level, a near-impulsive burn would require an engine cluster in excess of 1800 mT (far larger than the most massive 90-Day Study mission). Of the engine types studied, only FPBR and Cermet were capable of delivering the baseline payload to Mars at the IMLEO figures given. Clusters composed of NERVA, the Open Cycle engines, and the Closed Cycle Light Bulb were too massive to allow these vehicles to deliver the baseline payload for every mission; Option I's Flights 3,4, and 6, as well as Option V's Flight 5, were beyond the reach of missions propelled by those engines for the baseline IMLEO. These missions, save Option I-4, were manned missions with Space Station Freedom rendezvous, requiring a large expenditure of propellant mass at the end of the mission to brake the vehicle/engine cluster.

Both FPBR and the Cermet NERVA derivative reactor were capable of achieving greater payloads per mission, despite the handicap imposed by the lack of an aerobrake. Figure 28 clearly indicates that both Cermet NDR and Particle-Bed propelled vehicles could deliver twice

the payload to the Martian surface over the Option I timeframe. Interpreted in a different way, the total payload (166.6 mT) brought to Mars by six baseline missions over the years 2015-24 could be performed by only two FPBR missions. The Cermet NDR, which could be thought of

**Table 17 NTP Engine Staging for Fixed IMLEO/ All-Propulsive Missions**

| Engine Option | Engines firing: | TMI | EOI | MOI | EOI |
|---|---|---|---|---|---|
| NERVA | MTV-P | 7 | 5 | 1 | 1 |
| | MTV-C | 6 | 6 | | |
| FPBR | MTV-P | 35 | 21 | 5 | 5 |
| (T/W = 7) | MTV-C | 26 | 26 | | |
| FPBR | MTV-P | 8 | 5 | 1 | 1 |
| (T/W = 30) | MTV-C | 6 | 6 | | |
| Cermet NDR | MTV-P | 18 | 12 | 5 | 5 |
| | MTV-C | 14 | 9 | | |
| Light Bulb | MTV-P | 7 | 5 | 2 | 2 |
| | MTV-C | 5 | 4 | | |
| Open Cycle 2 | MTV-P | 2 | 1 | 1 | 1 |
| | MTV-C | 1 | 1 | | |

as a logical successor to NERVA and perhaps as an upper performance ceiling for NERVA-type propulsion, was superior to the cryo/aerobrake system but nevertheless could not equal the higher T/W FPBR. Table 18 illustrates that this very-low weight FPBR system emplaces 73.35 mT on Mars--compared to the 15.4 mT delivered by the cryo/aerobrake system in Table 6. Mission event lists for baseline duration Mars missions can be found in Appendix A.

For lunar missions, only the first 26 flights of Option I were considered. This was thought to be sufficient to extrapolate the performance of NTP engines over the range of that option's 44 flights and to those of Option V. $\Delta v$ figures were taken to be those given within the 90-Day Study--they did not conflict with basic astrodynamics and it was not necessary to produce MULIMP data to verify them. Assumptions differed from those used in Martian missions in only one significant way--no staging of engines on the transfer vehicles would occur--and the LTVs would thus be completely reusable. This conforms to the baseline architecture, which allowed for the reuse of LTVs and LEVs for five missions. Based on the maximum IMLEO for any lunar mission (that of Opt I-25, 197 mT), a NERVA LTV would require 2 engines to

perform the TLI burn. The Cermet NDR-propelled system would need 5 engines, while the FPBR LTV requires 9.

**Table 18 Option I Mars Flight 6 Mission Event List (FPBR-propelled)**

| *Mission Event* | *Total Vehicle Mass (MT)* | *Change in Mass (MT)* | *Delta-V (m/s)* |
|---|---|---|---|
| IMLEO | **678.70** | | |
| Pre-injection preparation propellant | 649.41 | 29.29 | 0 |
| Trans-Mars injection propellant | 401.10 | 248.31 | 4250 |
| Jettison 14-engine TMI stage | 387.10 | 14.00 | |
| Jettison Earth-Mars consumables | 383.30 | 3.80 | |
| Trans-Mars coast propellant | 379.41 | 3.89 | 90 |
| Mars orbit insertion propellant | 287.26 | 92.15 | 2454 |
| Mars orbit operations propellant | 284.34 | 2.92 | 90 |
| Deploy payloads/jettison 16-engine MOI | 261.74 | 22.60 | |
| Mars payload to Mars surface | 114.69 | 147.05 | |
| Mars orbit consumables | 114.69 | 0.00 | |
| Trans-Earth injection propellant | 95.39 | 19.30 | 1625 |
| Jettison TEI stage | 95.39 | 0.00 | |
| Mars-Earth consumables | 91.59 | 3.80 | |
| Trans-Earth coast propellant | 90.55 | 1.04 | 101 |
| Earth orbit insertion propellant | 49.74 | 40.81 | 5284 |
| Earth orbit operations propellant | 48.98 | 0.76 | 136 |
| Jettison 5-engine EOI stage | 43.98 | 5.00 | |
| Final MTV-P mass in LEO | 43.98 | | |
| | | | |
| Mars payload total mass | **147.05** | | |
| Pre-deorbit preparation propellant | 147.05 | 0.00 | |
| Mars descent propellant | 109.11 | 37.94 | 1360 |
| Mars payload (dry) | 46.51 | 62.60 | |
| Mars surface science | 46.51 | 0.00 | |
| Mars surface consumables | 37.18 | 9.33 | |
| MEV-P ascent stage prior to ascent | **37.18** | | |
| MEV-P ascent propellant | 10.50 | 26.68 | 5763 |
| Crew | 10.50 | 0.00 | |
| MEV-P final mass | **10.50** | | |

Figure 29 shows the performance of FPBR and Cermet versus the Option I baseline. Once again, NERVA, both Open Cycle engines, and the Light Bulb were discounted by their inability to perform the majority of missions (i.e. deliver the baseline payload) at the given IMLEO. An FPBR-propelled LTV allows the Option I schedule to emplace the entire required payload mass on the moon after only 25 flights. This would allow Option I to be accomplished in the span of eleven years, rather than the twenty-six planned. Table 19 shows the Cermet NDR-propelled Opt I-0 flight. Comparing this event list with Table 2 shows that the Cermet's large TLI propellant mass savings, approximately 30 mT, is partially negated by its need to retrobrake at

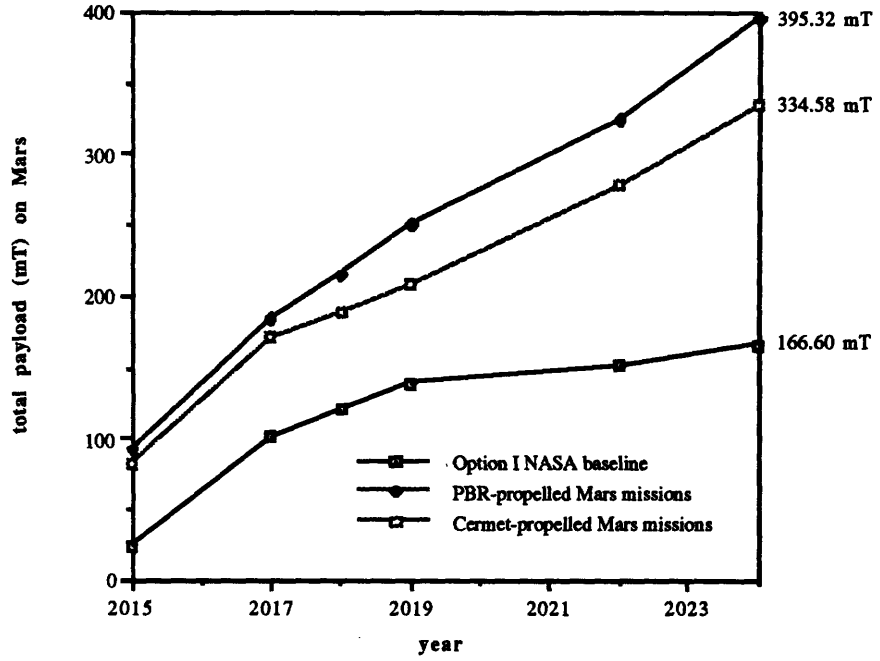


**Figure 28 Performance of nuclear thermal options against NASA's baseline Option I; total payload delivered to the Martian surface by various engine types**

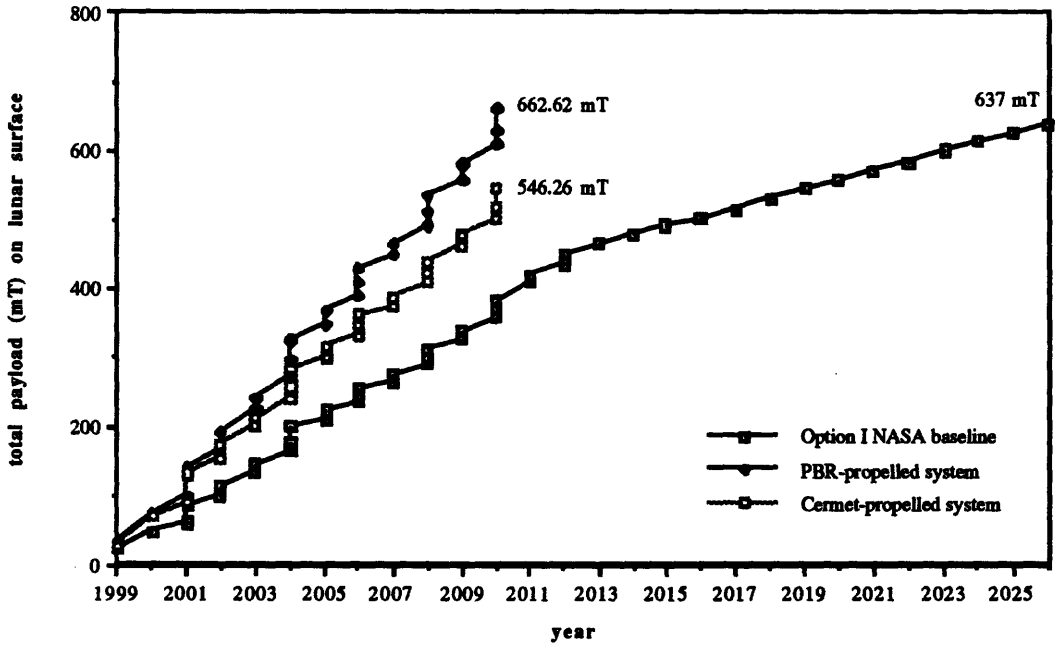


**Figure 29 Performance of nuclear options versus the NASA baseline Option I; total payload deliveries to the lunar surface, 1999 - 2026**

EOI. The Cermet LTV's extra structural mass, 14.88 mT, and this EOI propellant mass (~ 11 mT) can be seen to nevertheless be smaller than the initial propellant savings, resulting in a lunar payload increase of 5 mT. This is not small--and, it allows the Cermet system to greatly outdo the baseline after 26 flights.

**Table 19 Option I Lunar Flight 0 Mission Event List (Cermet NDR-propelled)**

| *Mission Event* | *Total Vehicle Mass (MT)* | *Change in Mass (MT)* | *Delta-V (m/s)* |
|---|---|---|---|
| IMLEO | **159.80** | | |
| Pre-injection preparation propellant | 159.80 | 0.00 | |
| Translunar injection propellant | 113.13 | 48.67 | 3300 |
| Jettison TLI tanks | 106.83 | 4.30 | |
| TLI coast propellant | 106.71 | 0.12 | 10 |
| Lunar orbit insertion propellant | 94.54 | 12.17 | 1100 |
| Lunar orbit operations propellant | 94.54 | 0.00 | |
| Deploy additional payloads | 94.54 | 0.00 | |
| Lunar payload to lunar surface | 41.95 | 52.59 | |
| Jettison LOI tanks | 40.65 | 1.30 | |
| Trans-Earth injection propellant | 36.01 | 4.64 | 1100 |
| Trans-Earth coast propellant | 35.97 | 0.04 | 10 |
| Earth orbit operations propellant | 35.95 | 0.02 | 6 |
| Earth orbit insertion propellant | 25.00 | 10.95 | 3300 |
| Less orbital transfer engine mass | 10.13 | 14.88 | |
| Final LTV-C mass in LEO | **10.13** | | |
| | | | |
| Lunar payload total mass | **52.59** | | |
| Pre-deorbit preparation propellant | 52.02 | 0.57 | 50 |
| Lunar descent propellant | 33.54 | 18.48 | 2000 |
| Lunar payload (dry) | 5.85 | 27.69 | |
| Moon surface science | 5.85 | 0.00 | |
| Moon surface consumables | 5.85 | 0.00 | |
| LEV-C total mass prior to ascent | **5.85** | | |
| LEV-C ascent propellant | 5.85 | 0.00 | |
| Crew | 5.85 | 0.00 | |
| LEV-C final mass | **5.85** | | |

The large engines (NERVA et. al.) thus require even more massive a propellant savings in order to recoup their initial structural mass investment. In the case of an Open Cycle 2 engine, this investment is 157.5 mT, too large for its increased specific impulse (1800 s.) to make up in propellant savings.

**3.1.1.1.2 Aerobraked Missions:** The combination of nuclear thermal propulsion and aerobraking to decrease IMLEO or increase delivered payload is quite promising--taking away as it does the greatest advantage the baseline design has over the other options. The study was performed under essentially the same conditions as the one described in 3.1.1.1.1. Mars missions were assumed to have used the baseline design aerobrake (MTV-P, 20.7 mT; MTV-C,

14 mT), which required only the addition of this mass to the NTP missions. Lunar missions used the baseline Earth-return aerobrake (3.1 mT), which had been left in the mission manifest but not used. For this study, aerobrake mass is considered 'active.'

*Fixed payload/variable IMLEO:* For aerobraked NTP options and fixed payload delivery at the baseline level, all but the low-thrust Open Cycle 1 engine performed substantially better than the cryo/aerobrake missions. Figure 30 demonstrates that an architecture incorporating NERVA could achieve the baseline with only 65% of the materiel emplaced in LEO. This savings is equivalent to the throwweight of 10 heavy-lift launch vehicles. Cermet and FPBR provided even more favorable numbers--the total Mars payload could be established for 2128.43 mT and 2122.97 mT, respectively.

Finally, for aerobraked lunar missions, FPBR and Cermet again require the least LEO mass for a fixed lunar payload (Fig. 31). Both NERVA and the Light Bulb engine benefit, however, from the reusability scheme, with the total Light Bulb LEO mass at 3639.53 mT.

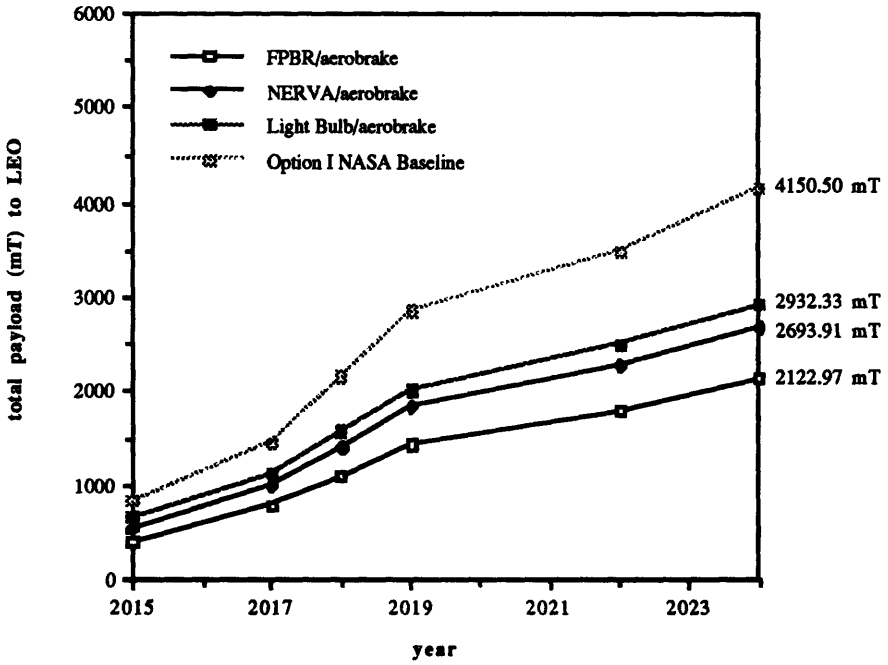


**Figure 30 Total payload in LEO required to support Mars operations for various NTP/Aerobrake alternatives to the Option I baseline**

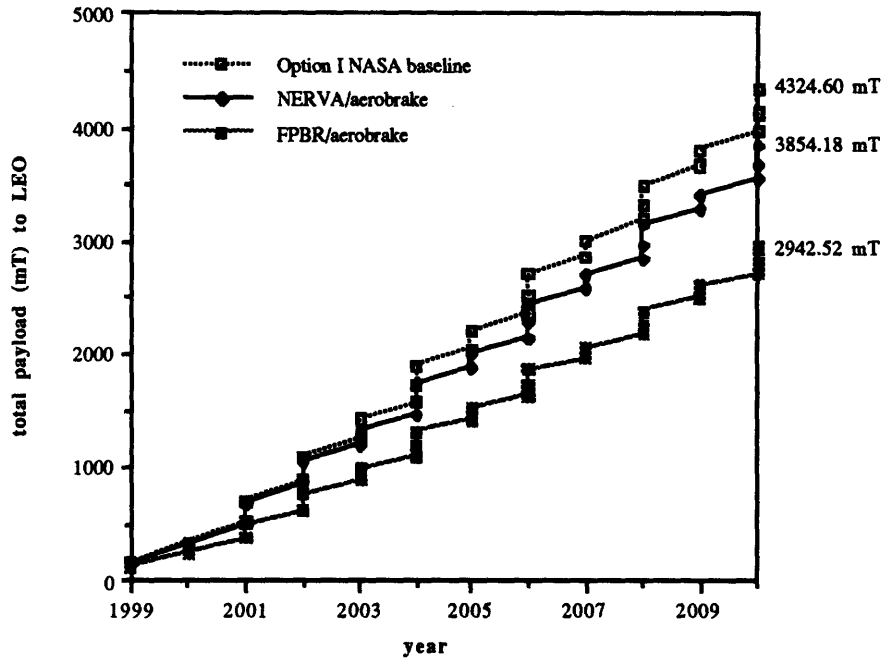


**Figure 31 Total payload delivery to LEO required to support lunar operations (1999-2010) for two NTP alternatives to the Option I baseline**

*Fixed IMLEO/variable payload:* Since NTP engines allow arrival at Mars with substantially reduced propellant expenditure, the encounter mass in low Mars orbit (EMLMO) is necessarily higher than the baseline for fixed IMLEO missions. Table 20 illustrates the EMLMO figures for Option I Mars Flight 6. The question naturally arises as to whether the baseline aerobrake would be capable of slowing the much heavier NTP encounter masses. A simple aerobrake model would be based on the following familiar equation for drag:

$$D \approx \rho v^2 C_D A \qquad (18)$$

$C_D$ is the drag coefficient, while A represents the effective area of the brake. If the atmosphere is taken to be of reasonably constant composition (constant $\rho$), the drag force on the aerobraked vehicle can be approximated, knowing the atmospheric entry velocity. The key here is to gain a rudimentary understanding of how the mass of the brake will vary with the mass of the vehicle. Clearly, the force required to brake the vehicle, and thus the necessary drag, will vary directly with the vehicle mass. Then, if the aerobrake has a reasonably constant mass/area, the brake mass will vary directly with the vehicle mass. A doubling of vehicle EMLMO will then be construed to roughly require no less than a doubling of the brake mass (although it is clear that

the increase of stress in the aerobrake as the brake mass increases will cause the relation to be of a higher than linear order).

**Table 20 Encounter Mass in Low Mars Orbit for Various NTP/Aerobrake Alternatives (Option I Mars Flight 6), for Fixed IMLEO/FMLEO**

| *Propulsion System* | *Total Vehicle EMLMO (mT)* | *Payload to Mars (mT)* | *Brake Mass (mT)* |
|---|---|---|---|
| 90-Day Baseline (678.7 mT) | 197.29 | 15.40 | 20.70 |
| NERVA/Aerobrake | 320.83 | 110.39 | 33.66 |
| FPBR/Aerobrake | 367.81 | 160.80 | 38.59 |
| Cermet/Aerobrake | 367.67 | 159.26 | 38.58 |
| Open Cycle 2/Aerobrake | 346.96 | 27.73 | 36.40 |
| Light Bulb/Aerobrake | 346.66 | 91.35 | 36.37 |

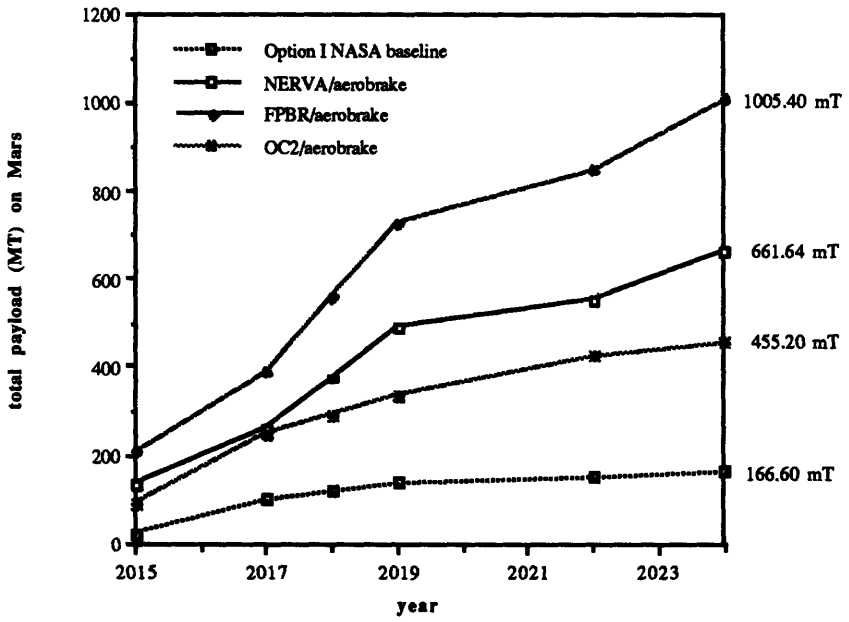


**Figure 32 NTP with Aerobraking versus Option I; total payload delivered to Mars for fixed IMLEO**

The FPBR/Aerobrake and Open Cycle 2/Aerobrake missions were reanalyzed for an augmented Mars/Earth aerobrake massing 40.7 mT, 20 mT *higher than that assumed in Figures 32 and 33*. For the FPBR mission, it was found that the payload deliverable to the Martian

surface decreased by 18.31 mT (from 160.8 mT to 142.49 mT); this overall decrease was seen to be the effect of increased TEI propellant consumption--as the difference in mass would have to be returned to Earth in the form of extra aerobrake--and decreased MEV propellant consumption at lower (465 s.) $I_{sp}$. As these propellant requirements approximately cancelled each other, the net effect of the increased aerobrake mass was to decrease the deliverable payload by almost exactly the amount of mass added to the brake. Similarly, the Open Cycle 2 mission had a deliverable payload decrease of 16.5 mT. The smaller difference results from the trade between increased MTV fuel consumption at an $I_{sp}$ of 1800 s. and MEV consumption at 475 s. In any case, extrapolating this result to Figure 32 indicates approximately 100 mT of delivery capability lost--a substantial loss but certainly not enough to change the nature of the results. The FPBR still would be capable of almost six times higher payload emplacement on Mars[55], while the Open Cycle 2 MTV could double payload on the Martian surface. However, the Open Cycle 2 was not able to place the baseline payload for Option V Flight 5 for the specified IMLEO.

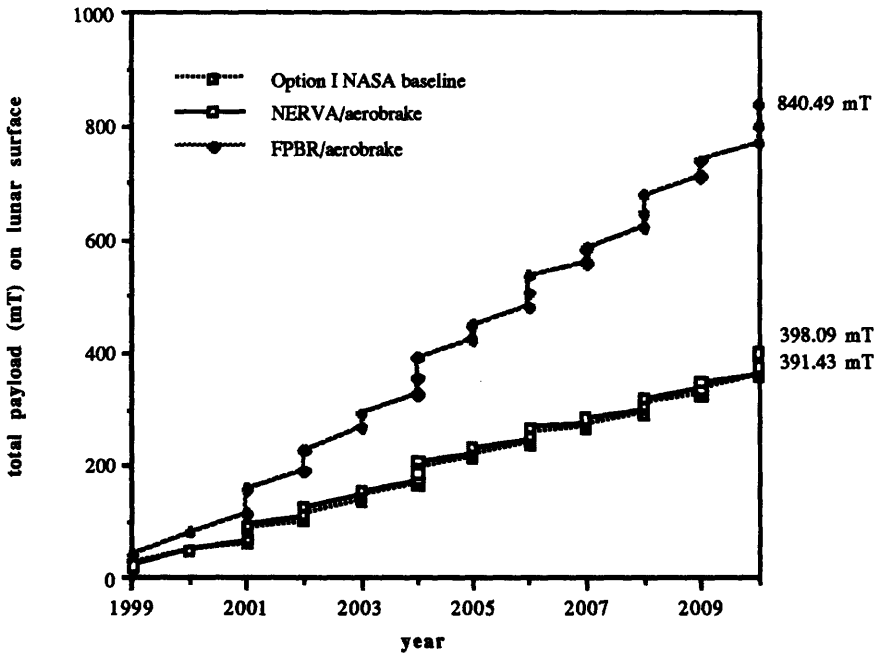


**Figure 33 NTP with aerobraking versus Option I; total payload delivered to the lunar surface for fixed IMLEO**

---

[55] The Cermet NDR mission is capable of delivery nearly on par with the FPBR-propelled MTV, approaching within 100 mT of its performance.

Lunar NTP missions augmented by aerobraking were not as promising for the high-$I_{sp}$ alternatives--none of the gas-core LTV's were able to perform a majority of the baseline missions, although the Light Bulb LTV could deliver some payload to the lunar surface for 15 of the 26 missions examined. Interestingly, the NERVA/Aerobrake combination produced results exceedingly similar to the 90-Day Study architecture (Fig. 33); the propellant savings achieved through the use of NERVA was entirely negated by its lower thrust/weight and consequently higher cluster mass. Both the Cermet and FPBR missions were capable of doubling the baseline payload.

As to the question of increased aerobrake mass to handle NTP transfer vehicles, the rationale offered for Mars missions holds true for lunar missions. An additional 3 mT of aerobrake mass to cover the increased mass on return to Earth results in approximately a 3 mT lunar payload decrease. Yet the FPBR would still be capable of over 750 mT in deliveries. NERVA would slip below the baseline.

**3.1.1.2 LV Upper Stage NTP:** There is substantial promise in the prospect of upper stage nuclear engines; the possibility was addressed late in the NERVA program and has been considered seriously for both SEI and the Strategic Defense Initiative. Clearly, lower stage use is ruled out on the basis of the engines' radioactivity and possible contamination of the environment. The engines examined in this section will be lightweight solid-core (NERVA, FPBR, and Cermet), as only they have sufficient T/W to be considered for ETO deliveries. The advanced engines are certainly not suited to this role, owing to their large mass.

The most important issue in upper stage use will be the eventual determination of nuclear safe orbits (NSO)--this could affect further development of NTP-enhanced launch vehicles. The upper stage will be activated only after first stage burnout and separation--the assumed $\Delta v$ provided to the vehicle at this point is 2000 m/s out of a total of 9200 m/s. This places the launch vehicle at approximately 60 km above the earth's surface, essentially beyond the atmosphere and far enough downrange from inhabited areas to pose little if any threat in the event of a failure of the second stage.

The baseline heavy-lift launch vehicle (Fig. 34) developed for this study is a simple design: three solid rocket motors (possibly STS-derived, $I_{sp}$ = 250 s., thrust/engine = 11000 kN at sea level) constitute the first stage. The second stage would consist of an SSME-style liquid engine ($I_{sp}$ = 465 s.). The assumed structural mass fractions of both stages of the baseline non-nuclear LV is .05. The gross lift-off weight (GLOW) was assumed to be 2000 mT; this will be held constant for the study.

The rocket equation gives a burnout mass prior to first-stage separation of 884 mT; once the

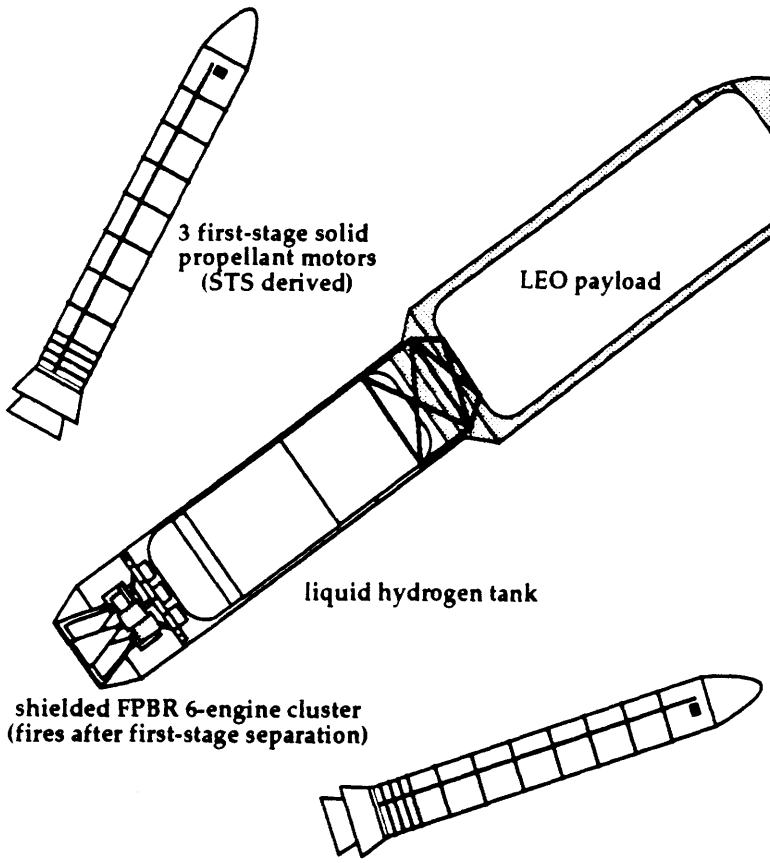


**Figure 34 Hypothetical next-generation launch vehicle with nuclear thermal propulsion aboard the second stage**

solids are ejected (58.7 mT), the liquid motor fires for the actual orbital insertion burn. On reaching orbital velocity, the vehicle mass is 170 mT, with a total delivered payload to LEO of 135.5 mT; this is only slightly less than the capability stated for the 90-Day Study Mars HLLV. The calculated structure is therefore 34.5 mT.

Replacing the liquid system with one of the SCR options could conceivably raise the amount of payload on-orbit for a given GLOW. If an FPBR ($I_{sp}$ = 900 s.) were used in the place of the SSME derivative, and the structural mass fraction ($\varepsilon$) of the second stage given to be .20, four times that for the chemical-propelled stage, the resulting delivered payload would be 249.7 mT, with the remaining mass of 115 mT being extra structure required due to the engine design. This assumption of high $\varepsilon$ is in line with the requirements for heavy shielding to protect crew aboard a manned mission, sensitive cargo, and to prevent propellant heating. If the engine's $I_{sp}$ is fixed at 900 s.(Fig. 35), and the structural mass fraction allowed to vary, it can be seen that, for the baseline payload of 135.5 mT, the nuclear stage could have an $\varepsilon$ as high as .33. Conversely, fixing $\varepsilon$ at .20 and allowing the $I_{sp}$ to decrease shows that the nuclear stage breaks even with the chemical system for an $I_{sp}$ of about 675 s. (Fig. 36). This is lower than all tested NERVA engines and far lower than that expected from either NERVA derivatives or the particle

bed. A four-engine FPBR cluster would mass only 4 mT--including a 10 mT radiation shield would prevent the difficulties associated with the high radiation flux from the engines, leaving

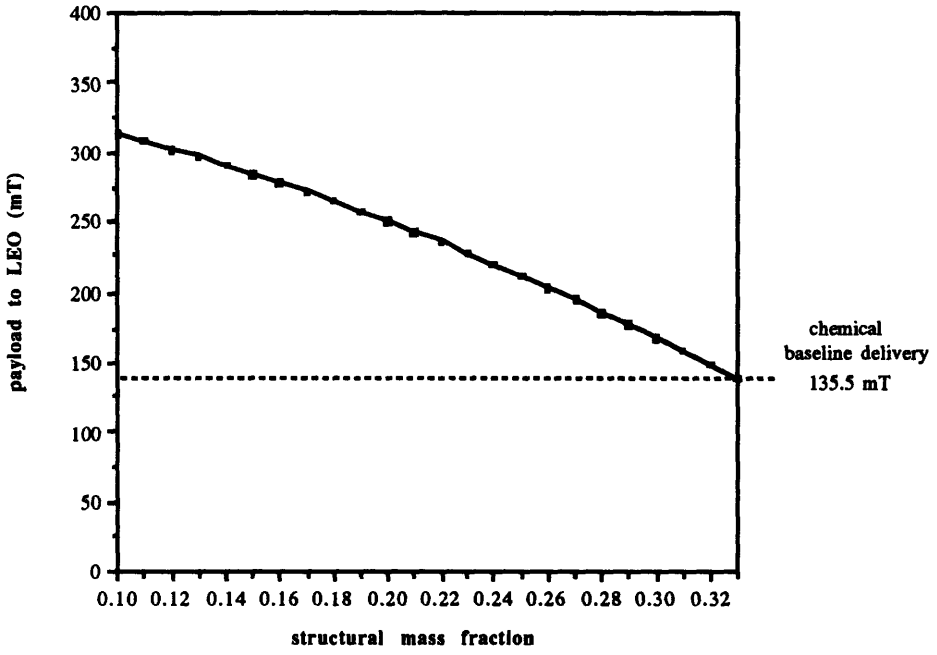


**Figure 35 Payload delivered to LEO by a nuclear second stage as a function of the stage's structural mass fraction ($I_{sp}$ = 900 s.)**

over significant mass to structure. This seems to indicate that the initial assumption of .20 for ε may be overly conservative, allowing even greater payload deliveries.

The number of launch vehicle flights is obviously dependent on the payload capability, and, if such a heavy-lift booster were used in place of the 90-Day Study HLLV, with the consequent doubling of payload to LEO, the number of flights could be halved. This would bring the total number of flights down from 187 (in the case of Option I) to almost 90. Coupled with the use of NTP on the orbital transfer vehicle and the use of split missions (discussed in the next section), this would further lower the total number of required missions or allow for even faster transfers than those picked in 3.1.2.

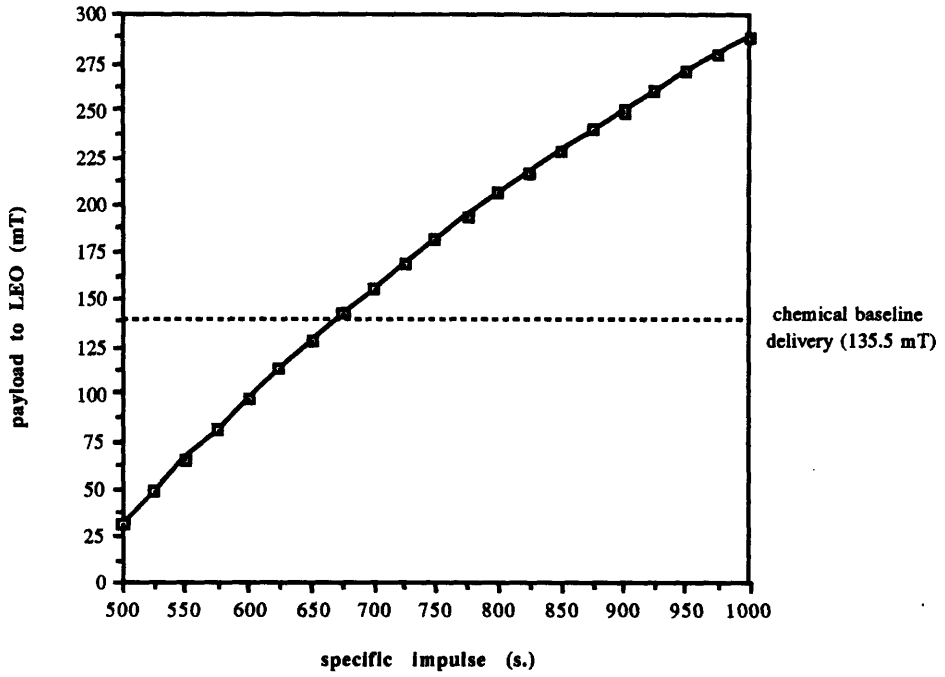


**Figure 36 Payload delivered to LEO by a nuclear upper stage as a function of the stage's specific impulse ($\varepsilon$ = .20)**

**3.1.1.3 Ascent/Descent NTP:** A trade study was performed to determine the amount of propulsion system mass freed up by exchanging the LOX/$LH_2$ engines of the 90-Day Study for NTP engines with increasing specific impulse. The lunar vehicle gross weight prior to descent was taken to be 50 mT, with a total dry weight (no propellant, no payload, no propulsion system) of 10.44 mT. The 90-Day Study states that the LEV contains four 230 kg. chemical engines.

Given the $\Delta v$ requirements in Table 21, the baseline system delivers 15 mT to the lunar surface. If the specific impulse of the propulsion system is raised while the delivery is held constant, extra mass is available to allocate to the nuclear propulsion system (including whatever extra shielding and structure was deemed necessary). If this propulsion system is substantially smaller than the amount of mass freed up by increased specific impulse, then the nuclear option could be considered viable. If an NTP option would weigh on the order of the free mass or more, then the chemical system would be preferred. The results of this trade are shown in Figure 37 for $I_{sp}$ values ranging from 465 to 1100. For the FPBR ($I_{sp}$ = 900 s.), the total propulsion system mass would have to be lower than 9600 kg. for it to be a viable alternative. A NERVA system would have to mass 9000 kg. or less.

**Table 21 Mars Mission Δv requirements**

| Mission | Lunar descent | Lunar ascent | Mars descent | Mars ascent |
|---|---|---|---|---|
| delta-V (m/s) | 2000 | 1900 | 1360 | 5763 |

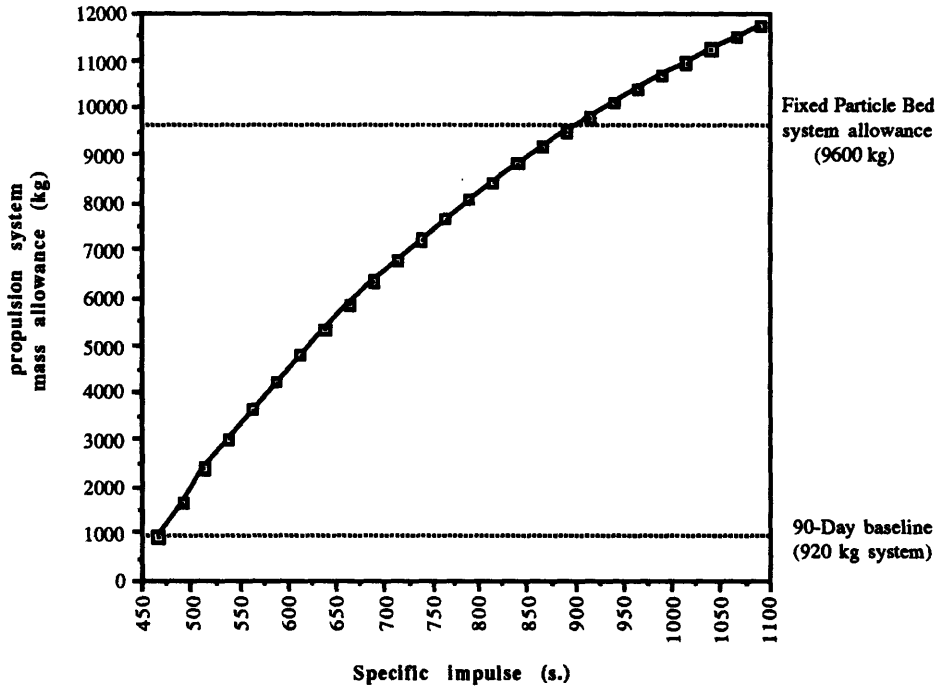


**Figure 37 Lunar excursion vehicle mass allowance for its propulsion system as a function of increasing specific impulse**

A similar trade was conducted for a Mars Excursion Vehicle (Fig. 38). The total vehicle weight prior to descent was taken to be 80.5 mT, with a 6 mT mass on return to orbit following descent and jettisoning of the aeroshell (9.3 mT), delivery of 25 mT of Mars cargo, and discarding of the descent stage (6.5 mT). The FPBR system would have to be somewhat lower than 10 mT to replace the chemical ascent/descent scheme.

While ascent/descent use is favorable at first glance on the basis of specific impulse considerations alone, further research shows that operation of the reactors on or near the surface of the moon or Mars will cause unacceptable contamination problems and require extensive precautions against exposure (detailed in Section 3.2.2). Additionally, the shielding necessary to hold the crew's absorbed radiation dose to 5 rem over the engine's operating period would be

on the order of the mass margin (10 mT) afforded by doubling the specific impulse to 900 s.

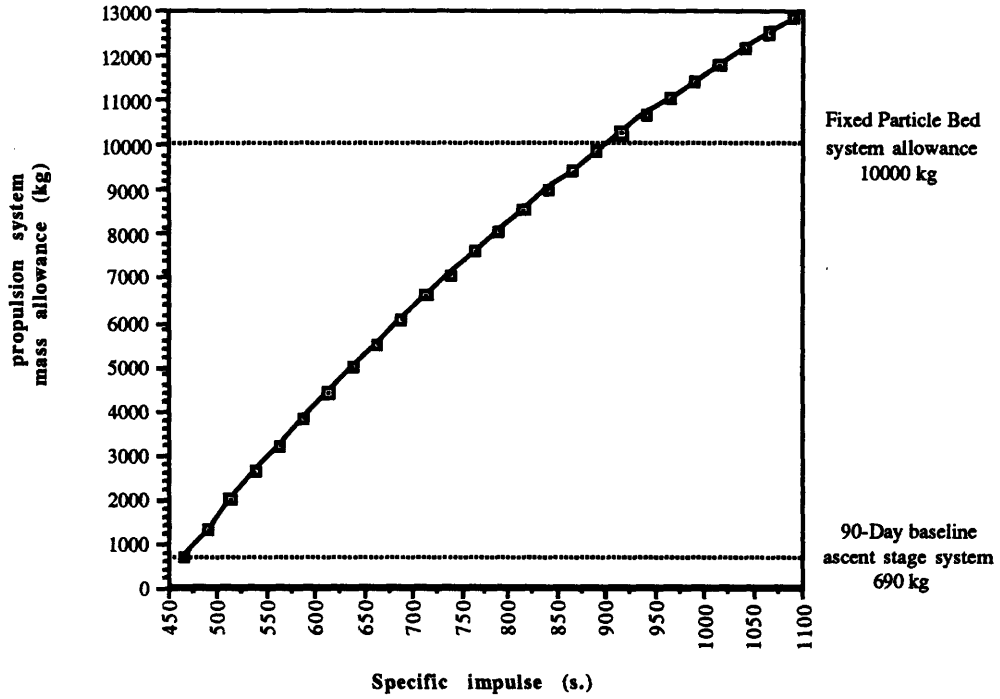


**Figure 38 Mars excursion vehicle mass allowance for its propulsion system as a function of increasing specific impulse**

### 3.1.2 Variable Duration Missions

This section examines the variation of performance displayed by NTP options versus the NASA 90-Day Study baseline missions. The severe life support requirements for the Martian missions are not encountered in the lunar transfers, due mostly to their relatively short duration; hence, for this portion of the study, lunar missions will not be considered. Heretofore, gas-core engines have performed fairly badly. At the low Δv transfers of the 90-Day Study, the propellant savings is clear but not even an order of magnitude better than the baseline. This handicapps the gas-core rocket, which is capable of high performance at larger Δv's. As transfer times shorten appreciably (time spent aboard the spacecraft under 180 days, as opposed to the 500 or more of the baseline), Δv requirements grow drastically--beyond the means of a low-$I_{sp}$ engine cluster such as the cryo/aerobrake system to handle for reasonable cost. Additionally, the use of an aerobrake sets strict limits on insertion velocity: The baseline missions propose an upper limit on Mars and Earth entry of 9500 m/s and 12500 m/s, respectively. This severely restricts the cryo/aerobrake system to very low transfer Δv's and long transfer times.

To find useful trajectories to trade against the baseline, MULIMP was used extensively. Missions were divided into (1) Short stay times (30-90 days), (2) Medium stays (180-300 days), (3) Long stays (500-550 days), and (4) Protracted stays (700+ days).[56] All figures for $\Delta v$ are given assuming all-propulsive transfers, with no aerobraking. Aerobraking tends to half the figures; however, as explained above, for significant decreases in transfer time it is necessary to go to trajectories with MOI and EOI figures higher than is considered acceptable (or practical) for forecasted aerobrakes.

MULIMP produced optimum trajectories based on the following assumptions:

(1) A fixed total trip time with a specified launch date,

(2) no use of Venus gravity-assist swingbys, and

(2) a fixed stay time

For instance, a 200-day/30-day stay mission (abbreviated 200/30) could be calculated for specified launch dates between 1 January 2000 and 1 January 2016--providing a clear picture of the entire periodic $\Delta v$ variation of this particular mission. Such a picture is displayed in Figure 39. If a certain launch date is requested, MULIMP will calculate the minimum $\Delta v$ mission given the parameters above, adjusting the 30-day stay time requirement within the 200-day window. In August 2007, the minimum-energy 200/30 trip is a 96-30-74 mission requiring a total $\Delta v$ expenditure of 51599 m/s. Yet a month later, the minimum-energy mission is an 85-30-85, with a $\Delta v$ of 54024 m/s. The increase is ~5%, but it is a much larger step than an equivalent margin on the baseline missions, where total $\Delta v$ seldom exceeded 10 km/s. Venus swingbys offer substantial $\Delta v$ savings but were discarded in this study on the basis of their long trip times. "Venus swingbys are seldom if ever helpful for one-way transfers...when the transfer time is required to be shorter than 250 days."[57] One goal of this study is to produce reasonable mission alternatives with one-way transfers near 90 days, significantly shorter than the 250-day minimum necessary to use Venus gravity-assist trajectories.

Figure 40 illustrates a compilation of data gathered from a number of charts like that in Figure 39. Here, the envelope of total mission $\Delta v$ can be seen and a general trend extrapolated. It

---

[56] The nomenclature followed in this section will be (outbound transit time)-(Mars stay time)-(inbound transit time), such that a 93-30-77 mission would entail a 93-day transfer from Earth to Mars, a 30-day Martian stay, and a return trip of 77 days. Incidentally, this 200-day/30-day stay mission would prove rather costly in terms of fuel--the minimum energy transfer for 200/30 occurs near the middle of 2003, for a total $\Delta v$ of 33912 m/s.

[57] Fast Round-Trip Mars Trajectories, p. 510.

seems intuitive that, as trip time decreases for a fixed Martian stay time on Mars, the total

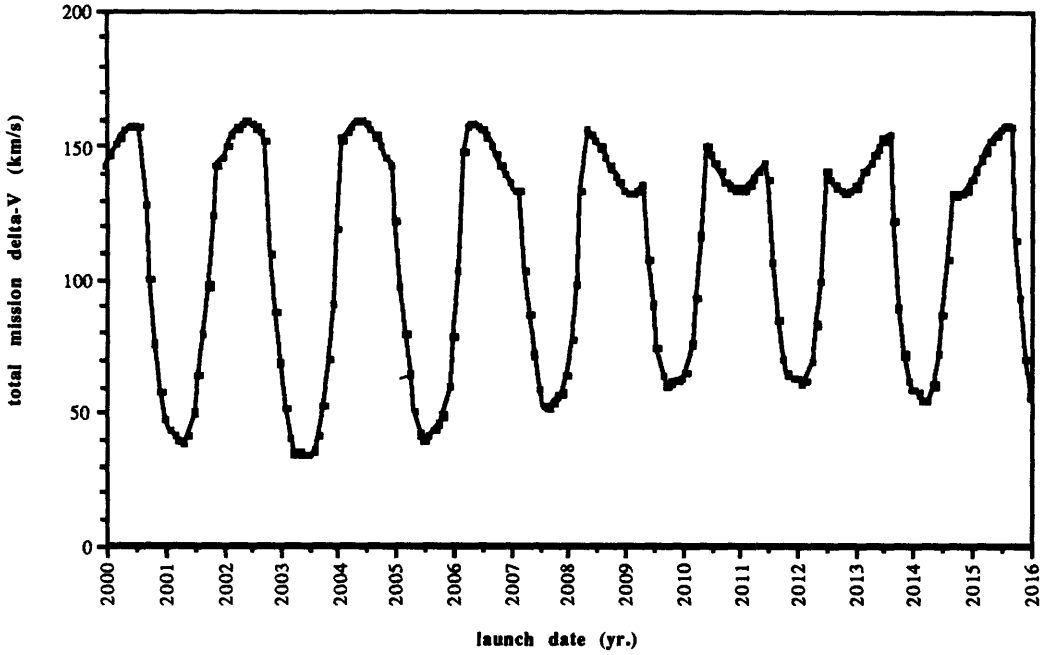


**Figure 39 200-day trip time with 30-day stay, for the period 2000-2016**

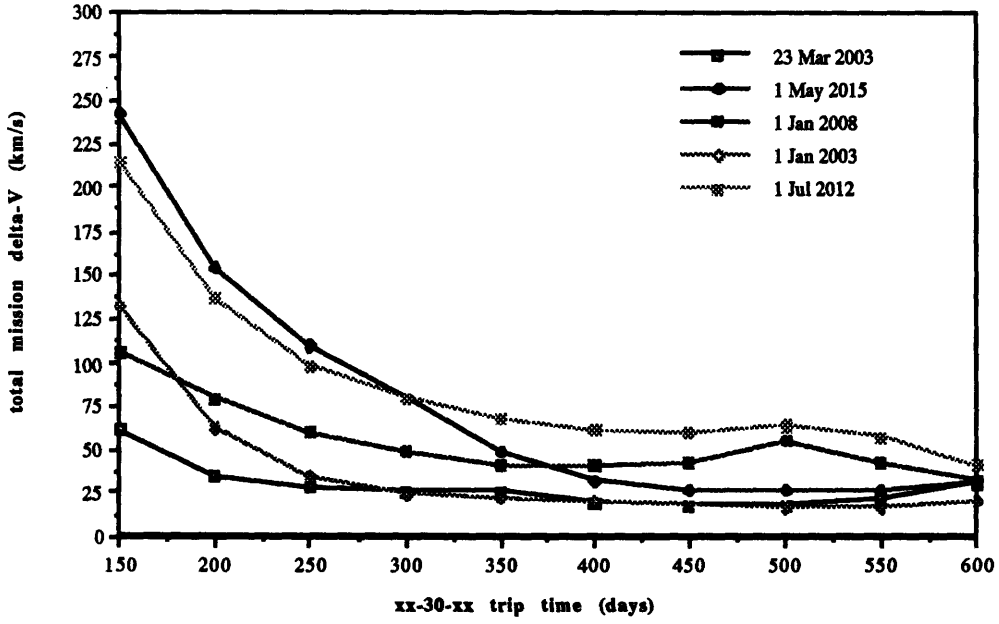


**Figure 40 Envelope of 30-day stay missions for variable trip time**

mission Δv should rise; however, this is not always the case. It certainly does not hold for very lengthy missions, where the outbound transit may pass far beyond the orbit of Mars before encountering the planet. As these missions become longer and longer for the fixed stay, the Δv moves through a minimum and begins to rise slowly. The dates chosen represent minima or maxima of the Δv for various trip times. Comparing the rise and ebb of the 200/30 trip to its envelope in Figure 40 shows remarkably close agreement.

**3.1.2.1 Short Stay Missions:** The 30-day stay case was examined in detail, and the variations in total propulsive Δv from trip times of 150 days to as high as 650 days shown in figures 40-42. As mentioned in Section 1.2, the cycle of variations recurs with a period of 15 years--this is true for missions of all classes. The best cases for departure occur in 2001, 2003, and 2005, with the global minimum in 2003 (therefore 2018, 2033, etc.)--total mission Δv for a 550/30 in 2003 is approximately 17 km/s. These minima are consistent as the total trip time varies from 150-500 days. Both the 60-day and 90-day stay cases (Figures 41, 42) follow the 30-day pattern, with a global minimum Δv in 2003. However, their minimums are slightly higher[58], and it can be seen that, as the stay time increases from 30 to 90 days, there is a steady increase in Δv requirements and an incentive to keep short trips as short as can be achieved. Essentially, conditions for return are best immediately upon arrival at Mars. Worst-case minima occur in 2009 (2024, 2039, ...) and 2011-12 (2026-27, 2041-42, ...).

Very long trip times (850-900 days) produce minimum Δv figures lower than the 500/30 value. An 850/30 flight is capable of a total Δv approaching 14 km/s--yet this trip is not under consideration in this study for piloted missions, due to the very lengthy transit time it enforces upon potential Mars explorers.

Very short trip times (150-200 days) require immense propellant expenditures from all but the gas-core engines. This is clearest in the 150/90 case, where the minimum Δv is approximately 150 km/s. To understand the significance of such a large velocity change, a 1000 mT mission propelled by a 5000-s. $I_{sp}$ gas-core engine would achieve this change by expelling over 953 mT of propellant, leaving over 47 mT to structure and payload. A mission powered by a cryogenic LOX/$LH_2$ engine ($I_{sp}$=475 s.) could achieve a 47 mT payload for this Δv only with an initial mass of $4.64 \times 10^{15}$ mT, necessitating over a *trillion* times the propellant expenditure of a gas-core engine. The vast difference between initial masses for these high Δv figures shows why gas-core and other high-specific impulse alternatives are under examination.

---

[58] 60-day minimum = 18 km/s., 550-day stay; 90-day minimum = 20 km/s., 550-day stay

This was not as clear at minimum-energy transfer values, where high thrust/weight nullified the

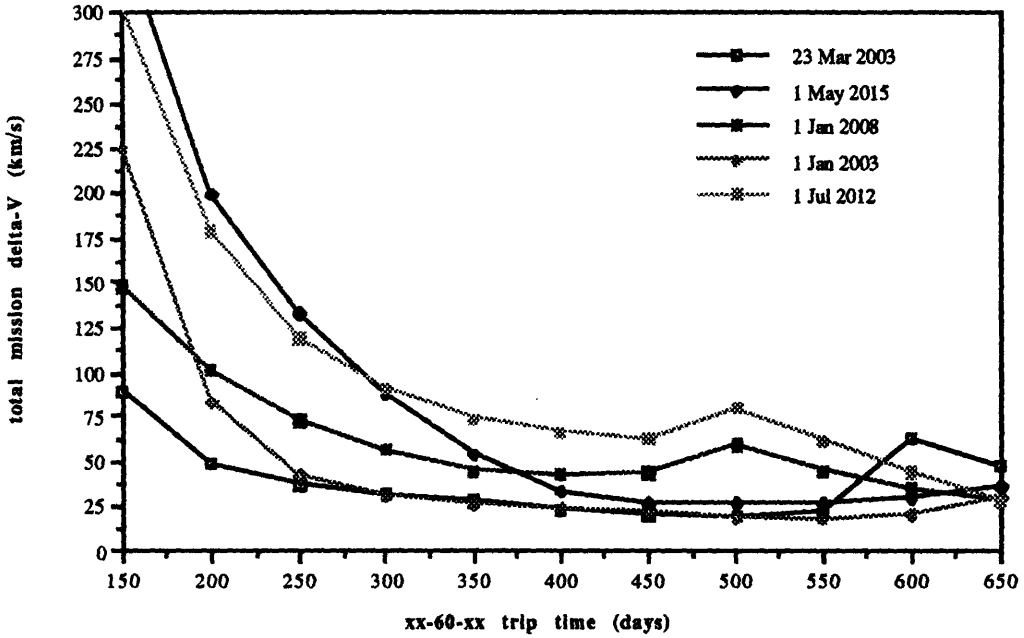


**Figure 41 Envelope for 60-Day stay times**

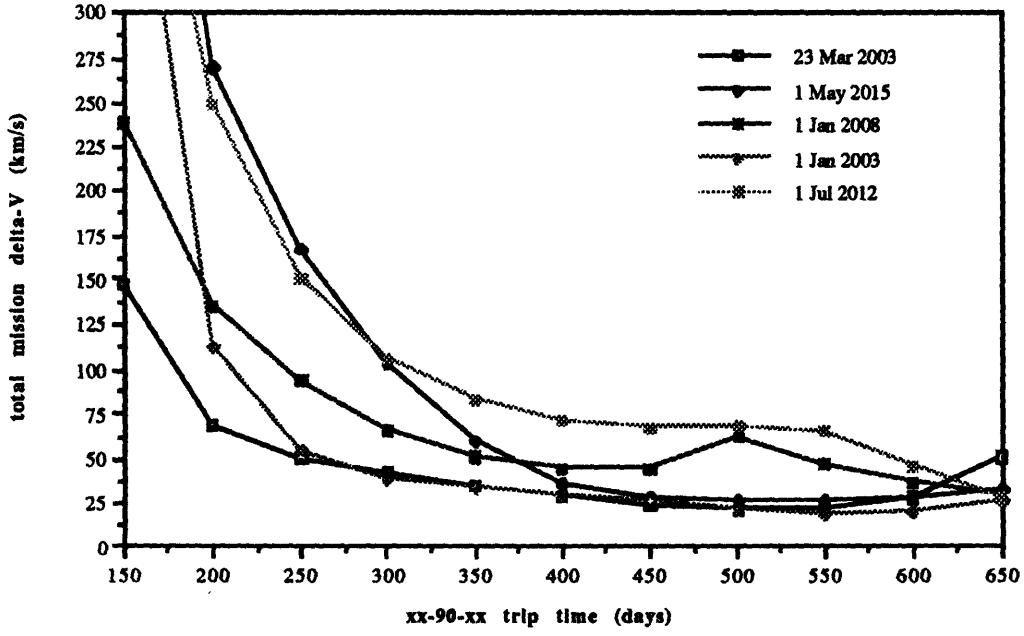


**Figure 42 Envelope for 90-Day stay times**

disadvantage of the cryo/aerobrake system's low $I_{sp}$. For fast transfers, chemical engines of any type can quickly and safely be disqualified from consideration. The question is not whether chemical engines can perform such missions--they are incapable--but if such transfers are desirable or perhaps even necessary, given the information presently known about the hazards of lengthy transits.

**3.1.2.2 Medium Stay Missions:** Figure 43 represents a typical succession of medium-length stay opportunities. The 500/240 trip can also be seen in Figure 44, where it ranges in $\Delta v$ from 37 km/s. (June 2002) to a maximum of ~100 km/s. in August 2012. The best cases occur in 2001, 2002-03, and 2004-05. Highest minimum $\Delta v$ missions can be seen to occur in 2009 and again in 2011. Figures 44, 45, and 46 show a remarkable flatness to the envelope in the 650-day range--with the effect most pronounced for 650/300 missions. The 650/300, ranging as it does from 39 to 47 km/s., does not provide single-mission performance as high as, say, an 850/300 mission ($\Delta v_{min}$ = 12 km/s.), but it would provide extended launch windows to future mission planners with access to high-$I_{sp}$ (gas-core) engines. Neither the cryo/aerobrake baseline nor solid-core systems can handle even these moderate $\Delta v$ requirements.

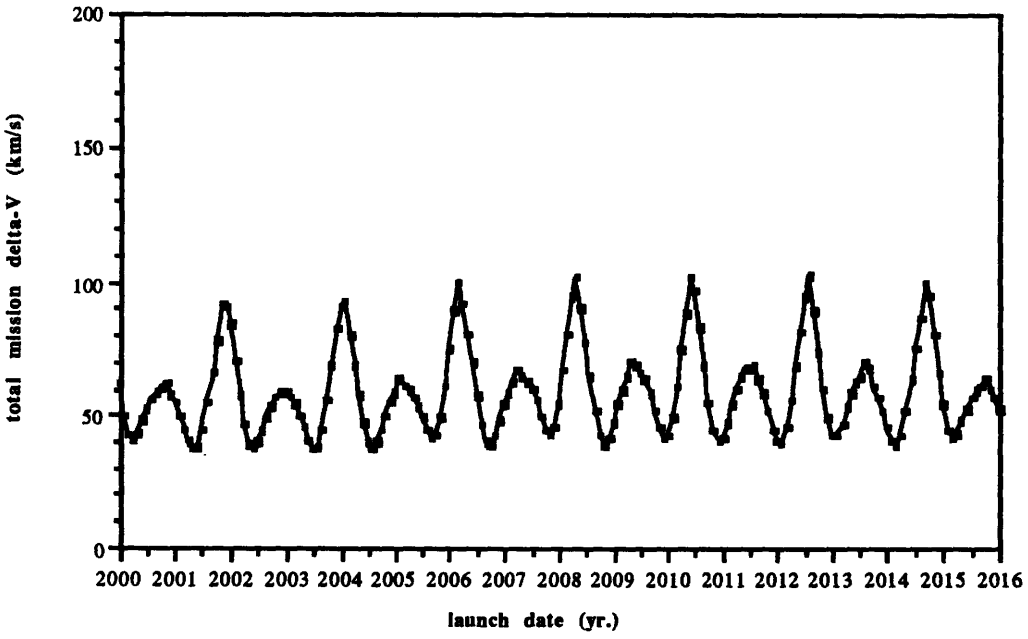


**Figure 43 500/240 mission opportunities**

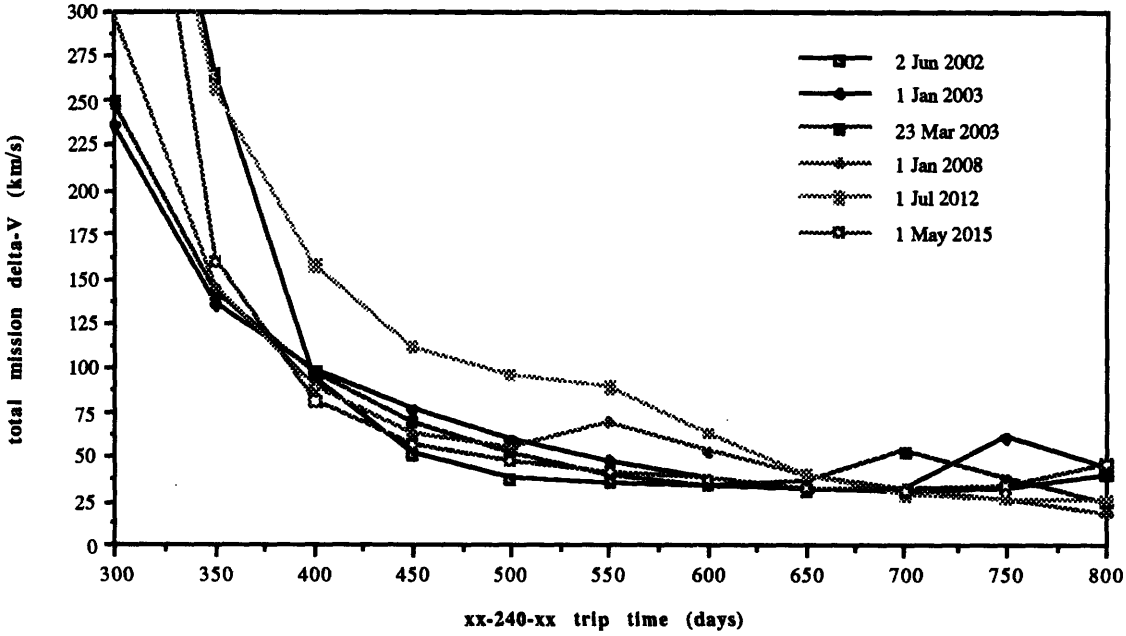


**Figure 44 Envelope for 240-Day stay times**

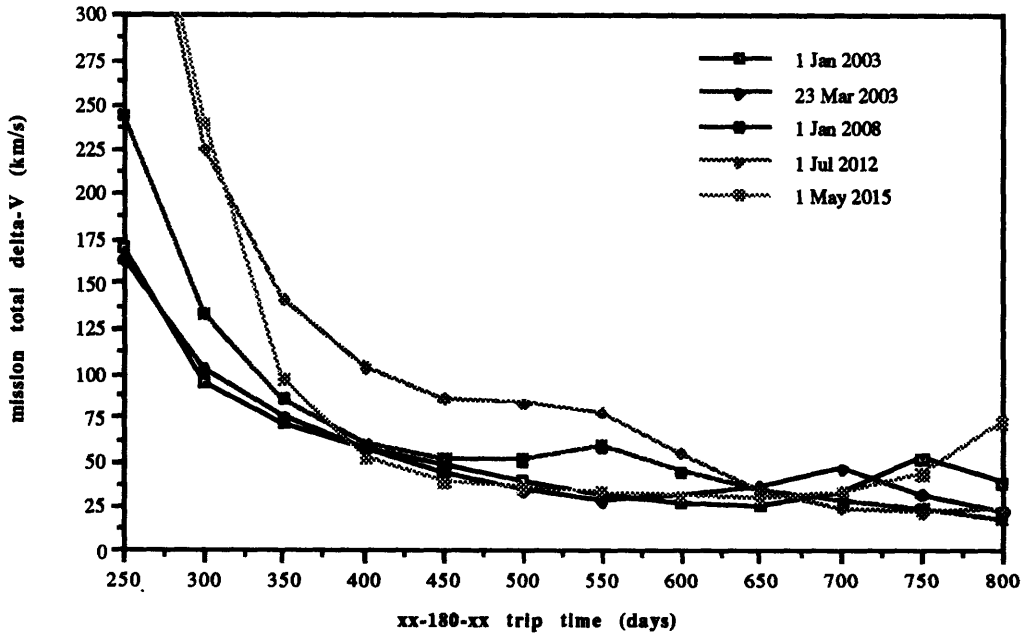


**Figure 45 Envelope for 180-Day stay times**

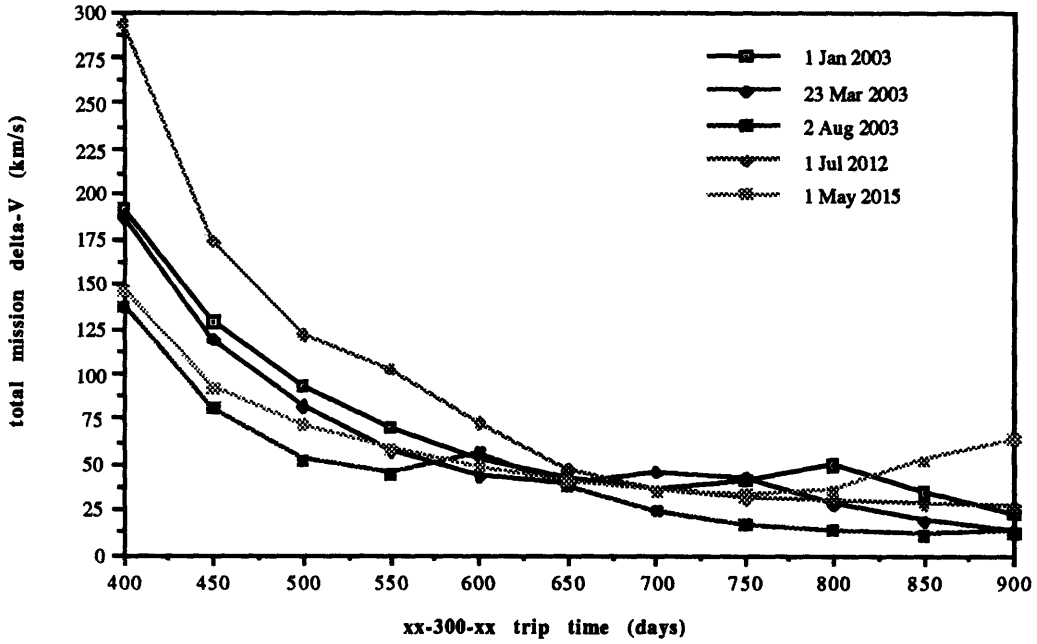


**Figure 46 Envelope for 300-Day stay times**

The general trend for 180-300 day missions is a tendency towards lower total Δv as trip time increases. This is understandable as "long stay" or conjunction class missions, examined in the next section, allow for the lowest total Δv of any mission type. Conditions become steadily less favorable as stays increase from 30 to 90 days, plateau in the region between 90 and 180 days, and then become increasingly better as the trip more and more resembles a conjunction-class (double-Hohmann) mission. Very short trips combined with these medium stays (e.g. 450/300) require upwards of 75 km/s. to accomplish, and are beyond the abilities of all but the gas-core engines.

**3.1.2.3 Long Stay Missions:** 500-day and 550-day stay times provide for the least propellant expenditure of all missions. Minimum Δv figures for 850/500, 900/500, and 950/500 all tend to bottom out at 11.5 km/s., whereas their 550-day counterparts have minima in the 1050-1100-day range. High variations, up to 50 km/s., in total Δv across a given synodic period creates tight launch windows (Figures 47, 48). Best cases can be achieved in 2001 and 2003 (reoccurring in 2016 and 2018), while these minima are at their largest in 2009-10 (2024,2025). There is only a very slight variation from synodic period to synodic period for these low-Δv opportunities (Figures 49, 50).

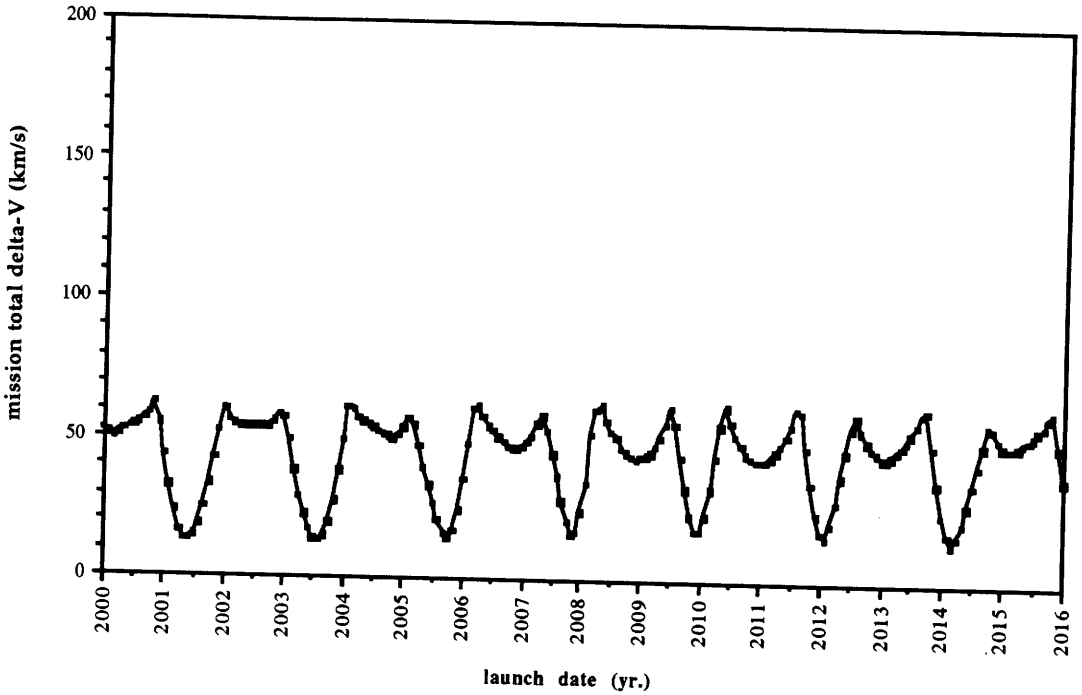


**Figure 47 850/500 mission opportunties**

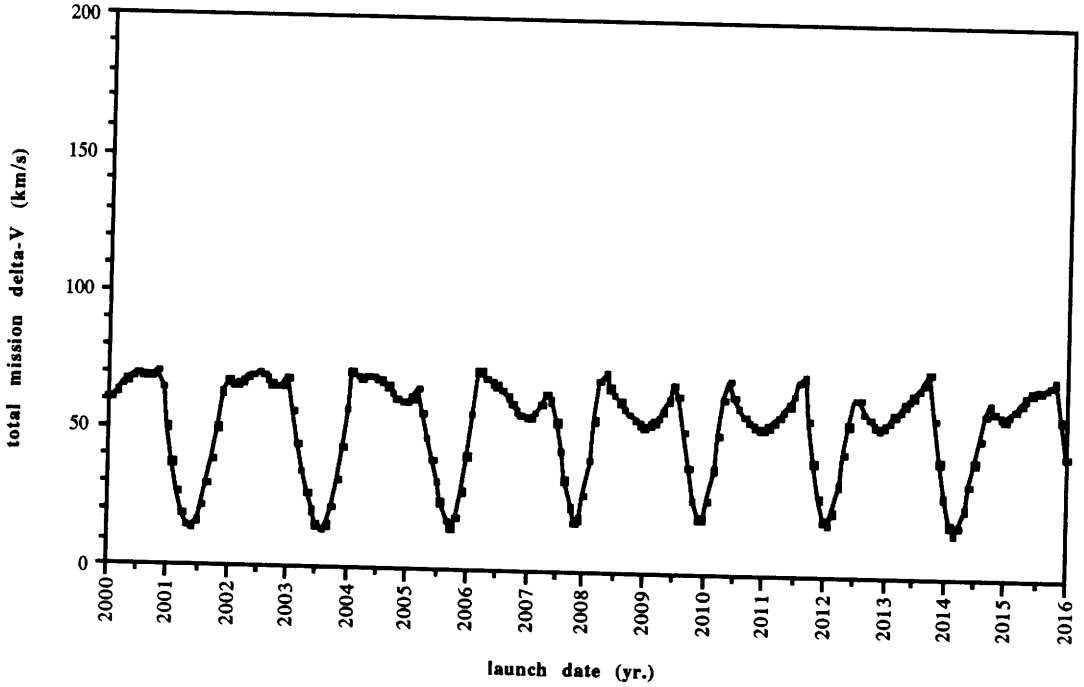


**Figure 48 850/550 mission opportunities**

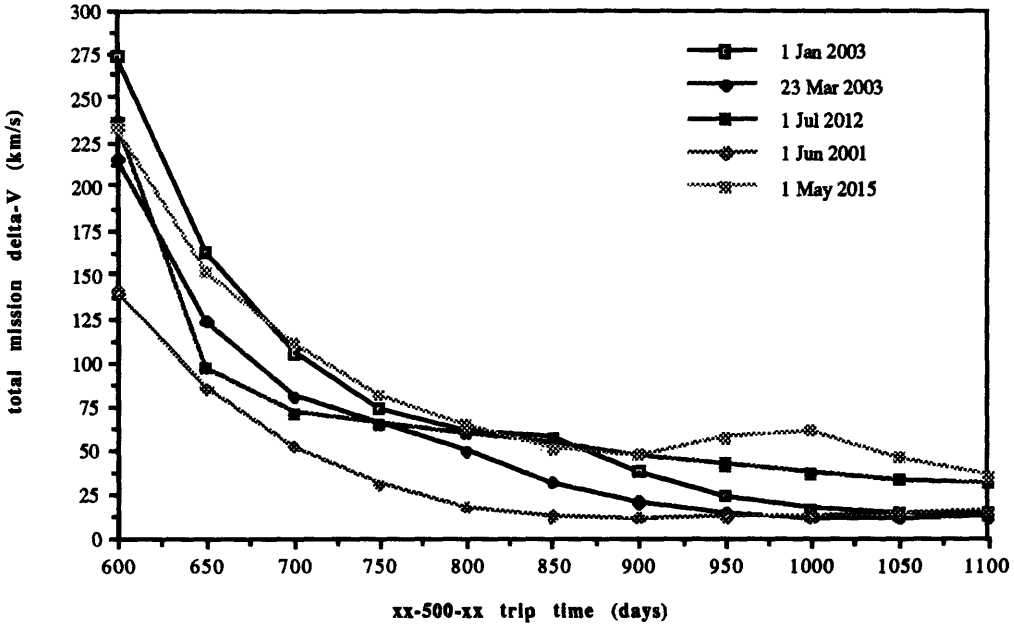


**Figure 49 Envelope of 500-Day stay times**

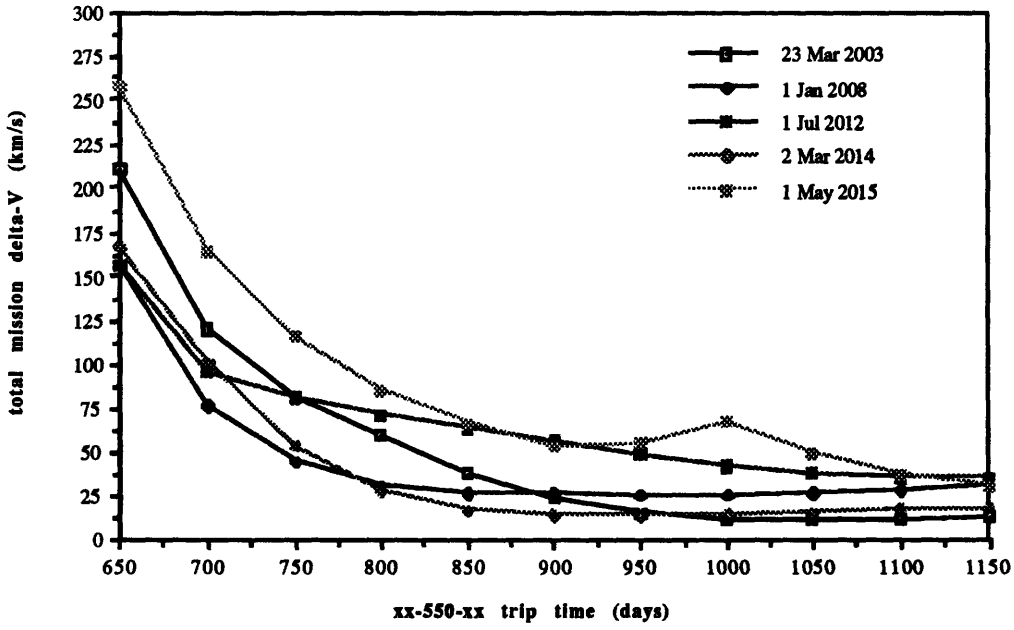


**Figure 50 Envelope of 550-Day stay times**

Several of the NASA baseline missions fall within this region or slightly above it, with stay times of 474-659 days.

**3.1.2.4 Protracted Stay Missions:** Increasing stay time beyond the conjunction class times (700-850 days) produces trajectories which are fairly expensive in terms of total Δv. These missions are usually not examined in depth due to their large Δv requirements but are presented here to explore possible limits on mission duration. Figure 51 shows a 1000/750 mission; it is reasonably shallow but never drops below 45 km/s. The 700-day and 750-day stays (Figures 52, 53) both exhibit this behavior, with shallow Δv envelopes but minima in excess of three times that of the minimum-energy transfers. The 850-day stay (Figures 54, 55) is characterized by decreased minima--in the range of 30 km/s. for 1050-day total trips. This appears to be the result of extending the wait significantly beyond the conjunction class figure of 500-550 days--an 850-day stay is equivalent to remaining on Mars almost halfway through the next synodic period. Were this extended to ~1300 days, it would in effect be waiting until the conjunction-class configuration reoccurs.

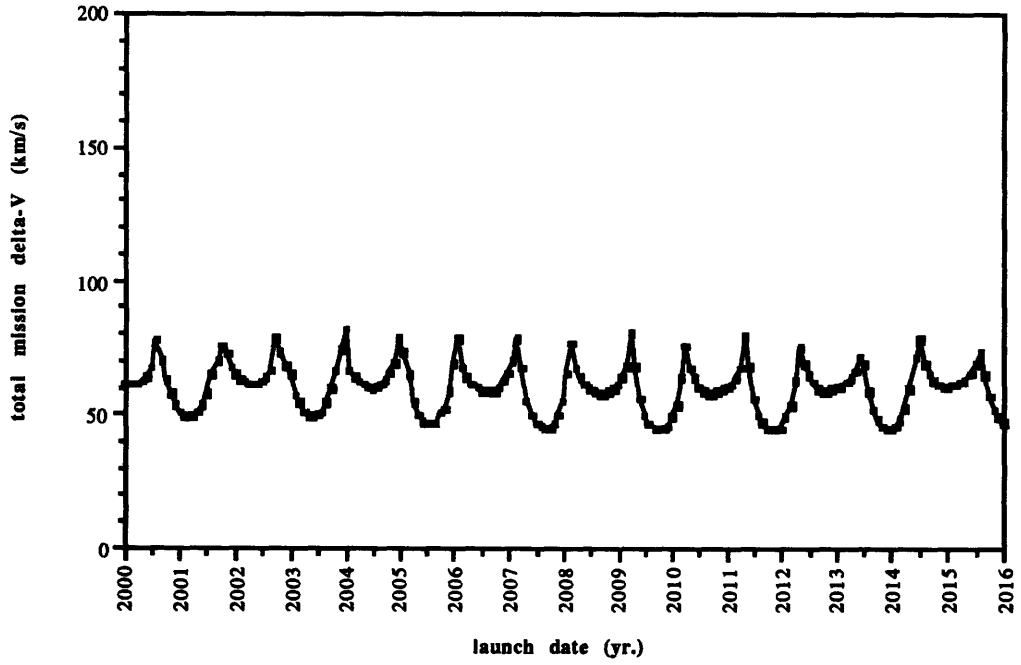


**Figure 51 1000/750 mission opportunities**

The 700-day stay is characterized by odd behavior of the minimum, which occurs at 900/700. This is a remarkably short trip time relative to the total stay, but is not very useful, as

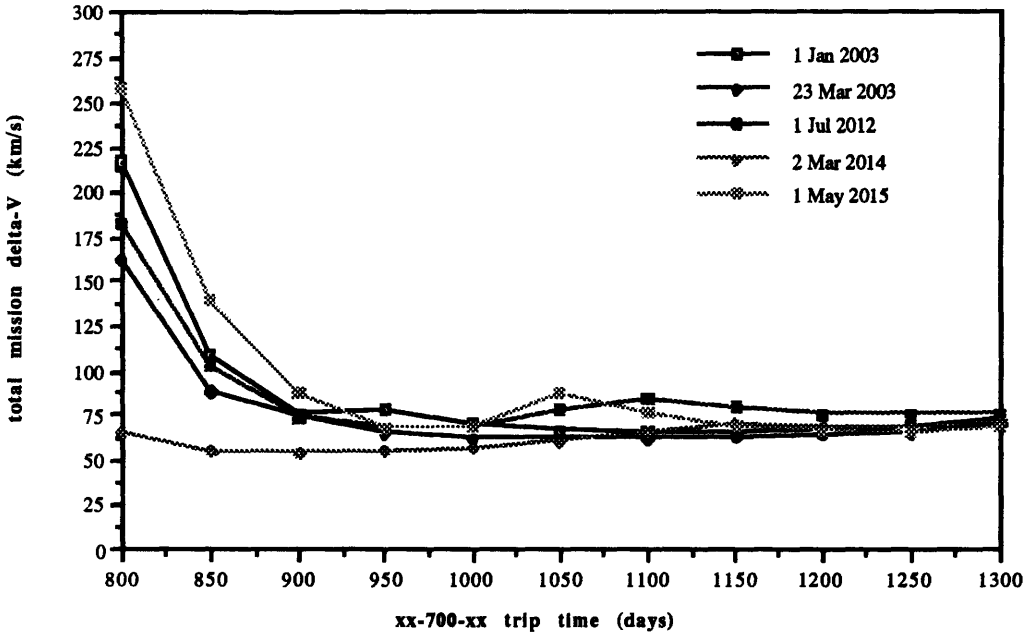


**Figure 52 Envelope of 700-Day stay times**

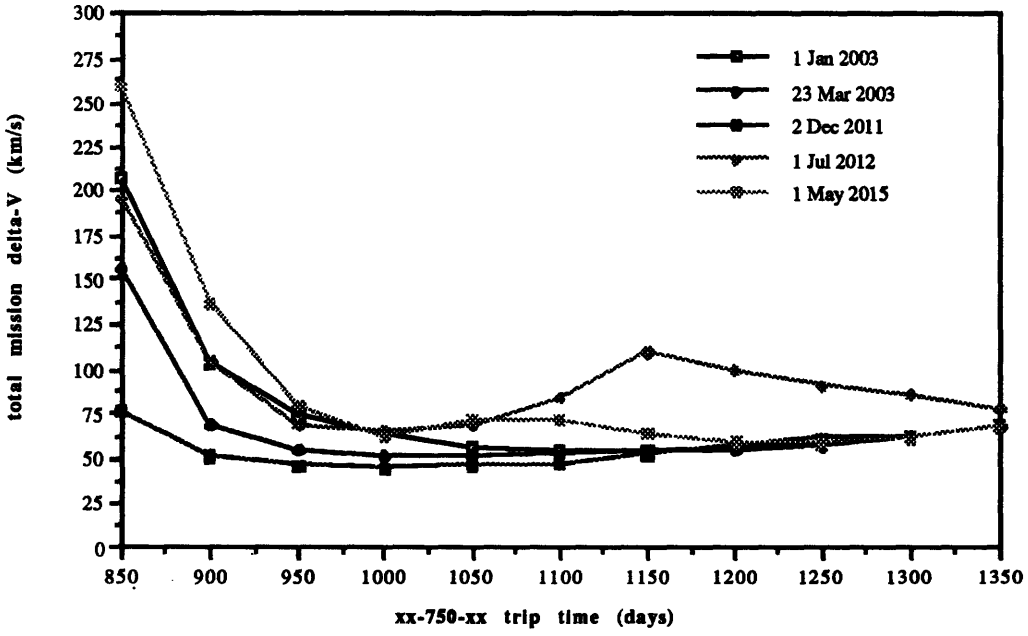


**Figure 53 Envelope of 750-Day stay times**

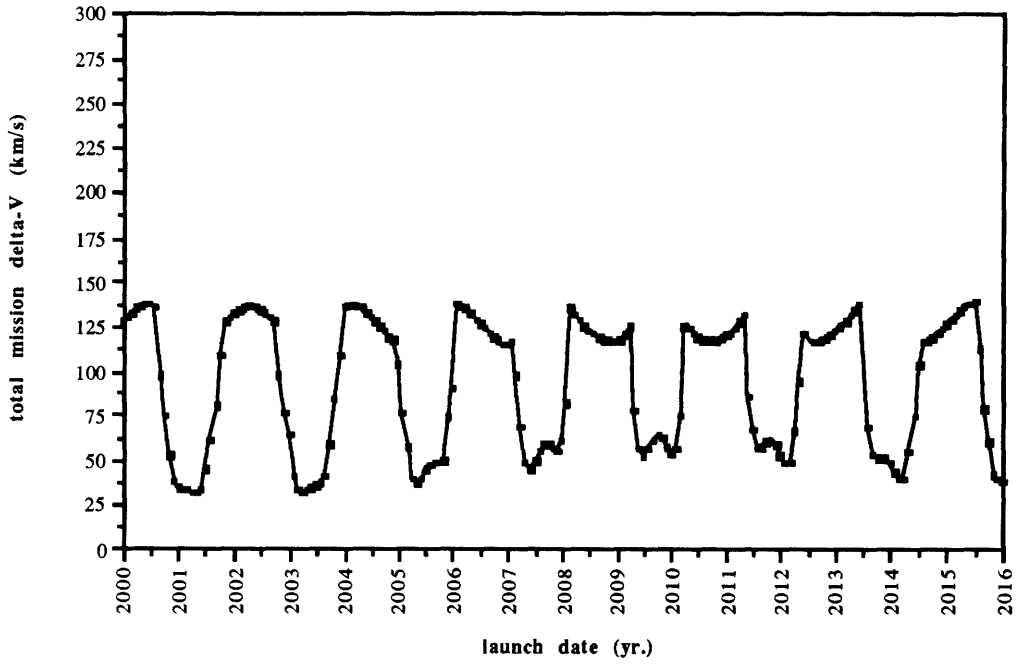


**Figure 54 1000/850 mission opportunities**

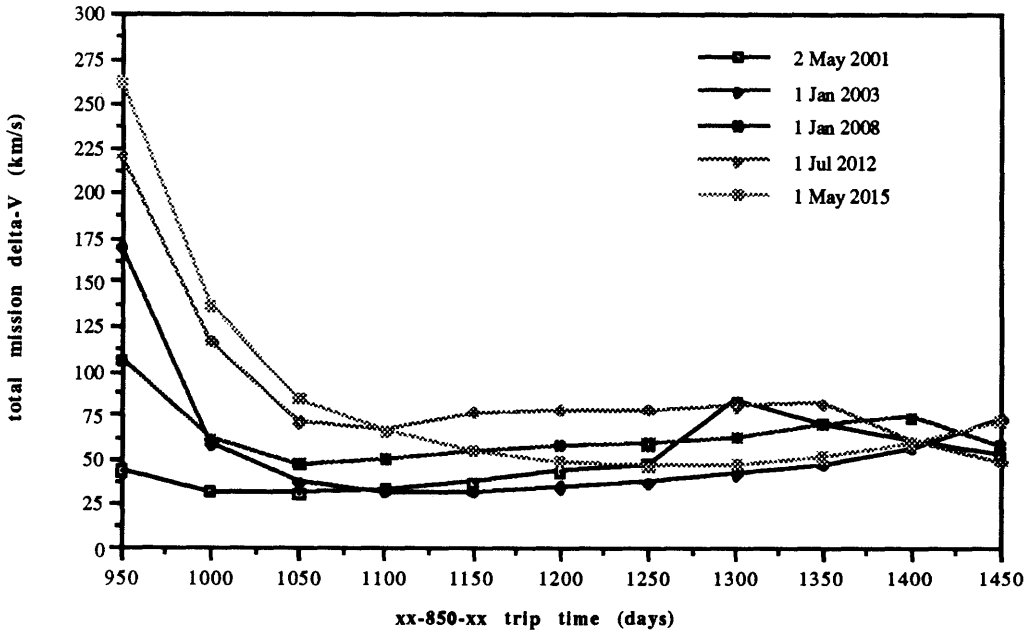


**Figure 55 Envelope of 850-Day stay times**

it happens for a $\Delta v_{min}$ of 55 km/s. These protracted missions appear to be fairly difficult, as they would not be simply expensive but would also require additional consumables and safeguards to protect against the failure of critical systems--especially life support--over such an extended journey. 1000/550 missions appear to be justifiable on the basis of their minimum propellant requirements, but longer trips do not seem to possess significantly greater benefits that could balance the increasing probability of catastrophe as trip time extends beyond three years.

**3.1.2.5 All-Up Alternatives to the Baseline:** This section analyzes the performance of NTP-propelled missions using the baseline IMLEO/FMLEO and fixing the payload deliveries to that established in the 90-Day Study. In this way, any surplus mass will translate into propellant mass that could be used to decrease transfer time between Earth and Mars. The 90-Day Study stay time for the missions, as well as the engine cluster configurations of Table 17, will also be held constant. Cargo missions (such as Option I Mars Flights 2, 5) will not be addressed, as the need for decreasing trip time apply mainly to piloted missions.

The first mission examined was Option I Mars Flight 1, a piloted opposition-class flight slated to launch in May 2015. The relevant statistics for the baseline mission, as well as those for reduced duration missions, are shown in Table 22. The $\Delta v$ figures used for the variable duration missions were typically not May 2015 values but global minima for their respective mission classes.

Option I Mars Flight 6, a piloted conjunction-class mission with a 484-day stay time, was also analyzed. Pertinent data relating to it and its alternatives in Table 23. 500-day stays were used as approximations to the 484-day stay.

The variable trip time missions shown here were calculated for their minimum total $\Delta v$ requirements over the 16-year period 2000-2016. For instance, the 350/30 mission in the table would be launched on 2 May 2001, the global minimum for trips of its type. This date was used as an example only; this mission type would reoccur with the 15-year period explained earlier, such that a similar trip could be performed in mid-2016. 15% margins were added to each $\Delta v$ figure to account for gravity losses and launch window variations.

Since the 90-Day Study relied on aerobraking for its MOI and EOI, there was no requirement to minimize the propulsive $\Delta v$ needed at these times--so long as entry velocities stayed below the ceilings set by the aerobrake design. All-propulsive systems would better be served by minimizing the total $\Delta v$ or by minimizing the first two burns, since they will of course require far and away the largest fuel expenditure (once the payload is dropped at Mars, an increase in TEI or EOI $\Delta v$ will not have the impact on propellant mass that it would have on departure from LEO, since the vehicle weight at TEI is significantly smaller than on departure). To simplify

this study, however, total Δv was minimized and the performance of NTP vehicles measured against these particular trajectories. Aerobraking was not taken under consideration for these shorter missions since, although it would eliminate the need for MOI and EOI propulsive changes, it would nevertheless severely restrict entry velocities.

**Table 22 Option I Mars Flight 1 and Alternatives**

| *Mission Type* | *TMI Δv (m/s)* | *MOI (m/s)* | *TEI (m/s)* | *EOI (m/s)* |
|---|---|---|---|---|
| 90-Day Baseline (565/30, 335-30-200) | 4500 | 4447 | 3400 | 7193 |
| 500/30 (230-30-240) | 6166 | 3098 | 3288 | 6554 |
| 450/30 (183-30-237) | 4195 | 2799 | 3903 | 8519 |
| 400/30 (146-30-224) | 4237 | 3372 | 4110 | 8293 |
| 350/30 (110-30-210) | 5388 | 4172 | 4672 | 8310 |
| 300/30 (183-30-87) | 7952 | 7367 | 6654 | 5224 |
| 250/30 (134-30-86) | 8197 | 10631 | 8227 | 5466 |
| 200/30 (92-30-78) | 7849 | 12733 | 11756 | 6693 |

It was determined that the Light Bulb, Cermet NDR, and FPBR were all capable of delivering the baseline payload to Mars at the given IMLEO on the 350/30 trajectory, a substantial decrease in time spent onboard the MTV (150 days). The Light Bulb's high $I_{sp}$ was

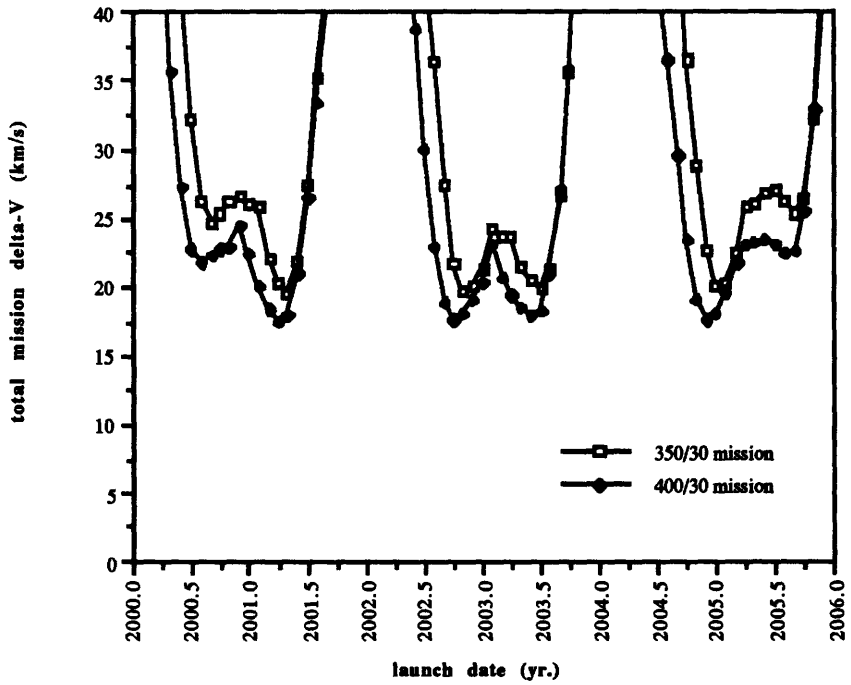


**Figure 56 Δv mission requirements for 350/30 and 450/30, 2000-2006**

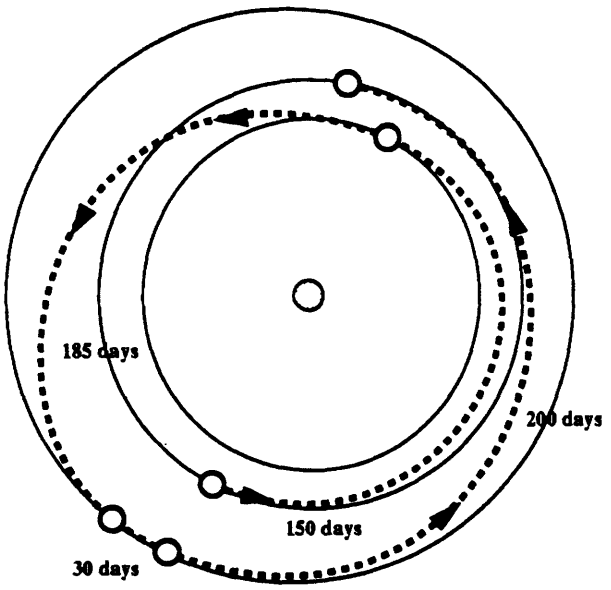


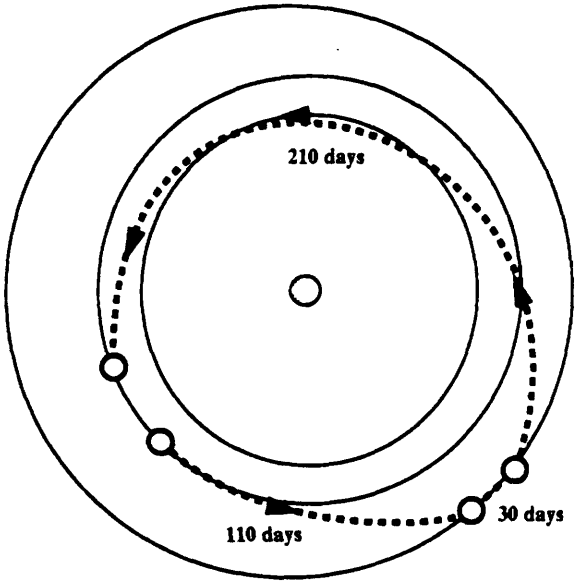


**Figure 57 Option I Flight 1 (565/30)** **Figure 58 Alternate 350/30**

partially negated by its greater weight. Both NERVA and the Open Cycle 2 engine were capable of a reduction to 400/30, but the large mass of the OC2 (and the relatively large mass of NERVA coupled with its lower $I_{sp}$) precluded better performance. Figure 56 shows a portion of the cyclical variation of 350/30 and 400/30 missions over time, while Figures 57 and 58 illustrate the trajectories of the baseline and one of its two shorter-duration alternatives.

Given the fixed IMLEO requirement, all engines can perform the 900/500 mission, since it calls for a lower total $\Delta v$ than the baseline. FPBR and the Cermet NDR can perform the 850/500 with some margin--FPBR can almost meet the 800/500 requirements. These reductions in trip time are not as useful as those seen for opposition-class missions, although total time spent onboard the MTV is decreased by two months, which is still substantial. However, the high propulsive requirements for 750/500 missions and those with even shorter transits cannot be met by any engine type.

A comparison of figures 40 and 49 shows that the minimum for 650/500 (~80 km/s.) is far higher than that for a 180/30 (~35 km/s.), although the time spent onboard is the same. The conjunction-class missions, while fairly steady for trip times over 850 days, produce very high propellant mass requirements for trips under this value. In contrast, while shortening opposition-class missions clearly increases propellant requirements, the rise is not as rapid as that seen for conjunction-class trips. Figure 59 illustrates the cyclic deviations of the 850/500 and 900/500 missions, while figures 60 and 61 show the baseline Flight 6's trajectory and its 850/500 counterpart.

**Table 23 Option I Mars Flight 6 and Alternatives**

| *Mission Type* | *TMI Δv (m/s)* | *MOI (m/s)* | *TEI (m/s)* | *EOI (m/s)* |
|---|---|---|---|---|
| 90-Day Baseline (927/484, 208-484-235) | 4250 | 2454 | 1625 | 5284 |
| 900/500 (200-500-200) | 4532 | 1783 | 1163 | 4306 |
| 850/500 (195-500-155) | 5497 | 2633 | 1412 | 5119 |
| 800/500 (180-500-120) | 7593 | 4054 | 2148 | 6762 |
| 750/500 (151-500-99) | 11616 | 6458 | 3555 | 9644 |
| 700/500 (118-500-92) | 18426 | 10832 | 6170 | 14027 |
| 650/500 (86-500-64) | 29100 | 18681 | 11341 | 21075 |

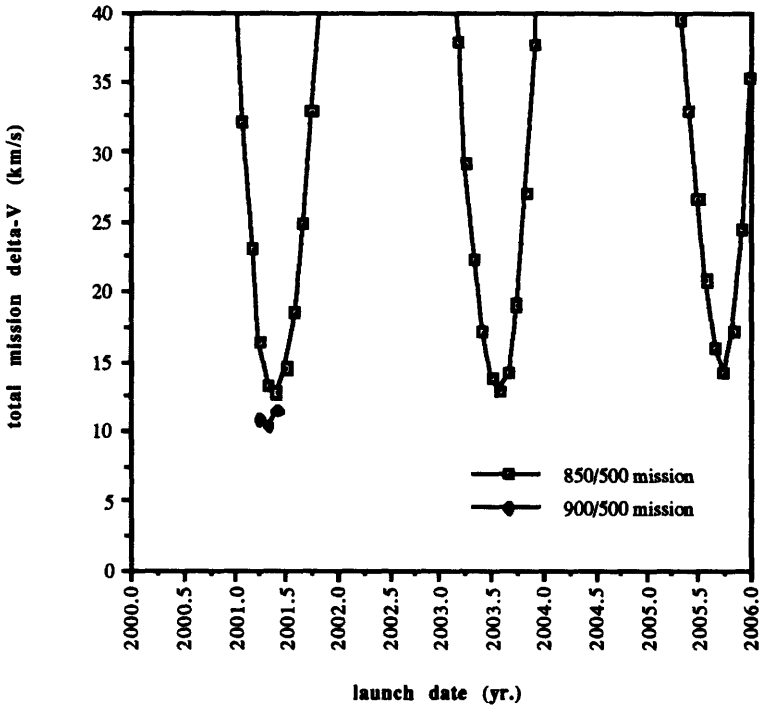


**Figure 59 Opportunities for the 850/500 and 900/500 class missions, 2000-2006**

In summary, baseline piloted missions concentrate on short (30-day) stays with total trip times of 500 to 600 days, resulting in over a year and a half being spent onboard the Mars transfer vehicle. For a fixed IMLEO, it has been shown that the transfer times associated with these short-stay missions can be decreased, given higher-$I_{sp}$ nuclear thermal systems. While the gas-core engines are too massive to provide a signficant decrease, the high thrust-to-weight FPBR system (and to an extent, the other solid-core options) can lower transfer time to the 350-day range, saving seven months spent in transit.

The 90-Day Study missions also plan longer-duration missions with surface stay times of over 500 days. These conjunction-class transfers require the crew to spend from 250 to 500

days in transit. Large reductions in trip time were not possible; Δv increased with decreasing trip time more drastically than with short-duration trips. Nevertheless, in the specific case of Option I Flight 6, the FPBR was capable of reducing transfer time by almost two months.

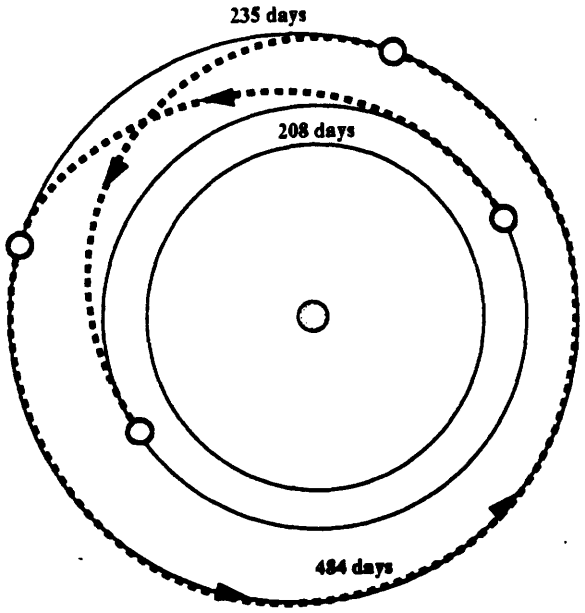


**Figure 60 Option I Flight 6**

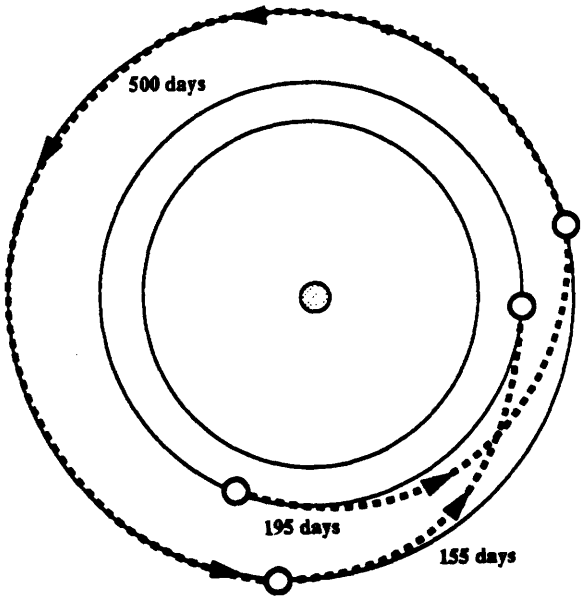


**Figure 61 Alternate 850/500**

This investigation of various mission types shows that an effective doubling of specific impulse from the baseline's nominal value of ~475 s. to the 900-1000 s. range provides large reductions of up to 200 days or more in short-duration stay missions and smaller yet still significant reductions, on the order of 50 days, for long-duration stay missions.

**3.1.2.6 Split Mission Alternatives to the Baseline:** This portion of the study will examine the effect of splitting perishable and/or consumable payload from nonperishables between an initial emplacement mission and a piloted mission during the next available launch window. The cargo MTV (Fig. 62) can be sent out on a minimum-energy trajectory, as there is no serious difficulty associated with long trip times for such missions. The piloted MTV will then follow a faster trajectory to Mars, to mitigate the problems associated with lenghty transfers (Fig. 63). The cargo mission will be able to carry (1) the Mars excursion vehicle, (2) habitat structure, power and resource generation facilities, (3) non-sensitive instrumentation and scientific apparatus, in addition to (4) MTV-P TEI/EOI propellant, including a portion of the TEI/EOI engine cluster. It has been argued that enough propellant for minimum-energy TEI should be placed aboard the piloted vehicle to enable it to return to Earth in the event that the

cargo mission fails or the propellant aboard is 'inaccessible.'[59] These 'contingency' missions are important and should be considered in detail; for this study, however, only the straightforward 'split' mission will be examined fully--to provide an understanding of the gains possible in dividing perishable payloads from nonperishables.

Following this analysis is a short aside detailing the compromises necessary to allow the crew transfer vehicle to transport its own propellant to Mars--it will be seen that the consequence of carrying fuel aboard the fast-transfer vehicle is either a very high IMLEO or an increased transfer time in order to make the baseline initial mass requirement at LEO.

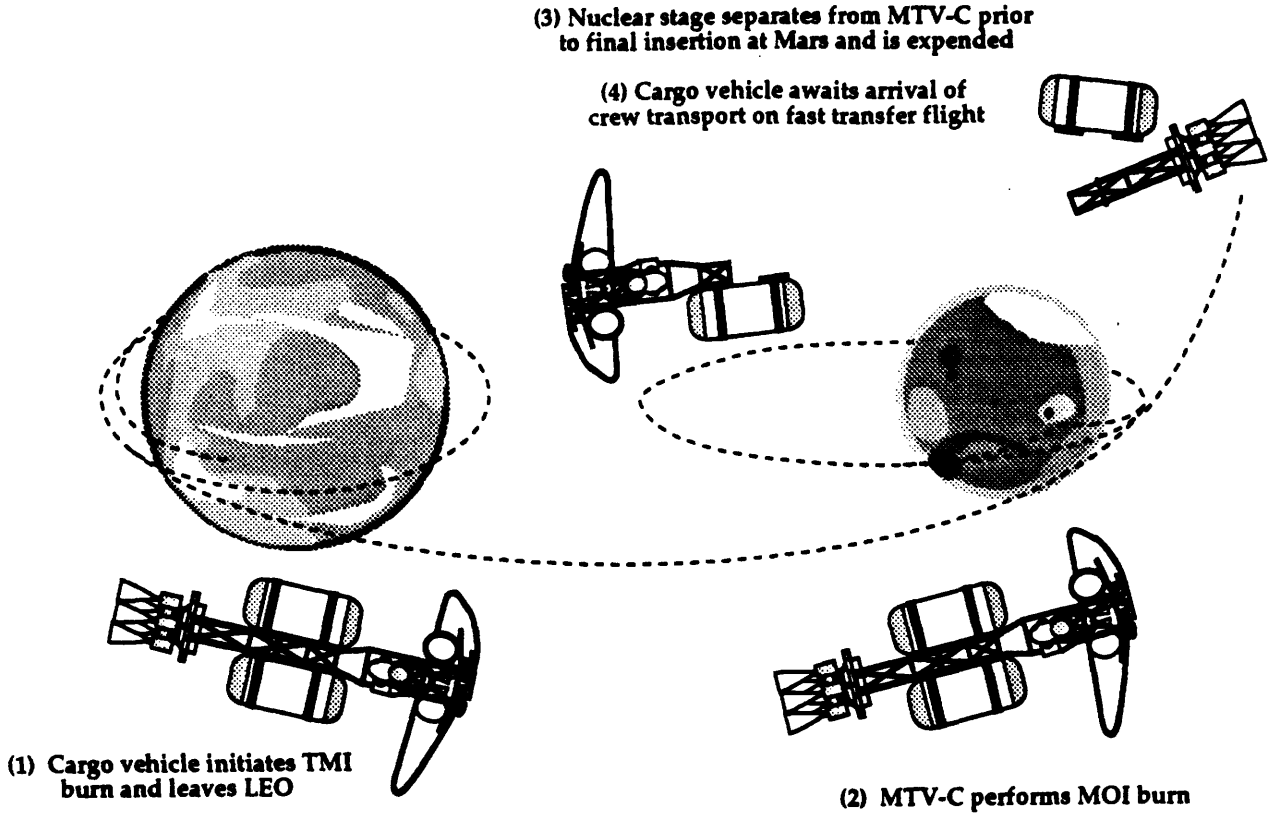


**Figure 62 Option I Mars Flight 1 Split Mission (cargo flight)**

As in Section 3.1.2.5, Option I's Flights 1 and 6 are examined and the consequences of a split mission shown. Flight 1, an opposition-class mission of type 565/30, includes a direct entry of the crew upon return to earth. The total baseline payload for the 90-Day Study mission is listed in Table 24. Included in the MTV-C payload were essentially all non-perishable items, those that could not be affected by an enhanced radiation environment or could be expected to decay or degrade over the length of a near-minimum energy transfer.

---

[59] Mars Mission Strategies, D. Weaver, NASA Office of Lunar & Mars Exploration Program Office, 1991

**Table 24 Option I Mars Flight I Payload and Division Among Split Missions**

| *Payload* | *Cargo MTV* | *Piloted MTV* |
|---|---|---|
| MEV-P and ascent/descent propellant | X | |
| Habitation module | X | |
| Airlock | X | |
| Power Plant | X | |
| Rover and Lab Instruments | X | |
| Crew Supplies | | X |
| EMUs | | X |
| TEI/EOI Propellant | X | |

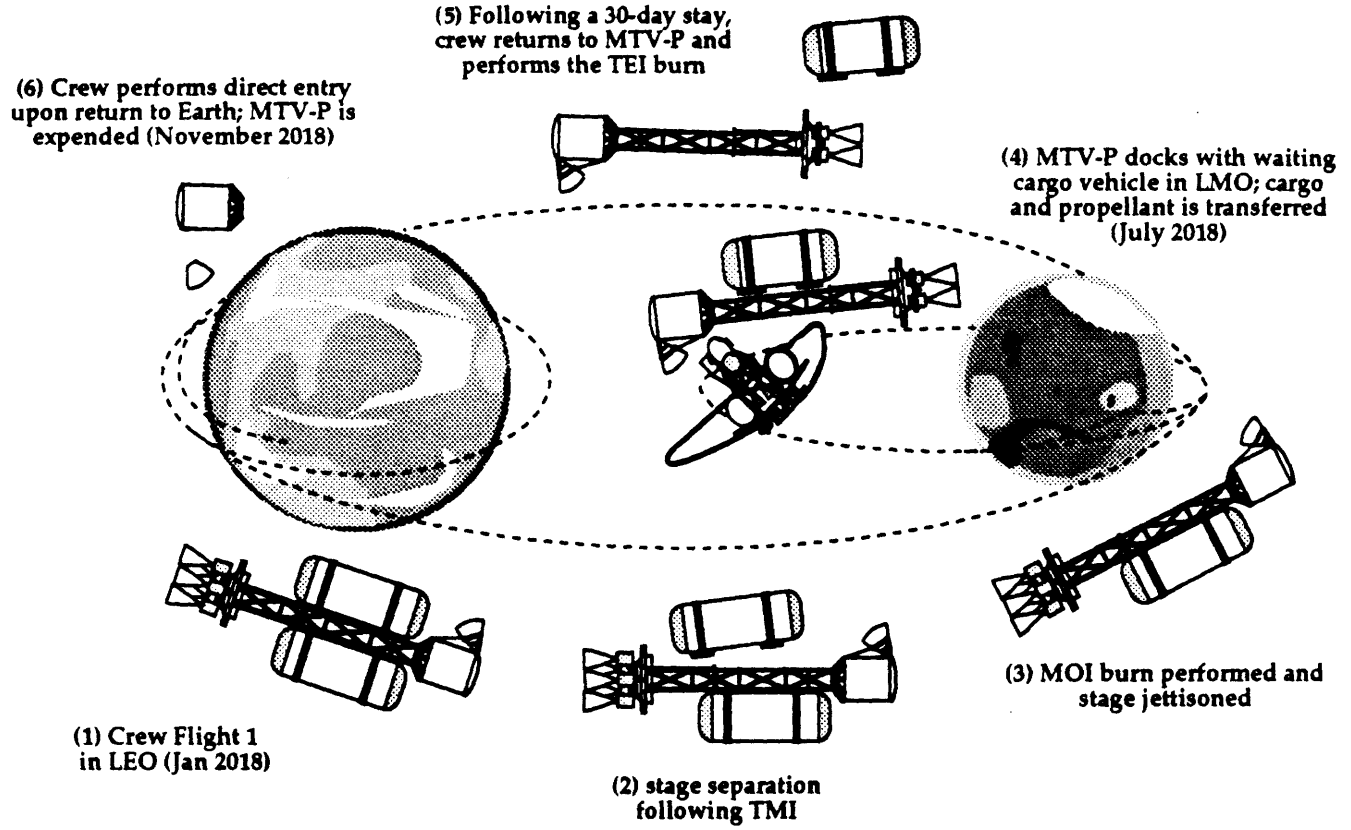


**Figure 63 Option I Mars Flight 1 Split Mission (crew flight)**

This greatly lowers the mass of the piloted MTV. The split Flight 1 would proceed as follows: (1) The MTV-C would set out on a near-minimum energy transfer for Mars ($\Delta v_{TMI}$ = 4250 m/s, $\Delta v_{MOI}$ = 2254 m/s). It would then wait in the 250 x 34000 km capture orbit used in the 90-Day Study until the MTV-P arrived with the crew on its fast flight. The crew, their supplies

for the 30-day stay (2.13 mT), and EMUs (0.89 mT) would be transferred to the waiting MEV and taken down to the surface. Upon return to low Mars orbit, propellant (and perhaps additional engines) would be moved from the cargo vehicle to the MTV-P. The crew would then initiate TEI and return to earth on a fast trajectory. At earth, the crew capture vehicle would perform a direct entry into the atmosphere. Table 25 illustrates the lowest transfer times achievable by the various engine technologies for the stated IMLEO ceiling. Since total $\Delta v$ values were known only for specific transfer times (300 days, 350 days, etc.), an engine's performance was evaluated by calculating the total mission IMLEO for two trip times and subsequently using linear interpolation to find a transfer time corresponding to the baseline IMLEO. Tables 26 and 27 show FPBR-propelled split missions. FPBR and the Cermet NDR were both capable of achieving 300/30 transfers, better than the all-up variable duration missions examined previously. All NTP options bettered the baseline by at least 200 days; even the massive Open Cycle gas-core was able to achieve 350/30 at a cost of 15 mT over the baseline--this is a result

**Table 25 Option I Mars Flight 1 and Alternative Propulsive Systems' Performance (for fixed IMLEO of 832.2 mT)**

| *Propulsion System* | *Achievable Transfer Time (days in transit / surface stay)* |
|---|---|
| 90-Day Baseline (cryo/aerobrake) | 565/30 |
| **FPBR** | **295/30** |
| **Cermet NDR** | **296/30** |
| NERVA | 347/30 |
| Light Bulb | 338/30 |

of the gas-core's better performance at higher $\Delta v$. For extremely short flights (e.g. 200/30, 150/30), the gas-cores would become the only options available, although they would certainly not be able to meet the baseline IMLEO.

Option I Flight 6 was also examined, but it could be seen that the lack of a direct entry by the Earth Crew Capture Vehicle (ECCV) at the end of a mission (and thus the additional propellant necessary to perform an expensive EOI burn) incurred substantial extra mass--enough to preclude any substantial transfer time savings by the MTV-P. The FPBR-propelled alternative to the baseline flight 6 was not even capable of an 850/500 transfer at the given IMLEO of 678.7 mT. To perform an 850/500, taking 93 days off the baseline's time in transit, requires the FPBR vehicle to have an IMLEO of 705.9 mT--the majority of the extra mass is in the form

**Table 26 Option I Mars Flight 1 Mission Event List**
**Prepositioning Cargo Mission (FPBR-propelled)**

| *Mission Event* | *Total Vehicle Mass* | *Change in Mass* | *Delta-V* |
|---|---|---|---|
| | *(MT)* | *(MT)* | *(m/s)* |
| IMLEO | **388.15** | | |
| Pre-injection preparation propellant | 377.31 | 10.84 | 0 |
| Trans-Mars injection propellant | 233.04 | 144.27 | 4250 |
| Jettison 8-engine TMI stage | 224.04 | 9.00 | |
| Jettison Earth-Mars consumables | 224.04 | 0.00 | |
| Trans-Mars coast propellant | 221.76 | 2.27 | 90 |
| Mars orbit insertion propellant | 171.75 | 50.01 | 2254 |
| Mars orbit operations propellant | 170.01 | 1.74 | 90 |
| Deploy payloads/jettison 8-engine MOI | 163.01 | 7.00 | |
| Receive perishable payloads from MTV-P | 166.05 | 3.04 | |
| Mars payload to Mars surface | 86.55 | 79.50 | |
| Mars orbit consumables | 86.55 | 0.00 | |
| Transfer TEI propellant | 10.00 | 76.55 | |
| Final Mass in LMO | 10.00 | | |
| | | | |
| Mars payload total mass | **79.50** | | |
| Pre-deorbit preparation propellant | 79.50 | 0.00 | |
| Mars descent propellant | 58.99 | 20.51 | 1360 |
| Mars payload (dry) | 37.19 | 21.80 | |
| Mars surface science | 36.19 | 0.00 | |
| Mars surface consumables | 34.04 | 2.15 | |
| MEV-P ascent stage prior to ascent | **34.04** | | |
| MEV-P ascent propellant | 9.61 | 24.43 | 5763 |
| Crew | 9.61 | 0.00 | |
| MEV-P final mass | **9.61** | | |

of TEI propellant carried out by the cargo mission. The crew fast transfer's IMLEO would only be 199 mT, but the cargo vehicle would leave LEO at 506.75 mT.

A final inspection of mission modes was undertaken in which the TEI propellant was carried to Mars aboard the *crew*, not the cargo, mission. Transporting the TEI propellant allows for a possible abort following initial departure from Earth orbit; also, it prevents any need for propellant transfer (in zero-g) at Mars. The driving reason behind carrying this fuel, however, is to take advantage of the stored liquid hydrogen as an active neutron shield; the fuel must be emplaced directly between the engine cluster and the crew habitat for it to block the neutron flux of the motors. Staging engines and propellant tanks is required even at the $I_{sp}$ range of SCR such as FPBR and NERVA; were they released in sequence, such that the second stage cluster were closer to the crew habitat than the first stage, a second (and larger, due to the decreased separation distance) gamma radiation shield would be necessary to protect the crew. This drives the design of a single modular cluster at constant separation; likewise, the propellant tanks would be mounted off a central truss to allow simple release. A propellant tank off the centerline would not shield the crew compartment unless it, too, was off-centerline (making for

complicated changes in the crew habitat or engine subsystems)--to simplify the design, the return propellant could be mounted between the central truss and the engine cluster, acting as a

**Table 27 Option I Mars Flight 1 Mission Event List**
**Crew Fast Transfer Mission (FPBR-propelled)**

| *Mission Event* | *Total Vehicle Mass* (MT) | *Change in Mass* (MT) | *Delta-V* (m/s) |
|---|---|---|---|
| IMLEO | **411.75** | | |
| Pre-injection preparation propellant | 394.19 | 17.56 | 0 |
| Trans-Mars injection propellant | 160.01 | 234.18 | 7952 |
| Jettison 15-engine TMI stage | 145.01 | 15.00 | |
| Jettison Earth-Mars consumables | 138.21 | 6.80 | |
| Trans-Mars coast propellant | 136.81 | 1.40 | 90 |
| Mars orbit insertion propellant | 59.34 | 77.47 | 7367 |
| Mars orbit operations propellant | 58.74 | 0.60 | 90 |
| Deploy additional payloads | 57.74 | 1.00 | |
| Perishable payloads transferred to MEV-P | 54.70 | 3.04 | |
| Mars orbit consumables | 53.60 | 1.10 | |
| Mass prior to propellant/engine transfer | 53.60 | | |
| | | | |
| Add TEI propellant | 130.15 | 76.55 | |
| Trans-Earth injection propellant | 61.21 | 68.94 | 6654 |
| Jettison TEI stage | 61.21 | 0.00 | |
| Mars-Earth consumables | 57.41 | 3.80 | |
| Trans-Earth coast propellant | 56.75 | 0.65 | 101 |
| Earth orbit insertion propellant | 56.75 | 0.00 | 0 |
| Earth orbit operations propellant | 55.89 | 0.87 | 136 |
| Jettison IMM/10-engine EOI stage | 12.59 | 43.30 | |
| Final MTV-P mass in LEO | 12.59 | | |

shield for all three impulsive burns. Unfortunately, placing the return fuel for the FPBR 300/30 aboard the much faster crew transfer vehicle raises the IMLEO of the crew vehicle from 411.75 mT to a very high 1135 mT--although it lowers the cargo mission IMLEO from 388 to 214 mT. The aggregate is clearly far higher than the baseline; to remain competitive with the baseline Option I Flight 1, the FPBR crew mission is forced to move to 350/30 to compensate for transporting the return propellant to Mars at a higher energy. The 350/30 FPBR mission would mass 336.7 mT (crew transfer) and 214 mT (cargo) in LEO.

While substantial abort capability is provided by crew mission transfer of its own TEI fuel, carrying it along on a fast transfer necessitates either an exceedingly large IMLEO or a slower transfer time to meet the baseline initial mass requirement. This would argue against emplacing the TEI fuel aboard the MTV-P.

**3.1.2.7 Results of Mission Analysis:** The prior studies were performed in order to select a suitable nuclear thermal propulsion system for further analysis in Section 3.2. The six

NTP alternatives were rated against the baseline mission for fixed duration and variable duration flights (Fig. 64). The combination of the baseline design's use of aerobraking to offset the $I_{sp}$ disadvantage of cryogenic LOX/$LH_2$ chemical engines and near-minimum energy transfers provided very low IMLEO figures for Mars and lunar missions. However, aerobraking is not a proven technology; the Aeroassist Flight Experiment (AFE) discussed earlier and currently slated for launch in 1994, may lose both its support and funding. If this occurs, a Mission From Planet Earth would have to focus on nuclear thermal or nuclear electric technologies since chemical propulsion alone is incapable of providing the performance necessary to reach Mars. For fast transfers, nuclear thermal propulsion, with its capacity for thrust-to-weight levels on the order of chemical systems, is the only option available.

*Gas-core infeasibility:* The primary question is which of the NTP options presents the most favorable combination of performance and technical feasibility. Gas-core engines, discussed at length in Section 2.2.2, have been the focus of theoretical research for decades, yet the work has yet to validate the various conceptual designs and serious questions remain. The open-cycle gas-core engine suffers from fuel-loss problems that may not be preventable, while the closed-cycle gas-core, or light-bulb, requires structural strength and thermal properties in materials that are beyond current and forseeable future technologies. This eliminates them from consideration in the short term ; however, their performance at high values of total mission $\Delta v$ (above 20 km/s.) might provide future mission designers with a useful propulsive option, if their design problems are overcome.

*Unfavorable gas-core performance:* The advanced engines are unable of competing against the 90-Day baseline primarily because they do not perform significantly better at the low values of total $\Delta v$ utilized by designers of the baseline missions. The mass ratio $R = m_o/m_f$, where $m_o$ corresponds to initial mass and $m_f$ to burnout mass following an impulsive burn, is a small number for the $\Delta v$ values under consideration in the 90-Day Study; for instance, R = 2.93, given a cryogenic engine with an $I_{sp}$ of 475 s. and a total mission $\Delta v$ of 5 km/s. As has been shown previously, R is defined by the rocket equation:

$$R = \frac{m_o}{m_f} = e^{\left[\frac{\Delta v}{g I_{sp}}\right]}$$

For a fixed $\Delta v$, two engines having different $I_{sp}$ values ($I_{sp,\ engine\ 1} = x$, $I_{sp,\ engine\ 2} = ax$) will produce mass ratios $R_1$ and $R_2$ that are simply related by:

$$R_1 = R_2^a$$

Thus, for a cryogenic engine ($I_{sp}$ = 475 s.) and a high-specific impulse gas-core engine ($I_{sp}$ = 5000 s.), the ratio of specific impulses is a = 10.99. Then the equation above can be solved for $R_2$, which gives a mass ratio for the gas-core of 1.10. This is on the order of the cryogenic engine's mass ratio, even if it is clearly superior performance (burnout mass constituting 91% of the gas-core initial mass, but only 34% of the chemically-propelled initial mass); because of this and due to the enormous structural mass investment needed for implementation of the gas-cores, aerobraking reduces baseline mission $\Delta v$ enough to make the chemical propulsion system competitive with other engines. If the total mission $\Delta v$ were increased to 10 km/s., the cryogenic engine's mass ratio would be $R_1$ = 8.57, while the gas core's ratio would only have increased to 1.22. The difference quickly becomes dramatic as $R_2$ increases beyond ~1.5, since $R_1$ is a function of $R_2$ raised to the eleventh power.

The closed-cycle Light Bulb was a partial exception to this--its mass of 40 mT was low enough so that, to some degree, its increased $I_{sp}$ was able to mitigate its mass penalty. To do justice to this and other gas-core engines would require an examination of very short trip times, where $\Delta v$ figures climb into the 50 km/s. range and even higher. For these substantial velocity changes, gas-cores would be the only viable alternative. However, these missions were beyond the scope of this study.

*Emphasis on the fixed particle bed reactor (FPBR):* Offering lower technical risk in addition to approximately twice the $I_{sp}$ of the highest-performance chemical systems, solid-core engines rely on the achievements of the ROVER/NERVA program terminated in the early 1970's. A number of test engines were fired over a twenty-year period and a large mass of accumulated data is available on the design and operation of solid-core systems. The NERVA and Cermet designs used in analysis have essentially the same characteristics and are a product of a technology that was successfully demonstrated twenty years ago. The fixed particle-bed reactor represents a departure from the traditional NERVA design and promises increased $I_{sp}$ (up to 1000 s.), greater throttleability, and thrust-to-weight ratios approaching 30, very near chemical engines. All three solid-core options performed quite well against the baseline for both fixed and variable trip times. Both FPBR and the Cermet engine demonstrated superior delivery ability at fixed IMLEO and reduced initial mass for baseline payload requirements. As shown in figure 65, every SCR options bettered the 832 mT IMLEO of the baseline's Option I Flight 1 to Mars. FPBR and Cermet reduced the required IMLEO to ~600 mT, saving 28% of the total mass requirement. Higher (~30) thrust-to-weight FPBR derivatives promise to lower this figure to perhaps 500 mT. NERVA was too massive to improve on the baseline--its thrust-to-weight hampered its performance enough to neutralize its 825 s. $I_{sp}$. The Cermet engine, which was examined in the foregoing analysis as a liberal estimate of what a NERVA-style engine could achieve, proved almost as capable as the particle-bed but nevertheless did not surpass it.

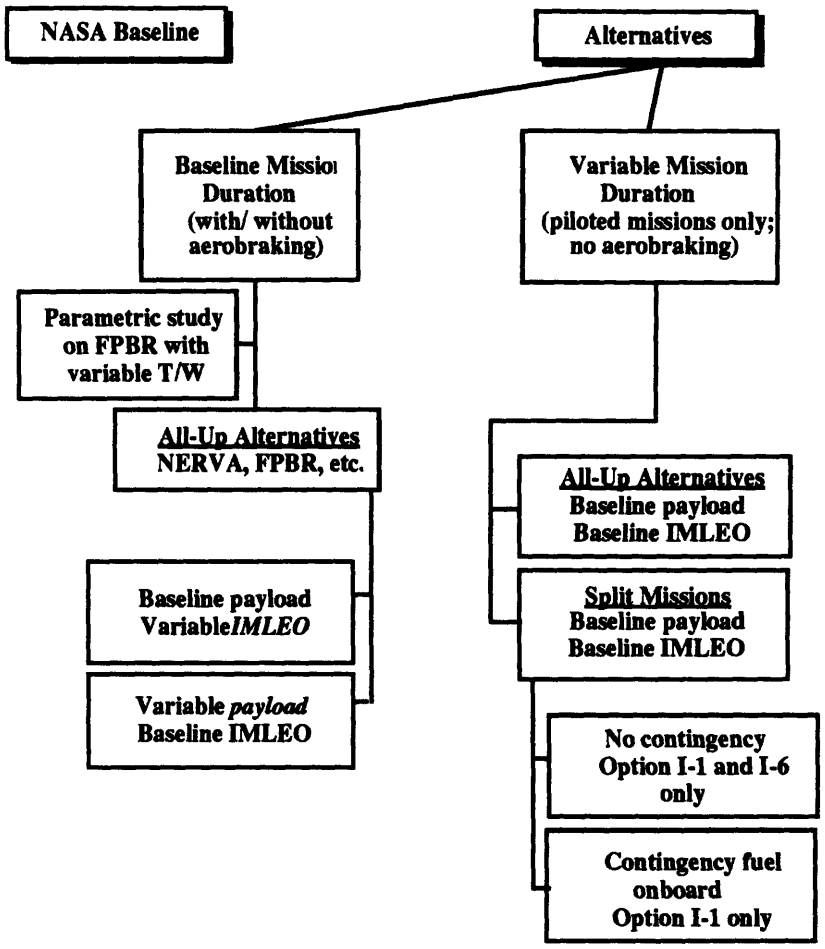


**Figure 64 Flowchart of mission analysis perfomed in this study**

The variable duration missions provided some surprises, as the FPBR and Cermet continued to outdo the higher-$I_{sp}$ options. All-up missions allowed both of these engine types to cut short-duration trip times by 200 days or more (from 565 to under 350), while split missions allowed a reduction of 250 days (Fig. 66). These two engine types were able to perform every mission of the baseline at reduced cost--a performance not equaled by the other options. In addition, they were able to perform far shorter missions for similar cost.

Being a NERVA derivative, Cermet would rely on the large NERVA database and might thus be simpler to build than the particle bed engine, which has not been tested to anything like the degree that the Cermet's predecessors have. However, the Cermet design in this study assumes a rather high specific impulse and, furthermore, would have ramp-up and shutdown difficulties explained in Section 2.0. If the baseline nuclear engine were used for either ascent/descent missions or precision orbit insertion on a launch vehicle upper-stage, the only presently conceivable alternative is the particle-bed, which is throttleable and can achieve full power on the order of several seconds. The particle-bed design is based on substantial work

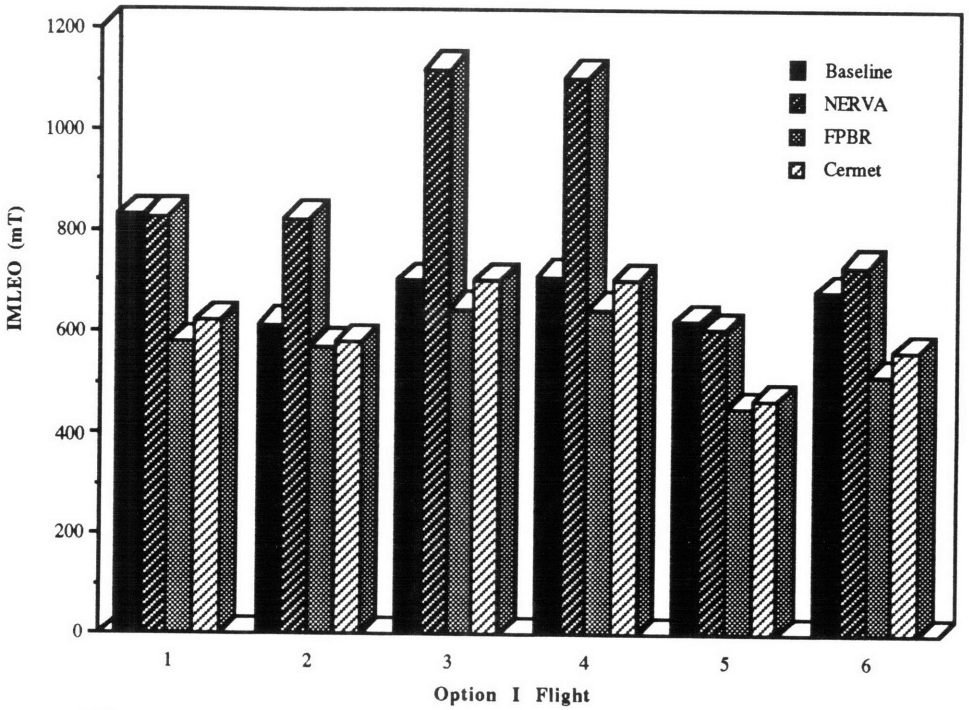


**Figure 65 Fixed payload, variable IMLEO results for Option I nuclear thermal alternatives**

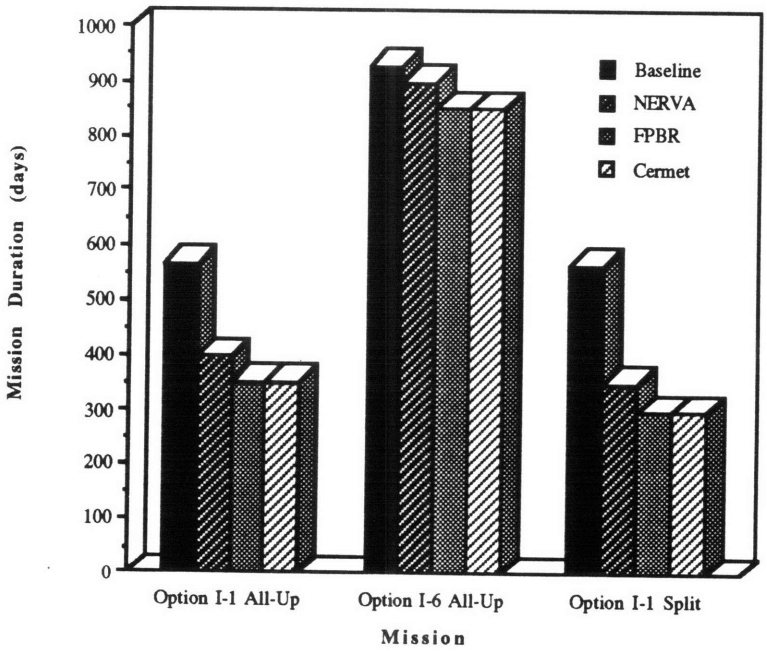


**Figure 66 Performance of NTP options versus the NASA baseline for variable duration missions**

done in HTGR's (high-temperature gas reactors) and promises up to 1000 s. of $I_{sp}$. Based on the design's robustness and its potential for improved performance, the Fixed Particle Bed Reactor will be studied to determine the impact of its substitution into an integrated SEI architecture. Also, the split mission alternative to Option I's Flight 1, which is capable of delivering the baseline payload to Mars with over a 250-day savings in transit time, will be used as the basis for further study into how the FPBR will produce new design requirements for transfer vehicles.

## 3.2 Impact on OTV, ADV, and LV Design

The enhanced radiation environment around the engine cluster drives most of the necessary design changes in the various vehicles. This section will discuss at length the modifications required for orbital transfer vehicles, ascent/descent vehicles, and launch vehicles to perform their missions. Figure 67 illustrates a possible NTP concept for a split mission Mars transfer vehicle.

### 3.2.1 Orbital Transfer Vehicle Design

#### 3.2.1.1 Engine Cluster Sizing

The number of engines in a lunar or Mars transfer vehicle and the thrust per engine will be determined by:

(1) the impulsive thrust required; the near-impulsive approximation mentioned earlier that limits LEO burns to 885 s. imposes a minimum thrust of ~500 kN for a transfer to the moon and twice that (1000 kN) for a Mars transfer;

(2) whether or not the engines in the propulsion system are capable of gimballed motion. The need for an engine-out requirement (in the event of a single engine failure, the vehicle should still be able to perform its mission), coupled with fixed-vector engines, would lead to a four-engine cluster as a minimum, due to symmetry. If the engines are gimballed, the minimum number of engines will be one. Clearly, however, one engine will not be enough to satisfy redundancy.

(3) the limits of the propulsion reactor used. Earlier analysis seemed to indicate that increasing thrust-to-weight values past 30 brought negligible additional IMLEO savings. Given the use of a very compact engine such as the FPBR, which is not likely to decrease significantly in mass during the design process, and a T/W goal of 30, a particle-bed reactor of comparable size will not be required to produce more than 300 kN of thrust.

This would tend to suggest the use of two gimballed engines for the lunar transfer vehicle. A cluster of four fixed engines could be used for the Mars mission; eliminating moving parts in the severe thermal and radiation environment near the reactors would simplify the engineering and reduce concerns about possible radiation damage--through embrittlement--to the gimbals. A square four-engine cluster contains the smallest number of engines possible that allow fixed (non-gimballed) thrusting; in the case of a single engine failure, a second engine (diametrically

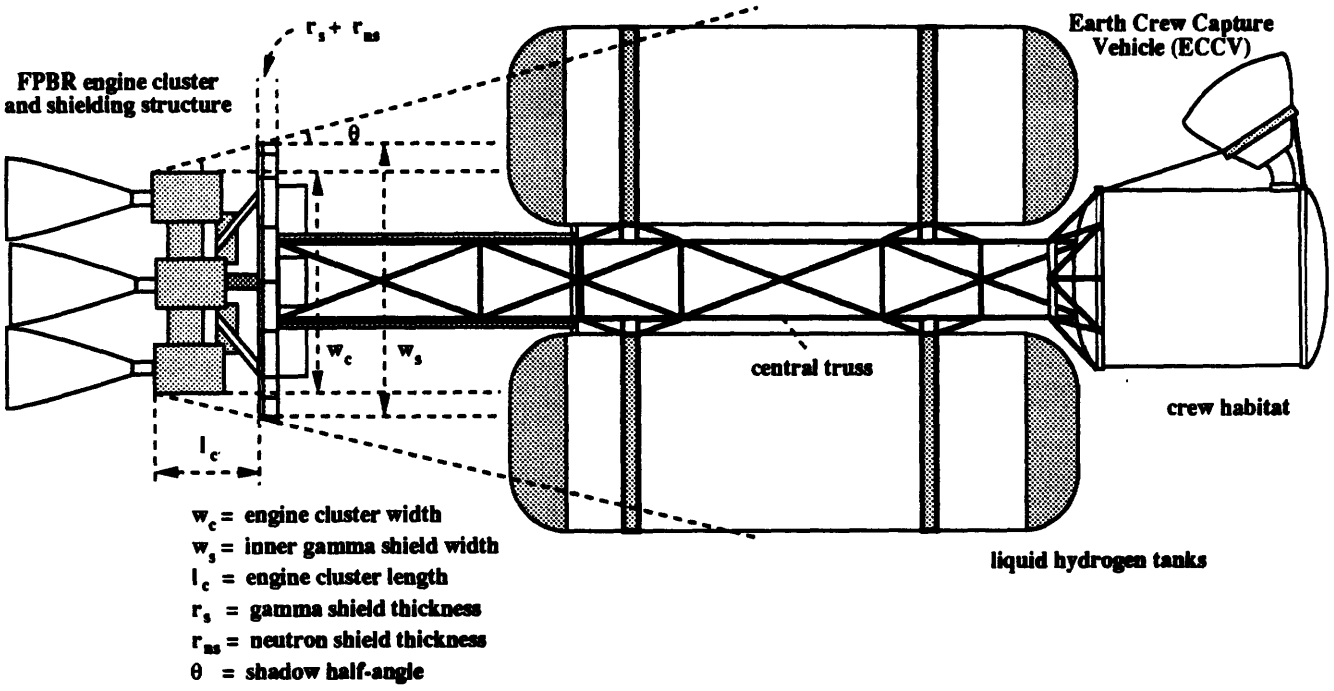


**Figure 67 Hypothetical Mars Transfer Vehicle incorporating a nuclear thermal propulsion system (radiation shielding geometry included)**

opposite the failed engine) could be shut down and the burn continued. Since the impulsive thrust requirement is very conservative, this engine requirement is high; for comparison, the 90-Day Study lunar transfer engines generate a combined thrust of 356 kN.

### 3.2.1.2 Engine Cycle and Pressurization Schemes

Two standard measures for pressurizing the hydrogen propellant are (1) gas pressurization, in which a high-pressure gas such as nitrogen or helium is released into the propellant tank to provide the impetus necessary to move the hydrogen into the reactor core, and (2) turbomachinery, which would raise the hydrogen from its low tank pressure to a value above the engine's chamber pressure. Gas pressurization is exceedingly simple and reliable, requiring none of the complicated mechanisms necessary to implement turbopumping. However, this

technique is suitable only for short-duration or low-thrust burns. Altman states, "Its [gas pressurization's] disadvantages can be serious...for certain applications. First, its weight increases rapidly with firing duration in a linear manner, due to the proportional increase in the volume and weight of the propellant tanks and the gas tank. This weight is prohibitive for durations longer than about 30 to 60 seconds..."[60] Given this study's assumptions involving burn times of 885 s. (LEO) and 1064 s. (at Mars), and due to the high thrust used, gas pressurization becomes extremely expensive. The mass of compressed gas, m, needed to evacuate a propellant tank can be determined from:[61]

$$m = \frac{pV}{RT_o}\left(\frac{\gamma}{1 - \left(\frac{p}{p_t}\right)}\right)$$

Here, p and V represent the pressure and volume of the liquid hydrogen tank, $p_t$ the gas tank pressure, v $T_o$, and $\gamma$ are all functions of the pressurizing gas. The pressure of the hydrogen tank must be higher than the FPBR chamber pressure in order for transport to take place, since pressure losses will necessarily occur in the feed lines, cooling jacket, and across the particle bed. $T_o$ is assumed constant, although the pressurizing gas temperature will drop appreciably as the pressure drops within the storage tank. A constant $T_o$ will give a lower than actual total gas mass.

Using the propellant requirements found in Table 27 (Section 3.1.2.6) for a split mission crew vehicle, a gas pressurization scheme utilizing air (R = 230 J/kg K, $T_o$ = 290 K, $\gamma$ = 1.4) to evacuate the TMI tanks (252 mT, with a required volume of 3600 $m^3$) was investigated for its feasibility. Assuming the ratio $p/p_t$ to be approximately zero and p to be 60 atm gives a required mass of air of nearly 460 mT, clearly an unacceptably large amount. The only figure of merit under the control of the designer of this pressurization system is p; it can be lowered only at the cost of decreasing engine performance, since dropping the propellant storage tank pressure will necessitate a drop in the chamber pressure as well. Since chamber pressure is directly related to the characteristic velocity of the propellant and therefore the engine's theoretical specific impulse, moving to a lower pressure to allow gas pressurization of the propellant would be ill-advised--a very low chamber pressure of 10 atm would still require 80 mT of air, nearly 32% of the total TMI propellant mass.

---

[60] Liquid Propellant Rockets, Altman et. al., Princeton University Press, 1960

[61] Rocket Propulsion Elements, p. 228

The alternative, turbomachinery, is therefore required to reduce overall pressurization system mass. Turbopump and turbine assemblies suffer from greater complexity and thus lower reliability than their gas pressurization counterparts, and are considered questionable in zero-g applications due to a lack of data and experience regarding the use of these systems in space. Zero-g fluid transfer is an issue under investigation by NASA and one that has not yet been settled; it is unclear how effective pumping systems are in the absence of gravity, and without further on-orbit testing to determine how to mitigate this, there is serious concern that turbopumps will not function properly during a burn. However, despite these possible problems, the low mass of turbopumping systems makes them very attractive. Sutton notes that turbopump feed systems are "usually used on high-thrust and long-duration rocket units. Their engine weight is essentially independent of duration." [Sutton, p. 153]

The three basic cycles that could conceivably drive a nuclear thermal propulsion system are (1) a gas generator cycle, (2) a bleed cycle, similar to that proposed for the NERVA engines, and (3) a closed or 'topping' cycle (Fig. 68). The gas generator cycle relies on a separate combustion process inside the generator to produce turbine inlet fluid to drive the turbopump. In the case of an NTP engine, this would necessitate the carrying of some oxidizer (e.g. liquid oxygen) and a portion of the $LH_2$ from the main propellant to produce combustion. The turbine exhaust gases would have to be vented overboard at substantially reduced specific impulse, since introducing $O_2$ and its combinations into the reactor core would introduce corrosion problems. The gas generator cycle would allow for a virtual decoupling of the reactor from the pumping mechanism, at the cost of carrying additional fluid and a reduction--perhaps of up to 5%-- in $I_{sp}$. For solid-core NTP (~900 s.), this is as much as 45 s. lost to turbine exhaust. Such a decrease in performance could mean as much as 10-15 mT of extra propellant and higher initial mass--for just the trans-Mars injection phase of a mission ($\Delta v$ of approximately 5 km/s).

The bleed cycle would 'bleed' off a fraction of the heated hydrogen from either the reactor core or the engine's cooling jacket and mix it with cold $H_2$ emerging from the storage tank. This fluid would enter the turbine and drive the turbopump assembly in the same manner as the gas generator, without the need for an oxidizer--thus making for a simpler overall system. However, like the gas generator, the bleed cycle would exhaust the turbine gases at lower velocity than the main flow and similarly lower the effective specific impulse of the engine. The reactor and pumping mechanisms are now partially linked.

The final possibility, the closed or 'topping' cycle, would bleed off coolant from the jacket or reactor core and allow it to enter the turbine in the same manner as the bleed cycle. However, instead of dumping the exhaust to space, the turbine exit fluid would enter the reactor core to

mix with the main propellant stream and exit with no decrease in the overall specific impulse. The 'full' topping cycle[62] would pass the entire propellant flow through both pump and turbine. Bussard notes that the topping cycles involve the greatest coupling between the reactor and its pumping system--clearly, this would complicate methods for controlling the engine and perhaps limit the design's flexibility.

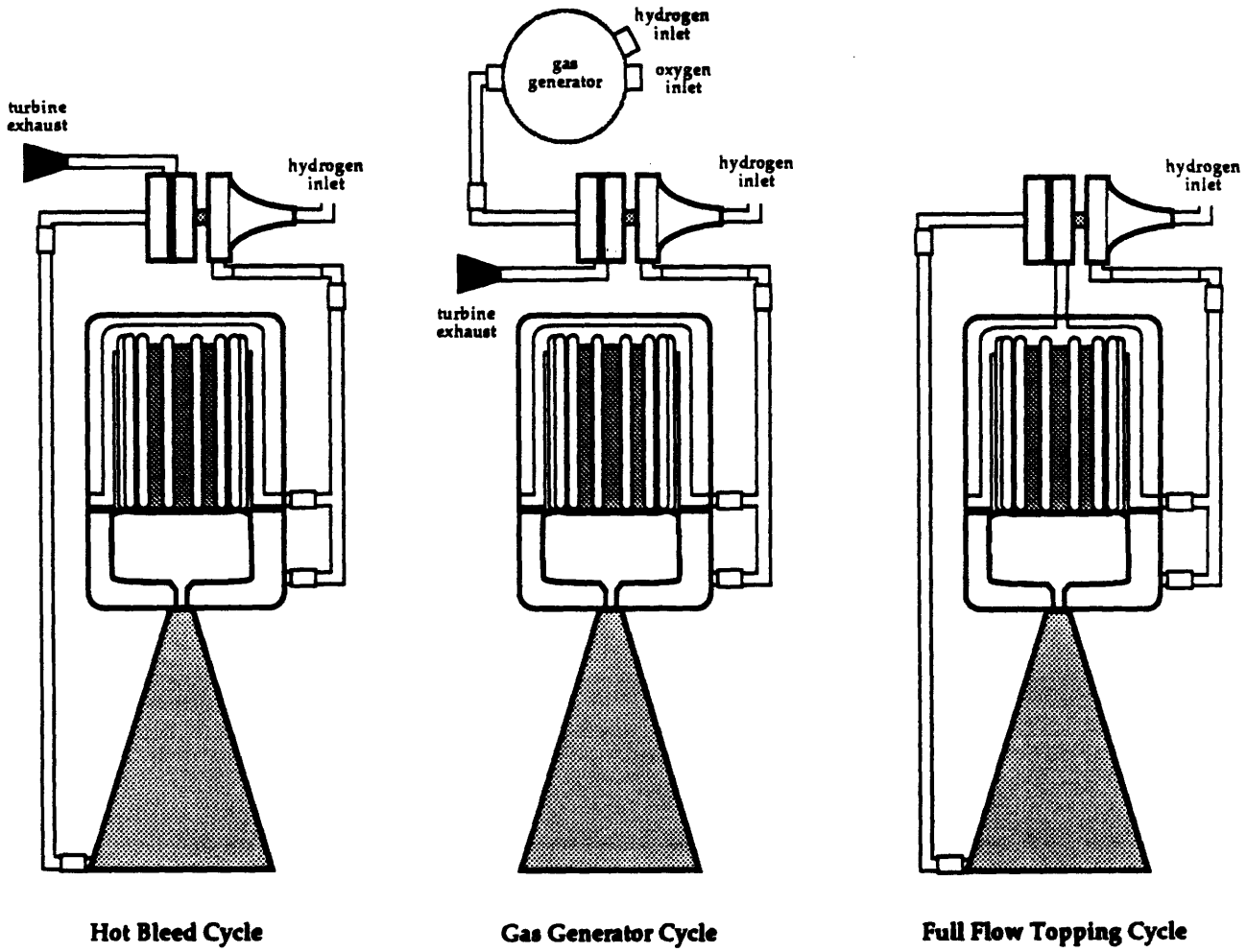


**Figure 68 Engine cycle options [Bussard and DeLauer, 1965]**

Gas pressurization is ruled out on the basis of its extremely high mass requirement. This leaves the three basic turbopumping cycles; the choice among cycles is primarily a qualitative trade between the design's complexity (and attendant reliability and cost) and vehicle

---

[62] Fundamentals of Nuclear Flight,R. Bussard and R. DeLauer, pp. 428-429, McGraw-Hill, 1965

performance. The gas generator cycle offers easier control of the total system by segmenting the engine into 'reactor' and 'pumping system,' yet requires a separate combustion to take place. The bleed cycle, used extensively during NERVA tests, has the advantage of being the simplest design. Both methods suffer from a 5% loss in specific impulse and thus an increased IMLEO for a given payload.

The topping cycle would not offer insurmountable technical difficulties but could nevertheless provide substantially improved performance and should therefore be implemented in the design of a particle-bed reactor engine. While more complex and requiring more monitoring and close control than its counterparts, it would rely on technological advances in both turbomachinery (that have made possible the Space Shuttle Main Engine) and reactor neutronics since the termination of the nuclear rocket program nearly twenty years ago. The coupling of reactor and pumping systems raises difficult problems in engine control and stability and figured prominently in Bussard's 1965 conclusion that the hot bleed cycle would prove easier and less costly to implement. Significant advances made in computer technology and architecture since that date would surely contribute to improved control of complicated systems, and allow the mission designer to choose the high-performance topping cycle.

#### 3.2.1.3 Radiation Enviroment and Shielding Requirements

The operation of nuclear reactors produces mostly neutrons and gamma radiation as harmful by-products; fission fragments, which retain the majority of the fission energy, are deposited close to the point of fission and pose no direct hazard. Likewise, $\alpha$- and $\beta$-particles--produced in the decay process--are charged particles and may be easily stopped without resorting to centimeters of lead or concrete. Neutrons and gamma have much more penetrating power and therefore are the two sources of radiation that require protection in the form of shielding. Clearly, a significant fraction of the neutrons must be retained in order to continue the fission process. $3 \times 10^{10}$ fissions must occur per second to generate one watt of thermal power--a 300 MW reactor thus requires $9 \times 10^{18}$ fissions/s.; moreover, a single fission event will spawn, on the average, two neutrons (assuming thermal neutrons in $U^{235}$). Any that do not contribute to new fission events will be lost to capture in the engine structure or, in the worst case, escape the engine cluster entirely. Fast neutrons (those having high energies, typically in the MeV range) are the hardest to shield against and therefore will be considered in the following analysis. Bussard and DeLauer note:

> "...we have ignored the leakage of thermal neutrons and the dose rate associated due to thermal neutrons produced by thermalization of fast neutrons escaping from the power source. This is in fact perfectly acceptable, for, as we shall see, any material capable of providing radiation protection against the fast-neutron

leakage will be more than adequate for protection against thermal neutrons."[63]

Gamma radiation is also produced in the fission event, making up approximately 10 MeV out of the 200 MeV or so available. The unattenuated dose rate (rads/s.) received at a separation distance r (cm) from a nuclear reactor operating at a power level $P_r$ (MW) is given by the following formula[64] :

$$D_\gamma(r) = 1.361 \times 10^{7}\left[\frac{1 + 0.8f_d}{1 + 0.08f_d}\left(\frac{P_r}{A_s r^2}\right)\right] \qquad (19)$$

The reactor is modelled as a point source and is considered to be radiating isotropically. $A_S$ is an empirical 'attenuation factor' that accounts for gamma loss between the source (engine) and the detector at distance r. This factor would include shielding provided by the engine structure or other spacecraft structure. For this analysis, $A_S$ will be assumed to be equal to one (corresponding to the worst case of no attenuation). The variable $f_d$ is the fraction of decay energy obtainable from the reactor--this increases as engine operating time increases, due to the greater fission product inventory in the reactor. For a near-impulsive burn in LEO (given earlier as having a burn time of 885 s.), the operating time is so short as to not allow a significant product buildup; thus, the value of $f_d$ will be assumed to be zero for simplicity. In a discussion with Professor Norman Rasmussen of the Department of Nuclear Engineering at MIT in October 1991, he stated that the decay power available to a reactor after operation for an extensive (essentially infinite) time is approximately 8%; a burn time of 885 s. was, in his opinion, too short to allow any kind of fission product buildup within the reactor that might produce additional power. Therefore (19) becomes:

$$D_\gamma(r) = 1.361 \times 10^{7}\left(\frac{P_r}{r^2}\right) \qquad (20)$$

The equation for the fast-neutron dose rate (again in rads/s.) is similar[65] :

$$D_n^f(r) = 1.474 \times 10^{7}\left[\frac{\left(1 - \frac{1}{\eta}\right)}{1 + 0.08f_d}\left(\frac{P_r}{B_s r^2}\right)\right] \qquad (21)$$

---

[63] Fundamentals of Nuclear Flight, pp. 270-271

[64] ibid., p. 268

[65] ibid., p. 269

Here, $\eta$ is the neutron yield per fission (usually ~2) and $B_S$ is the neutron attenuation factor; the other variables are noted above. It is important to note that this equation contains an implied macroscopic scattering cross-section for soft tissue--this value would change for fast neutron scattering in other material (e.g. propellant, tank and truss structure, engine structure). Like (19), (21) can be simplified given the assumption that $\eta = 2$, $B_S = 1$, and $f_d = 0$. Then the dose rate for fast neutrons can be represented by the equation:

$$D_n^f(r) = 7.37 \times 10^6 \left(\frac{P_r}{r^2}\right) \tag{22}$$

The gamma and neutron dose rates in rads/s. can be converted to rem (detailed in section 1.2.3.3); the relative biological effectiveness (RBE) factor for gamma radiation is 1, while that of fast neutron radiation is 10--RBE is a multiplicative value, such that 1 rad of neutron radiation will equal 10 rem. Clearly, then, neutron attenuation becomes paramount, since, although the total neutron dose is a little more than half that of the gamma dose, the relative adverse affect of the neutrons is ten times higher. If the neutron and gamma doses are converted to rem/s, the total dose can be described by:

$$D_t(r) = 8.371 \times 10^7 \left(\frac{P_r}{r^2}\right) \tag{23}$$

Since 5 rem is considered to be the ceiling for safe short-term exposure[66], and given that the maximum operating time of a nuclear vehicle in LEO will be 885 s. in order to adhere to the near-impulsive burn requirement, the per-second dose at this level will be .00565 rem/s. Solving for r in (23) gives:

$$r = \sqrt{\frac{8.731 \times 10^7 P_r}{D_t}} \tag{24}$$

For various values of $P_r$, and a given maximum allowable dose rate, a safe separation distance can be determined. Fig. 69 shows the separation distances required to reduce absorbed neutron and gamma doses to 5, 2, and 0.5 rem. This is clearly a conservative calculation, since it

---

[66] Analysis of a Nuclear Orbital Transfer Vehicle Accident, Horn, Powell, et. al, Brookhaven National Laboratories, 1987

neglects the attenuation effect of the engine (which partially self-shields), in addition to any structural material at the detector site. This calculation ignores the dose absorbed following shutdown of the reactor, the decay power, since the fission product buildup following the short burn time is negligible. Nevertheless, a single 300-MW FPBR would require unshielded personnel to remain at a distance of no less than 20 km to hold the absorbed dose to 5 rem. If the total allowed dose is reduced to 0.5 rem, personnel will have to retreat to a distance of 70 km. This will have a definite impact on orbital operations, and will be addressed later. Here, however, the issue is shielding of the crew and sensitive components--at a

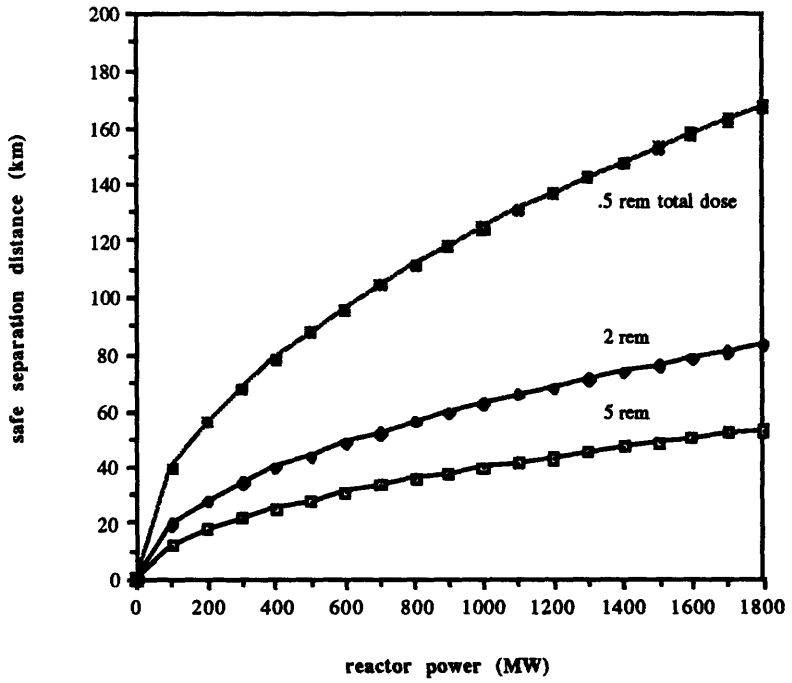


**Figure 69 Separation distances required to achieve given dose rates (.5, 2, and 5 rem)for various reactor power capacities, assuming no shielding of any kind between personnel and reactor**

plausible 30-m separation from the reactor, a crew member without benefit of shielding would see a dose rate in excess of 2700 rem/s, instantly fatal. To reduce this risk to an acceptable level--the 0.5 to 5 rem seen by unshielded personnel at vast distances--requires material shielding to block and absorb the neutron and gamma flux.

The mechanism for neutron attenuation at average energies--around 2 MeV--is accomplished through elastic collision between the neutrons and the surrounding materials' nuclei. Maximum energy transfer in such collisions is dependent on the factor $\alpha$ (A):

$$\frac{E}{E_o} = \alpha = \left[\frac{A-1}{A+1}\right]^2 \qquad (25)$$

where A is the atomic weight of the target nucleus, and $E/E_0$ is the ratio of neutron energy following the collision to its initial energy. For A=1 (hydrogen), $\alpha = 0$ and the maximum energy transfer from the neutron to the nucleus is the total neutron kinetic energy. Therefore it is advantageous to use hydrogenous or low-A materials to shield or moderate average-energy neutrons. High-energy neutrons (above 2 MeV) cannot easily be slowed through interaction with low-A materials. The scattering cross-section of these materials decreases with increasing neutron energy; low-A shields will tend to act as highpass filters, screening out less energetic neutrons while allowing fast neutrons through. Since the fast neutrons are more dangerous, this must be accounted for by positioning other forms of shielding in the path of the oncoming particles.

Bussard and DeLauer describe in detail the necessity for efficient *inelastic* scattering material in the shield--the process of inelastic scattering relies on the fast neutron's ability to be absorbed

**Table 28 Removal Cross-Sections for Fast Neutrons (8 MeV) in Various Materials[67]**

| *Material* | *Density* ($g/cm^3$) | *Z* | *A* | $\Sigma_f$ ($cm^{-1}$) |
|---|---|---|---|---|
| depleted uranium | 18.9 | 238 | 92 | .17 |
| tungsten | 19.3 | 184 | 74 | .22 |
| lithium hydride | .82 | --- | --- | .15 |
| liquid hydrogen | .07 | 1 | 1 | .04 |
| lead | 11.3 | 207 | 82 | .12 |
| bismuth | 9.8 | 209 | 83 | .10 |
| iron | 7.9 | 56 | 26 | .17 |
| concrete | 2.6 | --- | --- | .09 |
| air (sea-level) | .0012 | --- | --- | $4.7 \times 10^{-5}$ |
| carbon | .07 | 12 | 6 | .07 |

by a nucleus, which is thereby excited. The excited nucleus emits a neutron at lower energy.

---

[67] ibid., p. 293

Such scattering depopulates the high-energy region of the neutron spectrum, leaving lower-energy particles that can be further slowed by hydrogenous shielding. The neutrons continue to lose kinetic energy through a number of collisions until they are thermalized (having energies of approximately .025 eV). Research has indicated that higher-A materials tend to have lower energy excited states and therefore are better inelastic scatterers--this would tend to suggest the use of Fe, Pb, or W. Thermal neutrons can be absorbed by effective neutron poisons (boron, lithium, or cadmium are possibilities). $Li^6$ and $B^{10}$ are considered[68] likely candidates to play the role of shield poisons, given their relatively large capture cross-sections. $Li^6$, unlike $B^{10}$, absorbs a neutron and then decays via β-emission; the boron nucleus emits a γ-ray of almost 0.5 MeV energy. This tends to suggest the use of lithium over boron (even allowing for the factor of five advantage in boron's capture cross-section) given that β-rays are easily stopped by minimal shielding while the production of additional gamma inside the shield negates some of its intended usefulness. Neutron attenuation is modeled by:

$$I = I_o \frac{e^{-\mu r}}{4\pi r^2} \tag{26}$$

I (the intensity of the neutron radiation) is here a function of the source strength $I_o$. The beam is reduced by distance ($1/r^2$ dependence) and by collisions or captures within the material (of given linear attenuation coefficient μ). The use of poisons (Li, B) prevents production of additional neutrons within the shield mass and allows (26) to take the form:

$$I_n^f = I_{n_o}^f \frac{e^{-\Sigma_r^f r_s}}{4\pi r^2} \tag{27}$$

The fast-neutron flux is related to the source neutron strength by an inverse-square law (accounting for distance from the source) and an exponential decay within shielding. The exponential decay is calculated on the basis of the removal cross-section of the shielding material $\Sigma_r^f$. Representative values of the cross-section are given in Table 28. A neutron attenuation factor $B_s$ may now be specified for a particular shielding material:

$$B_s = e^{\Sigma_r^f r_s} \tag{28}$$

---

[68] Fundamentals of Nuclear Flight, pp. 277-278

Gamma radiation attenuation may be modeled in a similar manner, and occurs through one of the following three mechanisms:

(1) Photoelectric Effect: This process is an absorption; the incoming γ-ray strikes an electron shell of the target nucleus, whereupon it is absorbed. The excited atom emits an electron. This process contributes little to absorption above gamma energies of approximately 0.5 MeV, but is the prime mechanism below this value. "The probability of interaction via the photoelectric effect depends on the atomic weight [Z] of the absorber and the incident photon energy roughly as $Z^4E^3$..."[70] This can be seem in (26), where $\tau_u$ is the photoelectric scattering coefficient of a given element ($\tau_{Pb}$ is the coefficient for Pb)[71] :

$$\tau_u = \tau_{Pb}\left(\frac{\rho_u}{\rho_{Pb}}\right)\left(\frac{A_{Pb}}{A_u}\right)\left(\frac{Z_u}{Z_{Pb}}\right)^4 \tag{29}$$

(2) Compton Effect: This is a scattering process in which an incoming γ-ray strikes an electron, resulting in an energy gain to the electron (and corresponding energy loss to the γ-photon) via conservation of momentum. The electron becomes a β-ray which should be easily absorbed by the surrounding shield material, while the gamma photon continues through the shield but at reduced energy. This interaction is the most likely to occur in the range of gamma energies most likely to be encountered in the reactor's environment (~2 MeV). The dependence of the Compton scattering coefficient σ on atomic number is directly proportional to Z:

$$\sigma_u = \sigma_{Pb}\left(\frac{\rho_u}{\rho_{Pb}}\right)\left(\frac{A_{Pb}}{A_u}\right)\left(\frac{Z_u}{Z_{Pb}}\right) \tag{30}$$

(3) Pair Production: The third process involves the absorption of a gamma photon by a target atom's electron shell and the subsequent creation of an electron-positron pair. The paired particles are slowed through collision with other charged particles--while the positron is eventually annihilated by collision with an electron (gamma radiation is produced by this annihilation, but it is in the form of 2 γ-rays with energies slightly over that of the electron rest mass, ~ 0.5 MeV). Pair production is a high-energy phenomenon, accounting for the greater share of attenuation in materials for gamma energies above 5 MeV. The likelihood of interaction through pair production--where κ is the pair production coefficient--depends on the square of Z:

---

[70] ibid., p. 280

[71] Modern Physics for Engineers, McGraw-Hill

$$\kappa_u = \kappa_{Pb}\left(\frac{\rho_u}{\rho_{Pb}}\right)\left(\frac{A_{Pb}}{A_u}\right)\left(\frac{Z_u}{Z_{Pb}}\right)^2 \qquad (31)$$

The total attenuation coefficient $\mu_u$ ($cm^{-1}$) is the sum of the three individual coefficients for the material--some values for $\mu$ are given in Table 27. The Z-dependence of gamma attenuation drives the shield designer to materials having the highest possible atomic numbers--Pb, W, Ir, Os, Pt, and U seem to be logical choices. However, platinum, iridium, and osmium are all fairly scarce, and $U^{238}$ (depleted uranium) is susceptible to fission if exposed to a fast neutron source--the use of uranium would thus "place a fast-neutron source outside the primary source and vastly complicate the shielding problem."[72]

**Table 29 Linear Attenuation Coefficients for Gamma Radiation in Various Materials**

| *Material* | *Density* ($g/cm^3$) | *Z* | *A* | $\mu$ ($cm^{-1}$) |
|---|---|---|---|---|
| iridium | 22.5 | 192 | 77 | .87 |
| osmium | 22.4 | 190 | 76 | .87 |
| depleted uranium | 18.9 | 238 | 92 | .85 |
| platinum | 21.4 | 195 | 78 | .84 |
| rhenium | 21.0 | 186 | 75 | .80 |
| tungsten | 19.3 | 184 | 74 | .73 |
| lead | 11.3 | 207 | 82 | .47 |
| bismuth | 9.8 | 209 | 83 | .40 |
| iron | 7.9 | 56 | 26 | .20 |
| boron | 2.3 | 11 | 5 | .06 |
| carbon | 2.6 | 12 | 6 | .06 |
| air (sea-level) | .0012 | --- | --- | $3.6 \times 10^{-5}$ |
| liquid hydrogen | .07 | 1 | 1 | $5.9 \times 10^{-6}$ |

Equation 26 holds for gamma attenuation when the shield thickness is thin with respect to the characteristic relaxation length of the shielding material (where $\lambda$ = relaxation length = $\mu^{-1}$); however, it is necessary to account for forward propagation of gamma due to Compton

---

[72] Fundamentals of Nuclear Flight, p. 302

scattering--this makes (26) look more like a 1/r dependence for large r than the given inverse-square law. Therefore, a 'build-up' factor (1 + μr) is used to give a more accurate expression for gamma attenuation:

$$I_\gamma = I_{\gamma_0}\frac{(1+\mu r)\,e^{-\mu r}}{4\pi r^2} \tag{32}$$

This provides the ability to calculate a shield's gamma attenuation factor $A_S$ as:

$$A_S = \frac{e^{\mu r_s}}{(1+\mu r_s)} \tag{33}$$

Here, $r_S$ is the shield thickness.

Figure 70 shows the required shield thickness necessary to shield crew members situated 30 meters forward of a nuclear propulsion reactor. The total assumed dose to the crew is 5 rem--2.5 rem of gamma and 2.5 rem of neutron radiation delivered over a hypothetical 885-second burn. Of the metals examined, iridium is the best, iron by far the worst. It is important to note

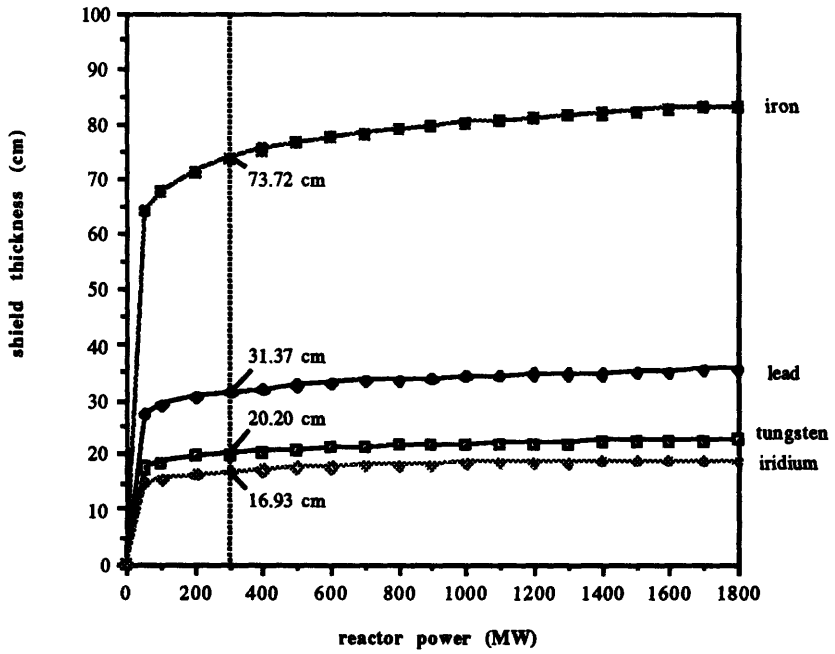


**Figure 70 Shielding depth necessary to hold absorbed gamma radiation dose to 2.5 rem for various materials and an assumed separation distance of 30 m.**

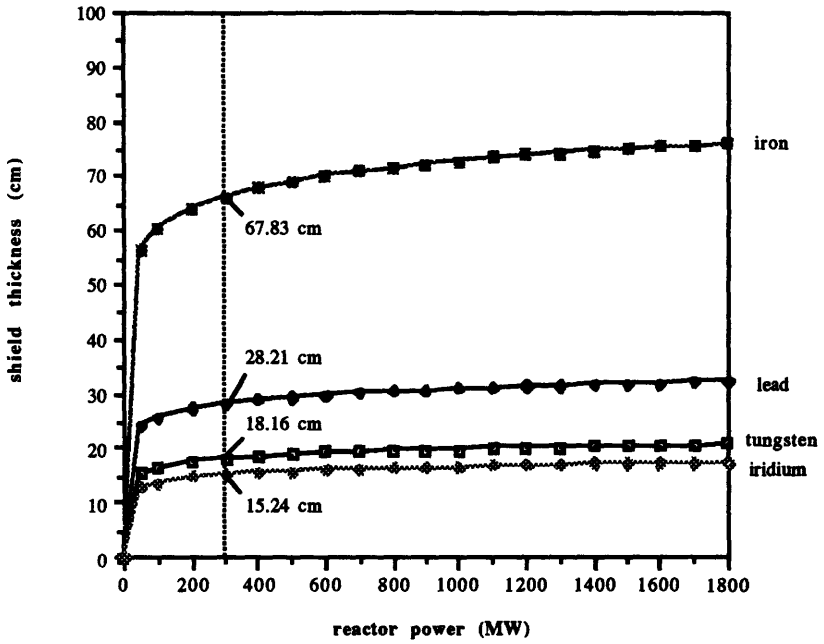


**Figure 71 Shielding depth for gamma dose of 2.5 rem (60 m. separation)**

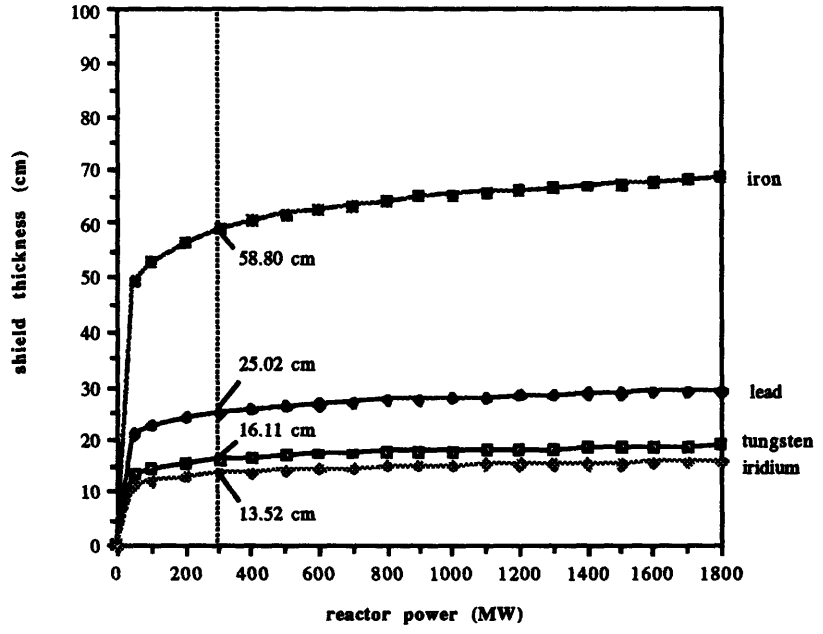


**Figure 72 Shielding depth for gamma dose of 2.5 rem (120 m. separation)**

that the gamma shield mass has yet to be calculated--the thinnest shield is not necessarily the least massive--although iron is clearly eliminated on the basis of its large size. Figures 70 through 72 illustrate the decline in required shield thickness as the separation distance between crew and reactor increase from 30 to 120 meters. For a tungsten shield (Fig. 73), increasing the separation to 120 meters allows the removal of 4 cm of material--for a 1-meter radius shadow shield and a 300-MW reactor, this would be a total mass reduction of 12250 kg - 9750 kg = 2500 kg. The gamma shield would nevertheless be quite massive (~10 mT).[73] These mass requirements drive the planner to consider as large a separation distance as is feasible, given vehicle structural requirements.

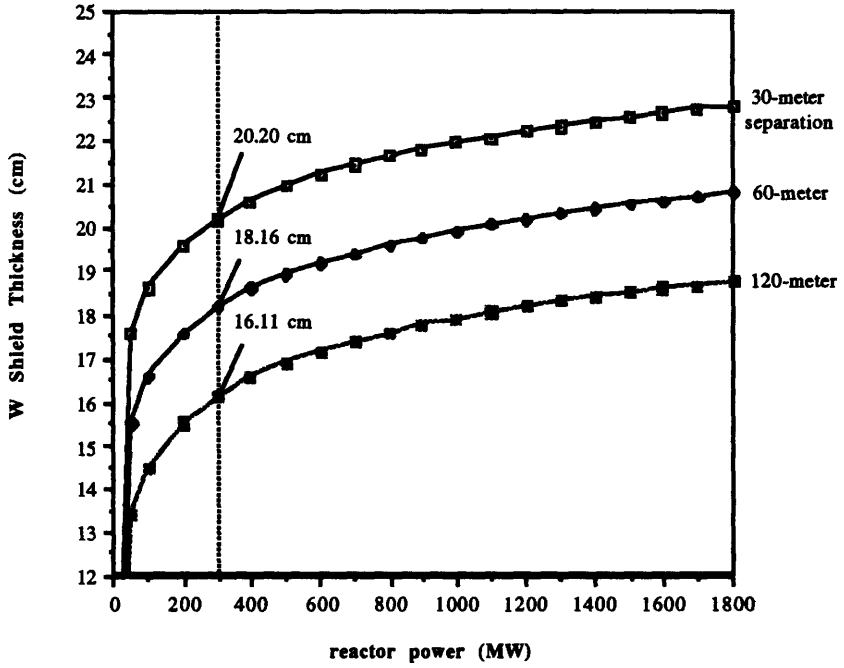


**Figure 73 Tungsten shield depth necessary to hold absorbed gamma dose to 2.5 rem, assuming separation distances of 30, 60 and 120 m.**

As previously mentioned, the gamma shield would provide partial protection against fast neutrons; however, a dedicated neutron shield will be necessary to depopulate the remainder of the high-energy neutron spectrum. High-Z materials provide the inelastic scattering needed to

---

[73] This analysis assumes that the crew compartment, propellant tank and fuel, and other structure provide no incidental shielding to the personnel aboard.

slow down the fast neutrons, but a low-Z, low-A material (LiH, $H_2$, etc.) with a high

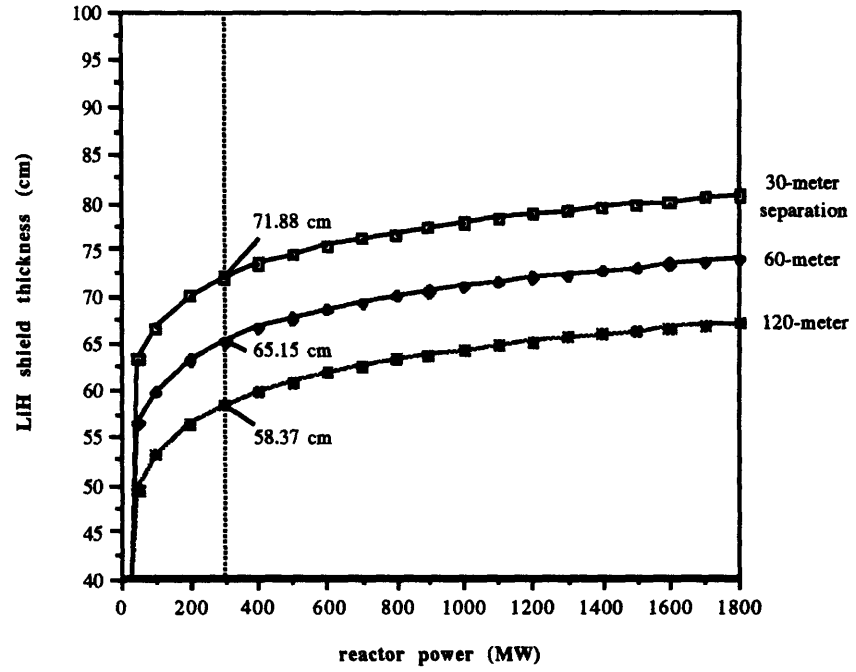


**Figure 74 LiH neutron shield thickness required to hold absorbed dose to 2.5 rem, for 30, 60, and 120 m. separation distances**

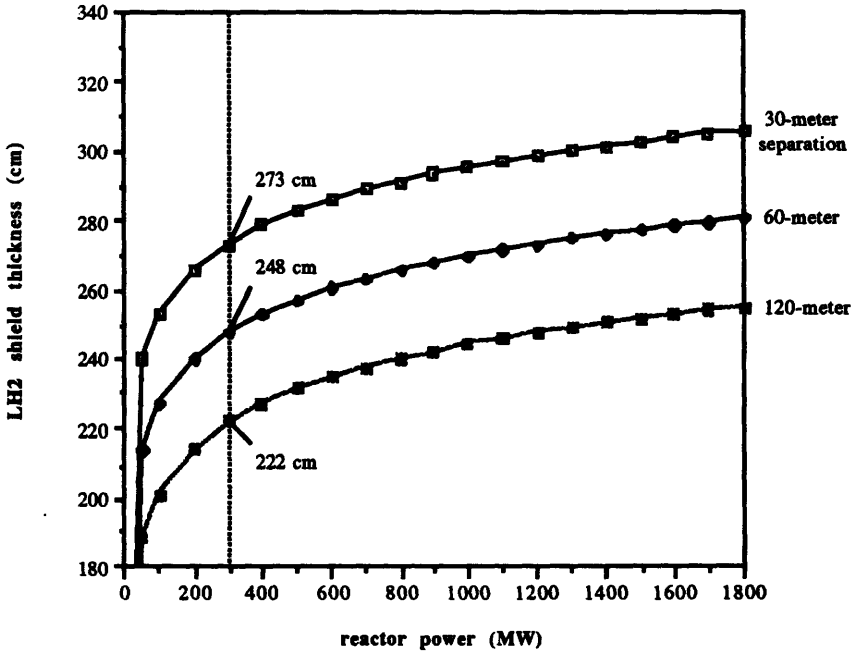


**Figure 75 $LH_2$ neutron shield depth (total dose = 2.5 rem)**

percentage of hydrogen are extremely effective in removing the remainder. Lithium or boron then completes the process by absorbing the thermalized neutrons. Figure 74 shows the dependence of LiH shield thickness on separation distance, given a total absorbed dose of 2.5 rem. The analysis assumed a tungsten shield (designed to the gamma attenuation specifications above) yielding partial neutron stopping ability. Since LiH is extremely light (Table 28) there is little incentive to the designer to move to larger separation distances as opposed to increasing shield mass--especially since full liquid hydrogen tanks, if distributed along or near the centerline of the orbital transfer vehicle, will provide additional neutron shielding (Fig. 75).

Since it is clear that liquid hydrogen will stop any high-energy neutrons emerging from the gamma shield, the question arises as to whether LiH (or other hydrogenous materials) are necessary, since there will be large quantities of $LH_2$ aboard in the form of propellant. However, leaving the task of neutron attenuation to the propellant tanks will impart energy to the cold fuel and lead to additional boil-off. Also, all the thermalized neutrons in the propellant tank would not be absorbed by the $LH_2$; instead, it would be necessary to place a fraction of neutron poison (again, Li or B) in the tank walls to provide this capability. The use of a boron-aluminum composite has already been accomplished in the case of the shuttle, where it is used in much of the center truss structure[74]. The greatest objection to the use of the propellant as a partial shielding mechanism would be that it is useful only while the tank is full--as its volume is depleted over the time of a burn, its usefulness as a shield against neutrons decreases. Additionally, the tank would need to be placed directly between the engine cluster and the crew habitat, which would probably entail the placement of the tanks along the centerline, where they would be required to act as load bearing structures. Since multistaging the Mars transfer vehicle is useful in decreasing the mission's IMLEO or trip time, given the high split mission $\Delta v$ requirements, the first stage would drop away after TMI, leaving a second engine cluster/tank system closer to the crew habitat. Such a scheme, discussed earlier, would require additional gamma shielding, since the first stage gamma shield would have been lost at jettison after TMI; it is not likely that the first stage gamma shield could be recovered before the stage is jettisoned and emplaced on the vehicle without major risk to the crew. One alternative--placing the gamma and neutron shields directly behind the crew habitat--is operationally hazardous, since the shadow cone width provided by a shield at the habitat's separation distance will be considerably reduced in size. A second alternative would be to carry the return propellant aboard the crew vehicle instead of aboard the prepositioning cargo vehicle--however, this was shown in Section 3.1.2.6 to require an unacceptably high crew vehicle IMLEO or, to meet the baseline IMLEO

---

[74] Space Vehicle Design, p. 367, M. Griffin and J. French, AIAA Education Series, 1991

requirement, at least a 50-day increase in time spent in transit. A dedicated LiH shield would prevent the necessity to incorporate poison in tank walls, obviate staging difficulties and allow placement of the tanks at nodes along the central truss structure of the vehicle, and would be quite light--at a meter in radius, LiH would mass only 1850 kg (given a 30-meter separation, a 300-MW reactor, and the 2.5 rem absorbed dose ceiling).

Now it is possible to minimize shielding mass given engine cluster parameters such as core length and cluster width. Figure 67 shows the geometry of shield design. For given cluster dimensions and a chosen shadow half-angle $\theta$, the mass of a flat shield of required thickness $r_s$ will be shown to be:

$$m_s = \frac{1}{2}\pi r_s \rho_s \left[ \left( w_c + 2l_c \tan\theta \right)^2 + \left( w_c + (2l_c + r_s)\tan\theta \right)^2 \right] \tag{34}$$

As the gamma shield thickness can be determined from (33), and the build-up factor $1 + \mu r$ can be taken as approximately equal to 10 for the cases studied, (34) becomes:

$$m_s = \frac{1}{2}\pi \left( \frac{2.3 + \ln A_s}{\mu} \right) \rho_s \left[ \left( w_c + 2l_c \tan\theta \right)^2 + \left( w_c + \left( 2l_c + \left( \frac{2.3 + \ln A_s}{\mu} \right) \right) \tan\theta \right)^2 \right] \tag{35}$$

The shield mass is obviously dependent on the material's density-to-linear attenuation coefficient ratio $\rho/\mu$ ($g/cm^2$)--this quantity, the inverse of what is typically known as the material's mass absorption coefficient (in $cm^2/g$), must be minimized to minimize shield mass. Values of $\rho/\mu$ are given in Table 30 for various materials.

Here it is seen that depleted uranium and lead are two of the best gamma shield materials; however, uranium suffers from its tendency to fission in the presence of fast neutrons (noted earlier) and lead is not extremely useful, being too soft to bear the nominal structural loads experienced during impulsive manuevers. This is not insurmountable, since a supporting truss structure or shell (perhaps of another effective gamma shielder such as tungsten) could be emplaced to take the impulsive loading. Platinum, osmium, and iridium are scarce and/or too expensive for use as bulk shield filler; tungsten offers a high elastic modulus ($341 \times 10^9$ $N/m^2$, as opposed to lead's $14 \times 10^9$ $N/m^2$) and excellent neutron and gamma-stopping ability.

Analysis of the neutron attenuation problem leads to the following formula for the neutron shield mass $m_{sn}$, assuming the neutron shield is placed forward of the gamma shield:

$$m_{sn} = \frac{1}{2}\pi r_{sn} \rho_{sn} \left[ \left( w_c + 2(l_c + r_s)\tan\theta \right)^2 + \left( w_c + (2l_c + 3r_s)\tan\theta \right)^2 \right] \tag{37}$$

Since the neutron shield thickness $r_{sn}$ can be replaced by $\ln B_s/m$, we have:

$$m_{sn} = \frac{1}{2}\pi\left(\frac{\ln B_s}{\Sigma_r^f}\right)\rho_{sn}\left[\left(w_c + 2\left(l_c + \left(\frac{2.3 + \ln A_s}{\mu}\right)\right)\tan\theta\right)^2 + \left(w_c + \left(2l_c + 3\left(\frac{2.3 + \ln A_s}{\mu}\right)\right)\tan\theta\right)^2\right] \quad (37)$$

**Table 30 Inverse Mass Absorption Coefficients for Gamma Radiation in Various Materials**

| *Material* | *Density* ($g/cm^3$) | $\mu$ ($cm^{-1}$) | $\rho/\mu$ ($g/cm^2$) |
|---|---|---|---|
| depleted uranium | 18.9 | .85 | 22.24 |
| **lead** | **11.3** | **.47** | **24.04** |
| bismuth | 9.8 | .40 | 24.50 |
| platinum | 21.4 | .84 | 25.48 |
| osmium | 22.4 | .87 | 25.75 |
| iridium | 22.5 | .87 | 25.86 |
| rhenium | 21.0 | .80 | 26.25 |
| **tungsten** | **19.3** | **.73** | **26.44** |
| air (sea-level) | .0012 | $3.6 \times 10^{-5}$ | 33.33 |
| boron | 2.3 | .06 | 38.33 |
| iron | 7.9 | .20 | 39.50 |
| carbon | 2.6 | .06 | 43.33 |
| liquid hydrogen | .07 | $5.9 \times 10^{-6}$ | $1.18 \times 10^4$ |

**Table 31 Inverse Mass Absorption Coefficients for Neutron Radiation in Various Materials**

| *Material* | *Density* ($g/cm^3$) | $\Sigma f$ ($cm^{-1}$) | $\rho/\Sigma f$ ($g/cm^2$) |
|---|---|---|---|
| **liquid hydrogen** | **.07** | **.04** | **1.75** |
| **lithium hydride** | **.82** | **.15** | **5.47** |
| air (sea-level) | .0012 | $4.7 \times 10^{-5}$ | 25.53 |
| concrete | 2.6 | .09 | 28.89 |
| carbon | 2.6 | .07 | 37.14 |
| iron | 7.9 | .17 | 46.47 |
| tungsten | 19.3 | .22 | 87.73 |
| lead | 11.3 | .12 | 94.17 |
| bismuth | 9.8 | .10 | 98.00 |
| depleted uranium | 18.9 | .17 | 111.18 |

So, again, the shield mass is dependent on an inverse mass absorption coefficient $\rho/\Sigma_r^f$. Table 31 gives values of this quantity for various hydrogenous and nonhydrogenous materials. Both liquid hydrogen and LiH are superior to all nonhydrogenous substances; the choice between the two, discussed earlier, would be based more on construction and operation considerations--a fixed LiH shield placed directly behind the gamma shield would prevent problems associated with propellant tank staging and construction.

The optimal separation distance between the nuclear engine cluster and the crew habitat would be the distance that minimizes the sum of the shielding mass and the supporting structural mass of the central truss. Lead provides the least mass for a given gamma shield requirement (Fig. 76) and the total shielding mass drops off fairly quickly as separation distance increases. Both Pb and W will be examined in the following study. LiH neutron shielding requires no more than ~15% of the shielding depth necessary for gamma attenuation (Fig. 77); liquid hydrogen will not be examined.

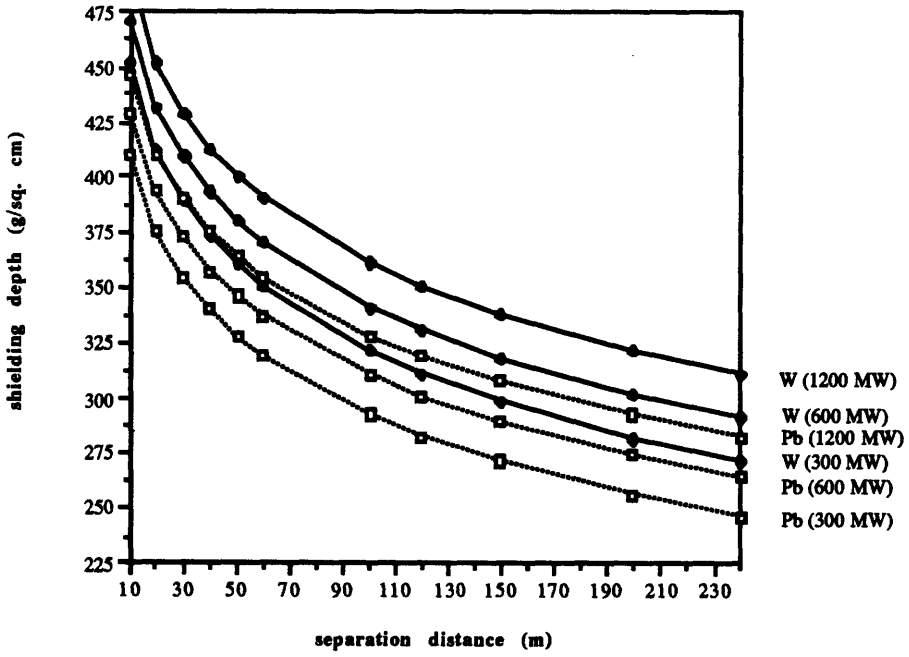


**Figure 76 Gamma shielding depth required for reactor power levels of 300, 600, and 1200 MW**

This trade argues strongly for low-density, high-stiffness support structure to maximize truss length (and therefore achievable separation) and close grouping of the engines within the cluster to lower the shield cross-section. Both Pb/LiH combinations save approximately a

metric ton over their W/LiH counterparts; therefore, Pb/LiH should be strongly considered for shield use. While Pb has little structural strength, it can be contained within a thin tungsten

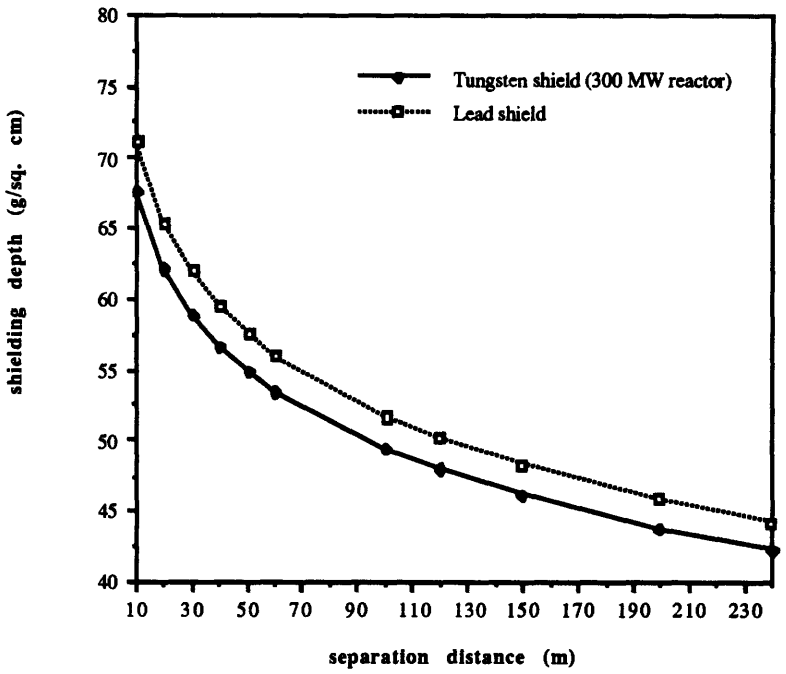


**Figure 77 LiH neutron shield depth (given a lead or tungsten shield providing partial attenuation)**

'shelf' structure with axial tungsten members to transmit loads through the shield--in this way, there is no reduction in gamma attenuation due to the use of inferior gamma shield materials (e.g. steel or aluminum). B/Al should be the material of choice for the supporting structure--it contains a significant boron component and would provide some small additional neutron absorption capability. Its chief rival, Be, delivers higher performance but requires stringent safety conditions on machining due to the toxicity of beryllium dust and filings. This would not preclude its use but should be taken into account.

While increasing the truss length will decrease shielding mass, the truss structure will itself have to increase in mass to maintain static stability. If the central truss connecting the cluster and habitat is modeled as a simple one-dimensional beam, the structure will buckle if the total axial force applied exceeds the Euler (or critical) buckling load[75] :

---

[75] Theory and Analysis of Flight Structures, p. 422, R. Rivello, 1969

$$P_{cr} = \frac{\pi^2 EI}{(L')^2} \tag{39}$$

E is the elastic modulus of the truss material ($N/m^2$), I is its area moment-of-inertia ($m^4$), and L' is the structure's effective length, determined by the boundary conditions imposed on the truss. L' was taken to be approximately L. Maximizing the truss length therefore calls for high elastic modulus and high moment-of-inertia, while minimizing weight requires low density; on the basis of these requirements, the two materials selected for further study were B/Al and beryllium. Their properties are given in Table 32. The assumed configuration of the structure was that of a 1m x 1m box truss, with four axial members, four transverse ties at 1-meter intervals, and a single diagonal beam on each face to stabilize the truss. $P_{cr}$ was taken to be the

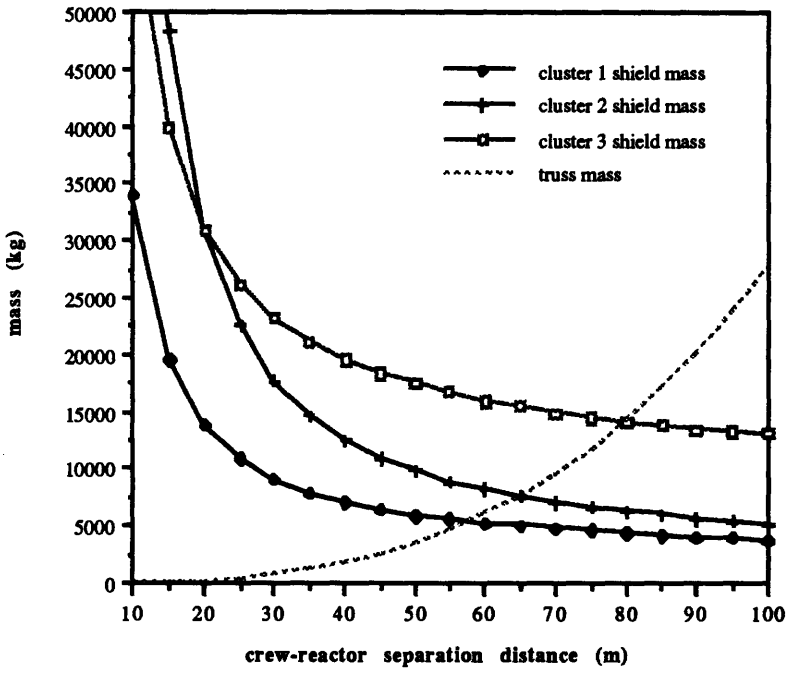


**Figure 78 Structural and shielding mass for various cluster types and crew-reactor separation distances (assumptions: reactor power of 300 MW; safe cone of 20 m diameter; truss assembled from B/Al)**

maximum thrust (assumed to be ~1000 kN) multiplied by a safety factor of 1.5. Then:

$$L = \sqrt{\frac{\pi^2 EI}{1.5F_{max}}} \tag{40}$$

Figure 78 shows the variation in shielding and structural mass with separation distance, given an assumed engine cluster power of 300 MW and a safe cone at crew separation having a diameter of ~20 m. Since the transfer vehicle habitat would be approximately 8 m in diameter, this would permit extravehicular activity by the crew during the transit, without requiring crew members to essentially cling to the sides of the transfer vehicle to remain out of the engine cluster's line-of-sight. Three clusters of variable geometry were considered: cluster 1, having a length of 1 m and a width of 50 cm, approximately the size of the FPBR examined in Section 2.0; cluster 2, with length 2 m and width 50 cm; and cluster 3, having a length of 1 m and a width of 1 m. Clearly, the trend in shield mass for clusters 1 and 2 is approximately the same for increasing separation distance, since as distance becomes infinite, the shield area decreases until it becomes the area of the engine cluster, which is the same for 1 and 2. Cluster 3 is wider and suffers a greater mass penalty for all values of separation distance.

Figure 79 shows the result of adding the curves in Figure 78 to find the overall minimum mass requirements for a given cluster type. All minima fall into the 40-50 m range, with

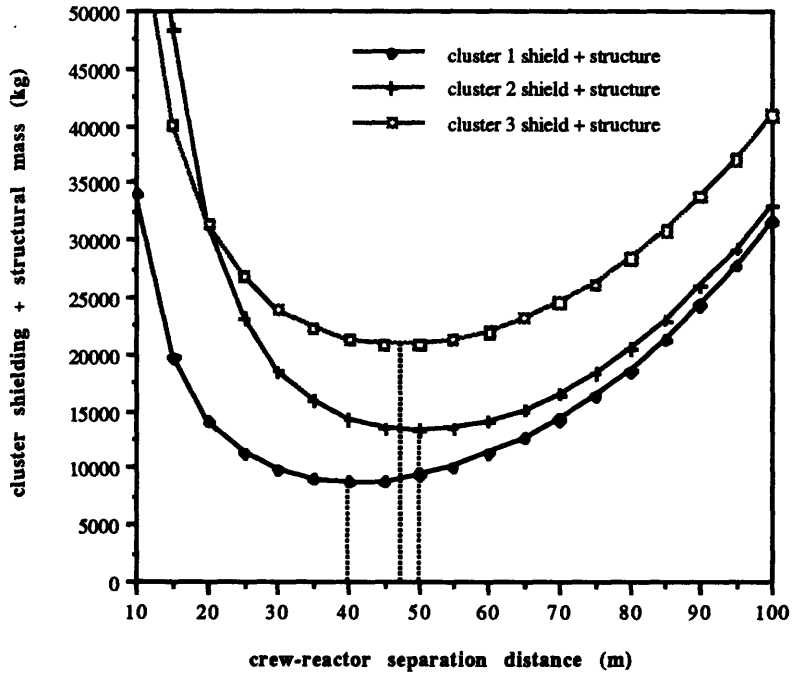


**Figure 79 Total structural and shielding mass (B/Al truss structure, Pb/LiH shield) for various shield area requirements**

signficant increases as separation decreases or increases. As will be seen shortly, stability requirements dictate truss structures of no greater than 9 m in length (for the assumed truss

cross-sectional area of 1 $m^2$); clearly, this would drive overall mass requirements up by a factor of two or possibly three.

As just mentioned, the more restrictive constraint on the truss is its susceptibility to external lateral vibrations, due to motors or engines on the vehicle, or even the sloshing of propellant within its tanks. The natural frequency of the truss structure, $f_{natural}$, should be high enough such that the truss cannot be excited into vibrational modes by other components onboard. This resonance could cause large lateral deflections and damage the structure. A value typically used for $f_{natural}$ aboard spacecraft is 35 hZ. The natural frequency of an equivalent cantilevered beam, of length L, elastic modulus E, cross-sectional area A, and having a mass M and tip mass $M_t$, can be described by the following equation[76] :

$$f_{natural} = 0.276\sqrt{\frac{AE}{M_t L^3 + 0.236ML^3}} \tag{41}$$

The tip mass was taken to be ~20 mT, which would approximate the aggregate mass of engine cluster and shielding in the worst case (prior to jettisoning of some engines after TMI). For the 30-meter B/Al case, the natural frequency was found to be only 5.47 hZ, far too low to guarantee that no resonance take place. To increase this value would require an increase in the

**Table 32 Properties of Structural Materials[77]**

| *Material* | *density* ($g/cm^2$) | *elastic modulus* ($10^9$ $N/m^2$) | *ultimate tensile strength* ($10^6 N/m^2$) |
|---|---|---|---|
| boron/aluminum | 2.60 | 214 | 1491 |
| graphite/epoxy UHM | 1.69 | 289 | 1337 |
| beryllium | 1.85 | 293 | 620 |
| aluminum 7075-T6 | 2.80 | 72 | 441 |

beam's cross-section (although $f_{natural}$ would increase only with the square root of the increase in A) or a reduction in the overall beam length, decreasing the truss mass in the process. To achieve the design floor of 35 hZ required the truss length to be shortened to 8.7 m. The total

---

[76] Space Mission Analysis and Design, p. 409, J. Wertz and W. Larson, Ed., 1991

[77] ibid., p. 394

truss and shield mass then increases from the minimum of 10 mT at 40 meters separation (given the assumptions of cluster 1 in Figures 78 and 79) to just short of 35 mT. This increase is substantial.

It will be seen in the next section that propellant mass requirements drive the design to larger separation distances than the simple truss above will allow. Coupled with the large shield mass penalty incurred by decreasing crew-reactor separation distance, there is a large incentive to find methods that will permit longer structures to be constructed. *The conflict between these issues and structural stability requirements necessitates either passive or active damping of lateral loading to compensate for the increased length of the structure.*

### 3.2.1.4 Tank Construction

The placement of the propellant tanks has been previously discussed; centerline tanks used as neutron attenuators were not deemed acceptable since use of split mission architectures would benefit from multistaging and would therefore require additional shielding. Jettisoning structure making up a portion of the centerline truss following trans-Mars injection would in effect "cut" the vehicle at the separation point (dropping engines and tankage behind it), requiring a second engine cluster to fire during MOI. This second cluster would necessitate a second heavier gamma shield (on the order of 10 to 15 mT). A simpler scheme would involve mounting the propellant tanks along the centerline truss and using a dedicated neutron shield composed of LiH. Two sets of tanks would be required--one for trans-Mars injection and one for the insertion at Mars several months later. These tanks would of necessity be symmetrically placed about the centerline to stabilize the center of gravity of the vehicle throughout impulsive burns.

**Table 33 Mass and Dimension Requirements for Proposed 90-Day Study Launch Vehicles**

| *Vehicle* | *Payload Mass (mT)* | *Dimensions* |
|---|---|---|
| NTS Mars HLLV | 140 | 12.5 x 30 m |
| NTS Lunar | 98.2 | 10 x 30 m |
| STS Mars | 140 | 12.5 x 30 m |
| STS Lunar (Large Fairing) | 61 | 4.6 x 25 m |
| STS Lunar (Small Fairing) | 71 | 7.6 x 25 m |

After the close of operations at Mars, propellant tanks would be transferred from the cargo vehicle to the crew vehicle in preparation for trans-Earth injection.

The single greatest constraint on propellant tank sizing is the payload fairing dimensions and mass ceiling of the launch vehicle; tanks must be constructed and filled with liquid hydrogen prior to placement on-orbit. This limits the baseline's throwweight to ~100 mT in the case of the NTS-derived lunar HLLV and 140 mT for the Mars HLLV. While the lunar mission's propellant requirement would never exceed its launch vehicle's payload ceiling, split mission Mars missions would require at least three chemical NTS launches from Earth to put the necessary liquid hydrogen on-orbit (for the crew transfer vehicle in Table 27, the total propellant requirement is 252 mT for TMI and 80 mT for MOI). A cylindrical $LH_2$ tank containing 126 mT of propellant (50% of the TMI load), having negligible thickness and the maximum diameter allowable for the ALS Mars vehicle, would have to be 14.7 m in length--this is clearly longer than the 9-meter truss length determined in the last section and therefore requires active or passive damping to be designed into the truss to ensure stability.

Tankage must be placed in the shadow of the gamma and neutron shield--direct exposure of tank structure to the radiation environment of the engine cluster will produce a large flux of secondary radiation due to scattering off the tanks, which could prove lethal to an unprotected crew and thus nullify the usefulness of the primary shielding. Prevention of secondary radiation forces the placement of cylindrical propellant tanks as far forward of the engine cluster as is required to put the tanks within the shadow cone of the shield. The alternative would be to design conical tanks that would allow close placement to the shield without any portion of the tank protruding outside the 'safe' cone (Fig. 80).

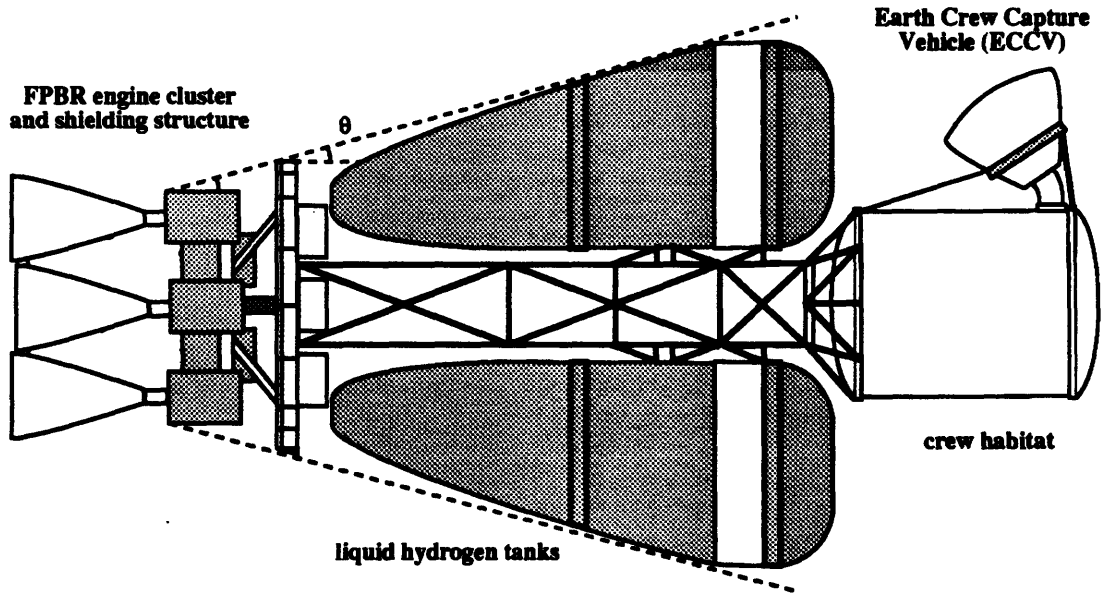


**Figure 80 Hypothetical Mars Transfer Vehicle with conical propellant tanks to reduce overall vehicle length**

### 3.2.2 Ascent/Descent Vehicle Design

This section will detail the operational and design considerations involved in the use of nuclear thermal propulsion for the ascent/descent mission at Mars or on the moon. The five major operational issues are:

(1) Rendezvous between two nuclear vehicles prior to descent and following ascent,

(2) Ensuring safety of the transfer vehicle during the descent burn,

(3) Protecting surface habitats from accidental radiation exposure,

(4) Ensuring crew safety during egress from a nuclear ascent/descent vehicle,

(5) Shielding sensitive cargo during offloading on the moon or Mars.

Using a nuclear thermal option in the ascent/descent phase further complicates the rendezvous procedure between the MEV and MTV, or between the LEV and LTV. Nuclear-propelled excursion vehicles will require radiation shielding similar to that discussed for transfer vehicles; their use will entail operational restrictions (Section 3.3) more severe since docking will require each vehicle to hold the other within its own safety cone.

The MEV or LEV will have to move to a safe separation distance from the transfer vehicle to initiate the descent burn, so that line-of-sight exposure during the burn will be tolerable to any crew remaining onboard the transfer vehicle. This issue is further discussed in 3.3; safe separation will be at least 20 km.

Landing on the lunar or Martian surface must occur far enough away from the habitat or other structures to ensure that there is no chance of accidental exposure, either due to the extreme situation involving an excursion vehicle crash, or simply the line-of-sight exposure during descent and while the vehicle is on the surface. A crash or pad failure near the surface base could conceivably irradiate a large area about the base and prevent further habitation at the site. This is perhaps the greatest argument against ascent/descent use; a single excursion vehicle mishap could have catastrophic consequences for the base itself and the entire planetary mission.

Egress from the excursion vehicle will have to take place in such a way to ensure that the crew remains within the safe zone protected by reactor shielding until alternate protection is made available. This could take the form of a shielded surface transport, since it would simply not be feasible to wait until the engine cluster radioactivity has decayed to acceptable levels--this could take several days to several weeks. An unshielded egress would have to be very fast, since it would be of utmost importance to increase the separation distance between crew and reactor as quickly as possible. This severely compromises crew safety and is clearly an unacceptable method. Protection against secondary radiation reflected from the planetary surface will also have to be considered. Similarly, cargo offloading must be handled so as not

to expose sensitive instrumentation or equipment to radiation from the propulsion reactors. This and crew egress will be difficult to implement without extensive radiation shielding.

It was shown in Section 3.2.1.3 that shadow shielding for the transfer vehicles would mass on the order of 10 mT--the shielding necessary to protect crew members aboard and MEV or LEV might be significantly higher, since:

(1) vehicle stability (during descent, ascent, and on touchdown) would prohibit large separation distances that would be available to a transfer vehicle designer. The requirement to maximize crew separation from the reactor(s) would conflict with a separate requirement for a short, squat design characteristic of landing vehicles. This would raise shield mass for a given reactor power.

(2) High thrust-to-weight requirements for the ascent/descent missions would drive designers to more powerful engine clusters (greater number of engines), thus increasing the shielding necessary, and

(3) egress and cargo offloading would probably necessitate protection beyond simple shadow shielding due to safety considerations--a mishap that could bring a crew member into a reactor's line-of-sight would probably be quickly fatal, and would have to be prevented. As crew safety is characteristically of paramount concern in manned space missions, it is conceivable that a nuclear ascent/descent vehicle might be implemented only if the reactor were totally encased in shielding material. This would drive the total propulsion system weight up considerably.

Given the mission analysis performed on a hypothetical 90-Day Study nuclear MEV and LEV, showing that such vehicles would be viable alternatives only if the total structural costs necessary to modify the vehicles to make them safe and man-rateable could be held significantly below 10 mT, *it would be inappropriate to use nuclear propulsion for either the lunar or Mars ascent/descent missions.*

### 3.2.3 Launch Vehicle Design

An analysis of Earth-to-orbit vehicles with a nuclear upper stage was discussed in Section 3.1.1.2; it was shown that, for the hypothetical launch vehicle under consideration, the second stage could have a fairly high structural mass fraction ($\varepsilon = .33$) or a low-Isp nuclear thermal propulsion system (Isp = 675 s.) for fixed $\varepsilon = .20$ and still remain competitive with an all-chemical system. In order for such a system to be implemented, however, it would certainly require much higher performance.

Like the ascent/descent and transfer vehicles, an ETO vehicle would require shadow shielding to protect crew and/or cargo from exposure to the engine cluster's high radiation flux. All payload and personnel would be required to remain within the safe cone during operation of

the engines. Propellant tanks would be tapered near the rear to allow the use of less massive shielding. Ignition of the nuclear stage would not occur until the vehicle emerges from the atmosphere, far enough downrange to prevent debris from falling on human habitations. A discussion of docking and maneuvering can be found in Section 3.3, and will impact on launch vehicle operations following insertion into LEO.

Operational problems would include failure of the vehicle at some point in its ascent trajectory and the method for disposing of the spent vehicle once its payload has been delivered to LEO. The second problem, disposal, is addressed more fully in Section 3.3.2, but it should be noted here that simply allowing the launch vehicle's orbit to decay and reenter would not be a politically acceptable solution, especially when the number of ETO flights necessary to implement the baseline architectures would be in the hundreds. This would require moving the spent vehicle to a 'safe' orbit, either in near-Earth space or beyond.

The launch vehicle could fail (1) on the pad before launch, (2) during the ascent stage but before ignition of the nuclear second stage, and (3) following nuclear stage ignition. Any failure prior to nuclear stage ignition would not result in any significant release of radioactives since the nuclear stage would not have been fired previously. Such failures would necessitate stringent engine-out requirements and high reliability on the first stage; the launch vehicle should be put into orbit if at all possible. Additionally, the nuclear stage would have to be designed to withstand an ocean impact intact in the event of a first-stage mishap and would have to be incapable of becoming critical on immersion in water.

The most acute failure would be one which occurred following second-stage ignition. At this point in the ascent, the engines would be operating and highly radioactive. A failure in the engine cluster itself might require only the shutdown of a single engine or, in the case of a reactor gone supercritical, jettisoning of the engine altogether. Clearly, propulsion system reliability is of greater concern here than onboard a transfer vehicle, since a failure after nuclear stage ignition would likely return radioactive debris to Earth. Even if such debris were widely dispersed and the consequent damage nil, public outcry could halt further launches:

> "In 1989, antinuclear activists, protesting potential 'Chernobyls in the skies,' organized the first civil-disobedience demonstrations aimed at halting a U.S. space shot. Their target: NASA's Galileo spacecraft, an interplanetary scientific mission that used as its power source two radioisotope thermoelectric generators fueled by plutonium. In October 1989, the Galileo launch went off without a hitch, despite the protests."[78]

Thus, operational considerations indicate that:

---

[78] "Star Wars Does It Again," Philip Elmer-DeWitt, Time, 15 April 1991

(1) lower and upper stages of a launch vehicle will require engine-out capability and high reliability to ensure that the vehicle will safely reach orbit,
(2) engine construction must include provisions for possible ocean impact in the event of failure before nuclear-stage ignition,
(3) radioactive engines must be disposed of by raising spent launch vehicles to safe orbits.

## 3.3 Impact on orbital operations

Replacing the chemical/aerobrake system of the NASA baseline with a nuclear system poses difficult operational problems on-orbit. These problems are all associated with the hazardous radioactivity released from the reactor(s) and affect:
(1) Propulsion system serviceability (and thus system design), in addition to extravehicular activity both during reactor operation and following shutdown,
(2) orbital maneuvering (rendezvous and docking procedures),
(3) low lunar orbit firing, and
(4) means for disposing of propulsion system components at end-of-life.

### 3.3.1 Cooldown, Serviceability, and EVA

A nuclear thermal propulsion system will remain lethally radioactive for days following even a short burn. When the system is shut down after use, decay products within the fuel elements will generate power (and radioactivity) at a fraction of the operating power. As mentioned earlier, Prof. Rasmussen (Dept. of Nuclear Engineering, MIT) states that this fraction is highly dependent on reactor operation time and can be taken to be approximately 8% of full power immediately following shutdown of a reactor that has been operating "for a period of months or longer." For the FPBR under consideration, the burn time will be no greater than 14 to 18 minutes, given the thrust requirements described earlier in the chapter detailing mission analysis. Long-duration operation of a reactor allows the inventory of fission products to increase as a function of specific products' half-lives. For a given product with a half-life of t seconds, the reactor will produce more and more of the product until a steady-state inventory is reached. This inventory is governed by the equation:

$$\frac{m_p(t)}{m_{p,\infty}} = 1 - e^{\frac{t}{\tau}}$$

Here, $m_p(t)$ is the mass of fission product for a given time t, while $m_{p,\infty}$ is the steady-state inventory, and $\tau$ incorporates the half-life of the fission product. Over 99% of the steady-state

mass is reached after three time constants, so a burn time of 885 seconds will clearly saturate all fission product inventories with half-lives of five minutes or less. However, these products will decay very quickly following shutdown. Products with substantial half-lives will not have time to build up in appreciable amounts.

The dose is essentially gamma radiation; other decay products which form by alpha or beta decay will be captured within the reactor and will not pose a hazard to crew or cargo. Bussard and DeLauer give the dose rate (in rem/hr./MW) for times after reactor shutdown as[79] :

$$\frac{A_s D_\gamma}{P_r} = 2.5 \times 10^{10}\left[\left(\frac{f_d}{1 + 0.08 f_d}\right)\left(\frac{t_o^{-0.2} - (t_o + t_b)^{-0.2}}{r^2}\right)\right]$$

$t_o$ is the time since reactor shutdown, while $t_b$ is the burn time. The separation distance r is, as always, given in centimeters. This equation can be simplified and solved for the dose rate per second, given an assumed attenuation factor $A_s$ of 1 and a decay fraction of .4:

$$D_\gamma = 1.495 \times 10^{8}\left[\frac{P_r}{r^2}\left(t_o^{-0.2} - (t_o + t_b)^{-0.2}\right)\right]$$

The decay fraction of .4 was calculated under the assumption that few product inventories would be saturated following engine shutdown. Dr. Glen Graves performs several calculations that illustrate the gamma radiation power supplied following short-term operation of a hypothetical nuclear thermal propulsion system[79] ; values of $f_d$ were found for Graves' data and a decay fraction determined from linear extrapolation. Assuming a linear increase in decay fraction with operating time is conservative, since the trend in $f_d$ was clearly less than linear in Graves' calculations. Additionally, the exponent of $t_o$, -0.2, is also conservative, since it takes into account the decay of the entire set of fission product inventories; the true value of this exponent for short-term operation will be smaller than -0.2. Figure 81 shows that the dose rate per unit reactor power decays quickly following shutdown. For instance, while approximately a week is required before unshielded crew members can approach within one kilometer of a 300 MW engine for a single hour (and receive 5 rem), the dose rate is still far too high to permit closer inspection. A one-hour exposure at a separation distance of 100 meters would not become possible for more than a year.

---

[79] Fundamentals of Nuclear Flight, p 272

[79] Radiation Enviromental Analysis: A Reference Reactor Concept and a Standard Operating Cycle, G. Graves, pp. 475-567, in Notes for the 1962 NSF Advanced Subject Material Institute on Nuclear Rocket Propulsion, Florida Engineering & Industrial Experimentation Station, 1962

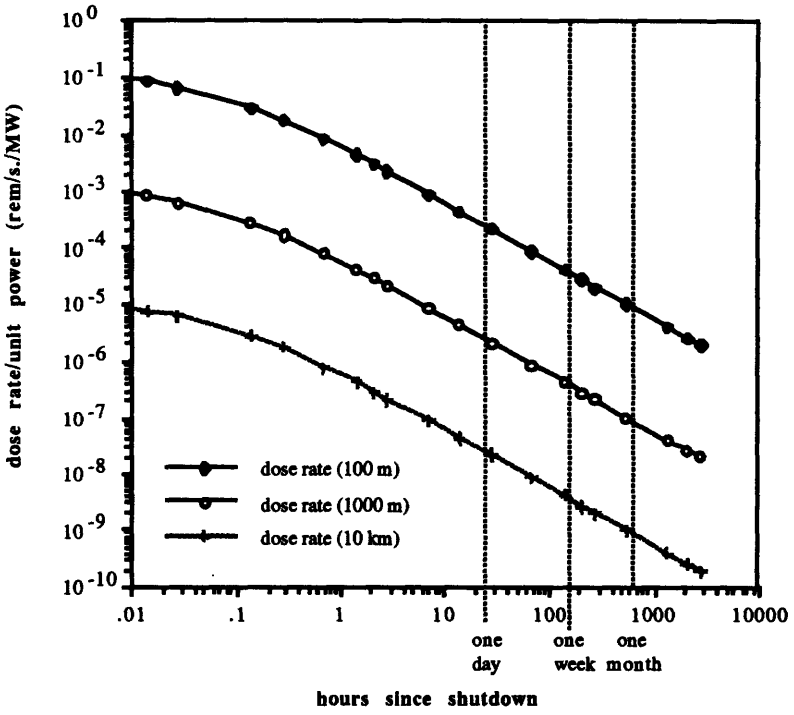


**Figure 81 Dose rate/unit power (rem/s./MW) for 100m, 1000 m, and 10 km separation distances following shutdown of an arbitrary reactor following an 885-s. burn (assumed decay fraction of .4)**

Presenting this data in a slightly different format displays the accumulated dose that exposed personnel would receive, assuming that their exposure began immediately following engine shutdown after an 885-second burn. Exposure is assumed to occur at a fixed distance. The equation for $D_\gamma$ can be integrated with respect to $t_0$ between two times following shutdown, giving the results seen in Figure 82.

Total accumulated dose following shutdown is approximately .01 rem/MW at a 20 km separation distance. For a 300-MW reactor, this translates to a 3 rem exposure. At two kilometers, the exposure would increase to 300 rem, usually a fatal dose. This data will be examined further in the next section, detailing docking and rendezvous restrictions.

Any servicing the engine system would therefore have to be done entirely by remote vehicle (via teleoperation) or dispensed with altogether as too expensive or time-consuming a process. Since the high radiation efflux very close to the engine following a burn could damage electronic and structural components within a repair vehicle, such a device would have to include shielding as a necessary requirement for its construction. Because of the problems associated with repair, serviceability should be discarded; this would drive a requirement for

very high reliability or requiring a number of engines to ensure redundancy in the event of a single reactor failure.

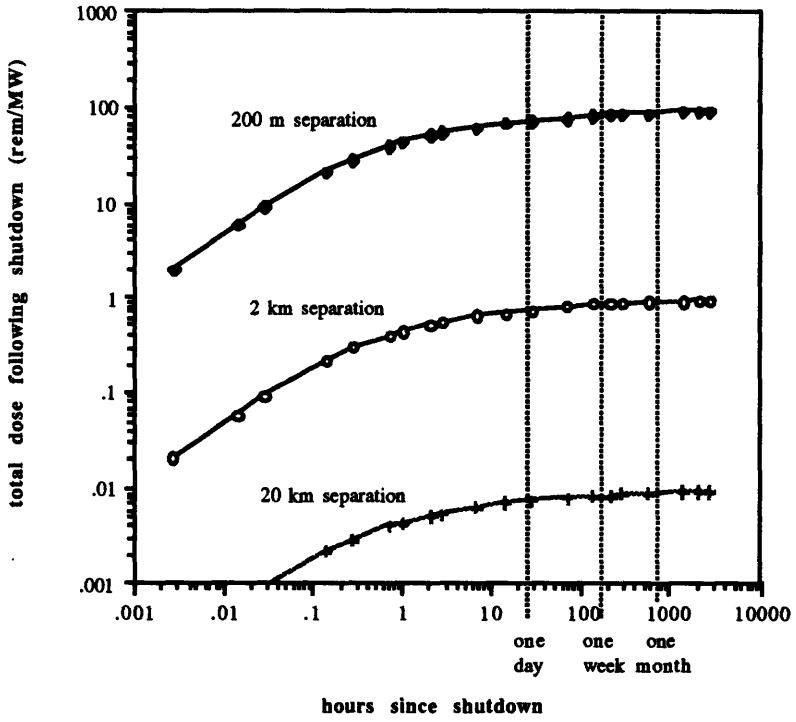


**Figure 82 Accumulated gamma radiation dose (rem/MW) at separation distances of 200 m, 2 km, and 20 km, assuming exposure begins immediately following shutdown after an 885-s. burn**

Given the work done in Section 3.2 involving restrictions on overall vehicle length, which suggest that the central truss structure of the vehicle be not much longer than stability principles would allow (perhaps ~10 m), the crew separation distance would be on the order of this value. Certainly, extravehicular activity (EVA) would need to be restricted to the safety cone provided by the shadow shield at all times after initial operation of the engine cluster.

### 3.3.2 Docking and Maneuvering Near Manned Stations

The use of transportation nodes in LEO, LMO, or lunar orbit will require strict docking and maneuvering procedures in order to prevent accidental exposure of station personnel or cargo to the unshielded radiation flux emerging from nuclear vehicles. Even if the use of transportation nodes such as Space Station Freedom were eliminated altogether, as is suggested by NASA's Synthesis Group, split missions would entail on-orbit rendezvous in low Mars orbit between crew and cargo vehicles. Routine transfer of personnel or fuel between

ascent/descent vehicles and orbital transfer vehicles would also necessitate careful maneuvering near nuclear propulsion clusters.

The types of maneuvers that pose safety hazards thus include:

(1) departure from an LEO transportation node,

(2) arrival at a LEO node,

(3) docking with ascent/descent vehicles prior to or following a stay on the moon or Mars.

Departure of a transfer vehicle containing pristine (never fired) engines from an LEO station would require no special precautions regarding engine line-of-sight with the station. Since--as explained in Section 3.2.1.3--the safe distance for unshielded personnel viewing a single active 300-MW FPBR is approximately 20 km, the transfer vehicle will have to achieve this separation distance either by non-nuclear means (perhaps a small chemical propulsion system) or a tug vehicle such as NASA's proposed OMV (Orbital Maneuvering Vehicle). The tug would ferry the transfer vehicle to the required separation and return to the LEO station.

In the case of a departing transfer vehicle with engines undergoing reuse (Fig. 83), the vehicle's shadow cone would have to include the station while en route to a safe separation point in order to prevent accidental exposure to station personnel and transfer vehicle crew (through secondary radiation scattered off of the station itself). This would apply primarily to reusable nuclear lunar vehicles returning to the moon. The 90-Day baseline options assume lunar flights occur on the order of (at most) three times per year and, during the operational phase of the base, once per year. This would allow the vehicle's engine cluster to cool down to fairly low radiation levels; small maneuvering errors near the station would not produce significant absorbed doses in the station personnel.

The case of an arriving transfer vehicle is more complex. The vehicle's engine cluster is highly radioactive after the insertion burn into Earth orbit and mistakes in rendezvous could be lethal to both station and vehicle crew. Initial approach to the station following insertion should begin after a cooldown period of 27 hours (engine clusters containing multiple engines will require a longer cooldown period). This will allow a safe one hour exposure at 100 meters in the event of manuevering errors. Again, the transfer vehicle's safety cone would have to include the station throughout approach. Actual docking of the transfer vehicle to the station would require extreme safety precautions due to the very short separation distance; a telescoping docking boom (to prevent the vehicle from rotating freely in space) in addition to the use of an OMV to ferry crew and cargo constitute a safer option.

While the nuclear vehicle is docked at the station, any extravehicular activity performed by station personnel would have to be conducted within the vehicle safety cone. Additionally,

other vehicles leaving or approaching the station will have to do so within the safety cone--this would apply mainly to OMV's and reentry vehicles.

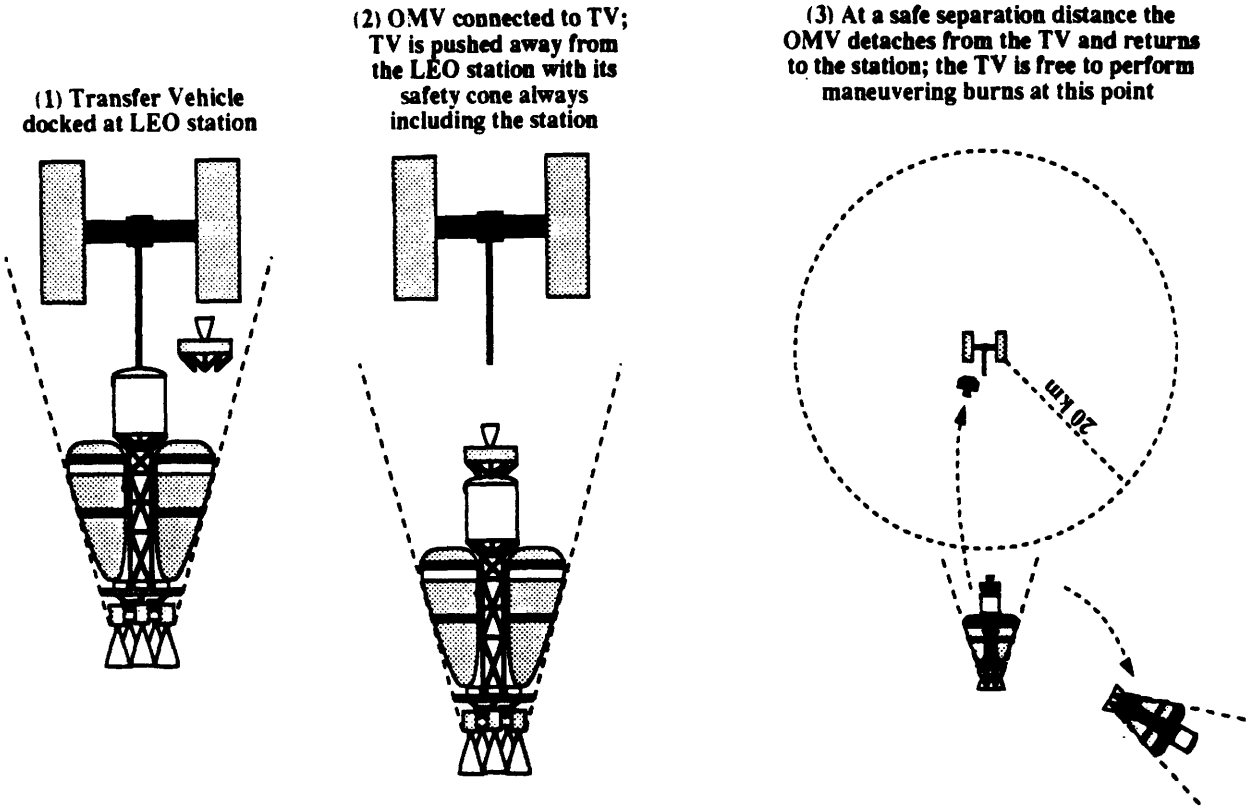


**Figure 83 Departure of transfer vehicle from Freedom or other LEO station; vehicle has previously used engines**

The rendezvous of ascent/descent vehicles with transfer vehicles or split mission vehicles presents the same difficulty as that found in docking with an LEO station. Following insertion into Mars or lunar orbit, the transfer vehicle will have only a short period of time before some form of docking procedure is required. At Mars, this is less stringent, since the mission stay time at the planet could last tens to hundreds of days and a day-long cooldown period could coincide with status checks and tasks that have to be performed before the crew and cargo could descend to the Martian surface. Thus, the procedure to be followed at Mars between split mission vehicles MTV and MEV would be essentially the same as at a LEO station: the MTV's safety cone would have to include the MEV throughout the entire approach/departure phase. At safe separation distances (20 kilometers), the two vehicles would be free to perform necessary maneuvers (descent to Mars, etc.). On ascent, the MEV would maneuver into the MTV's orbit but at safe separation. A slow 'catch-up' could then be performed.

Lunar docking procedures would be similar; however, adding two days for engine cooldown onto the lunar flight for each rendezvous (one in LLO, the other on return to LEO) would increase the total time spent aboard the transfer vehicle from 7 to perhaps 9 days. This should not require significant additional life support requirements.

Nuclear thermal propulsion will produce high radiation fluxes, in excess of 1000 rem/s, during operation, and a significant but quickly decaying flux will exist even following shutdown of the engine cluster. These fluxes represent extreme danger to personnel aboard both the nuclear vehicle and aboard vehicles or stations that come into contact with the nuclear vehicle. The possibility of exposure to lethal absorbed doses during operation require engine shutdown prior to the approach of the nuclear vehicle to other vehicles or stations. None of the precautions impose cooldown phases on the order of the mission transfer times. However:

(1) Departure from LEO by a pristine transfer vehicle will require that the transfer vehicle is moved to safe separation distance (20 km) before igniting its engine cluster. This will prevent exposure of LEO station personnel to an absorbed dose exceeding 5 rem; however, it is important to note that the transfer vehicle's burn will quickly take it far beyond this safe separation and 20 km will therefore provide more protection than is absolutely necessary. An unmanned or remotely piloted tug should be used to ferry the transfer vehicle to the 20 km separation.

(2) Departing lunar transfer vehicles that are undergoing reuse of their engines will be towed to safe separation distance in the same manner as pristine transfer vehicles. However, during the ferrying operation, the tug should maneuver to maintain the LEO station within the safe cone of the transfer vehicle. Following the tug's departure, the transfer vehicle can maneuver at will.

(3) Arriving transfer vehicles will be subjected to a cooldown phase of one day to reduce the danger of short-duration radiation exposure during final approach of the vehicle to a hypothetical LEO station. This requirement is necessary, since a 15-second exposure at 1 km immediately following shutdown would result in a total dose of ~.45 rem, while the same exposure after a one-day cooldown would only be ~.01 rem. Approach by tug vehicle would hold the station or approaching vehicle within the safe cone, while actual docking would necessitate a rigid docking boom and crew/cargo transfer within the same safe cone.

(4) Rendezvous of ascent/descent vehicles and the nuclear orbital transfer vehicle would be similar to station/vehicle rendezvous, with the transfer vehicle maneuvering to keep the ascent/descent vehicle within its safe cone throughout the docking maneuver. Removal to safe separation would be required before ignition of the transfer vehicle's nuclear engines.

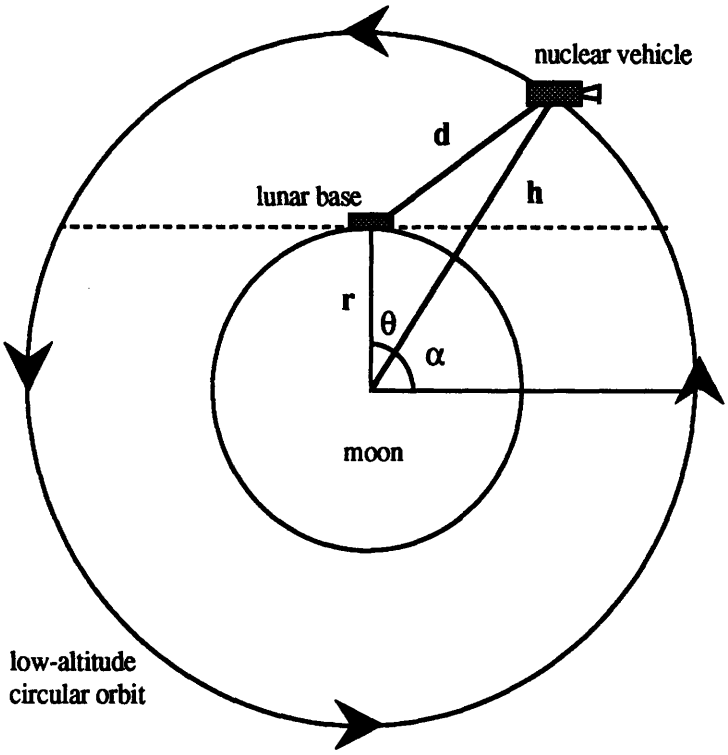


**Figure 84 Overflight Model**

### 3.3.3 Flyover

The issue of flyover radiation exposure is important only for the moon or other airless bodies. The atmospheres of both Earth and Mars are extremely effective radiation shields. To model the problem of a hypothetical lunar base coming into the line-of-sight of an orbiting nuclear transfer vehicle, the transfer vehicle's orbit was assumed circular. Then the separation distance (d) between the base and vehicle can be described by a law of cosines relation:

$$d = \sqrt{r^2 + (r + h)^2 - 2r(r + h)\cos\theta}$$

Figure 84 illustrates the geometry of the model; r is the lunar radius, h is the orbital altitude of the LTV, while $\theta$ defines the angle between the central force vectors of the base and the vehicle, respectively. $\alpha$ is the angle between the vehicle's central force vector and "horizontal," parallel to the tangent line through the lunar base. The vehicle emerges above the horizon when:

$$\theta = \theta_1 = \sin^{-1}\left(\frac{r}{r + h}\right)$$

and descends below the far horizon when $\theta = \theta_2 = \pi - \theta_1$. The base-vehicle distance was calculated for twenty-five points spaced at equal angular separation along the arc within the line-of-sight, and an average separation distance calculated. Assuming the engine to be operating at full power, the dose rate from Section 3.2.1.3 would be:

$$D_t = 8.371 \times 10^7 \left(\frac{P_r}{d^2}\right)$$

Given the orbital period of the transfer vehicle, the total dose received by unshielded lunar base personnel would then be the dose rate at the average separation distance multiplied by the time the vehicle spends above the local base horizon.

Results are shown in Figure 85. For decreasing orbital altitude, the stay time above the horizon decreases but not enough to prevent a slow rise in the total absorbed dose. Yet for the values considered (10 - 80 km), it is apparent that the total dose received at the base is small, ranging from
.02 to .06 rem for a single pass by a 300-MW propulsion system. For a given altitude, this dose increases linearly with reactor power. Since the lunar base will require some form of radiation protection to guard against galactic cosmic radiation and solar particle events, both of which will amount to doses in the tens of rems, it can be seen that flyover radiation, even for very low-altitude passes, will not present danger to the base or personnel inside. No special precautions will be necessary when designing the base structure. However, since unshielded crew members performing experiments outside the base proper could receive unnecessary radiation exposure, surface visits would have to be strictly scheduled to keep personnel inside the base during overflight. The alternative would be to perform all lunar-orbit maneuvers below the local horizon; this would simplify the problem by not requiring surface visit restrictions.

The radiation hazard posed by the overflight of a lunar base by an active nuclear vehicle is negligible; the vehicle's average separation distance within the range of altitudes investigated is too large to expose crew to any significant dose. Simple precautions will prevent crew exposure to the low radiation flux. These include:

(1) Requiring crew members not to venture outside the habitat during overflight. It is assumed that the lunar habitat will be well-protected from SPE and cosmic radiation; the radiation flux of a particle event or even the constant galactic cosmic radiation flux will be much higher and will have to be guarded against. The habitat's protection against these forms of radiation will easily be sufficient to attenuate the flux from a small engine cluster

at long distances.

(2) Requiring all vehicles in orbit to perform their maneuvering burns below the base's horizon.

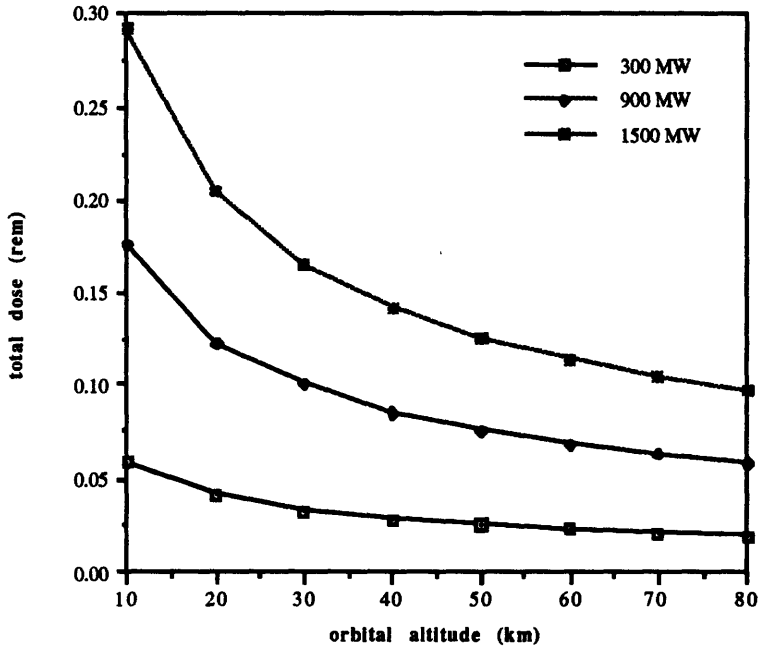


**Figure 85 Total absorbed dose received at a lunar base due to overflight by a nuclear transfer vehicle at altitudes of 10 - 80 km.**

### 3.3.4 Disposal methods

After use, particle bed reactors will remain radioactive and will require some form of disposal method to ensure that they do not come in contact with manned vehicles, bases, or stations, or reenter the Earth's atmosphere to endanger civilian populations. The various scenarios include:

(1) Reactors jettisoned following the TMI and TEI phases of Mars missions: These will not take part in subsequent insertion burns and would follow the original--and probably elliptical--path of the vehicle. (If the original path were parabolic or hyperbolic, which might occur on a high-energy trajectory, clearly no return would occur.) In order to mitigate the possibility of an early return by an engine cluster to near-Earth space, mission designers will have to carefully plan the trajectory followed by the jettisoned cluster to ensure that such a return would occur after the reactor radioactivity has decayed to acceptable levels.

(2) Split mission cargo vehicles: The reactors would reach end-of-life in Mars orbit following docking and cargo transfer with the crew vehicle. The cargo vehicle and its engine cluster would remain in the 250 x 34000 km capture orbit.

(3) Return of the split mission crew vehicle to Earth: The Earth Crew Capture Vehicle will perform a direct reentry at Earth after minor propulsive maneuvering. The nuclear stage would have to be jettisoned before these maneuvers occurred to prevent its reentry as well. Risk mitigation should include design of a reentry trajectory that would allow jettisoning of the nuclear stage prior to the final reentry maneuvers and placement of the stage on a course that would take it out of near-Earth space.

(4) Reusable lunar transfer vehicle: At end of life, the vehicle returns to LEO.

The issue of disposal is most important in LEO, where the expended LTV's will have to be moved to higher orbits to prevent reentry of radioactive material. Less serious is the disposition of split mission cargo vehicles in Mars orbit. The alternatives available consist of:

(1) transfer to a high, stable orbit at Earth or Mars (this could include Lagrange points),

(2) transfer to a heliocentric orbit that would not intercept the path of the Earth,

(3) transfer to a hyperbolic escape orbit (including sun intercept),

(4) burial on moon or Mars.

The decision among these options consists of a tradeoff between the expense of reaching the desired disposal zone and the safety afforded by placing the radioactive waste in that zone. The safest options (depositing waste in the sun or putting it on an escape trajectory) are the safest and also the most expensive. Sun-intercept would cost on the order of 30 km/s. of $\Delta v$, since the disposal mission would have to lose most of its velocity relative to the sun in order to reach it. Escape from LEO and then the solar system would require a $\Delta v$ of ~10 km/s. With respect to the third, Griffin and French note:

> "...interplanetary space seems the most desirable arena for disposal, preferably in an orbit far from that of the Earth. One approach would steal a page from the Mariner 10 mission. For a total expenditure of energy less than that for a landing on the moon, the material could be sent on a trajectory to flyby Venus. This could move the perihelion of the orbit to a point between Venus and Mercury. A relatively minor velocity change at the perihelion of the orbit would then lower aphelion inside the orbit of Venus. The package would then be in a stable, predictable orbit that would never again come close to the Earth."[80]

The least safe options (burial or transfer to high orbits) are fairly cheap in terms of propellant expenditure. Moving waste to a long-lifetime Earth orbit would require velocity changes on the order of hundreds, not thousands of meters per second. Such "safe" orbits are

---

[80] Space Vehicle Design, p. 40

generally considered to be circular with lifetimes exceeding 1000 years[81]. While these orbits will decay and eventually fall to Earth, the material aboard will have become inert by the time of reentry. To determine a baseline orbit for waste disposal, it is necessary to know how the orbit's semi-major axis will change due to induced atmospheric drag. An approximate circular orbit lifetime can be found using:[82]

$$\Delta a_{rev} = -2\pi\left(\frac{C_D A}{m}\right)a^2\rho$$

$\Delta a_{rev}$ denotes the change in the semi-major axis per revolution--it is related to the ballistic coefficient $C_D A/m$, the semi-major axis itself, and $\rho$, the atmospheric density at altitude. The lifetime is then:

$$L = \frac{-H}{\Delta a_{rev}}$$

H is the scale height of the atmosphere at altitude. Wertz and Larson note that this lifetime is affected principally by solar activity. By using an initial orbit altitude of 1000 km, a ballistic coefficient of .022, and assuming maximum solar activity, these equations give a lifetime of only 220 years. Assuming minimum activity raises this value to 4825 years.

Orbits exceeding 1000 km fall in the lower regions of the Van Allen belts, the zone of trapped particles circling the Earth. These orbits are not typically used by satellites due to the effect of the high-energy particle streams in the belts; non-hardened electronic components would quickly be rendered useless. Thus, these regions, which provide fairly stable orbits for hundreds of years but are generally not considered for other uses, could be used to store long-term radioactive materials. Wertz and Larson note:

> "Those who launched SNAP 10A with a nuclear reactor in 1965 launched the reactor in a subcritical mode, designed it to remain subcritical at or after impact if it should reenter the atmosphere before start-up, and delayed its startup until after it had reached orbit. It is in an almost circular polar orbit, which has a decay life of 4000 years. Additionally, this reactor was designed to come apart on reentry."[83]

However, the prospect of adding to the growing amount of orbital debris already present in near-Earth orbit is not attractive; additionally, nuclear waste left in Earth orbit might prove

---

[81] Space Reactor End of Life Issues, Albert, Science Applications International Corporation, p. 192

[82] Space Mission Analysis and Design, p. 127

[83] ibid., p. 698

politically infeasible with a public sensitized to nuclear issues, simply because it would 'eventually' fall--even if that time were far in the future.

**Table 34 Disposal of reactors in LEO**

| Mitigation strategy | Δv cost | Operational considerations |
|---|---|---|
| Allow to break up on reentry | None | Public perception would make this option impossible even if reentry would scatter material widely enough to make it safe |
| Boost to circular orbit ≥ 1000 km. | **≥ 300 m/s** | low propellant cost<br>material is still in near-Earth orbit which will eventually decay |
| Boost to escape system | ≥ 9200 m/s | high propellant cost<br>no return of waste to Earth possible |
| Deboost to sun-intercept (perihelion at 1 x $10^6$ km.) | 23200 m/s | very high propellant cost<br>waste is destroyed |
| burial on lunar surface | 6400 m/s | high propellant cost<br>no return of waste<br>lunar surface contaminated |
| Deboost to orbit between Venus and Mercury | **≥ 2500 m/s** | medium propellant cost<br>no return of waste |

Burial on the moon or possibly Mars will render certain areas of either body useless for human exploration and will require a large propellant cost, "since the material would need to be soft-landed to avoid scattering at impact."[84]

This would indicate that:

(1) Due to the high expense of most options, LTV engine clusters should either be boosted to circular orbits with altitudes exceeding 1000 km., or transferred to circular orbits with perihelions below the orbit of Venus. These missions are fairly low cost yet very safe; however, it is important to note that leaving radioactives in Earth orbit may prove difficult to implement regardless of the relative safety afforded by such orbits. The American public might feel that, given that such an orbit would have a finite decay period and that material placed in such an orbit must come down (even if such an eventuality is far in the future), no near-Earth orbit would prove acceptable.

(2) Mars split mission cargo vehicles should remain in their parking orbits or should have their pericenter raised to prevent premature decay of the orbit and the cargo vehicle's impact on

---

[84] Space Vehicle Design, p. 40

the Martian surface; missions to Mars will remain relatively rare for the forseeable future and it is unlikely that the derelict cargo missions will pose a major threat to Mars operations.

## 3.4 Impact on Surface Facilities and Surface Operations

### 3.4.1 Earthbound facilities

NTP engines will have to be tested, transported to the launch facility, launched, and tracked while on or orbiting the Earth. The main issues involved in building and operating surface facilities on Earth are:

(1) Test stand and flight engine test safety,

(2) transportation and launch pad safety, and

(3) handling of crises during the ascent of nuclear systems

Nuclear engines will have to undergo a rigorous ground testing procedure before flight qualification and further tests before vehicles will be considered man-rateable. ROVER/ NERVA tests were conducted at a remote location in Nevada, far from any civilian population. NERVA engine effluent was released directly to the atmosphere (although later efforts were made to scrub the effluent for radioactives). Koenig describes the Nuclear Furnace (NF-1), the final NERVA reactor:

> "The hydrogen exhaust gas was handled differently than in previous reactors. Instead of being exhausted through a convergent-divergent nozzle directly into the atmosphere, the hot hydrogen was first cooled by injecting water directly into the exhaust gas stream....The resulting mixture of steam and hydrogen gas was then ducted to an effluent cleanup system to remove fission products before release of the cleaned gas to the atmosphere."[85]

This method, while capable of scrubbing the effluent, would probably not be able to deal effectively with some of the problems experienced very early in the nuclear rocket program:

> "The Kiwi-B test series was initiated with the Kiwi-B1A test in December 1961 and culminated two years and eight months later with the successful Kiwi-B4E test accomplished in August 1964....During this test series...severe structural damage to the core was experienced...when the hot ends of seven fuel modules were ejected from the core during the transient rise to full power."[86]

The possibility of core meltdowns on the test stand and production of highly radioactive ejecta drive a requirement for containment of all effluent and confinement of this material

---

[85] Experience Gained from the Space Nuclear Rocket Program, D. Koenig, p. 12, Los Alamos National Laboratories LA-10062-H

[86] ibid., p. 9

underground. Disposal of the test stand engines themselves would have to be at a radioactive waste storage facility, such as the one presently under construction at Yucca Mountain, Nevada. Alternately, radioactive engines could be stored onsite at a facility constructed specifically for this purpose.

Flight engines would be required to undergo only very limited testing to ensure their transportability and safety while being moved to the launch facility and placed aboard a launch vehicle. Depending on the total operating time prior to launch, the reactor will have to be quarantined for an extensive period of time before it can be moved. If, for example, a 300-MW reactor is tested for a time equal to the maximum Earth-orbit burn time (885 s.) considered in this report, it will not be possible for unshielded personnel to move within 1000 m of the reactor for a single hour for 24 hours after firing. (This assumes no atmospheric shielding--the actual dose will be lower.) Nevertheless, it clearly indicates that only minimal testing of a flight engine can be performed unless radical precautions are taken later to ensure safety during handling if such handling is to be conducted soon after testing. The alternative is to provide a long cooldown period (on the order of months) to allow decay of radiation to reasonably safe levels. An accident during transit or during checkout at the launch facility could be prevented by completely encasing the reactor in a lead- or tungsten-lined container and by using remote means to place the engine aboard the launch vehicle.

Test crew and transport personnel should be thoroughly familiar with safety precautions required around nuclear engines. The possibility of a pad explosion or downrange accident following launch should be prepared for; standby recovery teams would have to be available to retrieve possibly radioactive debris in the event of premature reentry (after second stage ignition).

While testing, transporting, and launching nuclear systems present some of the greatest dangers of environmental contamination in case of mishap, strict safety procedures will prevent both the civilian population and personnel in contact with the engines from exposure to radioactivity. Conducting engine testing in remote locations and requiring the containment of all effluent will prevent the release of any radioactive propellant (or, in case of a core meltdown, the highly radioactive core structure) into the environment. Flight engines would be tested only to criticality and then shut down to keep residual radioactivity to an absolute minimum while satisfying the need for testing of the flight article. Short-duration testing will also decrease the level of precautions necessary for personnel safety while the engines are being transported to the launch facility and loaded aboard the launch vehicle. Stringent range safety protocol will have to be observed during the firing of launch vehicles with nuclear upper stages or nuclear cargo; this will include personnel to retrieve radioactive debris in the event of a vehicle failing on the pad or prior to reaching orbit.

### 3.4.2 Extraterrestrial Facilities

The use of nuclear ascent/descent vehicles would have the strongest impact on operations of a lunar or Martian facility. Many difficulties would arise due to possible contamination of an extraterrestrial habitat in the event of an excursion vehicle failure and crash near the habitat on landing or ascent, as well as shielding of crew and cargo during egress from the vehicle. Since nuclear excursion vehicles were dismissed on the basis of (1) their lack of cost-effectiveness, and (2) the lack of uncomplicated solutions to the operational problems, it will not be necessary to further discuss their impact.

Essentially, the two remaining problems are possible irradiation of unprotected personnel during flyover and the crash of a nuclear transfer vehicle near a lunar or Martian base. Lunar flyover, discussed in an earlier section, was shown to be important only during engine operation over unshielded personnel (such as crew members outside a lunar habitat). Since the lunar habitat will require radiation protection to guard against solar particle events and galactic cosmic radiation, both having greater magnitude than flyover doses, no extra habitat protection will be required. Personnel on the lunar surface should schedule their visits so as not to be outside during an 'active' flyover.

## 4.0 SUMMARY AND CONCLUSIONS

This report covered NASA's 90-Day Study and its baseline missions to the moon and Mars. The use of nuclear thermal propulsion for launch vehicles, ascent/descent vehicles, and orbital transfer vehicles was investigated, with heavy emphasis on the possible use of NTP for orbital transfer. Various solid-core and gas-core designs were evaluated to determine if NTP offered substantially higher payload delivery and/or lower initial mission mass requirements than the NASA chemical/aerobrake baseline. All-Up and Split missions were examined.

On the basis of the mission analyses performed in Section 3.1, the impact of using nuclear thermal engines on various vehicles and facilities was examined to find if the engines would pose insurmountable hazards or require large complications in operations to ensure safety both on-orbit and on planetary surfaces.

### 4.1 Conclusions

The conclusions discussed in this section are divided into issues of performance and issues of construction, operation and testing.

#### 4.1.1 Issues of Performance

• The fixed particle bed reactor outperformed the chemical/aerobrake baseline design and other nuclear thermal options, providing the lowest overall IMLEO for lunar and Mars missions. FPBR engines with thrust-to-weight ratios of 30 and specific impulses near 1000 s. could, for a given payload and trip time, reduce Mars mission IMLEO by almost 40%. T/W levels over 30 provide diminishing returns. For fixed IMLEO and payload delivery to Mars, the FPBR engine again outperforms the baseline and other nuclear thermal systems. All-up trip times to Mars can be reduced from over 550 days to 350 days, using the additional fuel fraction to enable higher-energy transfers.

• Split missions in which the TEI propellant is sent ahead on a low-energy trajectory on a cargo vehicle (these are referred to as 'no-contingency' missions, since an abort prior to Mars encounter would not be possible) could achieve crew trip times as low as 300 days with the use of the particle bed reactor, decreasing the time spent in transit by a factor of two, from ~500 to 250 days.

• The gas-core engines' low thrust-to-weight ratio (<1) disqualified gas-core systems from serious competition with their solid-core counterparts, despite the gas-core advantage in specific impulse. In the case of the open-cycle gas-core, engine structure typically constituted almost half of the total IMLEO.

• The use of an FPBR system as an upper stage for an Earth-to-orbit launch vehicle could approximately double the payload inserted into LEO, even allowing for a higher structural mass fraction to reflect the requirement for heavy onboard radiation shielding.

• The mass margin gained by replacing the baseline ascent/descent vehicles' chemical propulsion systems with nuclear thermal systems such as the FPBR is on the order of 10 mT. This margin is not large enough to justify such replacement, especially in view of the operational complications the use of nuclear engines would impose upon the ascent/descent mission.

*Fixed Particle Bed Reactor performance*: The FPBR was seen to be a lightweight, moderate $I_{sp}$ alternative to a chemical propulsion system that consistently outperformed both the high-$I_{sp}$ gas-core engines and NERVA, its solid-core predecessor. Its thrust-to-weight, the highest of any of the options studied, allowed it to decrease the IMLEO of several baseline missions by 40%. Specifications for the engine would require a T/W of 30, given a fixed engine mass of ~1 mT. Beyond a value of 30, there is little return in the form of decreased propellant mass. A specific impulse requirement of 1000 s. would place the FPBR at the edge of current material temperature limitations.

Fixed-IMLEO/Fixed payload Mars missions were examined to determine the reduction in trip time afforded by replacing the baseline chemical/aerobrake system by nuclear thermal options. While all of the solid- and gas-core variants improved upon the baseline to some degree, the FPBR system was capable of decreasing overall trip time for Mars Option I Flight 1 from 565 to 350 days. Short-duration stays with direct entry on Earth return were amenable to such reduction while conjunction-class missions (requiring stays of 500 days or more) and short-stay trips without direct entry upon return to Earth were not.

*Split missions:* Splitting the crew and cargo between two flights allowed further trip time reduction for short-duration stay missions. An FPBR-propelled Mars transfer vehicle could achieve baseline delivery at the baseline IMLEO in only 300 days (round trip), with a total time in transit of 270 days--as opposed to the 90-Day Study's 535 days aboard the transfer vehicle.

*Gas-Core flexibility problems:* The large mass--and low thrust-to-weight ratios--of the gas-cores negated their single advantage, high specific impulse. A single Open Cycle (2) engine, which masses 126 mT, has an Isp of 1800 s. and a thrust of 1760 kN, would be more than sufficient to meet the thrust requirement explained early in Section 3.0. It would incur a propellant savings of ~100 mT relative to a 900 s. FPBR system. However, the FPBR propulsion system, given a T/W of ~30, would mass only 1 mT. As subsequent burns are

performed, the robust FPBR system can stage unnecessary engines; the single Open Cycle engine must be retained for the entire mission, requiring extra propellant to accelerate the engine mass during each boost.

*Ascent/descent vehicle performance:* A trade study was performed to determine the amount of additional mass freed up by exchanging ascent/descent vehicle engines for the higher specific-impulse FPBR system. Lunar ascent/descent vehicles were assumed to mass 50 mT; Mars vehicles were 80 mT. Gross weight prior to descent and total payload mass were held fixed and $I_{sp}$ allowed to vary from 500 to 1000 s. As seen in Section 3.1.1.3, the total mass bonus accrued was approximately 10 mT for both the lunar and Mars excursion vehicles. This is too small to accomodate onboard radiation shielding, which would mass at least 10 mT and nullify the FPBR's $I_{sp}$ advantage.

*Nuclear upper stage performance:* A generic two-stage Earth-to-orbit vehicle massing 2000 mT and capable of placing 135 mT of payload in LEO was examined and its chemical second stage replaced by a hypothetical FPBR system. A structural mass fraction of .20 was assumed. The use of a high-$I_{sp}$ system onboard the second stage allowed the nuclear vehicle to deliver almost 250 mT to low Earth orbit, nearly doubling the chemical vehicle's payload and providing a large incentive to move to nuclear upper stages as a means of decreasing the number of vehicle launches required to sustain a particular lunar or Martian mission.

### 4.1.2 Issues of Construction, Operation, and Testing

- The use of nuclear thermal propulsion onboard Mars and lunar transfer vehicles will require heavy shadow shielding (lead and/or tungsten) to protect against gamma radiation, in addition to lighter LiH shielding to guard against exposure to neutron radiation. Total shielding depth will be on the order of 400 to 500 g/cm$^2$. Problems with vehicle structural stability prohibit extremely long truss structures to take advantage of the inverse square drop in absorbed dose with distance.
- Use of nuclear thermal propulsion aboard ascent/descent vehicles is inadvisable; its use introduces complex operational problems including protection of surface habitats from radiation exposure during landing and in the case of accidents upon landing, and safe crew egress and cargo offloading from a 'hot' vehicle. Additionally, ascent/descent vehicle design requirements are at odds with radiation shielding requirements; for instance, the need for a stable landing platform drives the designer to a vehicle with a low center-of-mass, while the use of nuclear engines would require the largest crew-reactor separation distance possible.
- On-orbit rendezvous between a nuclear vehicle and a transportation node or other vehicle will require approach and departure protocol including a one-day cooldown phase prior to docking,

keeping the docking node/vehicle within the safe cone of the nuclear vehicle at all times, and transfer of crew or cargo within this same safe cone.

- The radiation hazard posed by the overflight of a lunar base by an active nuclear vehicle is negligible; base shielding against galactic cosmic radiation and solar particle events will be more than sufficient to protect crew members against the comparatively low radiation flux of a reactor cluster at high altitude above the lunar surface.
- To decrease the possibility of environmental danger resulting from proximity to radioactive materials, engines at their functional end-of-life in Earth orbit should be boosted to high circular orbits above 1000 km. It has been shown that this would require an additional $\Delta v$ of ~300 km/s. Alternatively, engines could be placed on an interplanetary trajectory to remove waste entirely from high-traffic near-Earth space. These trajectories would require velocity changes in excess of 2500 m/s.
- Nuclear-augmented launch vehicles must reach orbit in order to prevent any debris from impacting on or near civilian populations--this translates to an engine-out requirement for all stages in addition to very high reliability requirements on the stages and their component engine clusters. Disposal of nuclear upper stages will involve measures similar to that used for transfer vehicle engines.
- Specific precautions will have to be taken with respect to engine testing, including permanent storage of reactor effluent and safe disposal of test articles such as used engines and test stands.
- Actual flight engines would be subjected to minimal testing, assuring only that the device may safely operate at criticality. Testing must be limited to prevent buildup of fission products within the engine which would require extensive radiation protection for all personnel contacting the engine.

*Radiation shielding requirements:* Shadow shielding provides low-cost radiation protection for transfer vehicle crew and sensitive cargo; encasement of the reactor systems, while preventing problems associated with maneuvering near nuclear-propelled vehicles, would drive the total shielding mass to unacceptably high levels. High-density, high-atomic number materials such as lead and tungsten prove most effective in stopping the gamma radiation flux from the engine cluster. Low atomic number materials, lithium hydride or liquid hydrogen, provide efficient absorption of thermalized neutron radiation. Since the total radiation flux declines as a function of the square of the separation distance between reactor and crew, a trade must be made between decreased shielding requirements for large distances and requisite increases in structural mass necessary to maintain vehicle stability. The trade specifically examined a 1 $m^2$ cross-section truss connecting a simplified crew vehicle to the propulsion

cluster. The truss was found to buckle for lengths over ~10 m. The resulting vehicle configuration required 400 to 500 g/cm$^2$ of neutron and gamma shielding; this translates to 4000 to 5000 kg/m$^2$ or about 15 mT for a 3 m$^2$ shield.

*Ascent/descent vehicle operations:* Complex operational problems both in space and during descent and touchdown contribute to making the ascent/descent mission an unlikely beneficiary of nuclear thermal propulsion. Placing an NTP cluster aboard an excursion vehicle will require shielding similar to that aboard transfer vehicles to protect crew and cargo; it has been shown that, for the payload requirements and excursion vehicle masses under consideration, the use of nuclear propulsion systems only frees up approximately 10 mT for additional modifications or increased payload. This 10 mT is lower than the 15 mT shielding that will be required to protect the crew. Docking and rendezvous in low lunar or low Martian orbit will have to take into account the shadow cones of two vehicles. More importantly, there appears to be no simple solution to the problem of effecting crew egress and cargo unloading on the surface following touchdown. The presence of a very 'hot' engine will require an egress to occur within the safety cone, but given the obvious 'engine-down' configuration of the vehicle on the surface, it is unlikely that the crew will be able to emerge onto the planetary surface without leaving the safety cone--this implies the need for an extremely fast egress, due to the high radiation flux. This problem, and the problem of a possible nuclear excursion crash near a surface habitat (which could make the surface facility uninhabitable) argues most strongly against the use of NTP aboard ascent/descent vehicles.

*Ascent/descent vehicle design:* The necessity for a stable landing configuration drives a requirement for a short, squat vehicle, while reactor shielding can only be decreased by increasing the crew separation distance and thus the overall vehicle length. High thrust-to-weight drives a requirement for larger engine clusters, again necessitating further shielding against the higher radiation flux. These factors combine to suggest that the assumption of 15 mT for transfer vehicle shielding constitutes a definite lower limit to ascent/descent vehicle shielding; the actual shield mass will be larger. Since the mass 'bonus' achieved by using NTP will clearly only be on the order of 10 mT, the ascent/descent vehicle should not be considered as a candidate for its use on the basis of these design issues.

*On-orbit rendezvous with a nuclear vehicle:* The difficulties posed by the use of nuclear thermal engines such as the FPBR during docking maneuvers with other vehicles or a transportation node can be solved by imposing a cooldown phase prior to transfer vehicle approach to the node/vehicle. For a 300-MW reactor, approximately 27 hours of standoff at a distance of 20 km would be required before approach; this would allow crew within 100 m of the reactor cluster for an hour and experience no more than 5 rem of absorbed dose. This level of radiation exposure is small enough to ensure that minor errors during the docking procedure

will not result in dangerous radiation doses delivered to crew onboard the other vehicle (or to the crew aboard the nuclear transfer vehicle via secondary or scattered radiation). Nevertheless, docking would have to be performed in such a manner as to ensure that the other vehicle would always remain within the shadow shield's safe cone. Crew transfer and cargo offloading would also occur within the safe cone.

This protocol would not be necessary for any nuclear vehicle prior to engine startup, since the cluster will be nonradioactive before ignition. The only necessary precaution to be taken would be moving the transfer vehicle to safe separation (again, 20 km) before initiating the transfer burn.

*Nuclear vehicle overflight:* A nuclear vehicle overflying a hypothetical lunar base and initiating an impulsive burn while in line-of-sight of the base does not allow any significant absorbed dose to unshilded crew members in the vicinity of the base. An active 1500-MW cluster of nuclear engines would deliver 0.3 rem to unshielded crew at a circular orbit altitude of 10 km. This indicates that such doses can be easily avoided by requiring crew to remain within the confines of the lunar habitat during overflight or by restricting impulsive burns to occur only below the base horizon.

*Disposal of engines following end-of-life:* Disposal is an important issue only when engines reach end-of-life in orbit at the moon, Mars, or Earth. Discarded or staged engines, lost following transfer burns between the various bodies, will follow trajectories that could be designed parabolic or hyperbolic so as not to allow a return to near-Earth space. Split mission cargo vehicles reach end-of-life in Mars orbit, and could be left there with the provision to move them to higher orbits at a later date if they prove to interfere with Mars operations. Engines discarded in low Earth orbit will have to be placed in (1) higher orbit, or (2) on an escape trajectory from Earth. These methods are the cheapest in terms of propellant expenditure and allow safe storage of spent engines for the conceivable future. Burnup of engines on reentry is not necessarily assured--the consequences of radioactive materials falling on inhabited areas make this option infeasible.

*Nuclear upper stage safety and disposal:* It is of the utmost importance that the upper stage reach orbit intact. This drives an engine-out requirement for all vehicle stages of a nuclear launch vehicle and high reliability, especially for the NTP stage. Failure of the first stage would not cause the release of any significant radioactivity as the nuclear stage is essentially inert prior to ignition. Engine construction would require that the reactor cluster could not achieve criticality in the event of an ocean impact, nor should the reactor break apart upon such impact. Additionally, nuclear upper stages could not be left in low Earth orbit but would have to be disposed of in much the same manner as transfer vehicle engines, either boosted to higher Earth orbits or allowed to escape Earth entirely.

*Testing program:* Test engines would require shielding and effluent scrubbing to prevent environmental contamination; early NERVA tests vented exhaust directly to the atmosphere with no precautions. If core material (structure and particles from the fluidized bed) remains intact, the effluent would be essentially non-radioactive, since hydrogen's neutron absorption cross-section is extremely small. Following engine tests, all radioactives would have to be interred and shielded; such storage could take place onsite or in a national storage facility.

*Testing of flight engines:* The protocol for testing flight articles would follow guidelines established for test engines; however, flight engines should only be tested to criticality and then shut down to prevent a sizeable buildup of fission products that could raise the engine's radioactivity and necessitate expensive and intricate procedures to safeguard personnel from contamination. Transportation and launch preparation of tested flight engines should nevertheless be conducted carefully, protecting transporters and launch pad workers from unnecessary exposure. This would include teleoperation of equipment for handling flight engines, in addition to light shielding and cooldown phases before moving tne engines following tests.

## BIBLIOGRAPHY

Albert, T., Space Reactor End of Life Issues, Science Applications International Corporation, 1987

Altman, et. al., Liquid Propellant Rockets, Princeton University Press, 1960

Altseimer, J., Operating Characteristics and Requirements for the NERVA Flight Stage, AIAA 70-676, 1970

Battin, R., An Introduction to the Mathematics and Methods of Astrodynamics, AIAA Education Series, 1987

Bhattacharyya, S., Use of Cermet-Fueled Reactors for Direct Nuclear Propulsion, 1988

Borowski, S., Nuclear Propulsion--A Vital Technology for the Exploration of Mars and the Planets Beyond, NASA Technical Memorandum, 1987

Bussard, R., and R. DeLauer, Fundamentals of Nuclear Flight, McGraw-Hill, 1965

Cohen, Aaron, et. al., Report of the 90-Day Study on Human Exploration of the Moon and Mars, 1989

Cooke, Doug, et. al., Databook for the 90-Day Study on Human Exploration of the Moon and Mars, 1989

DeCampli, W., Medical Problems Associated with Long-Duration Space Flights, in The Human Quest in Space (24th Goddard Memorial Symposium), AAS Science & Technology Series, Vol. 65, 1987

Elmer-DeWitt, P., "Star Wars Does It Again," Time, 15 April 1991

Graves, Glen, Radiation Environmental Analysis: A Reference Reactor Concept and a Standard Operating Cycle, pp. 475-567, Notes for the 1962 NSF Advanced Subject Material Institute on Nuclear Rocket Propulsion, Florida Engineering & Industrial Experimentation Station, 1962

Griffin, M., and J. French, Space Vehicle Design, AIAA Education Series, 1991

Harms, S., Evaluation of Advanced Nuclear Reactor Concepts for Space Applications, NRRT-N-89-023, 1987

Henry, A., Nuclear Reactor Analysis, MIT Press, 1986

Horn, F., J. Powell, et. al., Analysis of a Nuclear Orbital Transfer Vehicle Accident , Brookhaven National Laboratory, 1987

Koenig, D., Experience Gained from the Space Nuclear Rocket Program, Los Alamos National Laboratory, LA-10062-H, 1986

Latham, T., Criticality Studies of a Nuclear Light-Bulb Engine, Journal of Spacecraft, Vol. 6, No. 19, 1969

Latham, T., Summary of the Performance Characteristics of the Nuclear Light-Bulb Engine, AIAA 71-642, 1971

McCormack, P., Radiation Hazards in Low Earth Orbit, Polar Orbit, Geosynchronous Orbit, and Deep Space, in Working in Orbit and Beyond: The Challenges of Space Medicine, AAS Science & Technology Series, Vol. 72, 1989

McLafferty, G., Gas-Core Nuclear Rocket Engine Technology Status, Journal of Spacecraft, Vol. 7, No. 12, 1970

Nicogossian, A., and V. Garshnek, Consideration for Solar System Exploration: A System to Mars, in Working in Orbit and Beyond: The Challenges of Space Medicine, AAS Science & Technology Series, Vol. 72, 1989

Papadopolous, P., Aerobraking in a Dusty Martian Atmosphere, AIAA 90-1700, 1990

Powell, James, et. al., Particle-Bed Reactor Propulsion Vehicle Performance and Characteristics as an Orbital Transfer Rocket, from Space Nuclear Power Systems, Brookhaven National Laboratory, 1986

Rivello, R., Theory and Analysis of Flight Structures, 1969

Robbins, H., An Analytic Study of the Impulsive Approximation, AIAA Journal, 1966

Sutton, G., Rocket Propulsion Elements: An Introduction to the Engineering of Rockets, Wiley-Interscience, 1986

Thom, K., Review of Fission Engine Concepts, Journal of Spacecraft, Vol. 9, No. 9, 1972

Weaver, D., Mars Mission Strategies, NASA Office of Lunar and Mars Exploration, 1991

Wertz, J., and W. Larson, Ed., Space Mission Analysis and Design, Kluwer Academic Publishers, 1991

Wilson, Sam, Fast Round-Trip Mars Trajectories, NASA LBJ Space Flight Center, 1990

Zubrin, R., Nuclear Thermal Rockets Using Indigenous Martian Propellants, Martin-Marietta, 1989

## APPENDIX A

This section contains information derived from the Databook for the 90-Day Study on Human Exploration of the moon and Mars. The following pages are Excel spreadsheets, containing mission event lists from lunar (Option I Flights 0-7) and Mars (both options, all flights) baseline missions for comparison to the nuclear options discussed within the body of the study.

Opt1 Lunar Flt00

| | A | B | C | D |
|---|---|---|---|---|
| 1 | Mission Event | Total Vehicle Mass | Change in Mass | Delta-V |
| 2 | | (MT) | (MT) | (m/s) |
| 3 | IMLEO | **159.80** | | |
| 4 | Pre-injection preparation propellant | 159.80 | | |
| 5 | Trans-Lunar injection propellant | 79.35 | 80.45 | 3300 |
| 6 | Jettison TLI tanks | 75.05 | 4.30 | |
| 7 | Trans-Lunar coast propellant | 74.89 | 0.16 | 10 |
| 8 | Lunar orbit insertion propellant | 59.30 | 15.59 | 1100 |
| 9 | Lunar orbit operations propellant | 59.30 | | |
| 10 | Deploy additional payloads | 59.30 | | |
| 11 | Lunar payload to Lunar surface | 15.00 | 44.30 | |
| 12 | Jettison LTV/LOI tanks | 13.70 | 1.30 | |
| 13 | Trans-Earth injection propellant | 10.85 | 2.85 | 1100 |
| 14 | Trans-Earth coast propellant | 10.83 | 0.02 | 10 |
| 15 | Earth orbit operations propellant | 10.81 | 0.01 | 6 |
| 16 | Post-Aerobrake circularize | 10.13 | 0.69 | 310 |
| 17 | Final LTV-C mass in LEO | **10.13** | | |
| 18 | | | | |
| 19 | Lunar payload total mass | **44.30** | | |
| 20 | pre-deorbit preparation propellant | 43.82 | 0.48 | 50 |
| 21 | Moon payload propellant | 28.25 | 15.57 | 2000 |
| 22 | Moon payload (dry) | 5.85 | 22.40 | |
| 23 | Moon surface science | 5.85 | | |
| 24 | Moon surface consumables | 5.85 | 0.00 | |
| 25 | LEV-C total mass (prior to return to LLO) | **5.85** | | |
| 26 | LEV-C ascent propellant | 5.85 | | 0 |
| 27 | Crew | 5.85 | | |
| 28 | LEV-C (dry) | 5.85 | | |

Opt1 Lunar Flt01

| | A | B | C | D |
|---|---|---|---|---|
| 1 | Mission Event | Total Vehicle Mass | Change in Mass | Delta-V |
| 2 | | (MT) | (MT) | (m/s) |
| 3 | IMLEO | **178.80** | | |
| 4 | Pre-injection preparation propellant | 178.80 | | |
| 5 | Trans-Lunar injection propellant | 88.78 | 90.02 | 3300 |
| 6 | Jettison TLI tanks | 84.48 | 4.30 | |
| 7 | Trans-Lunar coast propellant | 84.30 | 0.18 | 10 |
| 8 | Lunar orbit insertion propellant | 66.76 | 17.55 | 1100 |
| 9 | Lunar orbit operations propellant | 66.76 | | |
| 10 | Deploy additional payloads | 66.76 | | |
| 11 | Lunar payload to Lunar surface | 12.46 | 54.30 | |
| 12 | Jettison LTV/LOI tanks | 11.16 | 1.30 | |
| 13 | Trans-Earth injection propellant | 11.16 | 0.00 | 0 |
| 14 | Trans-Earth coast propellant | 11.16 | 0.00 | 0 |
| 15 | Earth orbit operations propellant | 11.16 | 0.00 | 0 |
| 16 | Post-Aerobrake circularize | 11.16 | 0.00 | 0 |
| 17 | Final LTV-C mass in LLO | **11.16** | | |
| 18 | | | | |
| 19 | Lunar payload total mass | **54.30** | | |
| 20 | pre-deorbit preparation propellant | 53.71 | 0.59 | 50 |
| 21 | Moon payload propellant | 34.63 | 19.08 | 2000 |
| 22 | Moon payload (dry) | 10.48 | 24.15 | |
| 23 | Moon surface science | 10.48 | | |
| 24 | Moon surface consumables | 8.20 | 2.28 | |
| 25 | LEV-C total mass (prior to return to LLO) | **8.20** | | |
| 26 | LEV-C ascent propellant | 8.20 | | 0 |
| 27 | Crew | 8.20 | | |
| 28 | LEV-C (dry) | 8.20 | | |

Opt1 Lunar Flt02

| | A | B | C | D |
|---|---|---|---|---|
| 1 | Mission Event | Total Vehicle Mass | Change in Mass | Delta-V |
| 2 | | (MT) | (MT) | (m/s) |
| 3 | IMLEO | **189.00** | | |
| 4 | Pre-injection preparation propellant | 189.00 | | |
| 5 | Trans-Lunar injection propellant | 93.85 | 95.15 | 3300 |
| 6 | Jettison TLI tanks | 89.55 | 4.30 | |
| 7 | Trans-Lunar coast propellant | 89.36 | 0.19 | 10 |
| 8 | Lunar orbit insertion propellant | 70.76 | 18.60 | 1100 |
| 9 | Lunar orbit operations propellant | 70.76 | | |
| 10 | Deploy additional payloads | 70.76 | | |
| 11 | Lunar payload to Lunar surface | 26.26 | 44.50 | |
| 12 | Jettison LTV/LOI tanks | 24.96 | 1.30 | |
| 13 | Trans-Earth injection propellant | 19.77 | 5.19 | 1100 |
| 14 | Trans-Earth coast propellant | 19.72 | 0.04 | 10 |
| 15 | Earth orbit operations propellant | 19.70 | 0.03 | 6 |
| 16 | Post-Aerobrake circularize | 18.44 | 1.25 | 310 |
| 17 | Final LTV-P mass in LEO | **18.44** | | |
| 18 | | | | |
| 19 | Lunar payload total mass | **44.50** | | |
| 20 | pre-deorbit preparation propellant | 44.01 | 0.49 | 50 |
| 21 | Moon payload propellant | 28.38 | 15.64 | 2000 |
| 22 | Moon payload (dry) | 16.55 | 11.83 | |
| 23 | Moon surface science | 16.05 | 0.50 | |
| 24 | Moon surface consumables | 15.43 | 0.62 | |
| 25 | LEV-P total mass (prior to return to LLO) | **15.43** | | |
| 26 | LEV-P ascent propellant | 10.17 | 5.26 | 1900 |
| 27 | Crew | 10.17 | | |
| 28 | LEV-P (dry) | 10.17 | | |

Opt1 Lunar Flt03

| | A | B | C | D |
|---|---|---|---|---|
| 1 | Mission Event | Total Vehicle Mass | Change in Mass | Delta-V |
| 2 | | (MT) | (MT) | (m/s) |
| 3 | IMLEO | **178.80** | | |
| 4 | Pre-injection preparation propellant | 178.80 | | |
| 5 | Trans-Lunar injection propellant | 88.78 | 90.02 | 3300 |
| 6 | Jettison TLI tanks | 84.48 | 4.30 | |
| 7 | Trans-Lunar coast propellant | 84.30 | 0.18 | 10 |
| 8 | Lunar orbit insertion propellant | 66.76 | 17.55 | 1100 |
| 9 | Lunar orbit operations propellant | 66.76 | | |
| 10 | Deploy additional payloads | 66.76 | | |
| 11 | Lunar payload to Lunar surface | 12.46 | 54.30 | |
| 12 | Jettison LTV/LOI tanks | 11.16 | 1.30 | |
| 13 | Trans-Earth injection propellant | 11.16 | 0.00 | 0 |
| 14 | Trans-Earth coast propellant | 11.16 | 0.00 | 0 |
| 15 | Earth orbit operations propellant | 11.16 | 0.00 | 0 |
| 16 | Post-Aerobrake circularize | 11.16 | 0.00 | 0 |
| 17 | Final LTV-C mass in LLO | **11.16** | | |
| 18 | | | | |
| 19 | Lunar payload total mass | **54.30** | | |
| 20 | pre-deorbit preparation propellant | 53.71 | 0.59 | 50 |
| 21 | Moon payload propellant | 34.63 | 19.08 | 2000 |
| 22 | Moon payload (dry) | 22.48 | 12.15 | |
| 23 | Moon surface science | 10.48 | 12.00 | |
| 24 | Moon surface consumables | 8.20 | 2.28 | |
| 25 | LEV-C total mass (prior to return to LLO) | **8.20** | | |
| 26 | LEV-C ascent propellant | 8.20 | 0.00 | 0 |
| 27 | Crew | 8.20 | | |
| 28 | LEV-C (dry) | 8.20 | | |

Opt1 Lunar Flt04

| | A | B | C | D |
|---|---|---|---|---|
| 1 | Mission Event | Total Vehicle Mass | Change in Mass | Delta-V |
| 2 | | (MT) | (MT) | (m/s) |
| 3 | IMLEO | **189.00** | | |
| 4 | Pre-injection preparation propellant | 189.00 | | |
| 5 | Trans-Lunar injection propellant | 93.85 | 95.15 | 3300 |
| 6 | Jettison TLI tanks | 89.55 | 4.30 | |
| 7 | Trans-Lunar coast propellant | 89.36 | 0.19 | 10 |
| 8 | Lunar orbit insertion propellant | 70.76 | 18.60 | 1100 |
| 9 | Lunar orbit operations propellant | 70.76 | | |
| 10 | Deploy additional payloads | 70.76 | | |
| 11 | Lunar payload to Lunar surface | 26.26 | 44.50 | |
| 12 | Jettison LTV/LOI tanks | 24.96 | 1.30 | |
| 13 | Trans-Earth injection propellant | 19.77 | 5.19 | 1100 |
| 14 | Trans-Earth coast propellant | 19.72 | 0.04 | 10 |
| 15 | Earth orbit operations propellant | 19.70 | 0.03 | 6 |
| 16 | Post-Aerobrake circularize | 18.44 | 1.25 | 310 |
| 17 | Final LTV-P mass in LEO | **18.44** | | |
| 18 | | | | |
| 19 | Lunar payload total mass | **44.50** | | |
| 20 | pre-deorbit preparation propellant | 44.01 | 0.49 | 50 |
| 21 | Moon payload propellant | 28.38 | 15.64 | 2000 |
| 22 | Moon payload (dry) | 23.02 | 5.36 | |
| 23 | Moon surface science | 18.50 | 4.52 | |
| 24 | Moon surface consumables | 15.38 | 3.12 | |
| 25 | LEV-P total mass (prior to return to LLO) | **15.38** | | |
| 26 | LEV-P ascent propellant | 10.14 | 5.24 | 1900 |
| 27 | Crew | 10.14 | | |
| 28 | LEV-P (dry) | 10.14 | | |

Opt1 Lunar Flt05

| | A | B | C | D |
|---|---|---|---|---|
| 1 | Mission Event | Total Vehicle Mass | Change in Mass | Delta-V |
| 2 | | (MT) | (MT) | (m/s) |
| 3 | IMLEO | **189.00** | | |
| 4 | Pre-injection preparation propellant | 189.00 | | |
| 5 | Trans-Lunar injection propellant | 93.85 | 95.15 | 3300 |
| 6 | Jettison TLI tanks | 89.55 | 4.30 | |
| 7 | Trans-Lunar coast propellant | 89.36 | 0.19 | 10 |
| 8 | Lunar orbit insertion propellant | 70.76 | 18.60 | 1100 |
| 9 | Lunar orbit operations propellant | 70.76 | | |
| 10 | Deploy additional payloads | 70.76 | | |
| 11 | Lunar payload to Lunar surface | 26.46 | 44.30 | |
| 12 | Jettison LTV/LOI tanks | 25.16 | 1.30 | |
| 13 | Trans-Earth injection propellant | 19.92 | 5.24 | 1100 |
| 14 | Trans-Earth coast propellant | 19.88 | 0.04 | 10 |
| 15 | Earth orbit operations propellant | 19.86 | 0.03 | 6 |
| 16 | Post-Aerobrake circularize | 18.59 | 1.26 | 310 |
| 17 | Final LTV-P mass in LEO | **18.59** | | |
| 18 | | | | |
| 19 | Lunar payload total mass | **44.30** | | |
| 20 | pre-deorbit preparation propellant | 43.82 | 0.48 | 50 |
| 21 | Moon payload propellant | 28.25 | 15.57 | 2000 |
| 22 | Moon payload (dry) | 25.29 | 2.96 | |
| 23 | Moon surface science | 21.74 | 3.55 | |
| 24 | Moon surface consumables | 15.50 | 6.24 | |
| 25 | LEV-P total mass (prior to return to LLO) | **15.50** | | |
| 26 | LEV-P ascent propellant | 10.22 | 5.28 | 1900 |
| 27 | Crew | 10.22 | | |
| 28 | LEV-P (dry) | 10.22 | | |

Opt1 Lunar Flt06

| | A | B | C | D |
|---|---|---|---|---|
| 1 | Mission Event | Total Vehicle Mass | Change in Mass | Delta-V |
| 2 | | (MT) | (MT) | (m/s) |
| 3 | IMLEO | **173.30** | | |
| 4 | Pre-injection preparation propellant | 173.30 | | |
| 5 | Trans-Lunar injection propellant | 86.05 | 87.25 | 3300 |
| 6 | Jettison TLI tanks | 81.75 | 4.30 | |
| 7 | Trans-Lunar coast propellant | 81.58 | 0.17 | 10 |
| 8 | Lunar orbit insertion propellant | 64.60 | 16.98 | 1100 |
| 9 | Lunar orbit operations propellant | 64.60 | | |
| 10 | Deploy additional payloads | 64.60 | | |
| 11 | Lunar payload to Lunar surface | 15.40 | 49.20 | |
| 12 | Jettison LTV/LOI tanks | 14.10 | 1.30 | |
| 13 | Trans-Earth injection propellant | 11.17 | 2.93 | 1100 |
| 14 | Trans-Earth coast propellant | 11.14 | 0.02 | 10 |
| 15 | Earth orbit operations propellant | 11.13 | 0.01 | 6 |
| 16 | Post-Aerobrake circularize | 10.42 | 0.71 | 310 |
| 17 | Final LTV-C mass in LEO | **10.42** | | |
| 18 | | | | |
| 19 | Lunar payload total mass | **49.20** | | |
| 20 | pre-deorbit preparation propellant | 48.66 | 0.54 | 50 |
| 21 | Moon payload propellant | 31.38 | 17.29 | 2000 |
| 22 | Moon payload (dry) | 18.11 | 13.27 | |
| 23 | Moon surface science | 10.08 | 8.03 | |
| 24 | Moon surface consumables | 10.08 | 0.00 | |
| 25 | LEV-C total mass (prior to return to LLO) | **10.08** | | |
| 26 | LEV-C ascent propellant | 6.64 | 3.44 | 1900 |
| 27 | Crew | 6.64 | | |
| 28 | LEV-C (dry) | 6.64 | | |

Opt1 Lunar Flt07

| | A | B | C | D |
|---|---|---|---|---|
| 1 | Mission Event | Total Vehicle Mass | Change in Mass | Delta-V |
| 2 | | (MT) | (MT) | (m/s) |
| 3 | IMLEO | **150.10** | | |
| 4 | Pre-injection preparation propellant | 150.10 | | |
| 5 | Trans-Lunar injection propellant | 74.53 | 75.57 | 3300 |
| 6 | Jettison TLI tanks | 70.23 | 4.30 | |
| 7 | Trans-Lunar coast propellant | 70.08 | 0.15 | 10 |
| 8 | Lunar orbit insertion propellant | 55.50 | 14.59 | 1100 |
| 9 | Lunar orbit operations propellant | 55.50 | | |
| 10 | Deploy additional payloads | 55.50 | | |
| 11 | Lunar payload to Lunar surface | 23.50 | 32.00 | |
| 12 | Jettison LTV/LOI tanks | 22.20 | 1.30 | |
| 13 | Trans-Earth injection propellant | 17.58 | 4.62 | 1100 |
| 14 | Trans-Earth coast propellant | 17.54 | 0.04 | 10 |
| 15 | Earth orbit operations propellant | 17.52 | 0.02 | 6 |
| 16 | crew capsule reentry | 17.52 | 0.00 | |
| 17 | Post-Aerobrake circularize | 16.40 | 1.11 | 310 |
| 18 | Final LTV-P mass in LEO | **16.40** | | |
| 19 | | | | |
| 20 | Lunar payload total mass +LEV-P in LLO (8.7 mT | **40.70** | | |
| 21 | pre-deorbit preparation propellant | 40.26 | 0.44 | 50 |
| 22 | Moon payload propellant | 25.96 | 14.30 | 2000 |
| 23 | Moon payload (dry) | 22.96 | 3.00 | |
| 24 | Moon surface science | 22.96 | 0.00 | |
| 25 | Moon surface consumables | 16.72 | 6.24 | |
| 26 | LEV-P total mass (prior to return to LLO) | **16.72** | | |
| 27 | LEV-P ascent propellant | 11.02 | 5.70 | 1900 |
| 28 | Crew | 11.02 | | |
| 29 | LEV-P (dry) | 11.02 | | |

Opt1 Mars Flt01

| | A | B | C | D |
|---|---|---|---|---|
| 1 | Mission Event | Total Vehicle Mass | Change in Mass | Delta-V |
| 2 | | (MT) | (MT) | (m/s) |
| 3 | IMLEO | **832.20** | | |
| 4 | Pre-injection preparation propellant | 795.18 | 37.02 | 0 |
| 5 | Trans-Mars injection propellant | 302.43 | 492.75 | 4500 |
| 6 | Jettison TMI stage | 247.43 | 55.00 | |
| 7 | Jettison Earth-Mars consumables | 240.63 | 6.80 | |
| 8 | Trans-Mars coast propellant | 236.08 | 4.55 | 90 |
| 9 | Mars orbit insertion propellant | 235.23 | 0.85 | 17 |
| 10 | Mars orbit operations propellant | 230.79 | 4.45 | 90 |
| 11 | Deploy additional payloads/jettison aerobrake | 209.09 | 21.70 | |
| 12 | Mars payload to Mars surface | 129.59 | 79.50 | |
| 13 | Mars orbit consumables | 128.49 | 1.10 | |
| 14 | Trans-Earth injection propellant | 62.46 | 66.03 | 3400 |
| 15 | Jettison TEI stage | 52.06 | 10.40 | |
| 16 | Mars-Earth consumables | 48.26 | 3.80 | |
| 17 | Trans-Earth coast propellant | 47.24 | 1.02 | 101 |
| 18 | Earth orbit insertion propellant | 47.24 | 0.00 | 0 |
| 19 | Earth orbit operations propellant | 45.89 | 1.34 | 136 |
| 20 | Jettison IMM | 12.59 | 33.30 | |
| 21 | Final mass in LEO | **12.59** | | |
| 22 | | | | |
| 23 | Mars payload total mass | **79.50** | | |
| 24 | pre-deorbit preparation propellant | 79.50 | | 0 |
| 25 | Mars payload propellant | 58.99 | 20.51 | 1360 |
| 26 | Mars payload (dry) | 37.19 | 21.80 | |
| 27 | Mars surface science | 36.19 | 1.00 | |
| 28 | Mars surface consumables | 34.04 | 2.15 | |
| 29 | MCSV total mass | 34.04 | | |
| 30 | MCSV propellant | 9.61 | 24.43 | 5763 |
| 31 | Crew | 9.61 | | |
| 32 | MCSV (dry) | 9.61 | | |

Opt1 Mars Flt02

| | A | B | C | D |
|---|---|---|---|---|
| 1 | Mission Event | Total Vehicle Mass | Change in Mass | Delta-V |
| 2 | | (MT) | (MT) | (m/s) |
| 3 | IMLEO | **612.90** | | |
| 4 | Pre-injection preparation propellant | 586.42 | 26.48 | 0 |
| 5 | Trans-Mars injection propellant | 236.61 | 349.81 | 4225 |
| 6 | Jettison TMI stage | 201.61 | 35.00 | |
| 7 | Earth-Mars consumables | 201.61 | 0.00 | |
| 8 | Trans-Mars coast propellant | 199.48 | 2.13 | 50 |
| 9 | Mars orbit insertion propellant | 197.38 | 2.10 | 50 |
| 10 | Mars orbit operations propellant | 195.29 | 2.08 | 50 |
| 11 | Jettison Mars aerobrake | 174.59 | 20.70 | |
| 12 | Mars support to Phobos | 174.59 | 0.00 | |
| 13 | Mars science | 172.59 | 2.00 | |
| 14 | Mars payload to surface | 16.49 | 156.10 | |
| 15 | Mars cargo vehicle | 6.49 | 10.00 | |
| 16 | Final mass in LMO | **6.49** | | |
| 17 | | | | |
| 18 | Mars payload total mass | **156.10** | | |
| 19 | pre-deorbit preparation propellant | 156.10 | | 0 |
| 20 | Mars payload propellant | 115.82 | 40.28 | 1360 |
| 21 | Mars payload (dry) | 41.66 | 74.16 | |
| 22 | Mars surface science | 39.86 | 1.80 | |
| 23 | Mars surface consumables | 37.71 | 2.15 | |
| 24 | MCSV total mass | 37.71 | | |
| 25 | MCSV propellant | 37.71 | 0.00 | 0 |
| 26 | Crew | 37.71 | | |
| 27 | MCSV (dry) | 37.71 | | |

Opt1 Mars Flt03

| | A | B | C | D |
|---|---|---|---|---|
| 1 | Mission Event | Total Vehicle Mass | Change in Mass | Delta-V |
| 2 | | (MT) | (MT) | (m/s) |
| 3 | IMLEO | **698.70** | | |
| 4 | Pre-injection preparation propellant | 667.75 | 30.95 | 0 |
| 5 | Trans-Mars injection propellant | 253.97 | 413.78 | 4500 |
| 6 | Jettison TMI stage | 198.97 | 55.00 | |
| 7 | Jettison Earth-Mars consumables | 195.17 | 3.80 | |
| 8 | Trans-Mars coast propellant | 191.48 | 3.69 | 90 |
| 9 | Mars orbit insertion propellant | 190.79 | 0.69 | 17 |
| 10 | Mars orbit operations propellant | 187.18 | 3.61 | 90 |
| 11 | Deploy additional payloads | 186.18 | 1.00 | |
| 12 | Mars payload to Mars surface | 112.38 | 73.80 | |
| 13 | Mars orbit consumables | 112.38 | 0.00 | |
| 14 | Trans-Earth injection propellant | 73.52 | 38.86 | 2000 |
| 15 | Jettison TEI stage | 63.12 | 10.40 | |
| 16 | Mars-Earth consumables | 59.32 | 3.80 | |
| 17 | Trans-Earth coast propellant | 58.07 | 1.26 | 101 |
| 18 | Earth orbit insertion propellant | 58.07 | 0.00 | 0 |
| 19 | Earth orbit operations propellant | 56.41 | 1.65 | 136 |
| 20 | Mars-Earth Aerobrake | 42.41 | 14.00 | |
| 21 | Final mass in LEO | **42.41** | | |
| 22 | | | | |
| 23 | Mars payload total mass | **73.80** | | |
| 24 | pre-deorbit preparation propellant | 73.80 | | 0 |
| 25 | Mars payload propellant | 54.76 | 19.04 | 1360 |
| 26 | Mars payload (dry) | 50.79 | 3.97 | |
| 27 | Mars surface science | 45.79 | 5.00 | |
| 28 | Mars surface consumables | 36.46 | 9.33 | |
| 29 | Mars ascent stage total mass | 36.46 | | |
| 30 | ascent propellant | 10.29 | 26.16 | 5763 |
| 31 | Crew | 10.29 | | |
| 32 | ascent stage (dry) | 10.29 | | |

Opt1 Mars Flt04

| | A | B | C | D |
|---|---|---|---|---|
| 1 | Mission Event | Total Vehicle Mass | Change in Mass | Delta-V |
| 2 | | (MT) | (MT) | (m/s) |
| 3 | IMLEO | **707.90** | | |
| 4 | Pre-injection preparation propellant | 675.94 | 31.96 | 0 |
| 5 | Trans-Mars injection propellant | 251.62 | 424.32 | 4600 |
| 6 | Jettison TMI stage | 196.62 | 55.00 | |
| 7 | Jettison Earth-Mars consumables | 192.82 | 3.80 | |
| 8 | Trans-Mars coast propellant | 189.17 | 3.65 | 90 |
| 9 | Mars orbit insertion propellant | 188.49 | 0.68 | 17 |
| 10 | Mars orbit operations propellant | 184.93 | 3.56 | 90 |
| 11 | Deploy additional payloads/jettison aerobrake | 183.93 | 1.00 | |
| 12 | Mars payload to Mars surface | 110.73 | 73.20 | |
| 13 | Mars orbit consumables | 110.73 | 0.00 | |
| 14 | Trans-Earth injection propellant | 72.83 | 37.90 | 1975 |
| 15 | Jettison TEI stage | 62.43 | 10.40 | |
| 16 | Mars-Earth consumables | 58.63 | 3.80 | |
| 17 | Trans-Earth coast propellant | 57.38 | 1.24 | 101 |
| 18 | Earth orbit insertion propellant | 57.38 | 0.00 | 0 |
| 19 | Earth orbit operations propellant | 55.75 | 1.63 | 136 |
| 20 | Mars-Earth Aerobrake | 41.75 | 14.00 | |
| 21 | Final mass in LEO | **41.75** | | |
| 22 | | | | |
| 23 | Mars payload total mass | **73.20** | | |
| 24 | pre-deorbit preparation propellant | 73.20 | | 0 |
| 25 | Mars payload propellant | 54.31 | 18.89 | 1360 |
| 26 | Mars payload (dry) | 48.24 | 6.07 | |
| 27 | Mars surface science | 45.94 | 2.30 | |
| 28 | Mars surface consumables | 36.61 | 9.33 | |
| 29 | MCSV total mass | 36.61 | | |
| 30 | MCSV propellant | 10.34 | 26.28 | 5763 |
| 31 | Crew | 10.34 | | |
| 32 | MCSV (dry) | 10.34 | | |

Opt1 Mars Flt05

| | A | B | C | D |
|---|---|---|---|---|
| 1 | Mission Event | Total Vehicle Mass | Change in Mass | Delta-V |
| 2 | | (MT) | (MT) | (m/s) |
| 3 | IMLEO | **620.10** | | |
| 4 | Pre-injection preparation propellant | 593.30 | 26.80 | 0 |
| 5 | Trans-Mars injection propellant | 238.10 | 355.20 | 4250 |
| 6 | Jettison TMI stage | 200.30 | 37.80 | |
| 7 | Earth-Mars consumables | 200.30 | 0.00 | |
| 8 | Trans-Mars coast propellant | 198.19 | 2.11 | 50 |
| 9 | Mars orbit insertion propellant | 196.10 | 2.09 | 50 |
| 10 | Mars orbit operations propellant | 194.03 | 2.07 | 50 |
| 11 | Jettison Mars aerobrake | 173.33 | 20.70 | |
| 12 | Mars support to Phobos | 173.33 | 0.00 | |
| 13 | Mars science | 173.33 | 0.00 | |
| 14 | Mars payload to surface | 82.23 | 91.10 | |
| 15 | Mars cargo vehicle | 72.23 | 10.00 | |
| 16 | Final mass in LMO | **72.23** | | |
| 17 | | | | |
| 18 | Mars payload total mass | **91.10** | | |
| 19 | pre-deorbit preparation propellant | 91.10 | | 0 |
| 20 | Mars payload propellant | 67.59 | 23.51 | 1360 |
| 21 | Mars payload (dry) | 54.54 | 13.05 | |
| 22 | Mars surface science | 54.54 | 0.00 | |
| 23 | Mars surface consumables | 54.54 | 0.00 | |
| 24 | MCSV total mass | 54.54 | | |
| 25 | MCSV propellant | 54.54 | 0.00 | 0 |
| 26 | Crew | 54.54 | | |
| 27 | MCSV (dry) | 54.54 | | |

Opt1 Mars Flt06

| | A | B | C | D |
|---|---|---|---|---|
| 1 | Mission Event | Total Vehicle Mass | Change in Mass | Delta-V |
| 2 | | (MT) | (MT) | (m/s) |
| 3 | IMLEO | **678.70** | | |
| 4 | Pre-injection preparation propellant | 649.41 | 29.29 | 0 |
| 5 | Trans-Mars injection propellant | 260.62 | 388.79 | 4250 |
| 6 | Jettison TMI stage | 205.62 | 55.00 | |
| 7 | Jettison Earth-Mars consumables | 201.82 | 3.80 | |
| 8 | Trans-Mars coast propellant | 198.00 | 3.82 | 90 |
| 9 | Mars orbit insertion propellant | 197.29 | 0.71 | 17 |
| 10 | Mars orbit operations propellant | 193.56 | 3.73 | 90 |
| 11 | Deploy additional payloads/jettison aerobrake | 186.96 | 6.60 | |
| 12 | Mars payload to Mars surface | 116.06 | 70.90 | |
| 13 | Mars orbit consumables | 116.06 | 0.00 | |
| 14 | Trans-Earth injection propellant | 82.22 | 33.84 | 1625 |
| 15 | Jettison TEI stage | 71.82 | 10.40 | |
| 16 | Mars-Earth consumables | 68.02 | 3.80 | |
| 17 | Trans-Earth coast propellant | 66.58 | 1.44 | 101 |
| 18 | Earth orbit insertion propellant | 66.58 | 0.00 | 0 |
| 19 | Earth orbit operations propellant | 64.68 | 1.89 | 136 |
| 20 | Mars-Earth Aerobrake | 43.98 | 20.70 | |
| 21 | Final mass in LEO | **43.98** | | |
| 22 | | | | |
| 23 | Mars payload total mass | **70.90** | | |
| 24 | pre-deorbit preparation propellant | 70.90 | | 0 |
| 25 | Mars payload propellant | 52.61 | 18.29 | 1360 |
| 26 | Mars payload (dry) | 46.54 | 6.07 | |
| 27 | Mars surface science | 46.54 | 0.00 | |
| 28 | Mars surface consumables | 37.21 | 9.33 | |
| 29 | Mars ascent stage total mass | 37.21 | | |
| 30 | ascent propellant | 10.50 | 26.70 | 5763 |
| 31 | Crew | 10.50 | | |
| 32 | ascent stage (dry) | 10.50 | | |

Opt5 Mars Flt01

| | A | B | C | D |
|---|---|---|---|---|
| 1 | Mission Event | Total Vehicle Mass | Change in Mass | Delta-V |
| 2 | | (MT) | (MT) | (m/s) |
| 3 | IMLEO | **755.10** | | |
| 4 | Pre-injection preparation propellant | 721.42 | 33.68 | 0 |
| 5 | Trans-Mars injection propellant | 274.38 | 447.04 | 4500 |
| 6 | Jettison TMI stage | 219.38 | 55.00 | |
| 7 | Jettison Earth-Mars consumables + Comsats | 211.48 | 7.90 | |
| 8 | Trans-Mars coast propellant | 207.48 | 4.00 | 90 |
| 9 | Mars orbit insertion propellant | 206.73 | 0.75 | 17 |
| 10 | Mars orbit operations propellant | 202.83 | 3.91 | 90 |
| 11 | Deploy additional payloads/jettison aerobrake | 177.13 | 25.70 | |
| 12 | Mars payload to Mars surface | 97.63 | 79.50 | |
| 13 | Mars orbit consumables | 96.53 | 1.10 | |
| 14 | Trans-Earth injection propellant | 58.41 | 38.12 | 2368 |
| 15 | Jettison TEI stage | 47.11 | 11.30 | |
| 16 | Mars-Earth consumables | 43.31 | 3.80 | |
| 17 | Trans-Earth coast propellant | 42.39 | 0.92 | 101 |
| 18 | Earth orbit insertion propellant | 42.39 | 0.00 | 0 |
| 19 | Earth orbit operations propellant | 41.18 | 1.21 | 136 |
| 20 | Jettison IMM | 10.68 | 30.50 | |
| 21 | Final mass in LEO | **10.68** | | |
| 22 | | | | |
| 23 | Mars payload total mass | **79.50** | | |
| 24 | pre-deorbit preparation propellant | 79.50 | | 0 |
| 25 | Mars payload propellant | 58.99 | 20.51 | 1360 |
| 26 | Mars payload (dry) | 38.18 | 20.81 | |
| 27 | Mars surface science | 36.38 | 1.80 | |
| 28 | Mars surface consumables | 34.99 | 1.39 | |
| 29 | MCSV total mass | 34.99 | | |
| 30 | MCSV propellant | 9.88 | 25.11 | 5763 |
| 31 | Crew | 9.88 | | |
| 32 | MCSV (dry) | 9.88 | | |

Opt5 Mars Flt02

| | A | B | C | D |
|---|---|---|---|---|
| 1 | Mission Event | Total Vehicle Mass | Change in Mass | Delta-V |
| 2 | | (MT) | (MT) | (m/s) |
| 3 | IMLEO | **751.60** | | |
| 4 | Pre-injection preparation propellant | 719.05 | 32.55 | 0 |
| 5 | Trans-Mars injection propellant | 287.02 | 432.03 | 4275 |
| 6 | Jettison TMI stage | 232.02 | 55.00 | |
| 7 | Jettison Earth-Mars consumables + Comsats | 224.12 | 7.90 | |
| 8 | Trans-Mars coast propellant | 219.88 | 4.24 | 90 |
| 9 | Mars orbit insertion propellant | 219.09 | 0.79 | 17 |
| 10 | Mars orbit operations propellant | 214.95 | 4.14 | 90 |
| 11 | Deploy additional payloads/jettison aerobrake | 189.25 | 25.70 | |
| 12 | Mars payload to Mars surface | 108.35 | 80.90 | |
| 13 | Mars orbit consumables | 107.25 | 1.10 | |
| 14 | Trans-Earth injection propellant | 57.74 | 49.51 | 2919 |
| 15 | Jettison TEI stage | 46.44 | 11.30 | |
| 16 | Mars-Earth consumables | 42.64 | 3.80 | |
| 17 | Trans-Earth coast propellant | 41.73 | 0.90 | 101 |
| 18 | Earth orbit insertion propellant | 41.73 | 0.00 | 0 |
| 19 | Earth orbit operations propellant | 40.55 | 1.19 | 136 |
| 20 | Jettison IMM | 10.05 | 30.50 | |
| 21 | Final mass in LEO | **10.05** | | |
| 22 | | | | |
| 23 | Mars payload total mass | **80.90** | | |
| 24 | pre-deorbit preparation propellant | 80.90 | | 0 |
| 25 | Mars payload propellant | 60.03 | 20.87 | 1360 |
| 26 | Mars payload (dry) | 39.20 | 20.83 | |
| 27 | Mars surface science | 37.40 | 1.80 | |
| 28 | Mars surface consumables | 34.63 | 2.77 | |
| 29 | MCSV total mass | 34.63 | | |
| 30 | MCSV propellant | 9.78 | 24.85 | 5763 |
| 31 | Crew | 9.78 | | |
| 32 | MCSV (dry) | 9.78 | | |

Opt5 Mars Flt03

| | A | B | C | D |
|---|---|---|---|---|
| 1 | Mission Event | Total Vehicle Mass | Change in Mass | Delta-V |
| 2 | | (MT) | (MT) | (m/s) |
| 3 | IMLEO | **843.60** | | |
| 4 | Pre-injection preparation propellant | 805.37 | 38.23 | 0 |
| 5 | Trans-Mars injection propellant | 297.87 | 507.50 | 4630 |
| 6 | Jettison TMI stage | 242.87 | 55.00 | |
| 7 | Jettison Earth-Mars consumables + Comsats | 234.97 | 7.90 | |
| 8 | Trans-Mars coast propellant | 230.53 | 4.44 | 90 |
| 9 | Mars orbit insertion propellant | 229.70 | 0.83 | 17 |
| 10 | Mars orbit operations propellant | 225.36 | 4.34 | 90 |
| 11 | Deploy additional payloads/jettison aerobrake | 199.66 | 25.70 | |
| 12 | Mars payload to Mars surface | 117.36 | 82.30 | |
| 13 | Mars orbit consumables | 116.26 | 1.10 | |
| 14 | Trans-Earth injection propellant | 57.30 | 58.96 | 3335 |
| 15 | Jettison TEI stage | 46.00 | 11.30 | |
| 16 | Mars-Earth consumables | 42.20 | 3.80 | |
| 17 | Trans-Earth coast propellant | 41.31 | 0.89 | 101 |
| 18 | Earth orbit insertion propellant | 41.31 | 0.00 | 0 |
| 19 | Earth orbit operations propellant | 40.13 | 1.17 | 136 |
| 20 | Jettison IMM | 9.63 | 30.50 | |
| 21 | Final mass in LEO | **9.63** | | |
| 22 | | | | |
| 23 | Mars payload total mass | **82.30** | | |
| 24 | pre-deorbit preparation propellant | 82.30 | | 0 |
| 25 | Mars payload propellant | 61.06 | 21.24 | 1360 |
| 26 | Mars payload (dry) | 40.22 | 20.84 | |
| 27 | Mars surface science | 38.42 | 1.80 | |
| 28 | Mars surface consumables | 34.26 | 4.16 | |
| 29 | MCSV total mass | 34.26 | | |
| 30 | MCSV propellant | 9.67 | 24.59 | 5763 |
| 31 | Crew | 9.67 | | |
| 32 | MCSV (dry) | 9.67 | | |

Opt5 Mars Flt04

| | A | B | C | D |
|---|---|---|---|---|
| 1 | Mission Event | Total Vehicle Mass | Change in Mass | Delta-V |
| 2 | | (MT) | (MT) | (m/s) |
| 3 | IMLEO | **614.90** | | |
| 4 | Pre-injection preparation propellant | 588.42 | 26.48 | 0 |
| 5 | Trans-Mars injection propellant | 237.42 | 351.00 | 4225 |
| 6 | Jettison TMI stage | 202.42 | 35.00 | |
| 7 | Earth-Mars consumables | 202.42 | 0.00 | |
| 8 | Trans-Mars coast propellant | 200.28 | 2.14 | 50 |
| 9 | Mars orbit insertion propellant | 198.17 | 2.11 | 50 |
| 10 | Mars orbit operations propellant | 196.08 | 2.09 | 50 |
| 11 | Jettison Mars aerobrake | 175.38 | 20.70 | |
| 12 | Mars support to Phobos | 175.38 | 0.00 | |
| 13 | Mars science | 173.38 | 2.00 | |
| 14 | Mars payload to surface | 15.58 | 157.80 | |
| 15 | Mars cargo vehicle | 5.58 | 10.00 | |
| 16 | Final mass in LMO | **5.58** | | |
| 17 | | | | |
| 18 | Mars payload total mass | **157.80** | | |
| 19 | pre-deorbit preparation propellant | 157.80 | | 0 |
| 20 | Mars payload propellant | 117.08 | 40.72 | 1360 |
| 21 | Mars payload (dry) | 38.67 | 78.41 | |
| 22 | Mars surface science | 38.67 | 0.00 | |
| 23 | Mars surface consumables | 37.28 | 1.39 | |
| 24 | MCSV total mass | 37.28 | | |
| 25 | MCSV propellant | 37.28 | 0.00 | 0 |
| 26 | Crew | 37.28 | | |
| 27 | MCSV (dry) | 37.28 | | |

Opt5 Mars Flt05

| | A | B | C | D |
|---|---|---|---|---|
| 1 | Mission Event | Total Vehicle Mass | Change in Mass | Delta-V |
| 2 | | (MT) | (MT) | (m/s) |
| 3 | IMLEO | **571.90** | | |
| 4 | Pre-injection preparation propellant | 548.00 | 23.90 | 0 |
| 5 | Trans-Mars injection propellant | 230.81 | 317.19 | 4025 |
| 6 | Jettison TMI stage | 175.81 | 55.00 | |
| 7 | Jettison Earth-Mars consumables | 172.01 | 3.80 | |
| 8 | Trans-Mars coast propellant | 168.76 | 3.25 | 90 |
| 9 | Mars orbit insertion propellant | 168.15 | 0.61 | 17 |
| 10 | Mars orbit operations propellant | 164.97 | 3.18 | 90 |
| 11 | Deploy additional payloads/jettison aerobrake | 163.97 | 1.00 | |
| 12 | Mars payload to Mars surface | 92.87 | 71.10 | |
| 13 | Mars orbit consumables | 92.87 | 0.00 | |
| 14 | Trans-Earth injection propellant | 75.12 | 17.75 | 1000 |
| 15 | Jettison TEI stage | 64.72 | 10.40 | |
| 16 | Mars-Earth consumables | 60.92 | 3.80 | |
| 17 | Trans-Earth coast propellant | 59.63 | 1.29 | 101 |
| 18 | Earth orbit insertion propellant | 59.63 | 0.00 | 0 |
| 19 | Earth orbit operations propellant | 57.93 | 1.70 | 136 |
| 20 | Mars-Earth Aerobrake | 43.93 | 14.00 | |
| 21 | Final mass in LEO | **43.93** | | |
| 22 | | | | |
| 23 | Mars payload total mass | **71.10** | | |
| 24 | pre-deorbit preparation propellant | 71.10 | | 0 |
| 25 | Mars payload propellant | 52.75 | 18.35 | 1360 |
| 26 | Mars payload (dry) | 46.48 | 6.27 | |
| 27 | Mars surface science | 46.48 | 0.00 | |
| 28 | Mars surface consumables | 37.15 | 9.33 | |
| 29 | MCSV total mass | 37.15 | | |
| 30 | MCSV propellant | 10.49 | 26.66 | 5763 |
| 31 | Crew | 10.49 | | |
| 32 | MCSV (dry) | 10.49 | | |